Further investigation of the roles of fibronectin-binding proteins CadF and FlpA during *Campylobacter jejuni* interactions with intestinal epithelial cells

Mahjanah Hussein

Thesis submitted in accordance with the requirements for the degree
of Doctor of Philosophy of the University of London
February 2018

Department of Pathogens Molecular Biology
Faculty of Infectious and Tropical Diseases
London School of Hygiene & Tropical Medicine

Funded by MARA, Malaysia

Declaration

I, Mahjanah Hussein, confirm that the work presented in this thesis is my own. Where information has been derived from other sources, I confirm that this has been indicated in the thesis. All experiments were performed at London School of Hygiene and Tropical Medicine.

Abstract

Campylobacter jejuni is a leading cause of bacterial gastroenteritis in humans. The ability of *C. jejuni* to invade human intestinal epithelial cells (IECs) is pivotal for pathogenicity. Two highly conserved fibronectin-binding proteins CadF & FlpA have been shown to play an important role in *C. jejuni* adhesion to IECs. CadF & FlpA are also associated with outer membrane vesicles (OMVs) and may play a role in the binding of OMVs to IECs. Mutation of *cadF* & *flpA* in 11168H & 81-176 reduced binding to fibronectin *in vitro* and bacterial adhesion to and invasion of both Caco-2 & T84 IECs, however intracellular bacterial numbers increased over time between 3 and 24 hours. Both *cadF* & *flpA* mutants were able to translocate as efficiently as the wild-type strain across a T84 IEC monolayer, an event not associated with any change in membrane permeability as indicated by TEER values. Mutation of *cadF* reduced *C. jejuni* cytotoxicity in the *Galleria mellonella* larvae model of infection to a greater extent than mutation of *flpA*. OMVs isolated from *cadF* or *flpA* mutants were less immunogenic and cytotoxic than OMVs isolated from wild-type strains. Results from inhibitors studies showed that cytochalasin D, methyl-beta-cyclodextrin, colchicine and wortmannin all reduced 11168H invasion of T84 IECs. However the invasion mediated by CadF and FlpA was shown to initiate different invasion pathways as wortmannin showed no effect on the ability of the 11168H *cadF* mutant to invade T84 IECs whilst colchicine showed no effect on the ability of the 11168H *flpA* mutant to invade T84 IECs. Using a 11168H strain expressing GFP at high levels*, C. jejuni* was shown to invade IECs, either residing within the *Campylobacter* containing vacuole (CCV), free within the cytoplasm and also in close proximity to parts of the trans-golgi network. A LAMP-1 stain showed co-localisation with late endosomal compartments in parts of the trans-golgi network. *C. jejuni* infection of IECs leads to actin cytoskeleton rearrangement as seen by the formation of filopodia, lamellapodia, membrane ruffles and F-actin stress fibres after 24 hours infection as a result of activation of the small GTPase Rac1. Mutation of *cadF* or *flpA* reduces Rac1 activation compared to wild-type strain. The significant finding of this study is that CadF and FlpA appear to initiate different invasion pathways to allow *C. jejuni* invasion of IECs. The results of this study support the view that both CadF and FlpA play equally important roles in *C. jejuni* pathogenesis.

Table of contents

Acknowledgements

Bismillah, Alhamdullilah.

This PhD would not have been possible without the support of many people. First and foremost, I wish to express my heartfelt gratitude to my supervisor Prof Nick Dorrell who was extremely helpful and had offered assistance, support and guidance throughout my PhD. Thank you for your time and patience, Nick!

Deepest gratitude is also to my co-supervisor Dr Abdi Elmi who I have gained as a friend and without his advice, assistance and patience my project would not have been successful. Also to Dr Ozan Gundogdu for advice and suggestion to my work. Thank you, you both!

Special thanks to Dr Elizabeth McCarthy, for turning confocal microscopy's room from cold to warm with your friendship. Thank you.

Special thanks to Dorrell group members past and present. Special thanks also to the Wren group, especially to individuals from Lab 202. Thank you all!

Special gratitude to my family and friends; for their understanding, and support through the duration of my studies. Forever grateful!

Thank you also goes to Mestech, UniKL and finally MARA, for the sponsorship.

Finally, this work is dedicated to Aishah, my beloved daughter who has to 'endure' mummy, but with her endless love and duas, we made it to the end! I love you too, Aishah! And in loving memory of my mother Rahmah Md Noh.

Alhamdullilah.

List of abbreviations

ABC	ATP-binding cassette
AJs	adherence junctions
BamHI	Bacillus amyloliquefaciens type II restriction enzyme
BsAgs	bacterial superantigens (histo-blood group antigens)
BB	Brucella broth
BCA	Bicinchoninic acid
bp	base pair
BSA	bovine serum albumin
CadF	Campylobacter adhesion to fibronectin
CapA	Campylobacter adhesion protein
CBA	Columbia blood agar
CCV	Campylobacter-containing vacuole
Cia	Campylobacter invasion antigens
Cdc42	cell division control protein 42
cDNA	complementary DNA
CDC	Communicable Diseases Centre
CDT	cytolethal distending toxin
CFUs	colony forming units
CO_2	carbon dioxide
Cyto-D	cytochalasin-D
3-D	3 dimension
DAPI	4’6-diamidino-2-phenylindole
DCA	deoxycholic acid
DNA	Deoxyribonucleic acid

DMSO	Dimethyl sulfoxide
DMEM	Dulbecco Modified Eagle Medium
EBI	European Bioinformatics Institute
ECM	extracellular matrix
EcoRI	Restriction enzyme isolated from *E. coli*
EDTA	Ethylenediaminetetraacitic acid
EFSA	European Food Safety Authority
EGFR	epidermal growth factor receptor
EHEC	enterohaemorrhagic *Escherichia coli*
ELISA	enzyme-linked immunosorbent assay
EPEC	enteropathogenic *Escherichia coli*
EU	European Union
EVOM	Epithelial Voltohmmeter
FAs	focal adhesions
FALG	phenylalanine-arginine-leucine-serine
FAKs	focal adhesion kinases
FBLM	fibronectin-binding linear motif
FCS	foetal calf serum
FlpA	fibronectin like protein A
FlaA	major flagellin A
FlaB	minor flagellin B
Fn	fibronectin
FRLS	phenyalanine-alanine-leucine-glycine
FSA	Food Safety Authority
gDNA	genomic DNA
GFP	green fluorescence protein

GBS	Guillain-Barre' Syndrome
G-LISA	small GTPases activation assay
GuHCL	guanidine hydrochloride
GTPases	Guaninetriphospate
H_2O	hydrogen and oxygen
hBD-3	human beta defensin-3
HCT8	Homo sapiens colon ileocecal carcinoma cells
HDs	hemi desmosomes
HeLa	Henrietta Lack for cervical cancer cells
HtrA	high-temperature requirement A
HT29-MTXE-12	mucus secreting derivative of human colon adenocarcinoma ((HT29) cells
IECs	Intestinal epithelial cells
INT 407	HeLa derivative cervical cell line
IL-6	Interleukin-6
IL-8	Interleukin-8
IPTG	Isopropyl-B-thio-galactoside
JAMs	junctions adhesion molecules
JlpA	*Jejuni* lipoprotein A
katA	catalase A
kB	kilo base
Km	Kanamycin
kV	kilo volt
Lamp1	lysosome-associated membrane protein 1
LB	Luria-Bertani
LDH	lactate dehydrogenase

LMH	hepatocellular carcinoma epithelial cells
LOS	lipooligossaccharide
LPS	lipopolysaccharide
LSHTM	London School of Hygiene and Tropical Medicine
M cells	Microfold cells in the gut
MAPK	mitogen-activated protein pathways
MβCD	methyl beta cyclodextrin
MFS	Miller Fisher Syndrome
MDCK-1	Madin-Darby canine kidney cells
MKN-28	gastric cancer cell line
MFs	microfilaments
MH	Muller Hinton
MOMP	major outer membrane protein
MOI	multiplicity of infection
mRNA	messenger RNA
MSCRAMMs	microbial surface component recognising adhesive matrix molecules
MTs	microtubules
N_2	nitrogen
NCTC	National Collection Type Culture
NCBI	National centre for Biotechnology Information
NK-κB	nuclear factor-kappa
O_2	oxygen
OD	optical density
OM	outer membrane
OMVs	outer membrane vesicles

kDa	kilo Dalton
PBS	Phosphate Buffer Saline
pCJC1	plasmid *C. jejuni* with chloramphicol cassette
PCR	polymerase chain reaction
PEB1	periplasmic binding protein
PFA	paraformaldehyde
Pg	Pico gram
pH	potential of Hydrogen to show acidity or akalinity
PI3-K	Phosphoinositol-3-kinase
pMEK91	plasmid vector
PNS	Periphery nervous system
PHE	Public Health England
PldA	phospholipase A
PO	phenol oxidase
porA	outer membrane proteinA
pVir	plasmid virulence
Rac1	small GTPases
RFU	relative fluorescent unit
RNA	ribonucleic acid
ROS	reactive oxygen species
RT	room temperature
RT-PCR	reverse transcriptase PCR
Rpm	revolving per minutes
sodB	superdioxide dimutase
SOC	super optimal broth with catabolic repression

SBA	soya bean agglutinin
SCV	Salmonella-containing vacuole
Swiss 3T3	fibroblast cells
ST	sodium taurocholate
TAE	Tris-acetate-EDTA
TEER	trans epithelial electrical resistance
T3SS	type III secretion system
T4SS	type IV secretion system
T6SS	type VI secretion system
TJs	tight junctions
TNF-α	tumour nuclear factor-alpha
UV	ultraviolet
VAIN	Variable Atmosphere Incubator
VBNC	Viable But Non-Culturable
VDC	Vertical diffusion chamber
WGA	wheat germ agglutinin
WR	working reagent
units	
ng	nanogram
v/v	volume/volume
w/v	weight/volume
µM	micro Molar
µ/l	micro liter
mM	mili Molar

CHAPTER ONE: INTRODUCTION

1.1 Campylobacter

Almost 30 years ago, *Campylobacter* species were recognised as a human pathogen causing gastroenteritis, long after this bacterial infection was first described in 1886 by Theodor Escherich (Kist, 1986). In the UK since 1981, *Campylobacter* species have been identified as the major cause of acute bacterial enteritis in humans (Richardson et al., 2001).

Globally *C. jejuni* and *C. coli* are identified as a major cause of human gastroenteritis and are responsible for the majority of human cases of campylobacteriosis (Moore et al., 2005). *Campylobacter* species are the leading cause of human gastroenteritis compared to *Salmonella* species infections in many countries (Golz et al., 2014). The burden of the disease is important to human public health because of the clinical aspects emerging from the infection, such as Guillain-Barré Syndrome (GBS) and Miller Fisher Syndrome (MFS). Due to the association of *C. jejuni* with its natural host (poultry), the bacteria will always find their way into the food chain. As such, together with emerging trends in antibiotic resistance, this makes *C. jejuni* a significant foodborne human pathogen. At present, however, it is not feasible to eliminate *Campylobacter* species completely from poultry and thus the food chain. On-going research is aimed to understand the pathogenesis of *C. jejuni*.

1.2 *Campylobacter jejuni* bacteriology

C. jejuni is a Gram-negative bacterium which is curved or comma shaped, S or gull wing-shaped, or a spiral rod shape, 0.2 to 0.8 μm wide and 0.5 to 5 μm long. *C. jejuni* exhibits rapid darting motility with a corkscrew-like motion caused by a single polar flagellum at one or both ends of the cell. *C. jejuni* are microaerophilic and capnophilic, growing optimally in 5% O2, 10% CO2, 85% N2 at 42^{o}C rather than at 37^{o}C. However the bacteria cannot grow at temperatures below 30^{o}C. *C. jejuni* is highly susceptible to drying and does not grow well on dry surfaces (Fernandez et al., 1985). However a study has reported that *C. jejuni* can survive up to 4 h on some clean or soiled food contact surfaces at 27^{o}C and at around 62% relative humidity (De Cesare et al., 2003). In comparison to *Salmonella typhimurium* and *Listeria monocytogenes, C. jejuni* is not tolerant to high osmotic stress. *S. typhimurium* and *Listeria monocytogenes* can grow in the presence of

4.5% (w/v) and 10% (w/v) sodium chloride respectively, whilst *C. jejuni* cannot grow in the presence of 2% (w/v) sodium chloride (Doyle and Roman, 1982b). *C. jejuni* is able to grow in a pH range from 4.9 to 9.0, but the optimal growth pH is between 6.5 and 7.5 (Blaser and Wang, 1980, Blaser et al., 1980). *C. jejuni* can form biofilms and resist the impact of oxidative stress in the environment. Enzymes such as superoxide dismutase, catalase, peroxidase, gluthathione synthatase and gluthathione reductase play important roles in protecting *C. jejuni* from oxidative stresses (Pesci et al., 1994, Purdy and Park, 1994).

Older *Campylobacter* cells become coccoid in shape and non-culturable. The state of viable but non-culturable (VBNC) has been reported to be associated with the change of morphology from spiral to coccoid (Rollins and Colwell, 1986, Moran and Upton, 1986). More recent studies however suggested no correlation exists between cell morphology and culturable status (Medema et al., 1992, Lazaro et al., 1999). Non-culturable cells at 20 and 116 days kept in PBS at 4^{o}C were shown to contain the same intact DNA as fresh culturable control cells at day 0 (Lazaro et al., 1999). Furthermore, there are conflicting reports on the existence of the VBNC state in *C. jejuni* (Rollins and Colwell, 1986, Moran and Upton, 1986, Jones et al., 1991).

C. jejuni motility is phase variable (Karlyshev et al., 2002, Hendrixson, 2006, Hendrixson, 2008) and also growth-phase dependent (Konkel et al., 1992c). During *in vitro* culturing, motility can be reduced or lost due to phase variation (Gaynor et al., 2004). However, during infection experiments, motility can be regained (Jones et al., 2004). At the late logarithmic growth phase, motility was observed to be maximal and diminished during stationary phase (Wosten et al., 2004).

In comparison to other enteric bacterial pathogens like *Salmonella* species, the *C. jejuni* genome is small (1.64 Mbps) and has a relatively low G+C content of around 30% (Gaskin et al., 2009). A study in 2000 reported the complete circular genome of the *C. jejuni* NCTC 11168 wild-type strain has 1,641,481 base pairs (bp) encoding 1654 proteins. The *C. jejuni* NCTC 11168 genome contains many hypervariable gene sequences encoding different surface structures including lipo-oligosaccharide (LOS), capsular polysaccharide and flagella (Parkhill et al., 2000). During replication, these hypervariable sequences which encode for bacterial surface structures such as LOS, capsule and flagella, can result in slip-strand mispairing and cause phase variation to occur that leads to antigenic variation in the bacterial population. As a result of phase variation, the protein expression changes and causes phenotypic variation. *C. jejuni* was shown to demonstrate

extensive genetic diversity between human isolates (Dorrell et al., 2001). Studies have demonstrated that several strains contain a plasmid encoding for antibiotic resistance and a type IV secretion system (T4SS) (Bacon et al., 2000, Louwen et al., 2006, Batchelor et al., 2004). A study reported that in 2016, the complete assembled genome sequences for 142 *C. jejuni* species *jejuni* genome were available at the National Centre for Biotechnology Information (NCBI) genome databases (Mund et al., 2016). However, there are thousands more sequences deposited in NCBI, but not assembled and/or not annotated. In the European Bioinformatic Institute (EBI) bacteria website, there are currently 23 *C. jejuni* genomes, with the sequences fully assembled and annotated (EBI, 2018).

C. jejuni lacks the glycolytic enzyme phosphofructokinase and as such is not able to ferment glucose. However *C. jejuni* strains that have adapted to colonise livestock are able to utilise L-fucose (Zautner et al., 2012, Muraoka and Zhang, 2011). *C. jejuni* is able to metabolise free amino acids and keto acids directly from a host or generated by other bacteria in the same ecological environment (Lee and Newell, 2006). The non-livestock adapted strains that are incapable to utilise L-fucose and to metabolise amino acid (Zautner et al., 2011, Hofreuter et al., 2008). For respiration, *C. jejuni* is able to utilise many different electron donors such as D-lactate, formate, malate, succinate and NAD (P)H or hydrogen. In addition, *C. jejuni* has chemolithotropic characteristics so it is able to utilise inorganic sulphite as a respiratory electron donor (Tareen et al., 2011, Hoffman and Goodman, 1982, Kelly, 2001, Myers and Kelly, 2005).

1.2.1Transmission in chickens and humans

C. jejuni is found in the gastrointestinal tract of a wide range of animals particularly poultry (Gormley et al., 2014). The natural body temperature of poultry is around 42^{o}C and the microaerobic conditions in the gut are very favourable to *C. jejuni* colonisation (Gilbreath et al., 2011). Other animals can also harbour *C. jejuni* such as cats, dogs, pigs, cows and many wild animals (Gormley et al., 2014). As a natural host for *C. jejuni,* the poultry reservoir is linked to approximately 80% of all

campylobacteriosis infections (EFSA, 2011). *C. jejuni* colonises the chicken cecal mucosal crypts and numbers as high as 10^9 cfu/g of chicken ceacal contents can be found at any one time with chicks as young as 3 days old colonised (Shanker et al., 1990). Water, feed and litter gradually showed an increase of *C. jejuni* contamination as transmission within a flock increases (Shanker et al., 1990, Montrose et al., 1985). Other potential sources of transmission in broiler chicks were through contaminated fomites. These include farm workers clothing, transport such as trucks, tractors and forklifts as well as equipment such as crates and pallets (Ramabu et al., 2004).

It was previously thought that *C. jejuni* is a commensal in chickens and a study showed that colonisation of chickens does not affect the ceacal mucosa suggesting that no disease occurs in infected chickens (Meade et al., 2009). However, more recent studies have reported that *C. jejuni* colonisation of chickens causes damage to the mucosa and increased intestine permeability (Humphrey et al., 2014). High colonisation levels allow *C. jejuni* to spread throughout a flock and result in very high levels of contamination. It was shown that the majority of broilers could be infected within a month of hatching (Patriarchi et al., 2009, Golz et al., 2014). However, there was no evidence that vertical transmission occurs in commercial broiler production (Shanker et al., 1986, Cox et al., 2012). Another study in Sweden supported this, where 60,000 progeny parent breeders originating from *Campylobacter*-positive chickens were analysed and no evidence of vertical transmission was found (Callicott et al., 2006). In poultry processing, handling during slaughter and carcass processing pose the highest risk of contamination (Allen et al., 2007). Despite the hostile environment in the chicken gastrointestinal tract, *C. jejuni* thrives, indicating an adaptive ability to respond to *in vivo* stresses. One study has reported that the *C. jejuni* 81116 wild-type strain exhibits increased ability to colonise after one passage through chickens (Cawthraw et al., 1996).

However *C. jejuni* can cause severe disease in humans. Major sources of *C. jejuni* infection are the consumption of undercooked poultry as well as contaminated meats, milk and water (Doyle and Roman, 1982a). Despite implementation of various strategies to control this pathogen in poultry, chicken meat remains the most important source of infection in humans. It was reported that 75% of poultry sold in major supermarkets in the UK were contaminated by *Campylobacter* species (EFSA, 2011). *C. jejuni* and *Campylobacter coli* are responsible for around 85% and 15% of human infections respectively (Moore et al., 2005, Snelling et al., 2005). For the highly invasive *C. jejuni* 81-176 wild-type strain, as little as 100

bacteria are able to cause disease in humans (Black et al., 1988). Studies have shown in humans that 400 to 10,000 bacteria are sufficient to cause inflammatory gastroenteritis (Black et al., 1988, Alter et al., 2011). Humans can also become infected by consumption of contaminated meat, unpasteurised milk as well as contaminated water (Nachamkin et al., 1993, Fernandes et al., 2015, Perkins-Jones et al., 1982). The main infective route is through consumption of undercooked or raw poultry. Cross contamination to kitchen utensils also poses a significant risk during preparation of raw chicken products.

Flies have also been reported to be a seasonal vector in transmitting *Campylobacter* species to humans after contact with contaminated surfaces, human, bird or animal faeces. Rainfall increase the fly population, which starts in the late spring and peaks around June (Nichols, 2005, Royden et al., 2016, Shane et al., 1985). Another study supported this observation and reported that *C. jejuni* infection outbreaks increase during summer months and decrease during winter months, however the reason behind this still unclear (Casey et al., 2017).

Human to human transmission can occur, as reported in a study where an ill person contaminated a salad they prepared and caused an outbreak of gastrointestinal illness in a boys summer camp (Blaser et al., 1982). In another study, transmission between infected members of families was reported (Blaser et al., 1981). However, human-to-human transmission is thought to be a very infrequent event.

1.2.2 Disease presentation

Many host factors combine with the virulence factors expressed by *C. jejuni* to influence or determine the outcome of infection in humans. Acute symptoms are thought to be associated with *C. jejuni* invasion of the intestinal epithelium cells, which results in inflammatory bacterial diarrhoea. Symptoms range from mild diarrhoea with fever and abdominal pain to bacteraemia. These symptoms are not distinguishable from the gastrointestinal infections caused by other enteric bacterial pathogens such as *Salmonella, Shigella* or *Yersinia* species. Campylobacteriosis has an incubation period of 1 to 7 days and clinical symptoms will appear in most people after 3 to 7 days (Dasti et al., 2010) but these can last

far longer (5 to 21 days). More than 90% of patients reported fever of low grade or more than 40^{o}C and the fever could last for 1 week (Allos, 2001). The diarrhoea can be short lived, prolonged or recurrent. The diarrhoea can be watery and non-inflammatory or bloody and inflammatory. The frequency of diarrhoea can reach 10 instances per day and a person with diarrhoea poses the highest risk to their contacts (Ashkenazi et al., 1987).

Local complications can result from the direct spread of gastrointestinal infection including cholecystitis, pancreatitis, peritonitis and massive gastrointestinal haemorrhage. While systemic complications are rare, meningitis, arthritis, endocarditis and myocarditis have all been reported as manifestations of campylobacteriosis. In a rare case, *C. jejuni* mediated enterocolitis resulted in toxic megacolon in a 28 year old male (Schneider et al., 2000). In stools of healthy persons, *C. jejuni* is not commonly identified, as studies have shown up to 50% of infected persons during an outbreak are asymptomatic (Blaser et al., 1979).

Bacteraemia with campylobacteriosis can occur in patients (less than 1%) who are immunocompromised or among the very young or very old and can lead to sepsis and death. Death due to sepsis after *Campylobacter* infection occurs in 50 out of 1,000 cases (Allos, 2001). The duration of carriage may be quite long without treatment, however 90% of patients do become negative spontaneously within two months of infection. In the majority of cases, hospitalisation is not required, however death can occur in a minority of immunocompromised individuals.

1.2.3 Post-sequelae syndromes

Studies have shown that infection with *C. jejuni* can result in Guillain-Barré syndrome (GBS) (Rees et al., 1995, Yuki et al., 2004) or Miller Fisher syndrome (MFS) (Willison and O'Hanlon, 1999). GBS is an autoimmune disorder that causes a symmetrical ascending paralysis of the peripheral nervous system (PNS). GBS causes weakness of the limbs and weakness of the respiratory muscles (Ropper, 1992). Evidence of prior infection with *C. jejuni* and subsequent link to GBS has been reported in several studies. Patients with GBS were found to have evidence of prior *C. jejuni* infections, however no particular strains were implicated. C*. jejuni* infection resulted in a poor or severe outcome of GBS (Rees et al., 1995). *C. jejuni-*

positive patients showed significantly greater disability, such as requiring ventilation or walking aids and even death within one year after diagnosis.

Only infection with certain *C. jejuni* serotypes is known to increase the risk of developing GBS. *C. jejuni* strains from patients with GBS belong mostly to Penner serogroup type 19 (Kuroki et al., 1993). Many researchers have indicated that a ganglioside-like surface structure, such as GM1, which is found in some *C. jejuni* strains LOS, can induce GBS. (Gregson et al., 1997, Ropper, 1992, Ropper and Adelman, 1992). An experimental study using chickens infected with *C. jejuni* showed similar symptoms to GBS (Li et al., 1996). Many serotypes of *C. jejuni* have been reported to be associated with GBS such as Penner type O:1 to O:5, O:10, O:16, O:23, O:37, O:44, and O:64 (Nachamkin et al., 1998). However, infection with *C. jejuni* Penner type O: 19 increases the risk of developing GBS. A study by Yuki *et al.* reported that type 0:19 was identified in 52% in GBS patients (Yuki et al., 1997). In South Africa, *C. jejuni* Penner type O: 41 isolates were found to be associated with GBS patients (Wassenaar et al., 2000). Molecular mimicry by the LOS on the surface of *C. jejuni* with the human gangliosides in the PNS causes production of autoreactive antibodies that lead to an ascending paralysis (Yuki et al., 2004). In a study with rabbits injected with *C. jejuni* LOS, the rabbits developed anti-GM1 IgG antibodies and exhibited limb weakness. The changes in the rabbit PNS appeared to be identical to that of GBS patients (Backert et al., 2013). More recently it was reported that mice infected with *C. jejuni* developed GBS (St Charles et al., 2017).

Another complication is MFS, a rare variant of GBS, but potentially fatal. The Penner type O:2 is associated with MFS (Yuki, 1997). The paralysis causes abnormal muscle co-ordination and paralysis of the eyes with unmoving pupils (Willison and O'Hanlon, 1999, Dingle et al., 2001). Other conditions are also implicated with *C. jejuni* infection. It was reported that septicaemia can occur in immunocompromised individuals and irritable bowel syndrome is also commonly associated with campylobacteriosis (Spiller, 2007). Reactive arthritis can develop as a result of *C. jejuni* infection (Hannu et al., 2002). Myocarditis associated with *C. jejuni* infection has also been reported in a number of studies (Cunningham and Lee, 2003, Obafemi and Douglas, 2017, Hessulf et al., 2016, Pena and Fishbein, 2007, Westling and Evengard, 2001).

1.3 *Campylobacter jejuni* epidemiology

C. jejuni is the major cause of bacterial gastroenteritis worldwide (Zilbauer et al., 2008). *C. jejuni* infection is a significant public health problem globally because the number of cases of campylobacteriosis has surpassed by about 2-3 fold compared to the number of *Salmonella* infections (Figure 1.1) (Golz et al., 2014). Although other species of *Campylobacter* are also able to cause diseases in humans, such as *C. lari* and *C. uppsaliensis,* it is *C. jejuni* and *C. coli* that are responsible for around 85% and 15% of the human cases respectively (Moore et al., 2005). *C. jejuni* is responsible for as many as 400–500 million bacterial gastroenteritis cases per year worldwide (Boehm et al., 2011). In the USA it was estimated there are 1.3 million cases per year (14 cases per 100,000 population) (CDC, 2015). In the European Union (EU) alone, there are approximately 9 million gastroenteritis cases per year with a total cost estimated at €2.4 billion due to campylobacteriosis. This is equivalent to 55.5 incidences per 100,000 population (EFSA, 2015). *C. jejuni* is the major cause of food poisoning in UK with an economic burden predicted to be around £900 million. Annually, there are approximately 280,000 cases and there are over 100 deaths linked to campylobacteriosis (FSA, 2016).

The self-limiting nature of the disease results in many cases been unreported (Samuel et al., 2004). Therefore, the actual number of cases is almost certainly higher (Golz et al., 2014). It is estimated that the actual number of cases would be around 10 times higher. It also appears to be sporadic and consistent with a peak during the summer season where the activity of barbequing is popular (Tauxe and Blake, 1992, Nichols, 2005). The peak month for *Campylobacter* species reporting in 2015 was June (Figure 1.2B) (PHE, 2016).

Campylobacteriosis occurs in all age groups (Figure 1.2A). In developed countries, young children, young adults and the very elderly are susceptible, whereas in developing countries, young children are the high-risk individuals and many of the cases are fatal (Cody et al., 2012, Butzler and Skirrow, 1979a). Higher cases may occur in young children probably because of a lack of immunity and a lack of proper good hygiene practices as well as potentially higher contamination in food preparation (Cody et al., 2012). However, *Campylobacter* species were found in higher numbers in stool samples of young adults compared to young children, and higher in males than in females (Butzler and Lauwers, 1979, Butzler and Skirrow, 1979b). In England, the 50 – 59 year age group was the highest number of cases infected with Campylobacter (PHE, 2016).

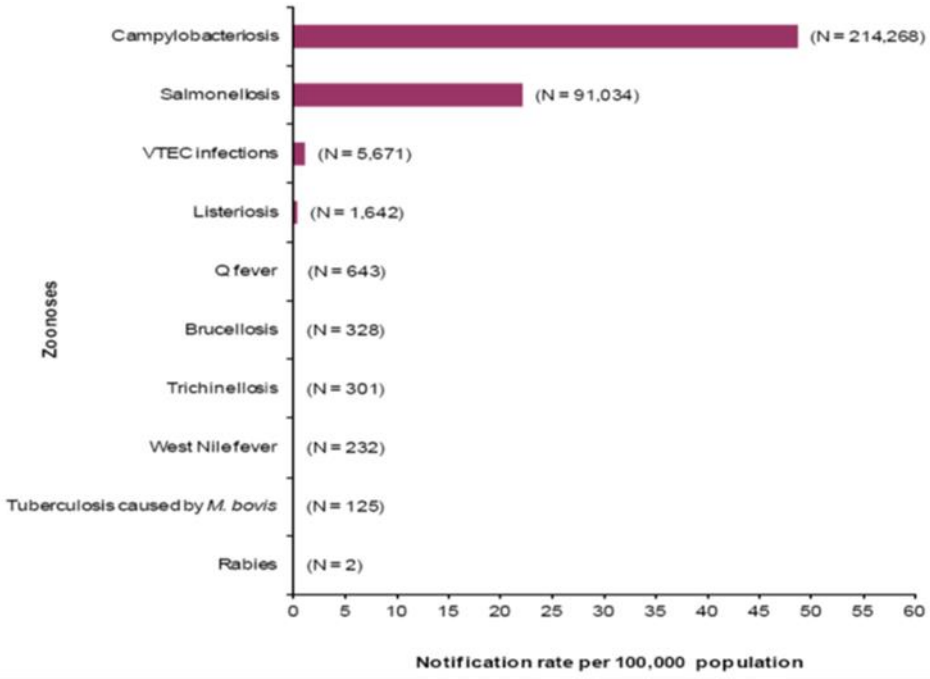

Figure 1.1. Campylobacteriosis causes more bacterial enteritis disease in humans compared to Salmonellosis. The underreporting of *Campylobacter* infections because of the self-limiting nature of disease would suggests that the true number of cases is probably higher. Report from human zoonoses cases and notification rates in EU in 2013. Reproduce from (EFSA, 2015).

A

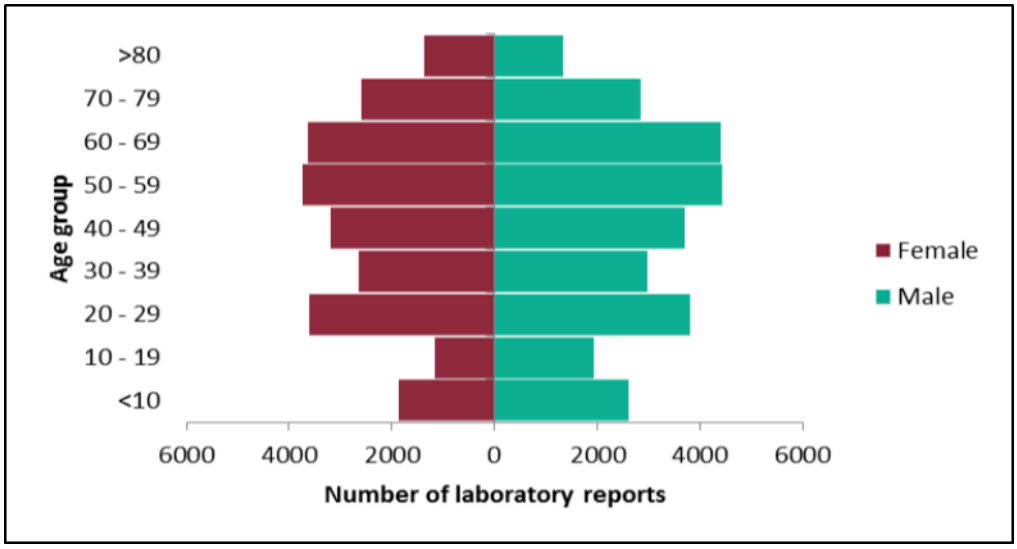

B

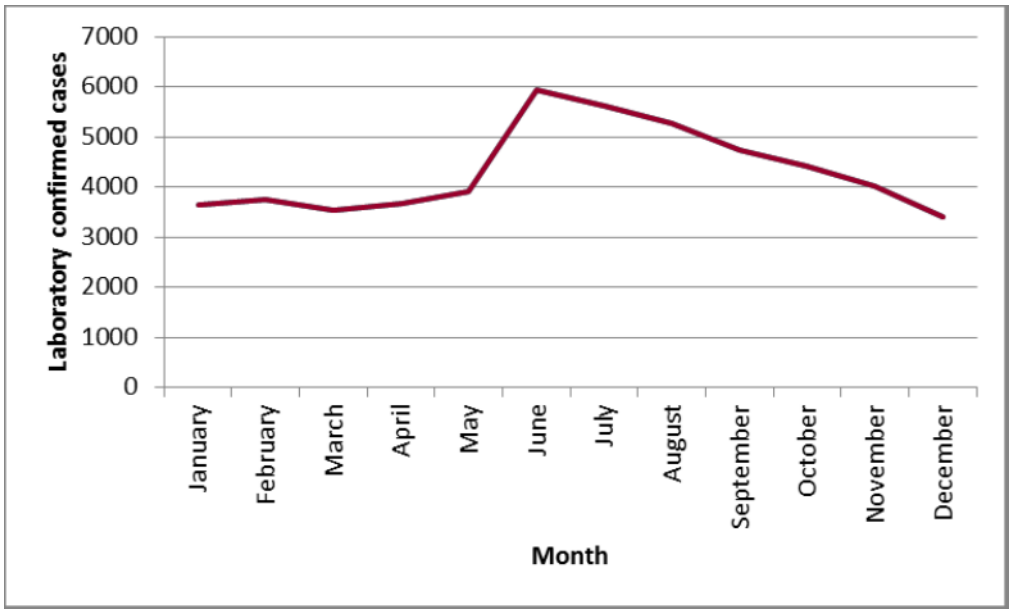

Figure 1.2. Campylobacteriosis incidence showing distribution in age and sex and seasonal occurance. A. Age/sex distribution of laboratory reports of *Campylobacter* species and B. Seasonality of laboratory reports of *Campylobacter* species reported in England in 2015. Reproduced from Public Health England (PHE, 2016).

1.4 Intestinal epithelial cells

Intestinal epithelial cells (IECs) form the first barrier in the intestine to harmful substances as well as offering a portal of entry for many enteric bacterial pathogens. Enteric bacterial pathogens ability to breach this barrier will potentially increase virulence and successful disease production (Wessler and Backert, 2008). The integrity of an intact barrier of IECs is maintained by several features exhibited by polarised epithelial cells. Structures such as distinct apical and baso-lateral surfaces, microvilli with a defined brush border, proper tight junctions (TJs) and adherence junctions (AJs), as well as a highly organised actin cytoskeleton, help form fully functional IECs (Laukoetter et al., 2008). The cell adhesion structures that are responsible for cell membrane integrity are the TJs, the AJs and in addition at the basal surface, the integrin-mediated cell matrix such as focal adhesions (FAs) and hemidesmosomes (HDs).

TJs are maintained by junction adhesion molecules (JAMs), claudins and occludins, as well as other proteins. TJs are localised laterally at the apical side and are responsible for tight sealing of cell monolayers. TJs control movement of membrane proteins, lipids and paracellular ion influx. AJs are maintained by an E-cadherin-based network of membrane proteins and associated molecules. AJs are localised basally to TJs and are responsible for mechanical adhesion between neighbouring cells. E-cadherin functions as an adhesive protein and also as a regulator of cell proliferation. In addition, E-cadherin is involved in transmitting a signal to the actin cytoskeleton via β-catenin via the intracellular domain of E-cadherin. At the basal membrane of IECs, FAs are maintained by transmembrane receptor protein integrins α5β1. This integrin with two subunits of α and β chains binds to extracellular matrix (ECM) proteins at the plasma membrane via fibronectin and to microfilaments of the actin cytoskeleton in the cytoplasm via various adapter proteins such as vinculin and paxilin, and also signalling enzymes including focal adhesion kinase (FAK). These linkages are able to transmit various signals from outside the cell and result in various changes or reorganisation of the actin cytoskleton inside the cell. HDs also have a complex network of protein interactions that involve integrin α6β4, laminin and plectin (Backert et al., 2013).

Previous studies have reported that *C. jejuni* is able to attach and invade both non-polarised and polarised intestinal cells (IECs) *in vitro* including INT 407 (Monteville et al., 2003), Caco-2 (Everest et al., 1992) and T84 cells (Monteville and Konkel, 2002). Although the adherence ability of different *C. jejuni* strains was similar to

some extent, invasion and transmigration capacities have been reported to be highly variable in different IEC lines. For translocation studies, polarised cells are widely used because the bacteria are required to cross tight polarised monolayer cells. Non-polarised cells express only FAs but polarised cells express TJs, AJs and HDs together with FAs. Typical polarised IECs include Caco-2, T84, MDCK-1 and MKN-28. In addition some polarised IECs are able to produce a mucus layer such as HT29 MTXE-12 (Alemka et al., 2010), hence providing a better mimic of the intestinal natural environment and may produce more relevant results.

Therefore, in order to impact, proliferate and survive in host cells, many enteric bacterial pathogens including *C. jejuni* employ various mechanisms to exploit and overcome TJs, AJs, HDs and FAs. Furthermore, studies have shown that *C. jejuni* invades cells of human origin more efficiently compared to non-human cells, indicating that *C. jejuni* is a successful human enteric bacterial pathogen (Konkel et al., 1992a).

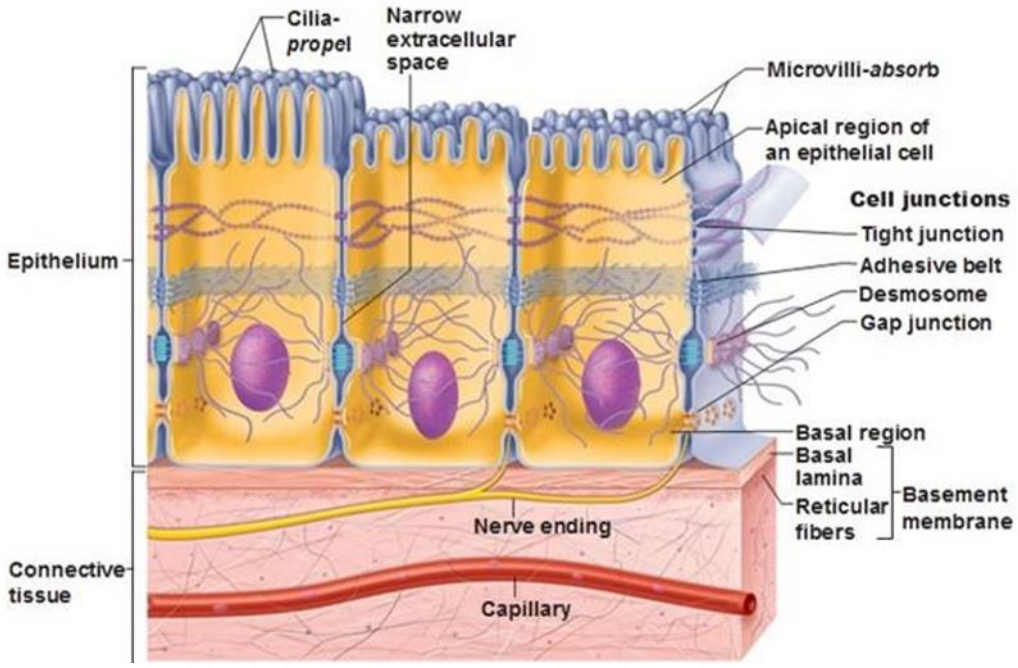

Figure 1.3 Schematic diagram showing characteristic of epithelial cell.
Barrier function of the mucosa is largely determined by tight junctions.
Reproduce from Antarnik.org

1.5 *Campylobacter jejuni* pathogenesis

C. jejuni interaction with host cells is a multifactorial processes and involve various identified and unidentified virulence factors. These complex host-pathogen interactions require motility, adhesion, translocation, invasion, protein secretion, toxin production, as well as intracellular survival of *C. jejuni* to successfully impact host cells and cause disease. Studies have suggested (Hu et al., 2008, Konkel et al., 1992b) *C. jejuni* pathogenesis involves multiple steps but during the initial stages of infection, *C. jejuni* appears to interact with host cell protrusions. This was visualised using electron microscopy, showing the *C. jejuni* 81-176 wild-type strain to adhere, invade, translocate across and exit polarised Caco-2 IECs (Hu et al., 2008). *C. jejuni* is reported to adhere to host cells via CadF and FlpA adhesins for maximal adherence (Konkel et al., 2010, Monteville et al., 2003). *C. jejuni* is capable of transcellular translocation across human polarised epithelial monolayers (Bras and Ketley, 1999). *C. jejuni* entry via the paracellular pathway was also reported and this involved no reduction in transepithelial electrical resistance (TEER). HtrA (high-temperature requirement A) protein has been shown to play a role in mediating the cleavage of E-cadherin (Boehm et al., 2012). In addition, a study reported an alternative entry pathway that *C. jejuni* may utilise referred to as subvasion. In the subvasion entry pathway, *C. jejuni* was suggested to enter host epithelial cells baso-laterally (Bouwman et al., 2013). Another study supported this showing *C. jejuni* preferentially entering T84 cells at the baso-lateral surface (Monteville and Konkel, 2002).

Following invasion of IECs, *C. jejuni* secretes putative invasion effectors into host cells that activate host cell signalling pathways and trigger C*. jejuni*-induced changes in many host cell signalling proteins. Krause-Gruszczynska *et al.* reported *C. jejuni*-induced GTPase activation including Cdc42 (Krause-Gruszczynska et al., 2011). Phosphorylation of host proteins as a prerequisite for *C. jejuni* invasion was also reported by studies using protein kinase inhibitors (Biswas et al., 2004, Hu et al., 2006). Internalised *C. jejuni* induces gastroenteritis through either inflammation or physical tissue damage (Young et al., 2007, Ketley, 1997). The ability of *C. jejuni* to induce pro-inflammatory cytokines in the host cells such as IL-8, is thought to be the major cause of gastroenteritis (Watson and Galan, 2005). HeLa cells infected with *C. jejuni* resulted in activation of the central immune modulator nuclear factor (NF-κB) (Mellits et al., 2002).

Previous studies have shown that the host cell cytoskeleton is reorganised to facilitate internalisation of *C. jejuni* with involvement of microfilaments (MFs) or microtubules (MTs) or both (Biswas et al., 2003, Kopecko et al., 2001). Hu & Kopecko reported that internalised *C. jejuni* moves along dynein (a molecular motor) in MTs to the perinuclear region of host cells (Hu and Kopecko, 1999). Moreover, *C. jejuni* 81-176 wild-type strain is able to replicate in a host cell vacuole and induce apoptosis via cytolethal distending toxin (CDT) (Hickey et al., 2005). CDT breaks double stranded DNA and causes cell cycle arrest (Lara-Tejero and Galan, 2000).

Intracellular survival may facilitate the dissemination of *C. jejuni* locally. *C. jejuni* 81-176 resides in a *Campylobacter*-containing vacuole (CCV) in T84 cells (Watson and Galan, 2008) and survives for several days in monocytes (Bouwman et al., 2013, Kiehlbauch et al., 1985). In addition, it was shown that *C. jejuni* 81-176 can form microcolonies / biofilms on human intestinal epithelial tissue (Haddock et al., 2010). Van Rhijn *et al.* reported that *C. jejuni* DNA was present circulating in myelomonocytic cells (Van Rhijn et al., 2003).

Recently, it was reported that not only is *C. jejuni* colonisation dependent on the host microbiota, but that this can also cause changes to the composition of the intestinal microbiota (Awad et al., 2016).

1.5.1 *C. jejuni* adhesion mechanisms

Colonisation of host tissues is an important step in bacterial infection. One of the mechanisms involved in colonisation is attachment of bacteria to host cells via specific interactions between bacterial adhesins and host cell receptors. Adherence to IECs is a multifactorial event that is proposed to be fundamental to *C. jejuni* pathogenesis (Backert et al., 2013, O Croinin and Backert, 2012). However, many of the precise molecular mechanisms involved in the attachment of *C. jejuni* to eukaryotic cells are still unclear.

Currently the hypothetical model of *C. jejuni* invasion involves two proposed pathways which are the zipper and trigger mechanisms (Figure 1.3) (O Croinin and Backert, 2012). The ‘zipper mechanism’ is commonly used by many pathogens that colonise the gastric intestinal tract. A high-affinity adhesin on the surface of

bacteria and a receptor on the host cell are required for the 'zippering' of the plasma membrane around the bacteria resulting in membrane engulfment. In the 'trigger mechanism' used by *Salmonella* and *Shigella* species, various bacterial effector proteins injected by either a type III secretion system (T3SS) or a type IV secretion system (T4SS) will initiate and activate rearrangement of the host cell cytoskeleton and allow entry of the pathogen into host cells.

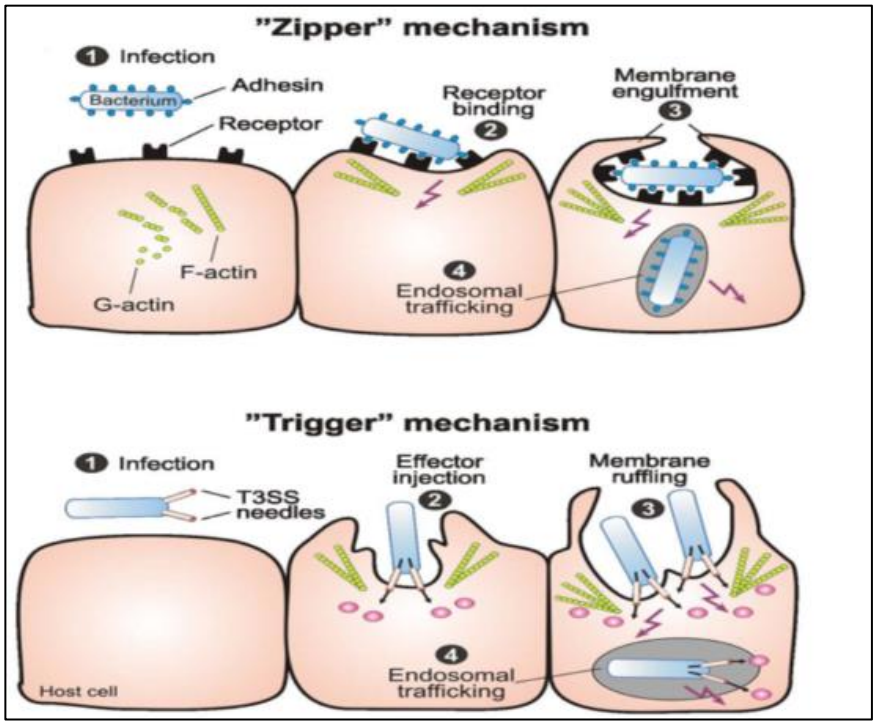

Figure 1.4 Primary mechanisms of bacterial invasion into non-phagocytic host cells. Schematic representation of the two different routes of entry by intracellular bacterial pathogens. The pathogens induce their own uptake into target cells by subversion of host cell signaling pathways using the "zipper" and "trigger" invasion mechanism, respectively. Reproduced from (O Croinin and Backert, 2012).

Many studies have reported different proteins and carbohydrates to play important roles in adhesion of *C. jejuni* to hosts cells both *in vivo* and *in vitro*. (Table 1.1)

1.5.1.1 Flagella

C. jejuni flagellin is thought to act as an adhesin for epithelial cells whilst motility is a virulence factor for C*. jejuni* (Guerry, 2007). FlaA and FlaB are the major and minor flagellins respectively and highly homologus (Guerry et al., 1991). A study reported that a flagellated and non-motile (*flaA flaB*$^{+}$ *Mot*$^{-}$*) C. jejuni* mutant showed similar ability in adherence to INT 407 cells when compared to a non-flagellated and non-motile (*flaA flaB Mot*$^{-}$) mutant. However, the *flaA flaB Mot*$^{-}$ mutant showed a reduction in invasion compared to the *flaA flaB*$^{+}$*Mot*$^{-}$ mutant (Grant et al., 1993). In addition, both mutants were inhibited in the ability to translocate across Caco-2 monolayers compared to control strains. This data suggests that *C. jejuni* flagella play a role in internalisation but not in adherence to epithelial cells (Grant et al., 1993). FlaC has sequence homology to the N- and C-terminal regions of the FlaA and FlaB flagellins but lacks the central domain (Song et al., 2004). However, a study showed that FlaC binds to Hep-2 cells and *flaC* mutants show a reduction in invasion of epithelial cells (Song et al., 2004).

1.5.1.2 PEB1A

One of the first proteins identified to play a role in *C. jejuni* adherence was PEB1A. PEB1A is a periplasmic binding protein component of an ABC transporter. PEB1A is a 28 kDa common antigen highly conserved and found in all *C. jejuni* and *C. coli* strains (Pei and Blaser, 1993, Pei et al., 1998). PEB1 from *C. jejuni* 81-176 wild-type strain was suggested to be involved in binding to intestinal cells and also in transporting amino acids, hence the suggestion of a dual function (Pei and Blaser, 1993). In another study, colonisation studies in a mouse model with a *peb1A* mutant showed a reduction in the rate and the duration of colonisation significantly lower and shorter compared to the wild-type strain (Pei et al., 1998). Peb1 in the *C. jejuni* F38011 wild-type strain was also reported to play a role *in vivo* in colonising broiler chicks (Flanagan et al., 2009). However in another study, a 81-176 *peb1A* mutant was reported to show no difference in cellular adhesion (Novik et al., 2010).

1.5.1.3 PEB3

PEB3 is a 30 kDa cell surface glycoprotein (Pei and Blaser, 1993) and was shown to be involved in *E. coli* interactions with host cell receptors (Batisson et al., 2003). PEB3 is required for binding of the *C. jejuni* 11168H wild-type strain to immobilised soya bean agglutinin (SBA) lectin (Rubinchik et al., 2014). Although the mutation of *peb3* in *C. jejuni* 11168H wild-type strain resulted in a reduced binding, this was restored by complementation. In addition, it was also suggested that other *C. jejuni* glycoproteins may be involved in adhesion to host cells. However in another study, PEB3 was found to play more of a role as a transport protein (Min et al., 2009). In this study, the PEB3 structure was shown to have some homology to transport proteins and linked to 3-phosphoglycerate (3-PG) utilisation.

PEB4 was thought initially to function as adhesion (Asakura et al., 2007), however a recent study demonstrated that PEB4 is a chaperone that transports other proteins such as CadF to the outer membrane (Kale et al., 2011).

1.5.1.4 CapA

In the genome of *C. jejuni* NCTC 11168, CapA (Campylobacter adhesion protein A) was identified as putative autotransporter protein (Ashgar et al., 2007). CapA was identified as an outer membrane protein of 116 kDa and the presence of a lipid attachment site suggested that CapA is also a lipoprotein. A *capA* mutant exhibited reduced adhesion to and invasion of Caco-2 cells (Ashgar et al., 2007). CapA has also been reported to play a role in the ability of *C. jejuni* to colonise chickens. The ability of *capA* mutants to colonise and persist in chickens was reduced (Ashgar et al., 2007, Jin et al., 2001). Further, *C. jejuni* CapA was reported to play a significant role in adherence to chicken epithelial cells *in vitro* (Flanagan et al., 2009).

1.5.1.5 Type VI Secretion System

Recent studies have reported that some *C. jejuni* strains possess a functional type VI secretion system (T6SS) which plays roles in survival against bile salt (deoxycholic acid (DCA)) stress and also in adherence and invasion of host cells (Lertpiriyapong et al., 2012). The T6SS was demonstrated to play an important role in *C. jejuni* ability to bind to T84 cells and murine RAW 2657.7 macrophages (Lertpiriyapong et al., 2012). Interestingly however, the T6SS was demonstrated to have opposing functions in survival and in interactions with host cells. For survival, the T6SS was 'not required'; as a T6SS mutant was able to resist the effect of DCA compared to the wild-type strain. When *C. jejuni* was exposed to DCA, *cmeA* was up-regulated in the wild-type strain but not in the T6SS mutant and as a result wild-type proliferation was inhibited. In contrast, during interactions with host cells, the T6SS was 'required'; as a T6SS mutant showed reduced adherence to and invasion of T84 cells *in vitro* and also reduced ability to colonise mice *in vivo.* When T84 cells were infected with *C. jejuni*, a haemolysin co-regulated protein was over-expressed in the wild-type strain, but not in the T6SS mutant and as a result the adherence and invasion abilities of the T6SS mutant was reduced. Furthermore, when *C. jejuni* was inoculated into B6.129P2-IL-10 mice, the T6SS mutant demonstrated a reduced ability to colonise compared to the wild-type strain (Lertpiriyapong et al., 2012).

1.5.1.6 JlpA

C. jejuni lipoprotein A (JlpA) is a novel surface-exposed lipoprotein, which has a molecular mass of 42.3 kDa and 372 amino acids residues. JlpA is released by the *C. jejuni* TGH9011 strain into culture media. This study by Jin *et al.* also showed that JlpA has a lipoprotein processing site at the N-terminus. JlpA was easily extracted from OMVs using detergents such as Triton X-100. The mutation of *jlpA* by insertion and deletion was shown to reduce binding to Hep-2 cells compared to that of the TGH9011 wild-type strain (Jin et al., 2001). In contrast, in other studies, *jlpA* mutants were observed to be able to bind to T84 cells at levels similar to the wild-type controls (Novik et al., 2010). A further study by Flanagan *et al.* reported that *jlpA* mutants can colonise broiler chickens and bind to chicken

hepatocellular carcinoma epithelial cells (LMH) as efficiently as the wild-type strain (Flanagan et al., 2009). JlpA is highly conserved in *C. jejuni* and also identified in the genomes of *C. coli* RM 2228, *C. lari* RM2100 and *C. upsaliensis* RM3195 (Jin et al., 2001). The crystal structure showed that JlpA was composed of a single domain of a large β-sheet in the middle with 11 α-helices (Kawai et al., 2012). However, results from the study above demonstrated that the impact of JlpA on adhesion may be strain dependent and also the type of cells used that results in the inconsistency in the published data.

1.5.1.7 MOMP

A *C. jejuni* major outer membrane protein (MOMP) is encoded by the *porA* gene (Islam et al., 2010) and has been shown to bind to ECM components such as fibronectin (Moser et al., 1997). A 42 kDa MOMP in *C. jejuni* 10945 was shown to bind to INT 407 cells (Moser et al., 1997, Schroder and Moser, 1997). Recently, an O-linked glycosylated MOMP in NCTC 11168 was shown to bind to histo-blood group antigens (BsAgs) and also adhere to host cells. In this study, a 45 kDa MOMP was reported to promote cell to cell adhesion, adherence to Caco-2 cells, promote biofilm formation but was also required for optimal colonisation of chickens (Mahdavi et al., 2014).

1.5.1.8 PldA

Phospholipase A is a 35 kDa outer membrane protein. A *pldA* mutant showed reduced ability to colonised chicks ceacum (Ziprin et al., 2001). Another study suggested that PldA played role in *C. lori* virulence (Grant et al., 1997).

1.5.1.9 pVir

Some strains of *C. jejuni* carry a plasmid termed pVir which is 37 kb in size (Guerry et al., 2000). The *C. jejuni* 81-176 strain but not the NCTC 11168 strain contains pVir. pVir expresses proteins that show some homology to T4SS transport

proteins. Mutations of two of the pVir genes encoding ComB3 and VirBII that are involved in natural transformation and protein transport respectively, significantly reduced *C. jejuni* 81-176 wild-type strain adherence to and invasion of INT 407 (Bacon et al., 2000).

1.5.1.10 CadF and FlpA

Probably the most established adhesion proteins and also the most highly conserved in *C. jejuni* are Campylobacter adhesion to fibronectin (CadF) (Konkel et al., 1997) and Fibronectin-like protein A (FlpA) (Flanagan et al., 2009). Both proteins are able to bind to fibronectin on host cell membranes that could possibly provide a linkage platform towards bacterial invasion (Eucker and Konkel, 2012). CadF and FlpA are described in more detail in Section 1.7.1 and 1.7.2 respectively.

Table 1. 1. *C. jejuni* virulence factors reported to be involved in adhesion to intestinal epithelial cells.

Virulence factor(s)	Encoding gene(s)	References
CadF, outer membrane protein	*cadF*	(Konkel et al., 1997)
CapA, Campylobacter adhesion protein A	*capA*	(Jin et al., 2001)
Phospholipase A	*pldA*	(Ziprin et al., 2001, Dekker, 2000)
JlpA, lipoprotein involved in adhesion to Hep-2 cells	*jlpA*	(Jin et al., 2001)
PEB1, periplasmic binding protein	*peb1A*	(Pei and Blaser, 1993)
PEB3, transport protein	*peb3*	(Min et al., 2009)

PEB4, chaperone playing an important role in exporting proteins to the outer membrane	*peb4*	(Kale et al., 2011)
FlpA, fibronectin–like protein	*flpA*	(Flanagan et al., 2009)
Type IV secretion system possibly involved in adhesion	*virB1*	(Bacon et al., 2000, Dasti et al., 2010)

Reported *C. jejuni* adhesion factors reproduced from (Bolton, 2015).

1.5.2 *C. jejuni* invasion mechanisms

Invasion of *C. jejuni* into IECs is well established as a result of many studies (Konkel et al., 2013, Kopecko et al., 2001). These studies have shown that *C. jejuni* is able to penetrate the IECs mucosal layer resulting in successful colonisation and invasion of IECs (Backert et al., 2013, Boehm et al., 2012, Corcionivoschi et al., 2009). In studies using microscopy, *C. jejuni* was observed to invade polarised cells such as Caco-2 IECs *in vitro* from the baso-lateral surface (Bouwman et al., 2013), where once internalised the bacteria will move towards the apical surface. Many routes of entry into intestinal cells have been reported for *C. jejuni*. Some are dependent on MTs and MFs (Kopecko et al., 2001, Monteville et al., 2003, Hu and Kopecko, 1999); others are independent of both (Bouwman et al., 2013). Table 1.2 shows virulence factors reported to be involved in *C. jejuni* invasion into host cells.

Table 1.2. *C. jejuni* virulence factors reported to be involved in invasion of intestinal epithelial cells.

Virulence factor(s)	Encoding gene(s)	References
FlhA, FlhB, FliQ, Flip,FliO & FliR, components of the flagellar Type III secretion system	*flhA, flhB, fliQ, flip,fliO & fliR*	(Carrillo et al., 2004)
FlaC, essential for colonisation and invasion	*flaC*	(Konkel et al., 2004, Carrillo et al., 2004)
CiaB, involved in adhesion	*ciaB*	(Konkel et al., 2004)
CiaC, required for full invasion of INT 407 cells	*ciaC*	(Eucker and Konkel, 2012)
CiaI, plays a role in intracellular survival	*ciaI*	(Buelow et al., 2011)
IamA, invasion associated protein	*iamA*	(Rivera-Amill et al., 2001)
HtrA, protease involved in the proper folding of adhesins, cleaves E-cadherin	*htrA*	(Baek et al., 2011, Elmi et al., 2016)
VirK, may have a role in protection against antimicrobial proteins	*virK*	(Novik et al., 2009)
FspA, role in apoptosis	*fspA*	(Poly et al., 2007)

Proteins reported to be associated with *C. jejuni* invasion of IECs. Reproduced from (Bolton, 2015).

1.5.2.1 CiaB

C. jejuni does not possess a T3SS like other enteropathogenic bacteria such as *E. coli*, *Salmonella* and *Shigella* to directly inject effector proteins into host cells. However, *C. jejuni* can utilise the flagellar apparatus to function as a secretion system to secrete virulence proteins into surrounding environments (Konkel et al., 2004). These proteins are termed *Campylobacter* invasion antigens (Cia) and have been identified to play a role in the invasion of and intracellular survival within host cells (Konkel et al., 1999b, Rivera-Amill and Konkel, 1999, Konkel et al., 2004). CiaB was reported to be important for internalisation of C*. jejuni* into INT 407 cells (Konkel et al., 1999c). A *ciaB* mutation in *C. jejuni* F38011 wild-type strain resulted in a non-invasive phenotype (Rivera-Amill and Konkel, 1999). However, Novik *et al* showed that *C. jejuni* 81-176 *ciaB* mutant does not exhibit reduced invasion into T84 cells (Novik et al., 2010).

1.5.2.2 CiaC

CiaC has been reported to play a role in *C. jejuni* invasion into INT 407 cells. The study showed that CiaC was delivered into the host cytosol upon *C. jejuni* adhering to epithelial cells via a flagellar hook complex that consisted of FlgE, FlgK and FlgL. Furthermore, the genes encoding the Cia proteins are up-regulated during *C. jejuni* infection of INT 407 cells. In addition, CiaC is also involved in host cell cytoskeleton rearrangements and causes membrane ruffling via activation of Rac1. However, a *flgL* mutant was not able to induce membrane ruffles in INT 407 cells (Neal-McKinney and Konkel, 2012, Eucker and Konkel, 2012).

1.5.2.3 CiaD

CiaD is another a Cia effector protein identified in 2013 (Samuelson et al., 2013). The study reported that CiaD activated host cell MAP kinase signalling pathways

that involved p38 and Erk1/2. Activation of these pathways promotes invasion by *C. jejuni* and release of IL-8 from the host cell (Samuelson et al., 2013).

1.5.2.4 CiaI

CiaI was reported to be involved in *C. jejuni* intracellular survival as a *ciaI* mutant exhibited reduced survival in INT 407 compared to the wild-type strain. In addition, epithelial cells infected with a *ciaI* mutant showed the Campylobacter-containing vacuole (CCV) to be more frequently co-localised with a lysosomal marker (Cathepsin D) compared to the cells infected with the wild-type strain (Buelow et al., 2011).

1.5.3 Translocation

Translocation is a virulence mechanism employed by pathogens to enable dissemination in the host cells. Enteropathogens such as *Salmonella*, *Shigella* and *Listeria* traverse host IECs using different translocation mechanisms including transcytosis of enterocytes or M cells and phagocytosis (Bras and Ketley, 1999). Transcytosis is apical endocytosis followed by basolateral exocytosis (Hu et al., 2008). Although translocation in *C. jejuni* was suggested to involve passing both across and between cells, this is still not confirmed. However, studies suggest that penetration of the intestinal mucosa by *C. jejuni* may be the cause of inflammation and enteritis disease (Black et al., 1988, Blaser et al., 1983).

IECs grown on Transwell filters can form polarised monolayers and exhibit characteristics of normal small intestine epithelial cells. Polarised cells exhibit a defined brush border and TJs that separate apical and baso-lateral surfaces which form a permeability barrier (Konkel et al., 1992c, Finlay and Falkow, 1990). These cells have been used in many studies to investigate the pathogenic potential in crossing cell barriers (Finlay and Falkow, 1990, Grant et al., 1993, Boehm et al., 2012). Bacteria passing through IECs is termed the transcellular route and will not interrupt TEER. Bacteria passing between cells is termed the paracellular route

(Figure 1.4). In the paracellular pathway, TEER will decrease as a result of disruption of TJs and AJs caused by bacterial invasion. Some studies have shown data that supports *C. jejuni* translocation across IECs through the transcellular pathway while other studies have shown data that supports the paracellular pathway (Boehm et al., 2012, Monteville and Konkel, 2002, Wine et al., 2008, Louwen et al., 2012).

C. jejuni translocation has been shown to be time-dependent and reached a maximum rate 4 h post-infection. This study also indicated that low temperature inhibited *C. jejuni* adherence to, invasion of and translocation across Caco-2 cells (Konkel et al., 1992c). Flagella are suggested to play a role in translocation because a study showed that non-flagellated non-motile *C. jejuni* mutants were not able to translocate across polarised Caco-2 cells compared to the wild-type strains. However, the non-flagellated non-motile mutants were found to adhere to INT 407 cells equally as well as flagellated non-motile mutants (Grant et al., 1993).

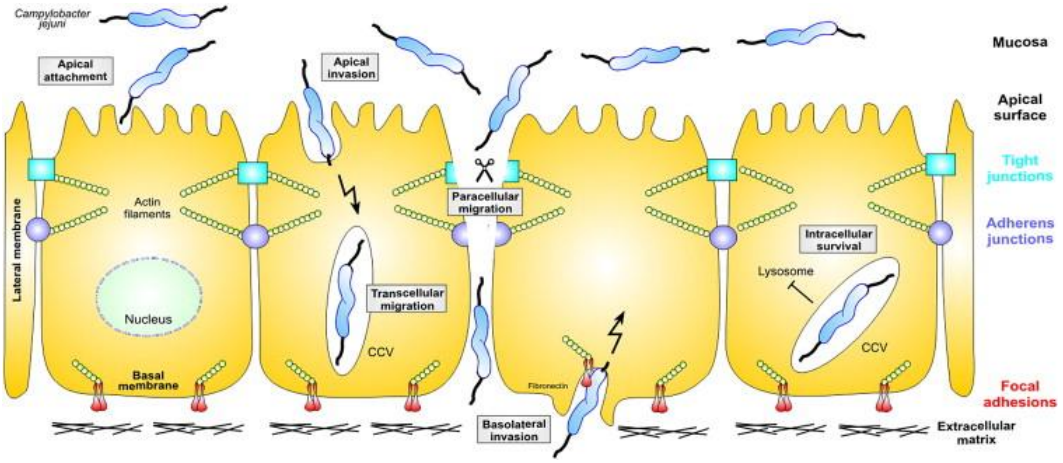

Figure 1.5. Hypothetical model for *C. jejuni* transmigration across intestinal epithelial cells. Polarised cells such as Caco-2 and T84 exhibit defined apical and baso-lateral surfaces with TJs and AJs that provide tight monolayers when grown on a Transwell filter membrane. *C. jejuni* is suggested to use transcellular or paracellular routes or both to translocate into the lamina propria. Reproduced from (Backert and Hofreuter, 2013).

1.6 Intracellular survival

Several studies have investigated the fate of *C. jejuni* after entering the host cell. In an earlier study, *C. jejuni* wild-type strains 2964 and 1702 were observed to be phagocytosed more successfully by human monocytes compared to murine macrophages (Kiehlbauch et al., 1985). The internalised *C. jejuni* appeared to be inside a vacuole, either as a single spiral bacterium or a mixture of spiral and coccoid bacteria in a larger vacuole. Once phagocytosed, *C. jejuni* changes shape from spiral to coccoid within 4 h to 6 h compared to within 24 h in controls (Kiehlbauch et al., 1985). Also in that study, *C. jejuni* was observed to survive intracellularly for up to 7 days, whereas a later study reported *C. jejuni* can only survive up to 48 h (Bouwman et al., 2013).

In another study using Hep-2 cells, a strong lysosomal response was observed following invasion by *C. jejuni* (De Melo et al., 1989). Endosome-lysosome fusion was observed with acid phosphatase activity evident at the surface of the internalised bacteria, most of which then showed signs of degradation by changing to a coccoid form. A gentamicin protection assay indicated that bacterial viability declined after 6 h, with few bacteria remaining viable after 36 h. *C. jejuni* were also found in INT 407 cells up to 96 h post-inoculation if gentamicin treatment was reduced in steps and electron microscopy confirmed the presence of viable intracellular *C. jejuni* (Konkel et al., 1992b). Removal of the antibiotic resulted in a cytopathic effect after 48 h, which was coincident with an increase in extracellular bacteria.

The bacterial and host factors important in determining the fate of intracellular *C. jejuni* are not clearly understood. Endosome acidification may not play a role as inhibition of acidification with monensin did not affect intracellular survival (Oelschlaeger et al., 1993). Reduction of the short-term intracellular survival in INT 407 cells of a *C. jejuni sodB* mutant when compared to the wild-type strain, indicates that reactive oxygen species influence intracellular survival (Pesci et al., 1994, Purdy and Park, 1994). The identification of a catalase KatA (Grant and Park, 1995) indicated that *C. jejuni* may have other determinants that form part of a defence system against oxidative stress as catalase was suggested to play a role in intracellular survival (Day et al., 2000). Interestingly, oxidative stress can increase the invasive potential of *C. jejuni* (Harvey and Leach, 1998). *C. jejuni* may not necessarily remain within membrane-bound vacuoles in the cytoplasm of tissue culture cells (Konkel et al., 1992a) although some reports did not observe

cytoplasmic bacteria (Oelschlaeger et al., 1993) (Konkel and Cieplak, 1992). In other studies, free *C. jejuni* within the cytoplasm were observed and were associated with a cytopathic effect (Ketley, 1997, Russell et al., 1993).

In a study in 2008, *C. jejuni* was found to co-localise in a membrane-bound compartment (Watson and Galan, 2008). The compartment was termed the Campylobacter-containing vacuole (CCV) as it contains and is induced by *C. jejuni* bacteria just like previous studies that had observed *C. jejuni* inside a vacuole once internalised in host cells (Kiehlbauch et al., 1985, Konkel et al., 1992b, Hickey et al., 2005). By residing in this CCV, *C. jejuni* avoids being lysed by lysosome because the CCV somehow follows a different pathway instead of the lysosomal one (Watson and Galan, 2008). This phenomenon can also be seen with the Salmonella-containing vacuole (SCV) created by *Salmonella* upon entry into intestinal cells (Finlay et al., 1988, Steele-Mortimer, 2008, Knodler and Steele-Mortimer, 2003, Steele-Mortimer et al., 2002, Steele-Mortimer et al., 2000). However, one study has shown that *C. consicus* co-localised with the autophagosome, which has a double membrane that subsequently will fuse with the lysosome for the continuing process of lysing the engulfed bacteria (Burgos-Portugal et al., 2014).

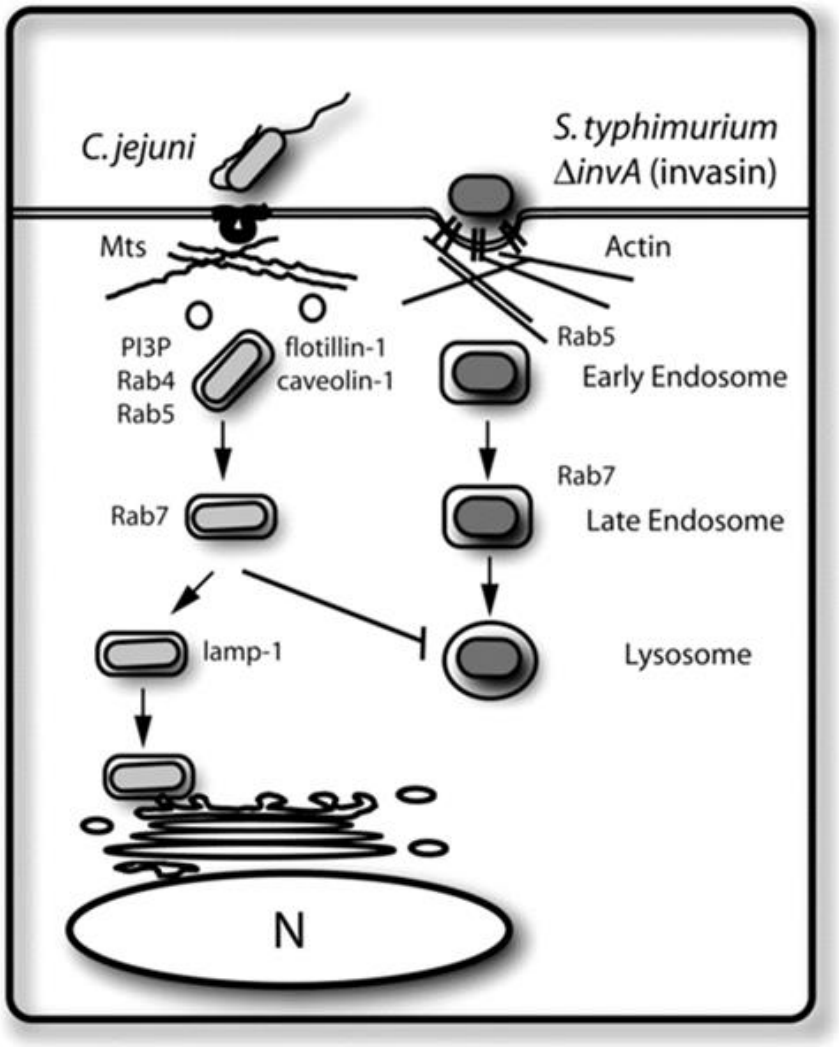

Figure 1.6. Schematic model of *C. jejuni* intracellular survival within IECs. Following internalisation, *C. jejuni* resides in a CCV. The CCV has different markers from the markers for endocytic pathways, and is prevented from lysis by lysosome. Reproduced from (Watson and Galan, 2008).

To date, many studies have shown that *C. jejuni* resides in a CCV and that being within that CCV or phagocytosed increases the intracellular survival of *C. jejuni* and may result in successful replication within the cells (Figure 1.5).

1.7 Outer membrane vesicles

C. jejuni lacks the specific virulence-associated secretion systems of other enteric pathogens such as T3SS and T4SS, so an alternative method to deliver virulence factors is using outer membrane vesicles (OMVs). OMVs were first thought of as an artefact of bacterial growth. Since that initial discovery, it has become evident that almost all Gram-negative bacteria produce OMVs as part of their normal growth. Many pathogenic bacterial species have been reported to produce OMVs include *E. coli, Shigella* species, *Salmonella* species (Bae et al., 2014, Elhenawy et al., 2016), *Helicobacter pylori* (Turner et al., 2015, Fiocca et al., 1999), *Vibrio* species (Chatterjee and Chaudhuri, 2011), *Pseudomonas aeruginosa* (Bomberger et al., 2009, Bauman and Kuehn, 2006), *Yersinia pestis* (Eddy et al., 2014) and *C. jejuni* (Elmi et al., 2012, Lindmark et al., 2009, Jang et al., 2014).

1.7.1 Biogenesis and composition of OMVs

Most Gram-negative bacteria release OMVs (Bauman and Kuehn, 2006) and in all phases of growth (McBroom and Kuehn, 2005, Mayrand and Grenier, 1989). This was first observed when a cell free filtrate of *Vibrio cholera* was able to trigger an immune response in rabbits (Kulkarni and Jagannadham, 2014). OMVs were suspected to contain the immunogenic properties of the Outer Membrane (OM) components of Gram-negative bacteria that could somehow manage to leach into the medium. OMVs are now known to play roles in secreting virulence factors that increase bacterial survival in host cells (Kuehn and Kesty, 2005).

Both Gram–negative pathogenic and non-pathogenic bacteria are known to release extracellular membrane–bound vesicles (Kulkarni and Jagannadham, 2014) that have a size range from 20 to 500 nm (Kulp and Kuehn, 2010). OMVs are formed from a ‘pinched’ section of the OM (Klimentova and Stulik, 2015). OMVs are also known by other names such as ‘membrane vesicles’, ’blebs’ or ‘outer membrane fragments’ (Ellis and Kuehn, 2010, Kulp and Kuehn, 2010). OMV production can be triggered when cross-linking between peptidoglycan and the OM is reduced. OMVs are released to relieve the turgor pressure exerted by PG during cell wall synthesis (Rolhion et al., 2005). Other suggested mechanisms for OMVs formation are increased phosphoslipids in OM, LPS and other proteins

result in curvature and leads to vasculation of OMVs from the OM. OMVs are not a product of cell lysis as they contain newly synthesised proteins. Bacteria produce OMVs on solid media, in liquid culture and during intracellular infections, also within biofilms (Klimentova and Stulik, 2015, Unal et al., 2011, Bjerre et al., 2002). Maximum OMV production was shown during exposure to physical and chemical stresses, as well as during the late log phase of bacterial growth (McBroom and Kuehn, 2007, Klimentova and Stulik, 2015). Other studies showed temperature, antibiotics and lack of nutrients increased release of OMVs by bacteria (Klimentova and Stulik, 2015, Collins, 2011). OMV composition and production can change as a result of host-pathogen interactions (Kuehn and Kesty, 2005).

Generally, OMVs have similar components as the OM (Figure 1.6). OMVs have lipo-polysaccharides (LPS), phospholipids, peptidoglycan, outer membrane proteins (OMPs), proteins originating from periplasmic, cytoplasmic and membrane bound compartments, nucleic acids (DNA and RNA), ion metabolites, signalling molecules and cell wall components (Lindmark et al., 2009, Vanaja et al., 2016, Koeppen et al., 2016).

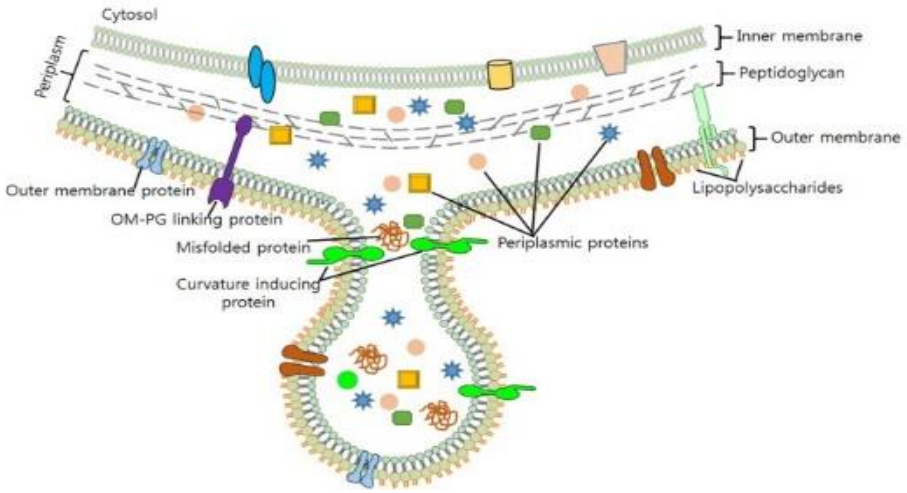

Figure 1.7. Biogenesis of OMV production in Gram-negative bacteria. The OMVs composition reflects OM protein components such as LPS, glyserophospholipids, enclosed periplasmic components as well as OM proteins. Reproduced from (Jan, 2017).

1.7.2 Functions of OMVs

With such a diverse composition from many aspects of cell interactions, OMVs will also have diverse functions depending on their composition. OMV roles can be offensive to the host cell or defensive to the bacterial cell as well as a tool for delivery of various effector molecules (Jan, 2017). OMVs have numerous functions that contribute to bacterial pathogenesis such as delivering bacterial virulence factors to host cells (Klimentova and Stulik, 2015), acting as metabolite and small molecule transporters, secreting toxins, as stress response mechanism promoters (McBroom and Kuehn, 2007), as a decoy or weapon for bacteriophages and initiation of biofilm formation (Yonezawa et al., 2009).

OMVs act as delivery vehicle in *P. aeruginosa* to transport virulence factors such as β-lactamase, alkaline phosphatase, haemolytic phospholipase C and Cif. Fusion of the OMVs with lipid rafts in the plasma membrane facilitate virulence molecule entry directly into the host cytoplasm (Bomberger et al., 2009). *H. pylori* has also been reported to use OMVs to secrete the vacuolating cytotoxin VacA (Fiocca et al., 1999).

It was hypothesised that *C. jejuni* may use OMVs to deliver bacterial virulence factors which promote the interaction with and invasion of IECs, as well as the modulation of the host response (Elmi et al., 2012, Klimentova and Stulik, 2015). One of the potent virulence mechanisms is vesicle-mediated toxin delivery. The CDT toxin including all subunits (CdtA, CdtB and CdtC) was found to be released by *C. jejuni* OMVs to the surrounding environment in infected host tissues (Lindmark et al., 2009). OMVs are reported to elicit inflammatory responses from infected host cell. OMVs from *P. aeruginosa* induced a significant IL-8 response from lung epithelial cells (Bauman and Kuehn, 2009).

As a general stress response, OMVs have been found to be secreted more when the bacteria are under environmental stress (Klimentova and Stulik, 2015, McBroom and Kuehn, 2007). In non-pathogenic bacteria, the OMVs play protective roles by secreting properties that reduce toxic compound levels in the surrounding environment (Kuehn and Kesty, 2005). However, non-pathogenic bacteria produce less OMVs compared to pathogenic bacteria (Horstman and Kuehn, 2002).

OMVs have many prospective applications such as drug delivery vehicles, communication tools, secretory systems, vaccines and adjuvants. Due to that, OMVs have the potential to become an agent for vaccine production.

1.7.3 *C. jejuni* outer membrane vesicles

C. jejuni produces OMVs (Elmi et al., 2012). OMVs isolated from *C. jejuni* were shown to have different functions as described above. Proteomic analysis of *C. jejuni* OMVs isolated from the 11168H strain identified 151 proteins that included all three components of CDT (CdtA, CdtB and CdtC), the HtrA and Cj0511 proteases, 16 *N*-linked glycoproteins including the major antigenic protein PEB3 (Elmi et al., 2012). The fibronectin binding proteins CadF and FlpA were also identified in 11168H OMVs (Elmi et al., 2012) and in 81-176 OMVs (Watson et al., 2014). In another study, proteomic analysis of OMVs from the C*. jejuni* NCTC 11168 wild-type strain identified 134 vesicular proteins including some N-glycoproteins (Jang et al., 2014).

C. jejuni OMVs can trigger host innate immune responses from human T84 cells (Elmi et al., 2012). *C. jejuni* OMVs trigger production of IL-8, IL-6, TNF-α and hBD-3 in a dose-dependent manner. IL-8 production depends on the concentration of 11168H OMVs incubated with T84 cells. However, pre-treatment of host cells with methyl-beta-cyclodextrin prior to co-incubation with OMVs, resulted in a reduction in induction of IL-8, IL-6 and TNF-α (Elmi et al., 2012). This suggests that OMV entry into T84 cells is partially dependent on intact lipid rafts that require a cholesterol-rich microdomain. Studies have also shown a *C. jejuni* mutant lacking the CDT toxin exhibits reduced ability to induce IL-8 (Hickey et al., 2000), however other studies have shown OMVs isolated from a *cdtA* mutant induce IL-8 production to the same extent as wild-type OMVs, suggestive that IL-8 production by OMVs is CDT-independent (Elmi et al., 2012).

OMVs are also cytotoxic to cell lines as seen after Caco-2 cell exposure to OMVs which results in an increase of extracellular LDH released by the cells. Using *G. mellonella* as a model of *C. jejuni* infection showed that OMVs caused mortality to infected *G. mellonella* larvae. However, heat-treated OMVs showed reduced cytotoxicity in infected larvae (Elmi et al., 2012).

In another study, OMVs isolated from the 81-176 strain were shown to play a role in adhesion and biofilm formation. In this study, the outer and inner membranes of 81-176 were analysed. In addition CadF was up-regulated and a *cadF* mutant showed reduced adhesion to inert surfaces in oxygen-enriched conditions (19% O_2) (Sulaeman et al., 2012).

Recently OMVs isolated from the 81-176 wild-type strain were shown to have protective properties in chicks challenged with *C. jejuni* by reducing ceacal colonisation. CjaA is a glycosylated extracytoplasmic highly immunogenic protein and conserved in different Campylobacter serotypes (Godlewska et al., 2016). In this study, OMVs from the 81-176 wild-type strain and OMVs that contained a high amount of CjaA were used as a vaccine in 18 day old chicken embryos. The immunisation showed a significant effect a week after infection, but this effect was short lived and was lost 2 weeks after infection (Godlewska et al., 2016).

1.8 *Galleria mellonela* model of infection

The human and insect immune systems, both humoral and cellular, share many similarities (Harding et al., 2013, Senior et al., 2011, Hoffmann, 1995). These include humoral immune responses via antibacterial peptides, coagulation, melanisation and production of reactive oxygen species (ROS), as well as cellular responses via the process of encapsulation and phagocytosis (Lavine and Strand, 2002). Even though insect immune systems lack an acquired immune system mediated by B and T lymphocytes, insects have a well-developed innate immune system that reacts rapidly to infectious agents (Lavine and Strand, 2002). Insects have cells known as haemocytes that function to phagocytose pathogens and form aggregates that encapsulate and neutralise bacteria. Insect haemolymph detects LPS from bacteria and results in a rapid coagulation response. In addition, haemolymph also contains inhibitors and antibacterial peptides which are produced and released to eliminate the bacteria (Hoffmann, 1995). Foreign antigens are recognised by receptors on haemocyte surfaces or through opsonisation. Activation of the haemocytes will trigger a phenoloxidase (PO) which results in melanisation and production of anti-microbial compounds (Senior et al., 2011, Lavine and Strand, 2002). Melanisation is an important cellular mechanism as a result of phagocytosis and encapsulation. The melanogenesis in insects produces cytotoxic molecules which are capable to interact with ROS, thus providing an effective immune response against foreign invaders (Nappi and Christensen, 2005).

Many studies have established a good correlation between insect infection and the pathogenicity of several microorganism such as *Listeria* species*, Legionella*

species*, Streptoccoccus pyogenes* and several pathogenic fungi (Harding et al., 2012, Mukherjee et al., 2010).

Although several animal models have been used in *Campylobacter* research including primates (Russell et al., 1993), ferrets (Yao et al., 1997), mice (Watson et al., 2007), piglets (Babakhani and Joens, 1993), chicks (Flanagan et al., 2009, Nachamkin et al., 1993) and chick embryos (Field et al., 1986), all come with limitations and showed limited success (Chang and Miller, 2006). An alternative needed to be found and due to the lack of a convenient small animal model available to study *C. jejuni* pathogenesis, investigators turned to the use of insects as a model of infection.

Galleria mellonella larvae are from the greater wax moth. The larvae are bred as live food for domestic reptiles and readily available commercially. Some of the advantages of using *G. mellonella* larvae include: 1. Easy to maintain as feeding is minimal, usually the wood chips that come with the box suffice; 2. Larvae can survive and be kept at 37^{o}C before and during infection; 3. The larvae are small around 1-2 cm long so easy to handle; 4. Larvae can live for up to 3 weeks before turning into pupae; 5. Injection of a bacterial inoculum can be performed without anaesthetic (Harding et al., 2012) but simply by putting the larvae on ice for 20 minutes renders them easy to handle. *G. mellonella* larvae have been used to study many aspects of pathogenesis such as cytotoxicity and antibiotic toxicity. *G. mellonella* larvae have become widely adopted as an insect model of infection to study a wide range of bacteria such as *Yersinia pseudotuberculosis* (Champion et al., 2009), *Legionella pneumophilla* (Harding et al., 2013), *Listeria monocytogenes* (Mukherjee et al., 2010), *Shigella* (Barnoy et al., 2017), *E. coli* (Heitmueller et al., 2017) and *C. jejuni* (Champion et al., 2010). Larvae of *G. mellonella* have been shown to be susceptible to *C. jejuni* infection as previously described (Champion et al., 2010, Senior et al., 2011). Some studies have even successfully recovered *C. jejuni* 24 h post-infection (Senior et al., 2011).

1.9 Role of the fibronectin binding proteins

Fibronectin is a non-integral protein found on the surfaces of cells and in the extracellular matrix (ECM) (Henderson et al., 2011). Fibronectin is an essential large multi-domain glycoprotein that functions as a host adhesion (Pankov and

Yamada, 2002). Fibronectin links the cell through integrins to the extracellular environment, thus becoming a common major target for bacterial pathogens (Pankov and Yamada, 2002). Fibronectin also binds to many biologically important molecules including collagen, heparin and fibrin. In addition, fibronectin plays important roles in cell development such as growth, differentiation, adhesion and transmigration (Pankov and Yamada, 2002).

Fibronectin is a major component of the ECM of epithelial cells. Fibronectin is a dimer of two very similar 220 kDa subunit glycoproteins linked by a pair of disulphide bonds present at regions of cell-to-cell contact between IECs (Konkel et al., 2010, Pankov and Yamada, 2002). Each monomer has three types of repeating units (Fibronectin repeats): type I, type II or type III. Type I contains two disulphide bonds and is about 40 amino acids in length; type II contains two intra-chain disulphide bonds and is about 60 amino acids in length; type III has no disulphide bonds but is about 90 amino acids in length. Almost 90% of fibronectin sequences are made up of 12 type I repeats, 2 type II repeats and 15-17 type III repeats (Pankov and Yamada, 2002).

Fibronectin acts as an adhesion molecule that anchors cells to ECM components via molecules called integrins. Integrins are cell-surface receptors that link the intracellular cytoskeleton to the ECM. Fibronectin acts as a ligand for many integrin receptors including the fibronectin classic receptor α5β1. The location for α5β1 binding receptor can be found at $FnIII_9$ and $FnIII_{10,}$ FnI_{1-9} and $FnII_{1-2}$ (Pankov and Yamada, 2002). Many cellular interactions including tissue repair, blood clotting and cell migration and adhesion are facilitated by fibronectin.

Cells rely on the surface protein fibronectin to interact with the cells surroundings, but many pathogens can also bind to this molecule and hijack the host cell signalling pathway mechanisms for the bacteria's advantage (Cossart and Sansonetti, 2004). The binding to fibronectin will trigger signal molecular pathways and result in subsequent formation of focal adhesion complexes that rearrange the cytoskeleton of the cells and that allow bacterial uptake by the host cells. During the infectious process, *C. jejuni* must interact with receptors of the human IECs. It was suggested that the ability of *C. jejuni* to bind to fibronectin increases the probability of bacterial virulence proteins to come into closer contact with host cell factors and promote bacterial internalisation (Konkel et al., 1992c). There are numerous *C. jejuni* proteins that mediate the interaction between the multiple components of the IECs including fibronectin. The two most characterised are

Campylobacter adhesion to fibronectin (CadF) and Fibronectin-like protein A (FlpA) (Konkel et al., 2010, Konkel et al., 1999c). Substantial evidence exists that mutation of *C. jejuni cadF* or *flpA* results in a reduction in host cell invasion (Monteville et al., 2003, Ashgar et al., 2007).

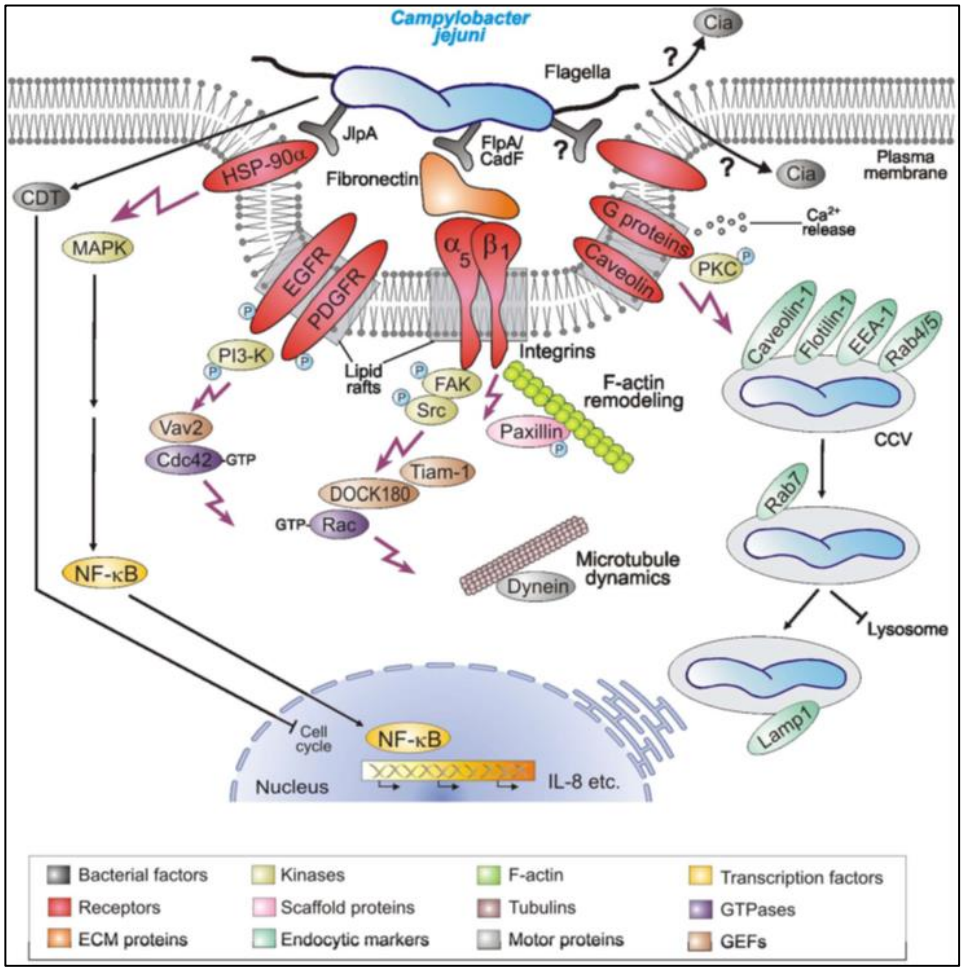

Figure 1.8. Hypothetical model of *C. jejuni* entry into host cell mediated by CadF and FlpA. *C. jejuni* adheres to host cells via numerous reported and unknown factors. Several indicated host cell receptors have been proposed to play a role in the uptake of the bacteria. This potentially causes localised F-actin and/or microtubule rearrangements at the site of *C. jejuni* entry, resulting in engulfment and bacterial uptake. Several indicated host cell signaling molecules and pathways including the intracellular survival in CCVs have been reported in *in vitro* infection models and may play a role during pathogenesis *in vivo*. Reproduced from (O Croinin and Backert, 2012).

1.9.1 CadF

The most extensively characterised C*. jejuni* fibronectin binding protein is CadF. CadF was first identified in 1997 (Konkel et al., 1997). CadF is a member of the microbial surface components recognising adhesive matrix molecules (MSCRAMMs) family. CadF has a molecular mass of 37 kDa and is an outer membrane protein that comprises 106 amino acid residues (Konkel et al., 1997). CadF is highly conserved amongst *C. jejuni* and *C. coli* strains which was initially confirmed by immunoblot analysis of 58 C. *jejuni* isolates of human and animal origin (Konkel et al., 1999a, Krause-Gruszczynska et al., 2007b). *C. jejuni* CadF showed 2 bands at a 37 kDa (p37) and 32 kDa (p32) whilst in *C. lori* the sizes were larger at 39 kDa (p39) and 34 kDa (p34) respectively. Four amino acids at position 134-137 exposed on the surface of *C. jejuni* CadF have been shown to be responsible for the binding to fibronectin (Konkel et al., 2005). *C. coli cadF* has an extra 39 base pair insertion and as a result the binding to fibronectin was inhibited (Konkel et al., 1999a). Infection assays revealed that *C. jejuni* bound and invaded INT 407 epithelial cells much more efficiently than *C. coli* and that this difference was considerably reduced in *C. jejuni cadF* mutants compared to the wild-type strains (Monteville et al., 2003, Monteville and Konkel, 2002). More recent work by Neveda Naz (LSHTM PhD student, Personal communication) has also established that CadF from *C. jejuni* strain 81-176 plays a role in *C. jejuni* adhesion to human IECs (Caco-2 and T84 cells). Substantial evidence exists that mutation of *C. jejuni* adhesin genes results in a reduction in host cell invasion (Monteville et al., 2003, Ashgar et al., 2007). It was shown that CadF was required for maximal adherence to and invasion of INT 407 cells through binding to fibronectin. As a result, the binding activated the paxillin-mediated pathway and transmitted signals that cause cell cytoskeleton rearrangement through microfilament reorganisation (Monteville et al., 2003).

Mamelli *et al.* attempted to purify CadF but this was found to be difficult and time consuming. They managed to purify small amount of CadF protein by extraction using mild detergent from the outer membrane of *C. jejuni* (Mamelli et al., 2006). A structural study analysis of the full length of the *C. lori* CadF was performed. This showed in comparison to the *C. jejuni* maximal fibronectin binding sequences that contain the residues phenylalanine-arginine-leucine-serine (FRLS) (Konkel et al., 2005), *C. lori* CadF had the residues phenylalanine-alanine-leucine-glycine (FALG) instead (Hirayama et al., 2009). In addition, a CadF-like protein in *C. lori*

is 9 amino acids larger than the one in *C. jejuni* (Hirayama et al., 2009). A previous study has also suggested that CadF can be cleaved into smaller polypeptides but still able to bind to fibronectin. However, CadF was shown to be immunogenic as a full length structure, but not as the cleaved variant (Scott et al., 2010).

A recent study reported that CadF was expressed in culture which is viable but non-culturable (VBNC) while incubated in fresh water at 4^{o}C for 48 days. This suggests the potential role of CadF in combating oxidative impact in environmental stress and increased survival (Patrone et al., 2013). In another study, CadF in the *C. jejuni* 81–176 strain was up-regulated in the outer membrane of oxygen-acclimatised cells, and *a* c*adF* mutant showed a reduction in adhesion to inert surfaces compared to the wild-type strain (Sulaeman et al., 2012).

These results demonstrate that CadF is one of the many pathogenicity factors that *C. jejuni* possesses. CadF mediates the binding of *C. jejuni* to fibronectin, promotes bacterium-host interactions, and facilitates the bacterial colonisation of chickens.

1.9.2 FlpA

A second fibronectin binding protein was identified and named FlpA for fibronectin-like protein A (Flanagan et al., 2009). In the study, it was reported that FlpA plays a role in colonising epithelial cells of chicks *in vivo* and a *flpA* mutant showed a reduction in adherence to chicken LMH hepatocellular carcinoma epithelial cells *in vitro* (Flanagan et al., 2009). Another study identified the amino acid sequence of *C. jejuni* NCTC 11168 FlpA (Cj1279c) that contained at least three Fibronectin type III domains which are surface-exposed domains (Konkel et al., 2010, Flanagan et al., 2009). In another study, FlpA was reported to be composed of three Fibronectin III-like repeats D1, D2 and D3, and binds the fibronectin-binding domain via a motif within the D2 repeat (Larson et al., 2013). FlpA binding affinity to fibronectin was reduced compared to CadF as shown by mutation in the *C. jejuni* F38011 strain (Konkel et al., 2010). It was reported that in addition to binding to fibronectin, FlpA also adheres to INT 407 cells. *flpA* mutants showed a reduction in adherence compared to wild-type strain, however, complemented strains restored the *C. jejuni* binding to INT 407 cells (Konkel et al., 2010). Further studies showed that the *flpA* mutant was completely prevented from colonising the chicken epithelium.

Accordingly, *C. jejuni* lacking a functional FlpA proved considerably less virulent than wild-type bacteria in a rodent model of infection, confirming the importance of this interaction.

In a study by Larson *et al.*, a residue of the Fibronectin-binding linear motif (FBLM) was identified in FlpA as a fibronectin binding domain (Larson et al., 2013). In addition, the study also reported that FlpA induced disease in a germ-free mouse model. FlpA is also required for maximal binding to intestinal epithelial cells and was able to activate Erk1/2 (Larson et al., 2013). Further, a *C. jejuni cadF flpA* double mutant was impaired in the activation of epidermal growth factor receptor (EGFR) and Rho GTPase Rac1 (Larson et al., 2013). Although these observations establish a role for fibronectin-binding proteins during *C. jejuni* invasion, their contribution to invasion mechanisms are unclear. Recent studies have highlighted the probability that FlpA and CadF may act collaboratively in targeting fibronectin on host cells (Eucker and Konkel, 2012). The resulting interaction from binding triggers a series of signalling events, including mechanisms that enable bacteria to penetrate the intestinal cell

1.10 Visualisation of *C. jejuni* expressing GFP interaction with host cells

Green fluorescent protein (GFP) usage in molecular microbiology has become increasingly common. GFP has been expressed in bacteria (Chalfie et al., 1994), yeast (Kahana et al., 1995), mould (Moores et al., 1996), plants (Casper and Holt, 1996) and mammalian cells (Ludin et al., 1996). GFP can function as a protein tag and allows the host protein fused to maintain native function (Cubitt et al., 1995). In mammalian cells, GFP is typically distributed throughout the cytoplasm and nucleus. GFP as a non-invasive real-time marker allows enormous flexibility during applications in research including investigation in cell, developmental and molecular biology such as linage tracer, reporter of gene expression and proteins interaction (Valdivia et al., 1996, Miller et al., 2000).

GFP is a 27 kDa protein isolated from the Pacific jellyfish *Aequorea victoria*. The protein is a monomer consisting of 238 amino acids and naturally fluorescent (Chalfie et al., 1994, Cody et al., 1993). GFP transduces the blue chemiluminecence of another protein, aequorin, into green fluorescence light, by energy transfer. The wild-type absorbance/excitation peak is at 395 nm and the

peak emission at 508 nm. The protein crystal structure is shaped as a cylinder, consisting of 11 strands of β-sheet wrapping around an α-helix. The protein fold cylinder is called 'β-can' and the fluorophores are protected within (Yang et al., 1996). GFP requires no substrate or any cofactors, with addition of near UV or blue light will detect the protein readily. GFP requires oxygen to be in oxidised to fluoresce (Heim et al., 1994). GFP is thermosensitive, with maximal fluoresce at 15^{o}C and decreasing to 75% levels at temperatures greater than 30^{o}C. Although GFP is a peptide, it is very resistant to denaturation. Partial or total denaturation can occur at a pH less than 4.0 or above 12.0 within minutes or with a strong oxidising agent such as 6 M of guanidine hydrochloride (GuHCL) at 90^{o}C, but this is reversible (Yang et al., 1996). Thus, once produced expression of GFP is stable and resistant to photo bleaching (Chalfie et al., 1994). Incorporation of GFP into cells of wide variety of organisms does not seem to have toxic effects on the cells (Chalfie et al., 1994, Valdivia et al., 1996).

Some studies have reported *C. jejuni* expressing GFP visualised in infected IECs. The first study showed *C. jejuni* expressing GFP fluorescence using flow cytometry and demonstrated that bacterial infection caused cell death (Konkel and Mixter, 2000). This was followed by a study by Miller *et al.* who constructed *C. jejuni* expressing GFP with two different plasmids. It was found that GFP transformed into *C. jejuni*, fluoresce strongly and can be detected on plant tissue, chicken skin and inside infected Caco-2 cells (Miller et al., 2000).

In 2003, a study by Mixter *et al.* reported that *C. jejuni* F38011 expressing GFP was readily detectable *in vivo* using fluorescence microscopy and flow cytometry. They constructed a shuttle vector pMEK91 using an *ompE* promoter with a tetracycline resistance cassette and *gfp* cloned into an EcoRI site. In the study, the *C*. *jejuni* GFP strain was injected into mice and the bacterial association was tracked with a marker for selected granulocytes (Mixter et al., 2003).

In 2015, a study by Jervis *et al.* reported that *C. jejuni* 11168 expressing GFP was visualised invading HeLa cells. In the study, they constructed a plasmid pCJC1 that contained a chloramphenicol resistance cassette (*cat*), with upstream and downstream sites. A region of *C. jejuni* pseudogene *Cj0223* flanked both sites. Three different promoters were cloned into the pCJC1 upstream of the *cat* gene, namely *porA* from *C. jejuni, ureI* from *H. pylori* and *flaA* from *Helicobacter pullorum*. In addition, a GFP reporter gene were inserted downstream of each of the different promoters. The *porA* promoter produced the highest fluorescence, whilst the *ureI*

promoter produced the lowest. Following that, strains constructed with *porA* /GFP were investigated for *in vitro* invasion ability with HeLa cells. The results showed, the strains were readily visualised within the actin following staining and viewed with fluorescence microscopy. In addition, no significant effect on growth between strains expressing GFP and controls were observed (Jervis et al., 2015).

GFP as a reporter protein is very versatile because it inherently fluoresces without the need for extra cofactors or substrates. This make it possible to visualise the fluorescence in live cells.

1.11 Aims

The aim of this study was to investigate the role of the CadF and FlpA fibronectin binding proteins during *C. jejuni* interactions with and invasion of human intestinal epithelial cells, comparing different wild-type strains and mutants. The effect of host immune responses to *C. jejuni* infection will also be investigated. Data from a previous study showed both *cadF* and *flpA* mutants had reduced interaction and invasion activity compared to the 81-176 wild-type strain (Neveda Naz, PhD Thesis, LSHTM, 2014). These studies showed that whilst 81-176 *cadF* and *flpA* mutants both exhibit reduced ability to adhere to IECs, the 81-176 *flpA* mutant exhibits a more significant reduction in invasion of IECs. This would suggest that FlpA plays a more important role in *C. jejuni* invasion than CadF. Therefore, this study aims to investigate whether the same phenotypic characteristics are observed in the 11168H wild-type strain, *cadF* and *flpA* mutants.

Specific objectives:

1. Investigation into the effects of mutation of *cadF* or *flpA* in the 11168H wild-type strain and comparison with the same mutations in the 81-176 wild-type strain;
2. Investigation into the role of CadF and FlpA in the *C. jejuni* interactions with intestinal epithelial cells;
3. Visualising *C. jejuni* 11168H wild-type expressing GFP during interactions with intestinal epithelial cells.

CHAPTER TWO: MATERIALS AND METHODS

2.1 Bacterial strains and growth techniques

2.1.1 Bacterial strains

In this study, two *C. jejuni* wild-type strains and isogenic *cadF* and *flpA* mutants were used. The *C. jejuni* 11168H wild-type strain is a hypermotile derivative of NCTC 11168 (Karlyshev et al., 2002) which shows higher levels of colonisation of the GI tract of chicks and as such is considered a better strain to use to investigate host-pathogen interactions (Jones et al., 2004). The 11168H GFP strain was kindly provided by Dr Dennis Linton (University of Manchester). The 11168H *cadF* mutant and the 11168H *cadF* mutant expressing GFP were constructed in this study. The 11168H *flpA* mutant was from a previous study by Neveda Naz (a LSHTM PhD student), whilst the 11168H *flpA* mutant expressing GFP was constructed in this study. The *C. jejuni* 81–176 wild-type strain was isolated from a patient with gastroenteritis (Korlath et al., 1985). This strain has been verified to infect human volunteers and promote commensal colonisation of chicks (Black et al., 1988). The *C. jejuni* 81–176 wild-type strain is probably the most widely studied laboratory strain. The 81-176 *cadF* and *flpA* mutants were from the previous study by Neveda Naz. A list of all strains and plasmids used in this study is provided in Table 2.1.

Table 2.1 Bacterial strains, mutants and plasmids used in this study

Bacteria strains/ mutants/plasmids	**Descriptions**	**References**
C. jejuni 11168H	Hypermotile derivative of the original sequenced strain NCTC 11168	(Karlyshev et al., 2002, Jones et al., 2004)
C. jejuni 11168H expressing GFP	Hypermotile derivative of the original sequenced strain NCTC 11168 expressing green fluorescent green under strong *porA* promoter control	(Jervis et al., 2015)
C. jejuni 81-176	Highly invasive wild-type laboratory passaged strain. A	(Korlath et al., 1985)

	strain isolated during outbreak in USA.	
C. jejuni 11168H *cadF* mutant	Isogenic mutant, *Cj1478* (*cadF*) gene function disrupted with insertion of 1.4kb Km^R cassette.	This study
C. jejuni 11168H *cadF* mutant expressing GFP	Isogenic mutant, *Cj1478* (*cadF*) gene function disrupted with insertion of 1.4kb Km^R cassette and expressing green fluorescent green under strong *porA* promoter control	This study
C. jejuni 11168H *flpA* mutant	Isogenic mutant, *Cj1279c* (*flpA*) gene function disrupted with insertion of 1.4kb Km^R cassette.	Neveda Naz (PhD Thesis, LSHTM, 2014)
C. jejuni 11168H *flpA* mutant expressing GFP	Isogenic mutant, *Cj1279c* (*flpA*) gene function disrupted with insertion of 1.4kb Km^R cassette and expressing green fluorescent green under strong *porA* promoter control	This study
C. jejuni 81-176 *cadF* mutant	Isogenic mutant, *Cjj1471* (*cadF*) gene function disrupted with insertion of 1.4kb Km^R cassette.	Neveda Naz (PhD Thesis, LSHTM, 2014)
C. jejuni 81-176 *flpA* mutant	Isogenic mutant, *Cjj81176*- (*flpA*) gene function disrupted with insertion of 1.4kb Km^R cassette.	Neveda Naz (PhD Thesis, LSHTM, 2014)
E. coli DH5α competent cells	*E. coli* cells used for transformation by electroporation	Invitrogen, Thermo Fisher Scientific, Paisley, UK
XL2-BLUE MRF high efficiency competent cells	*E. coli* cells used for transformation by electroporation	Agilent Technologies LDA, Cheadle,UK
SCS110 competent cells	*E. coli* cells used for transformation by electroporation	Agilent Technologies

		LDA, Cheadle, UK
pGEM-T easy	Commercial TA cloning vector with ampicillin resistance cassette	Promega, Southampton, UK
pGEMT+Cj1478 11168H	pGEMT-easy vector with inserted 0.96 kb 11168H *cadF* gene disrupted by insertion of Km^R cassette	This study
pJMK30	Plasmid containing a gene encoding for Kanamycin resistance (*aphA3*) (1.4 kb)	(Trieu-Cuot et al., 1985)
pCJC1	Plasmid contains a chloramphenicol resistance cassette (cat)	(Jervis et al., 2015)

2.1.2 Bacterial growth conditions

C. jejuni wild-type strains and mutants were routinely grown on Columbia Blood Agar (CBA) plates (Fisher Scientific, Basingstoke, UK) supplemented with *Campylobacter* selective supplement (Oxoid, Basingstoke, UK) and 7% (v/v) horse blood (TCS Microbiology, Botolph Claydon, UK). Where appropriate CBA plates were supplemented with 50 µg/ml kanamycin or 10 µg/ml chloramphenicol (Sigma-Aldrich, Poole, UK). For broth cultures, bacterial strains were cultured in Brucella broth (BB) or Muller Hinton broth (MH) (Oxoid). Both plates and broth cultures were incubated in microaerobic conditions in a Variable Atmosphere Incubator (VAIN) (Don Whitley Scientific, Sheffield, UK) that was supplied with a mixture of 5% Oxygen, 10% Carbon Dioxide and 85% Nitrogen to produce microaerobic conditions.

Escherichia coli DH5α and XL2 were grown on Luria–Bertani (LB) agar or in LB broth containing 100 µg/ml ampicillin, 100 µg/ml kanamycin or 15 µg/ml chloramphenicol as appropriate.

2.1.3 Bacterial glycerol stocks

C. jejuni were grown on CBA plates for 24 h. Bacteria were harvested with a sterile 10 µl plastic loop (VWR, Lutterworth, UK), and resuspended in media consisting of BB supplemented with 10% (v/v) Foetal Calf Serum (FCS) (Sigma-Aldrich) and 10% (v/v) glycerol (Sigma-Aldrich). The suspension was then aliquoted (100 µl) into 1.5 ml tubes (Starlab, Hamburg, Germany). Tubes were snap-frozen in a dry ice and 100% (v/v) ethanol mixture for 5 min in a polystyrene tray. Frozen bacterial suspensions were stored at -80°C in a New Brunswick Scientific Innova ultra-low temperature freezer (Eppendorf, Stevenage, UK). All *E. coli* strains were stored at −80°C in media consisting of LB broth supplemented with 20% (v/v) glycerol.

2.1.4 Bacterial resuscitation

To resuscitate *C. jejuni* from frozen stocks, a vial of glycerol stock containing the desired bacterial strain was thawed on ice. Once thawed, the contents were transferred onto a CBA plate and spread using a sterile loop in a circular motion over the plate. The plate was then placed into the VAIN incubator for 48 h. After 48 h of growth, a single colony was picked, subcultured onto a new CBA plate and then incubated for further 24 h.

2.1.5 Passaging of bacteria

C. jejuni strains were routinely passaged onto a fresh CBA plate for 3-4 days up to a maximum of 10 passages. Passages were routinely checked for contamination by streaking in a fashion aimed at obtaining single colony forming units (CFUs) and the morphology of individual CFUs examined, as extended passage can lead

to the development of a mucoidy colony phenotype. If a mucoidy phenotype was observed, the line was discontinued, and fresh bacteria resuscitated from the stocks as described in Section 2.1.4.

2.1.6 Bacterial suspension for assays

To prepare suspensions of *C. jejuni* for assays, bacteria were harvested from a 24 h CBA plate and mixed in 1 ml of BB or phosphate-buffered saline (PBS) in a 1.5 ml Eppendorf tube. The suspension was vortexed to obtain a homogenous suspension. The concentration of bacterial cells was then determined by measuring the OD_{600}. Briefly, 100 µl of bacterial suspension was diluted in 900 µl of BB or PBS in a cuvette (10 mm path length, Kartell, Noviglio, Italy). As a control, 1 ml of BB or PBS alone was prepared in another cuvette. The OD_{600} of the bacterial suspension was determined using a spectrophotometer at OD_{600} (S200UV/Vis Spectrophotometer, Jencons-VWR, Leighton Buzzard, UK). The formula below was used to obtain the required volume of the original suspension to add to a volume of media (Final volume) to produce a starting concentration of OD_{600} 0.1:

$$\text{Volume required} = \frac{\text{Inoculum required at } OD_{600} \text{ (e.g. 0.1)} \times \text{Final volume} \times 1000}{(10 \times OD_{600} \text{ reading})}$$

2.1.7 Bacterial competent cells

Bacteria were cultured under microaerobic conditions at 37°C for 16 h. When the OD_{600} reached 0.8, the culture was transferred into a 50 ml falcon tube and centrifuged at 4,000 rpm for 20 min. The supernatant was removed, and the pellet resuspended in 10 ml of ice cold EBF buffer until no clumps were visible. For 100 ml EBF buffer, it was made by mixing 10 ml 10% (w/v) sucrose and 15 ml 100% (v/v) glycerol in Milli-Q water. The bacterial cell suspension was centrifuged at 4,000 rpm at 4ºC for 15 min. The supernatant was removed, and the bacterial pellet was resuspended with the same volume of ice-cold EBF buffer. The centrifugation step was repeated twice more for a total of three washes. After the

last spin, the pellet was resuspended in 1 ml of ice cold EBF buffer and 100 µl aliquots were made and kept at -80^{o}C until required.

2.1.8 Bacterial colony forming unit quantification

100 µl of bacterial culture was serially diluted 1:10 in either PBS or BB. 200 µl of each dilution were plated onto a CBA plate and spread using a L-shaped spreader (Fisher Scientific). Each dilution was performed in triplicate. Plates were incubated for 24-48 h. Plates with between 50 to 300 colonies were selected for counting.

2.1.9 Bacterial growth curves

For the growth curve assay, 10 ml of BB in a 25 cm^3 tissue culture flask was pre-incubated for 18 h on a shaking orbital platform in the VAIN. Broth was then inoculated with a bacterial suspension to a final OD_{600} of 0.1 and further incubated for 24 h in the VAIN with shaking at 75 rpm. At intervals of every 2 h starting at 0 h, the OD_{600} readings of a 1 ml sample of the inoculated broth were recorded as an indication of bacterial growth.

2.1.10 Bacterial motility

Bacteria were cultured for 24 h then harvested in 1 ml PBS (Sigma Aldrich) and adjusted to an OD_{600} of 1.0, and 5 µl of this suspension was pipetted into the centre of a semi soft agar plate made by adding 0.4% (w/v) bacteriological agar (Oxoid) to BB. Plates were incubated under microaerobic conditions at 37^{o}C. At intervals of 24 h, 48 h and 72 h, plates were checked for growth indicated by a halo growing from the centre of injection site. Measurement of the diameter of the halo or growth zone was recorded, and images were captured using a Gene Genius Bio Imaging System (Syngene, Cambridge, UK).

2.2 Cell culture techniques

2.2.1 T84 and Caco-2 cultures

Two types of human IECs were used in this study: Caco-2 cells, a human enterocyte-like cell line (HTB37™) and T84 cells, a human colonic epithelial cell line (CCL-248™). Both cell lines were able to form polarised monolayers and displayed distinct apical and basolateral surfaces. Both lines were routinely cultured at 37^{o}C in a MCO15-AC humidified atmosphere containing air enriched with 5% CO_2 at 37^{o}C (Sanyo, Loughborough, UK).

2.2.2 Tissue culture media

The Caco-2 cell-line (HTB37™) was cultured in Dulbecco's Modified Eagle Medium (DMEM) (Fisher Scientific). The T84 cell-line (CCL-248™) was cultured in Dulbecco's Modified Eagle's Medium Nutrient Mixture F12 HAM with GlutaMAX-I (DMEM/F12) (Fisher Scientific). Both cell culture media were supplemented 10% (v/v) heat-inactivated FCS, 5% (v/v) essential amino acids and 5% (v/v) antibiotics that consists of streptomycin and penicillin (Fisher Scientific).

2.2.3 Storage of IEC cells

IECs cells were grown for 5-7 days until the cell density reached 80-90 % confluence. This was followed by washing and detaching the cells. Cells were pelleted and resuspended in media without antibiotics but supplemented with 5% (v/v) Dimethy sulfoxide (DMSO) to act as a cryoprotectant. 1 ml aliquots of this suspension was transferred into cryovials (Nunc, Roskilde, Denmark) and allowed to cool down slowly to -80^{o}C overnight using a Naglene Mr Frosty™ freezing box (Nunc). Cryovials containing IECs were placed in a liquid nitrogen storage tank (Statebourne, Washington, Tyne & Wear, UK).

2.2.4 Resuscitation of IECs

A cryovial of cryopreserved IECs cells (≈1 × 10^7 cells/ml) was taken out from the liquid nitrogen tank. The cryovial was immediately immersed in a water bath at 37ºC for 30–45 s. The surface of the cryovial was wiped dry and disinfected by spraying it with 70% (v/v) ethanol. Using a 1 ml pipette, the partially melted cells were mixed gently and carefully in order to melt the remaining frozen cells. The cells were aseptically transferred into 10 ml of pre-warmed complete media in a 25 cm^2 flask. The flask was then incubated in a MCO15-AC humidified atmosphere containing air enriched with 5% CO_2 at 37ºC. The culture media was changed every 2-3 days until the cells reach 90% confluence. Cells were subcultured at around 90% confluence. All work was performed in a biological safety hood (Envair, Haslingden, UK).

2.2.5 Splitting and seeding cells

Cells were sub-cultured at around 80-90% confluence. First, the culture medium was removed, and cells were washed three times in 10 ml of PBS (Fisher Scientific). 5 ml of Trypsin-EDTA (0.25%) phenol red (Fisher Scientific) were then added to cover the cell layers and flasks were incubated for 10 min. The action of trypsin was stopped by adding 20 ml of fresh culture medium. The suspension of cells was transferred into a 50 ml falcon tube. The cells were pelleted by centrifuging at 1,400 rpm for 10 min. The supernatant was removed and cells were resuspended in fresh complete media. Cells were seeded at a density of approximately 1 x 10^5 cells per well in a 24-well tissue culture plate (Fisher Scientific), containing 1 ml of complete medium per well. Plates were incubated for 5-7 days to obtain fully differentiated cell layers. During this period, the medium was changed every 2 days. Before use for virulence assays, cell layers were washed three times in PBS and 3 ml of fresh complete culture medium without gentamicin was added.

2.2.6 Counting cell with haemocytometer

To estimate the cell count for use in experiments, cells were enumerated using a haemocytometer (Weber Scientific, Teddington, UK). 100 µl of a cell suspension was mixed with 100 µl of trypan blue and 800 µl of cell media. 10 µl of the mix was filled into the glass chamber by capillary action onto the haemocytometer. The average number of cells present in the suspension was determined by counting the number of cells per square using an inverted microscope (Leica Microsystems, Milton Keynes, UK). The formula for concentration calculations is based on the volume underneath the cover slip.

A small square has a volume of length x width x height = 1 x 1 x 0.1 = 0.1 mm^3 = 0.0001 ml.

The cell concentration is calculated as follows:

$$\text{Cell concentration per ml} = \frac{\text{Average cells per small square X dilution factor}}{\text{Volume of a small square (ml)}}$$

2.2.7 Measurement of the Trans-Epithelial Electrical Resistance (TEER) of IECs

IECs were grown on a Transwell (Fisher Scientific) insert filter (3.0 µm pore size) in a 12 well plate and allowed to differentiate and form monolayers. Media was changed every 3 days from both apical and basolateral compartments. The TEER of Caco-2 and T84 monolayers were monitored using an electro volt ohm meter (EVOM) (World Precision Instruments, Sarasota, Florida, USA) with 'chopstick type' electrodes. Two voltage-sensing AgCl electrodes were placed close to the cell monolayer on apical and basolateral sites of the filter, passing a current through two further electrodes placed at the two distal ends of the insert and reading the voltage necessary to keep the current flowing. Resistance was calculated according to Ohm's law ($R = V/I$, where R = resistance, V = voltage, and I = current) and multiplied by the surface area of the monolayers (1.12 cm^2).

2.2.8 Sensitivity assay with Triton X-100 and gentamicin

1 ml of bacterial cells (≈1 × 10^8) from 24 h plate were incubated in 0.2% (v/v) Triton X-100 (Sigma-Aldrich) or gentamicin (150 µg/ml) for 20 min and 2 h respectively. Serial dilutions were performed down to 10^{-7} and 200 µl of the final dilution was plated in triplicates on CBA plates. Plates were incubated for 48 h and then the colonies counted. Sensitivity assays were performed on all the mutants and respective wild-type strains.

2.2.9 Pre-treatment of IECs with eukaryotic inhibitors and OMVs

Inhibitors of eukaryotic cell processes were added to the monolayer 1 h prior to the addition of bacteria. In this study, the inhibitors were then removed and not maintained throughout the 3 h infection period. The infected monolayers were then washed and incubated for another 3 h in fresh culture medium containing 250 µg/ml of gentamicin to kill extracellular bacteria. Subsequently, the monolayers were washed and internalised bacteria were enumerated by plate count as described in Section 2.1.8.

1 h prior to infection with *C. jejuni*, monolayers were treated with 1 ml of the required inhibitor and incubated for 1 h at 37°C in the CO_2 incubator. After incubation, the medium containing the inhibitor was removed and the cells were infected with 1 ml of *C. jejuni* suspension (MOI 100:1) and further incubated for the required length of infection. The list of inhibitors used in this study is provided in Table 2.2. All inhibitors were diluted in culture medium without antibiotics prior to addition to monolayers. The highest concentration of each inhibitor used was chosen for the maximal inhibitory effect without affecting the epithelial cell monolayers and following the protocol of a previous study by Neveda Naz (LSHTM PhD student). The absence of growth inhibition of inhibitors against bacteria was confirmed by inoculating the bacteria with culture media with 10% (v/v) FCS and with or without inhibitors at 37°C in a humidified 5% CO_2 incubator at the same condition as controls. The viable bacteria in both groups were compared.

Table 2.2. Inhibitors of eukaryotic cell processes used in this study

Inhibitors	Stocks	Concentration used (µM)
Methyl-β-cyclodextrin (MβCD)	10 mM in H_2O	5 µM
Cytochalasin D (CytoD)	0.2 mM in DMSO	3 µM
Colchicine	10 mM in DMSO	10 µM
Wortmannin	10 mM in DMSO	1 µM

2.3 Molecular techniques

2.3.1 Genomic DNA isolation

For experiments that required genomic DNA extraction from bacterial cells, a Pure Link Genomic DNA Mini Kit (Invitrogen, Carlsbad, USA) was used following the manufacturers' instruction for Gram-negative bacteria. Briefly, bacteria were grown on a CBA plate for 24 h under microaerobic conditions. A sterile loop was used to remove bacteria and re-suspended in 1 ml of PBS in a 1.5 ml Eppendorf tube. The suspension was centrifuged at 13,000 rpm for 1 min and the resulting supernatant was removed. After this time 180 µl of PureLink Genomic Digestion buffer was added to resuspend the pellet. 20 µl of Proteinase K at 20 mg/µl was then added and vortexed to lyse the cells. The sample was incubated at 55^{o}C for 30 min in a heat block and vortexed occasionally during this period. Then 20 µl of RNaseA was added, vortexed and incubated for 2 min at room temperature (RT). After that, 200 µl of PureLink Genomic Lysis/Binding buffer was added and vortexed. This was followed by addition of 200 µl of 100% (v/v) ethanol to the tube, and vortexed for 5 sec to form a homogenous solution. All of the lysate was transferred to a PureLink spin column and centrifuged at 10,000 rpm for 1 min. The column was then placed in a new collection tube and 500 µl of Wash Buffer 1 was added to the column and centrifuged at 10,000 for 1 min. In a new collection tube, the process was repeated with Wash Buffer 2, but this time centrifuged at 13,000 rpm for 3 min. Finally, the spin column was placed in a 1.5 ml Eppendorf tube. 50 µl of Milli-Q water was added to the centre of the column membrane and incubated for 1 min at RT, and then centrifuged at 13,000 rpm for 90 sec. The isolated DNA

concentration was quantified using a NanoDrop ND-1000 spectrophotometer (NanoDrop Technologies, Wilmington, USA) as described in Section 2.3.4. The genomic DNA samples were stored at -20^{o}C.

2.3.2 Plasmid DNA isolation from *E. coli*

A QIAprep Spin Miniprep Kit (Qiagen) was used to isolate plasmid DNA from overnight cultures of *E. coli* strains following the manufacturers' instructions.

2.3.3 DNA quantification

DNA was quantified using a NanoDrop 2000 platform. 1.5 µl of Milli-Q water was used to blank the initial measurement. Then, 1.5 µl of a DNA sample was pipetted onto the NanoDrop 2000 platform pedestal and the arm on top of the pedestal was closed, this resulted in the liquid sample contacting both ends of the fibre optic cable in the spectrophotometer. A ratio between absorbance readings at 260 nm and 280 nm was evaluated for DNA purity in samples. A ratio of 1.8 was considered as good quality DNA. Presence of proteins or other contaminants resulted in lower ratios that indicate poor quality DNA. DNA was stored at -20^{o}C for further use. RNA was also quantified using the NanoDrop. A ratio of 2.0 between absorbance reading at 260nm and 280 nm was considered as good quality RNA.

2.3.4 RNA isolation

Bacteria were grown on a CBA plate for 24 h in the VAIN and 10 ml BB was pre-incubated overnight under microaerobic conditions with shaking at 75 rpm. The next day, the pre-incubated broth was inoculated with a bacterial suspension from the 24 h plate at an OD_{600} of 0.1. The broth was further incubated for 18 h under microaerobic conditions with shaking at 75 rpm at 37^{o}C. After 18 h, 4 ml of the

culture was added to 8 ml of RNAprotect Bacteria Reagent (Qiagen, Manchester, UK), vortexed for 5 sec then incubated at RT for 5 min to stabilise the RNA. The stabilised RNA was then centrifuged for 10 min at 4,000 rpm at 4^{o}C and the supernatant discarded.

The following solutions were prepared prior to RNA isolation using buffers from an RNeasy Mini Kit (Qiagen):

Tris-EDTA (TE) buffer	- 1 part of lysozyme (1 mg/ml) added to 9 parts of TE buffer (Qiagen)
RLT buffer	- 10 µl of 14.4 M β-mercaptoethanol added to 1 ml of RLT buffer (Qiagen)
RDD buffer	- 10 µl of DNase I (1 U/µl) added to 70 µl of RDD buffer (Qiagen)

In the tube with the stabilised RNA, 200 µl of TE buffer was added and the pellet was resuspended for 1 min using a P1000 Gilson pipette (Anachem Ltd, Luton, UK). The suspension was incubated for 10 min at RT and vortexed every 2 min. 1 ml of RLT buffer was then added to the suspension and vortexed vigorously, followed by 500 µl of 100% (v/v) ethanol and mixed by pipetting. 700 µl of the suspension was then transferred into an RNeasy Mini spin column. The spin column was centrifuged at 10,000 rpm for 15 sec. The step was repeated with the remaining suspension. Then 350 µl of RW1 buffer was added and the spin column was centrifuged at 10, 000 rpm for 15 sec and the flow through discarded. 80 µl of RDD buffer was added to the centre of the spin column and incubated for 15 min at RT. After the incubation, 350 µl of RW1 buffer was added to the spin column, centrifuged at 10,000 rpm for 15 sec and the flow through discarded. This step was repeated with 500 µl of RPE buffer added to the spin column and the flow through discarded. Another 500 µl of RPE buffer was added and the spin column was centrifuged at 10,000 rpm for 2 min. To remove any remaining RPE buffer, the spin column was placed in a 2 ml collection tube and centrifuged at 13,000 rpm for 1 min. The spin column was then transferred to a 1.5 ml Eppendorf tube. To elute the RNA, 50 µl of RNase-free water was added directly to the centre of the membrane in the spin column and centrifuged at 13,000 rpm for 1 min. A NanoDrop was used to quantify the RNA concentration as described in Section 2.3.4. RNA samples were stored at -80^{o}C.

2.3.5. DNase treatment

Following RNA isolation, DNase treatment was performed to completely remove any traces of DNA present in the RNA samples using the TURBO DNA-free kit (Fisher Scientific).

The reactions were prepared as follows:

5 µl of 10X TURBO DNase Buffer

1 µl of TURBO DNase

x µl of RNA sample (2 µg)

Nuclease-free water (to 50 µl)

Mixed solutions were incubated at 37ºC for 30 min. Then, 5 µl of DNase Inactivation Reagent was added to each reaction and further incubated at RT for 5 min with occasional mixing to disperse the DNase Inactivation Reagent throughout the reaction mix. Tubes were centrifuged for 90 sec at 10,000 rpm. The concentration obtain for each sample was 40 ng/µl. The resulting supernatants containing pure RNA were carefully transferred to new tubes and stored at -80ºC.

2.3.5.1 Conversion of RNA to cDNA

The SuperScript III First-Strand Synthesis System for RT-PCR (Invitrogen) was used to convert total bacterial RNA to cDNA.

The reactions were prepared as follows:

2.5 µl of RNA sample (40 ng/µl)

1 µl of Random hexamers (50 ng/µl)

1 µl of 10 mM dNTP mix

5.5 µl of RNase-free water

Samples were incubated for 5 min at 65ºC, followed by 1 min on ice. Then 10 µl of the cDNA synthesis mix was prepared at the following concentration per sample:

2 µl of 10X RT buffer

4 µl of 25 mM $MgCl_2$

2 µl of 0.1 M DTT

1 µl of RNase OUT (40 U/µl)

1 µl of SuperScript III RT (200 U/µl)

As a control, a no RT reaction tube was prepared to analyse the reverse transcriptase enzyme efficiency and to check for any contamination by DNA. Samples were prepared in duplicate with one tube without the addition of SuperScript III RT. To each RNA sample, 10 µl of cDNA synthesis mix was added, mixed and incubated in a Thermal Cycler DNA Engine Tetrad 2 Peltier (Bio-Rad, Hemel Hempstead, UK) using the following program:

Step 1 at 25^{o}C for 10 min

Step 2 at 50^{o}C for 50 min and

Step 3 at 85^{o}C for 5 min

Once the program was finished, tubes were taken out and incubated for 1 min on ice. Reactions were briefly centrifuged and then 1 µl of RNase H was added and incubated for 20 min at 37^{o}C to degrade the remaining RNA. Finally, cDNA samples were stored at -20^{o}C until further use.

2.3.6 Primers design

Primers listed below were used in this study. All primers were designed manually based on the *C. jejuni* NCTC 11168 genomic sequence, then checked using Oligo analyser 3.1 software on the Intergrated DNA Technologies website (http://eu.idtdna.com/analyser/applications/oligoanalyser/) to confirm the percentage of G+C content, melting temperature, the absence of self-dimers and hairpin loops. The primers were then synthesised by Invitrogen. Primer suspensions were prepared by reconstituting the powder in Milli-Q water to produce 100 µM stock solutions. Each primer was used at a concentration of 15 pmol/µl in a PCR reaction. Primers were aliquoted and kept at -20^{o}C until required.

Table 2.3 Primers used in this study

Gene	Primers	Sequence 5'-3'
cadF	Cj1478cR	GAAGAGTGGATGCTAA
cadF	Cj1478cF	ATATTCTTATGTTTAGG
flpA	Cj1279cR	CTTTGCTTGAAGGTTCT
flpA	Cj1279F	ATTTCGCTTGAGTTT
Kan^R	Kan R	TGGGTTTCAAGCATTAGTCCATGCAAG
Kan^R	Kan F	GTGGTATGACATTGCCTTCTGCG
gyrA	R	CCTACAGCTATACCAC
gyrA	F	GGTCGTTATCACCCACATGGAG

2.3.7 Polymerase Chain Reaction

All PCR reaction mixes were prepared in a dedicated UV cabinet free of nucleic acid templates. All PCR reactions was routinely performed using MyTaq™ Red Mix (Bioline, London, UK). For complementation of desired genes, a high-fidelity DNA polymerase Accuprime Pfx supermix (Invitrogen) was used. The PCR mixtures were set up as follows:

All reactions were set-up on ice.

Template DNA	200 ng
Primers (20 µM each)	1 µl
MyTaq Red Mix, 2x	25 µl
Water (ddH_2O)	to 50 µl

Reactions were mixed in 0.6 ml Eppendorf tubes and placed into a Thermal Cycler DNA Engine Tetrad 2 Peltier and a PCR program cycle was run as follows:

Step 1: Denature at 94^{o}C for 15 sec

Step 2: Anneal at 55^{o}C for 1 min

Step 3: Extension at 72^{o}C for 1 min

34 cycles of step 1 to step 3 were repeated and ends with one cycle of step 4.

Step 4: End at 72^{o}C for 4 min

Steps 2 and 3 were varied to optimise PCR amplification conditions / amplification of larger products (usually 1 minute per Kb). Modifications to PCR reaction conditions were also dependent on the melting temperature (Tm) of the primers used.

2.3.8 Reverse transcription polymerase chain reaction (RT-PCR)

RT-PCR was used to investigate expression of *cadF* and *flpA* in the 11168H wild-type strain and mutants. This was a semi quantitative assay using the housekeeping gene *gyrA* as a control. RT-PCR reactions were performed using list of primers in Table 2.3. A minimum of three biological replicates were performed. PCR products were analysed and images were captured and recorded as described in Section 2.3.9. Image J software (NIH Image, Bethseda, USA) was used to analyse the images for band intensities.

2.3.9 Electroporation of *C. jejuni*

50 µl aliquots of electrocompetent *C. jejuni* cells were thawed on ice and 1 µl of plasmid (0.5 – 1.0 µg) DNA was added and mixed gently. The mix was kept chilled on ice for 30 min. Following incubation, the mixture was transferred to a pre-chilled 2 mm gap electroporation cuvette (Gene Pulser, Biorad, CA, USA). The settings for electroporation using a Gene PulserXcell electroporation system (Bio-Rad) were: 2.5 kV and 200 Ω. Immediately after electroporation, 1 ml of SOC media (Invitrogen) at RT was added into the cuvette and mixed using a pipette. The mixture was then pipetted onto a CBA plate, spread and incubated for 24 h at 37^{o}C in the VAIN. The next day, a sterile loop was used to collect the bacteria. The bacteria were then resuspended in 1 ml of BB. 200 µl of the suspension was plated onto an antibiotic supplemented CBA plate and incubated for 48 – 72h. The resulting colonies were restreaked and gDNA isolated as a boilate followed by PCR analysis to confirm homologous recombination of the correct construct.

2.3.10 DNA analysis by agarose gel electrophoresis

Agarose gels were prepared by dissolving 1.5 g agarose (Bioline) in 150 ml of 1 x Tris-acetate-EDTA (TAE) (40 mM Tris-acetate, 1 mM EDTA pH 8) buffer to obtain a desired concentration of 0.7% (w/v). The solution was heated for 3 min using a microwave. After cooling to 55^{o}C, 0.5 µg/ml ethidium bromide (Fisher Scientific) was added. The gel was swirled around to mix the contents, and then immediately

poured into a gel casket with the appropriate comb attachment. The gel was left to solidify for 20 min. To perform gel electrophoresis, the comb attachment was removed, and the gel immersed into 1X TAE buffer in an electrophoresis tank (AGE electrophoresis tank; Biorad, Hemel Hempstead, UK). 10 µl of each PCR sample was loaded into a gel well. 5 µl of Hyperladder 1 kb marker (Bioline) was also added to a separate well. Gel electrophoresis was performed at 120 mV for 30-45 min. PCR products were visualised using a transilluminator (UVP, Cambridge, UK) and gel images recorded using a Gene Genius Bio Imaging System (UVP).

2.3.11 Purification of PCR amplicons

PCR products were purified using a QIAquick PCR purification kit (Qiagen). Briefly, 20 µl of the PCR reaction was transferred to a 1.6 ml Eppendorf and 100 µl of binding buffer BP1 was added. The solution was mixed gently by pipetting and then transferred to a QIAquick spin column in a 2 ml collection tube. The tube was centrifuged at 13,000 rpm for 1 min and the flow-through discarded. The tube was placed back into the 2 ml collection tube, 750 µl of RPE buffer added to the tube, and centrifuged again at 13,000 rpm for 1 min. The QIAquick column was placed into a fresh 1.6 ml Eppendorf tube, 20 µl of sterile Milli-Q water was added to the centre of the QIAquick spin column and left to stand for 1 min at RT, followed by centrifuging at 13,000 rpm for 1 min to elute the DNA. The sample was incubated on ice and the purity of DNA was quantified using the NanoDrop. The purified PCR products were stored at -20^{o}C.

2.3.12 Restriction enzyme digestion

Prior to ligation with the kanamycin cassette, the plasmid DNA containing the gene to be mutated was digested and purified. Briefly, 2 µg of PCR product or plasmid DNA was added to 5 µl of 10X reaction buffer and 1 µl (10 U/µl) of the appropriate restriction endonuclease (New England Biolabs, England, UK) in a 1.5 ml Eppendorf tube, and then made up to a total volume of 48 µl with Milli-Q water.

The reaction tubes were incubated for 60-90 min in a 37°C water bath, followed by purification using the QIAquick PCR purification kit. Samples were checked for purity using the NanoDrop. Purified samples were stored at -20°C.

2.3.13 Plasmid DNA dephosphorylation

To avoid vector self-ligation, 8 µl of digested plasmid DNA was added to 1 µl of 10X dephosphorylating buffer and 1 µl of Antarctic phosphatise enzyme (10U/µl) in a 0.6 ml Eppendorf tube. The reaction was incubated for 15 min at 37°C and then further incubated for 5 min at 65°C in a heat block to inactivate the enzyme.

2.3.14 Insertion of a Kanamycin cassette

A BamHI digested fragment of plasmid pJMK30 containing the Kan cassette was ligated into the digested plasmid using the following procedures:

2 µl of plasmid DNA with unique restriction enzyme digested (250 µg/µl)

5 µl of digested Kanamycin cassette (29 ng/µl)

1 µl of Ligase buffer

2 µl of T4 DNA Ligase (3 U/µl)

The ligation reaction was mixed gently by pipetting, briefly centrifuged and incubated overnight at 4°C. The ligation reaction was transformed into DH5α cells and plated onto LB amp-kan plates. Plates were then incubated overnight at 37°C. Colonies from positive transformants were picked and restreaked onto fresh LB amp-kan plates and incubated as before. Boilates were prepared and used for PCR screening reactions. Gene specific primers were used to confirm the presence of a larger band due to the insertion of the Km^R cassette. Combinations of Kanamycin forward out or Kanamycin reverse out and gene specific forward or gene specific reverse primers were used to check that the Km cassette was in the correct orientation.

2. 3.15 Cloning PCR products into a plasmid vector

Ligation reactions were prepared with a ratio of insert to vector of either 1:1 or 3:1 and the amount of plasmid to insert was calculated using the following equation:

Insert size (kb) /vector size (kb) x ng of vector = ng of insert.

Three 0.6 ml tubes were prepared and labelled as test sample, negative control and positive control. The following were added into all tubes.

5 µl of 10 X ligation buffer

1 µl of pGEM T-easy vector (50 ng/µl)

0.4 µl of T4 DNA ligase (10 U/µl)

1 µl of water

Then either:-

2 µl of PCR products into the tube labelled test sample;

2 µl of water into the tube labelled negative control;

2 µl of control insert into tube labelled positive control

The reactions were gently mixed by pipetting and incubated overnight for 16 h at 4^{o}C.

2.3.16 Transformation of *E. coli* cells

E. coli cells were transformed with ligated plasmid from the above reactions. 100 µl of electrocompetent *E. coli* cells were thawed and mixed with 2 µl of β-mercaptoethanol for 10 min on ice with occasional gentle mixing. In pre-chilled 1.6 ml Eppendorf tubes, 2 µl of ligated plasmid were added to 50 µl of thawed electrocompetent *E. coli* cells. A control tube was set up and contained 2 µl of uncut plasmid DNA in 50 µl of electrocompetent *E. coli* cells. The tubes were incubated for 30 min on ice, heat shocked for 45 sec at 42^{o}C in a water bath, and then immediately incubated for 2 min on ice. Next, 950 µl of SOC broth (Bioline) was added to each tube and further incubated for 90 min at 37^{o}C with shaking at 250 rpm. Finally, 200 µl of transformant reactions were plated onto LB-amp plates

that contained 0.5 mM Isopropyl-B-thio-galactoside (IPTG) (Promega, Southampton, UK) and 80 µg/ml of X-Gal (Promega). Plates were incubated for 16 h overnight at 37ºC.

2.3.17 PCR screening of transformants

Fresh individual colonies from transformation plates were picked and restreaked onto fresh LB-amp plates and incubated overnight at 37ºC. After 16 h incubation, boilates were prepared by making a suspension of bacterial cells in 100 µl of Milli-Q water. The suspension was heated for 10 min at 95ºC, briefly chilled on ice and centrifuged for 5 min at 13,000 rpm. 1 µl of the supernatant was used as template in a 25 µl PCR reaction.

2.3.18 Construction of *C. jejuni* mutants expressing Green Fluorescent Protein Fusion (GFP)

C. jejuni 11168H *cadF* and *flpA* mutants expressing GFP were constructed by electroporation of the plasmid (pCJC1) that contains the *gfp* gene encoding the green fluorescent protein (GFP) under control of the strong *C. jejuni porA* promoter (Jervis et al., 2015). Briefly, competent *cadF* mutant or *flpA* mutant cells were prepared from a 24 h CBA plate as described in Section 2.1.7. Then, 50 µl of competent cells was mixed with 5 µl of GFP plasmid DNA and incubated on ice for 30 min. Electroporation was performed as described in Section 2.3.8. Electroporated bacterial cells were plated immediately onto CBA plates and incubated for less than 24 h. Colonies were picked and resuspended in 1 ml of BB. 400 µl and 200 µl of this bacterial suspension were spread onto separate CBA plates supplemented with kanamycin and chloramphenicol. Plates were incubated for 24 h to 72 h in the VAIN. The resulting colonies were collected, gDNA isolated as boilates, then analysed by PCR to screen for homologous recombination of the correct construct.

2.4 Assays

2.4.1 BCA assay

Bicinchoninic acid (BCA) kit (Fisher Scientific) protein assay was used to quantify protein concentrations according to the manufacturer's recommendations. Briefly, diluted albumin (BSA) standards were prepared at different concentrations in PBS, followed by the working reagent (WR). The volume of the WR needed was prepared by mixing 50 parts of reagent A with 1 part of reagent B from the kit. 25 µl of albumin standards and the unknown samples were added to microplate wells in duplicates, and then 200 µl of WR was added into each well. The plate was then incubated at 37°C in the dark for 30 min. The absorbance was measured at 562 nm using a SpectraMax M3 microplate reader (SpectraFluorPlus, Tecan, California, USA). From the absorbance reading output, a standard curve was generated. The average OD_{562} reading for each concentration replicate of the BSA standards was plotted against concentration in µg/ml. Protein concentration of the samples was then determined using the standard curve. Samples were diluted to the required concentration prior to performing the assays.

2.4.2 Enzyme-linked immunosorbent assay (ELISA)

T84 IECs were seeded into 24 well plates (≈ 1 x 10^5 cells per well) and grown for 5-7 days until confluent. A suspension of *C. jejuni* from a 24 h plate was prepared and adjusted to OD_{600} 0.1. T84 cells were incubated with 1 ml of the bacterial suspension for 24 h. The next day, supernatants were gently removed so as not to disturb the cells. The collected supernatants were probed for any cytokines present. The levels of Interleukin 8 (IL8 or chemokine (C-X-C motif) ligand 8, CXCL8) and Tumor necrosis factor alpha (TNFα) secretion were assessed using an ELISA kit according to manufacturer's instructions (Peprotech, London, UK). Detection was performed at an absorbance of 405 nm using a 96-well plate reader Dynex MRX II (Dynex, USA).

2.4.3 Lactate Dehydrogenase (LDH) Assay

Caco-2 and T84 IECs were seeded into 24 well plates (≈ 1 x 10^5 cells per well). IECs were grown for 5-7 days until confluent, then washed three times with PBS followed by the addition of the appropriate concentration of each inhibitor as well as a control without inhibitor. The IECs were incubated for 1 h with the inhibitor, and then the supernatants were removed and the IECs washed three times with pre-warmed PBS. This was followed by the addition of 1 ml fresh culture medium and the IECs were incubated for a further 24 h. After 24 h, the supernatant was collected, and extracellular lactate dehydrogenase levels were measured with the CytoTox 96 nonradioactive cytotoxicity assay kit (Promega) according to the manufacturer's recommendations. Total lysis of IECs following treatment with 1% (v/v) Triton X-100 represented the 100% cytotoxicity control. Medium without cells and inhibitors represented a 0% cytotoxicity control.

2.4.4 Rac1 activation with G-LISA assay

To determine Rac1 activation in infected IECs G-LISA™Rac1- activation assay (Cytoskeleton) (Cytoskeleton Inc., Denver, CO) was used according to the manufacturer's recommendations. Briefly, IECs were grown to 70% confluency in a 24 well tissue culture plate in DMEM/F12 containing 10% (v/v) heat-inactivated FCS, 5% (v/v) essential amino acids and 5% (v/v) antibiotics that consists of streptomycin and penicillin incubated in a 5% CO_2 incubator at 37^{o}C. The cells were serum-depleted, washed with DMEM once and incubated with DMEM containing 5% (v/v) FCS for 24 h. The next day, the procedure was repeated but this time the cells were incubated serum-free with DMEM and incubated for a further 24 h. The serum-depleted cells were then infected with *C. jejuni* for the indicated time per experiment. Subsequently, cells were washed with PBS, resuspended in the appropriate volume of G-LISA lysis buffer per well then harvested from the wells using a cell scraper. The lysate was clarified by centrifugation at 14,000 rpm at 4^{o}C for 2 min. The total protein concentration of each lysate was determined by the protein assay reagent of the kit. The concentrations of cell lysates were then normalised and equal amounts were added to a 96-well dish coated with Rac1. The plate was placed on a microplate

shaker at 400 rpm, 4°C for 30 min. Wells were then washed three times with wash buffer before adding 50 µl anti-Rac1 primary antibody (1:250). The plate was incubated on an orbital microplate shaker at 400 rpm, room temperature for 45min. The primary antibody was removed and wells were washed three times with wash buffer at room temperature. 50 µl diluted secondary horseradish peroxidase conjugate (HRP)-linked antibody (1:200) was added to each well before shaking the plate on a microplate shaker at 400 rpm, room temperature for 45 min. The plate was then washed three times with RT wash buffer before adding 50 µl HRP detection reagent into each well and incubate at RT for 20 min. Finally, 50 µl of HRP Stop Buffer was added into each well. The luminescence signal was quantified using a SpectraMax M3 microplate reader (SpectraFluorPlus, Tecan).

2.4.5 Interaction assay

For bacterial interaction assays, cells were cultured in either DMEM or DMEM/F-12 medium supplemented with 10% (v/v) heat-inactivated FCS, 5% (v/v) essential amino acids and 5% (v/v) antibiotics that consists of streptomycin and penicillin incubated in a 5% CO_2 incubator at 37°C. Interaction (adhesion and invasion) assays were performed in 24-well tissue culture plates with T84 cells which had reached at least 80% confluency. One day prior to infection, cells were washed once with 1 ml PBS and incubated overnight with antibiotic-free growth medium. On the day of infection, bacteria grown to mid-log phase were collected, resuspended in 1 ml of medium and adjusted to OD_{600} of 0.1 (≈1 x 10^8 cfu/ml).

The monolayers were infected with 1 ml of the bacterial suspension in each well, which is equivalent to multiplicity of infection (MOI) of 100:1 in pre-warmed DMEM, and then incubated in a humidified 5% CO_2 incubator at 37°C. After 3 h or 24 h, monolayers were rinsed 3 times with 1 ml of PBS each time, and then 500 µl of 0.2% (v/v) Triton X-100 in PBS was added and incubated for 20 min to lyse the IECs. The lysate was then serially diluted 1:10 down to 10^4. 200 µl of the diluted suspension was plated on CBA plates in triplicate. Plates were then incubated in the VAIN for 48 to 72 h. The number of interacting bacteria was determined by counting the resulting colonies.

2.4.6 Intracellular survival and gentamicin protection assays

The gentamicin protection assay was performed in a similar manner as above. Briefly, after incubating the cells with bacteria for the desired time point, cells were washed with 1 ml of PBS to remove non-adherent bacteria. The cells were then added with 1 ml of culture medium containing 150 µg/ml gentamicin sulfate and incubated under aerobic conditions for 2 h to kill extracellular bacteria. The cells were washed three times with 1 ml of PBS and lysed with 300 µl of 0.1 % (v/v) Triton X-100 in PBS for 15 min at 37^{o}C. Finally, serial tenfold dilutions of this lysate was performed and 200 µl of each dilution was spread on CBA plates using a sterile inoculation spreader. The plates were incubated for 72 h at 37^{o}C under microaerobic conditions, after which bacterial colony-forming units were formed, and the number of colony-forming units per ml was enumerated.

Intracellular survival assays were performed using the same protocol as gentamicin protection assay. However, after the first incubation with 150 µg/ml of gentamicin sulfate for 2 h, the monolayers were washed with 1 ml of PBS and further incubated with reduced concentration of gentamicin sulfate (10 µg/mL) for 19 h. Following incubation, the gentamicin-containing medium was removed, cells were washed three times with PBS, and lysed as described above.

2.4.7 Fibronectin and laminin binding assay

Fibronectin binding assays were performed as described previously (Konkel et al., 2010). Briefly, the wells of a 96-well flat-bottom plate (Fisher Scientific) were coated with a 1 mg/ml solution of fibronectin (Sigma-Aldrich) in PBS and then incubated overnight at 4^{o}C. For control, wells were also coated with 1% (w/v) BSA in PBS. *C. jejuni* was harvested from 24 h cultures on CBA plate and re-suspended in PBS at an OD_{600} of 2. Wells were rinsed with PBS and 50 µl of the bacterial suspension was added to each well and incubated at 37°C in a CO_2 incubator for 1 h. The wells were washed three times with PBS and adherent bacteria were removed by the addition of 0.05% (w/v) Trypsin / 0.02% (w/v) EDTA in Hanks' Balanced Salt Solution and incubated for 10 min at 37^{o}C. To enumerate the number of adherent bacteria, serial dilutions of the trypsin suspension were plated on CBA plates as described previously.

Pre-treatment of fibronectin with OMVs was performed as above, however OMVs (10 µg) were added to the fibronectin coated wells and incubated overnight at 4°C prior to the addition of bacteria.

2.4.8 *Galleria mellonella* model of infection

G. mellonella larvae were purchased from Live Foods Direct (Sheffield, UK) and kept on wood chips in the dark at RT for maximum of 2 weeks. Experiments were performed as described previously (Harding et al., 2013). Bacterial suspensions of OD_{600} 1 and OD_{600} 0.1 were prepared in PBS. 10 µl of suspension was injected into the right foremost leg of the larvae using a micro-syringe (Hamilton, Nevada, USA). The same procedure was also performed using 5 µg or 0.5 µg of OMVs isolated from the *C. jejuni* 11168H wild-type strain, *cadF* or *flpA* mutant. The larvae were incubated at 37°C. Larvae untreated with no injection or PBS only injection were also included as controls. Live *C. jejuni*-infected, OMV-injected, PBS-injected, and uninfected larvae in vented Petri dishes were incubated at 37°C under aerobic conditions. For each experiment, 10 *G. mellonella* larvae were infected and this was repeated at least three times. Survival was observed and recorded over 72 h. Cytotoxicity was determined by appearance of black pigmentation and unresponsiveness upon contact. Larvae that changed colour from white to dark brown or black were recorded as dead.

2.4.9 Translocation assay

T84 cells were seeded on Transwell 3.0 µm pore size filters in a 12-well plate (Fisher Scientific) at ≈ 1 x 10^5 cells per well and allowed to form a polarised monolayer for about 10 to 16 days. The media in both the apical and basolateral compartments were replaced with fresh media every 2-3 days. Once the cells had polarised, the cells were washed gently three times with 500 µl PBS. All media from the apical and basolateral compartment were then replaced with fresh media without antibiotics and incubated overnight. The following day, cells on the apical side were washed three times with PBS. Treated cells were infected with GFP expressing 11168H wild-type, *cadF* or *flpA* mutants at a MOI of 100:1. Control

wells were left untreated. At time intervals, the supernatant was collected from both apical and basolateral compartments and RFU read in 96 well black/opaque bottom to detect bacterial translocation using SpectraMax M3 microplate reader (SpectraFluorPlus Tecan). TEER values were taken before and after treatment at specified time points. Basolateral supernatants were collected to detect bacterial translocation from apical to basolateral side. For CFU counts, the basolateral supernatant was serially diluted, plated onto CBA plates and incubated in the VAIN. Bacterial CFUs were enumerated after 48 h incubation.

2.5 OMV isolations

OMVs were isolated as described previously (Elmi et al., 2012) . Briefly, *C. jejuni* strains were grown on CBA plates for 24 h, and harvested cells were re-suspended in 1 ml BB and adjusted to an OD_{600} of 0.1. This suspension was inoculated into 50 ml of BB which had been pre-incubated overnight in a 150 cm^3 tissue culture flask (Corning Incorporated, New York, USA) at 37ºC with shaking at 75 rpm. For every strain used, two flasks of 50 ml BB were prepared. The inoculated flasks were placed into the VAIN on an orbital shaker at 75 rpm for 16 h to achieve mid-log phase, and then transferred into 50 cm centrifugal tubes (Corning) and centrifuged (Eppendorf) at 4,000 rpm for 30 min at 4ºC. The supernatant from the two flasks were pooled, filtered using a 0.22 µm membrane syringe filter (Merck Millipore Ltd, Tullagreen, Ireland) and the cell-free supernatant collected into 50 ml centrifuge tubes. The filtered supernatants were transferred into Amicon centrifugal filter unit Ultra- 15 (Merck Millipore Ltd.) with a 10 kDa cut-off and concentrated to around 2 ml by centrifugation at 4,000 rpm for 30 min at 4ºC. The concentrated samples were transferred into ultra-clear centrifuge tubes (Beckman Coulter, CA, USA). Tubes were then centrifuged at 45,000 rpm for 3 h using a TLS 55 rotor at 4ºC in Optima TL Ultracentrifuge (Beckman Instruments, Palo Alto, CA). After ultracentrifugation, the supernatant was discarded and the pellet was resuspended in 200 µl sterile PBS. Aliquots were prepared and stored at -20ºC. Small volumes of each sample were taken for quantification of protein concentration using a BCA assay as described in Section 2.4.1.

2.6 Confocal fluorescent microscopy techniques

For confocal microscopy, IECs were processed using the following procedure: IECs were cultured on a glass cover slips for 24 h. Cells were grown to 50-60% confluence in a 5% CO_2 incubator. If inhibitors were used, these were added 1 h prior to infection with bacteria. Cells were then washed with PBS three times and infected with bacteria for the duration required. Once incubation ended, media were gently removed from the wells. 500 µl of 3.7% (v/v) paraformaldehyde (PFA) (Sigma-Aldrich) was added and incubated for 10 min at RT to fix the cells. Fixed cells were washed with PBS and permeabilised with 0.2% v/v Triton X-100 (Sigma-Aldrich) in PBS for 5 min. Once the cells and bacteria were fixed and permeabilised, the slide was now ready to be stained with any required stains to observe the specific structure or element (organelles) in the cell, as well as the extracellular or intracellular bacteria. Cells were incubated with stains and primary or secondary antibodies for the appropriate time at RT in the dark to protect the fluorescent dyes. After the final rinse with PBS, the edge of coverslips was dabbed with an absorbent paper to remove any remaining liquid. Coverslips were then mounted inverted on a drop of mounting medium containing 4'6-diamidino-2-phenylindole (DAPI) (Vector Laboratories, Peterborough, UK) at final concentration of 1.5 µg/ml with fluoresave (Sigma-Aldrich) on a glass slide (Fisher Scientific). Slides were left to air-dry for a minimum of 20 min, after which nail varnish was used to seal the coverslips ring to prevent further drying of the cells. Slides of a specimen could be observed straight away or kept at 4^{o}C for up to 1 week. Specimens were imaged on an inverted confocal laser-scanning microscope (LSM 510, Zeiss, Jena, Germany) using a ×63 oil immersion objective at ambient temperature. Images were acquired and processed using Zeiss confocal software and Image J (NIH) software. For each experiment, the confocal microscope settings and conditions were kept identical between control and treated cells monolayers. Random images were captured. The acquired images were analysed for each experimental condition. Islands of Caco-2 or T84 cells consisted of approximately 20-50 cells were analysed for bacterial internalisation. For each experiment, the entire slide was examined and on average a minimum of three representative islands of cells were imaged by capturing single image or making Z-stacks of the entire island. However, this only allowed a presumptive microscopic quantification of the number of intracellular bacteria.

2.6.1 Plasma membrane stain

For cell membrane staining, Wheat germ agglutinin (WGA) was used. WGA binds to glycoproteins of the cell membrane. However, the cells should not be permeabilised prior to staining and the incubation time should be limited to prevent WGA from staining internal structures. IECs were grown on glass cover slips for 24 h. Following treatment with inhibitors and bacterial infection as described in Section 2.5, cells were washed two times with PBS and fixed with 3.7% (v/v) paraformaldehyde (PFA) per well for 10 min at RT. After removal of PFA, cells were washed three times with PBS. Cells were then stained with 250 µl of WGA conjugated with Alexa Fluor 553 (Sigma-Aldrich) at a dilution of 1:500 in PBS per well and incubated for 10 min at RT. Cells were permeabilised by adding 250 µl of 0.2% (v/v) Triton X-100 per well and incubated for 5 min. Cells were washed again three times with PBS and excess fluid was removed by touching the coverslip edges onto tissue paper. Coverslips were then placed on top of a 3 µl drop of DAPI on a glass slide. Once dried, nail varnish was used to seal the coverslips. Slides were then ready to be viewed using confocal microscopy or stored at 4^{o}C in the dark.

2.6.2 Actin stain

IECs were grown on glass coverslips for 24 h. Following treatment with inhibitors and bacterial infection as described in Section 2.5, cells were washed and fixed with 250 µl 3.7% (v/v) paraformaldehyde per well for 10 min at RT. Cells were then washed three times with PBS. Permeabilisation was performed using 250 µl per well of 0.2% (v/v) Triton X-100 for 5 min. Cells were washed three times with PBS, and then 250 µl of Rhodamine phalloidin (Sigma-Aldrich) diluted at 1: 4000 in PBS was added and incubated in the dark for a minimum of 45 min. Cells were washed again three times with PBS. Excess fluid was removed and coverslips were placed on top of a 3 µl drop of DAPI on a glass slide. Once dried, nail varnish was used to seal the coverslips. Slides were then ready to be viewed using confocal microscopy or stored at 4^{o}C in the dark.

2.6.3 Late endosomal stain

IECs were prepared as described in Section 2.5. For visualisation of the late endosome, protein marker lysosome associated membrane protein 1 stain (Lamp-1 (H4A3): sc-20011) from Santa Cruz Bio technology Inc (Texas, USA) was used at a concentration of 1:100 according to the manufacturer's recommendations. The cells were infected with *C. jejuni* 11168H wild-type, *cadF* or *flpA* mutants for 2 h. After co-incubation with bacterial cells, the cells were washed three times with PBS, and then 250 µl of the lamp-1 conjugated with Alexa Fluor 647 (far red) was added to the cells and incubated for 1 h. Cells were washed again three times with PBS. Excess fluid was removed and coverslips were placed on top of a 3 µl drop of DAPI on a glass slide. Once dried, nail varnish was used to seal the coverslips. Slides were then ready to be viewed using confocal microscopy or stored at 4ºC in the dark.

2.6.4 Differential staining of adherent and intracellular bacteria

Cells were prepared as described in Section 2.5. Briefly, after the 2 h bacterial infection, cells were washed in sterile PBS to remove non-adherent bacteria and fixed by incubating infected cells in 500 µl of 3.7% PFA for 1 h at RT. Cells were blocked by incubating in blocking solution for 1 h at RT. To detect adherent bacteria, cells were probed with rabbit anti-*Campylobacter* polyclonal antibody at a concentration of 1:1000 (Abcam, Cambridge, UK) diluted in blocking solution for 1 h at RT or overnight at 4ºC. Following incubation with primary antibody, the cells were washed three times with PBS and 0.1% (v/v) Tween 20 for 5 min for each wash. The cells were incubated with secondary antibody Alexa Fluor far red conjugated mouse anti-rabbit anti-*Campylobacter*(Abcam anti-mouse ab25245) at a concentration of 1:1000 for 30-45 min. These steps were performed prior to cell permeabilisation at RT in the dark. 30 µl per well of intracellular bacteria were not stained with primary or secondary antibody since once bacteria were internalised, cells were not permeabilised and remained green (GFP). Cells were further washed with PBS three times. Excess fluid was removed and coverslips were placed on top of a 3 µl drop of DAPI on a glass slide. Once dried, nail varnish was used to seal the coverslips. Slides were viewed using confocal microscopy or

stored in the fridge at 4ºC in the dark. In each experiment, non-infected cells were used as internal controls of IECs auto-fluorescence. Adherent bacteria appear red as they have been stained red, while intracellular GFP *C. jejuni* appear green only.

2.7 Statistical analysis

Differences between mean values were tested for significance by performing unpaired two-tailed Student's tests using the GraphPad Prism software version 7.0 (GraphPad Software, California, USA).

CHAPTER THREE: COMPARISON OF THE EFFECTS OF MUTATION OF *cadF* or *flpA* IN THE 11168H AND 81-176 WILD-TYPE STRAINS

3.1 Introduction

Both *cadF* and *flpA* are highly conserved genes in *C. jejuni* (Flanagan et al., 2009, Konkel et al., 1997). Gene regulation in bacteria usually occurs at the level of transcription, when RNA polymerase transcribes genes to mRNA. Promoter sequences are usually located upstream of a gene and are the region that RNA polymerase binds to during the initiation of transcription. Different promoter activity levels were observed during expression of the two fibronectin binding proteins CadF and FlpA (Scanlan et al., 2017). This data showed that promoter region activity of *cadF* was at a higher level compared to promoter region activity of *flpA* in both the 11168 and 81-176 wild-type strains. However, there was a small increase in promoter activity of *flpA* in the 81-176 strain in comparison to promoter activity of *flpA* in the 11168 strain. The difference was linked to the different status of DNA supercoiling in the respective strains. The genomic DNA in the 11168 strain is more negatively supercoiled compared to the more relaxed genomic DNA in the 81-176 strain (Eoin Scanlan, PhD Thesis, UCD, 2014).

In addition, a previous study performed at the LSHTM showed that both the 81-176 *cadF* and *flpA* mutants had a similar significant reduction in bacterial interactions with intestinal epithelial cells (IECs). However, the 81-176 *flpA* mutant displayed a more pronounced reduction in bacterial invasion of IECs compared to the 81-176 *cadF* mutant (Neveda Naz, PhD Thesis, LSHTM, 2014). This suggested that FlpA plays a more important role in *C. jejuni* invasion than CadF, even though based on promoter activity levels, CadF may be expressed at higher levels than FlpA.

In many *C. jejuni* research studies, the strains used varies for example from recent clinical isolates to laboratory wild-type strains, to mutants constructed in lab, from less motile to highly motile strains, from non-invasive to highly invasive strains. In addition, the use of different experimental conditions together with the use of different tissue culture cell lines adds further confusion to an already complicated research area, making interpretation and comparison of different data sets more difficult. Because of all these factors, many of the results reported are diverse.

Due to the non-consensus over many of the mechanisms of *C. jejuni* interactions with human IECs described in the literature, further investigations are required to confirm whether the highly diverse data is strain-specific or species-specific.

Therefore, the aim of this chapter was to investigate and compare the role of the fibronectin binding proteins CadF and FlpA between two different *C. jejuni* wild-type strains and respective *cadF* and *flpA* mutants.

3.2 Results

3.2.1 Bioinformatic analysis of CadF and FlpA in the NCTC 11168 and the 81-176 strains

The similarity in nucleotide and amino acid sequences between CadF and FlpA from different strains was investigated. Gene sequences were obtained from NCBI and pairwise sequence alignment analysis was performed using ClustalW (Thompson et al., 1994). In the *C. jejuni* NCTC 11168 genome sequence, CadF is annotated as Cj1478c (an outer membrane fibronectin-binding protein) and FlpA as Cj1279c (a putative fibronectin domain-containing lipoprotein). In the 81-176 genome sequence, CadF is annotated as Cj81176_1471 (a fibronectin-binding protein) and FlpA is annotated as CJJ81176_1295 (a fibronectin type III domain protein) (Gundogdu et al., 2007).

Sequence alignment analysis showed CadF in NCTC 11168 differs from CadF in 81-176 at four amino acids at the N-terminus (Figure 3.1). In row 1 of Figure 3.1, one is a semi-conserved substitution where a serine is in the 81-176 strain whilst a glycine is in the NCTC 11168 strain. The other is a conserved substitution where an isoleucine is in the 81-176 strain and a phenylalanine is in the NCTC 11168 strain. In row 4, one is a non-conserved substitution where the 81-176 strain has a proline compared to an alanine in the NCTC 11168 strain and a conserved substitution of an alanine compared to a threonine.

Based on the sequence alignment analysis of CadF in the NCTC 11168 and 81-176 strains, FlpA was speculated to be highly conserved. FlpA showed seven amino acid differences (Figure 3.2), thus making it more difficult to infer FlpA function only by sequence analysis. In row 1 of Figure 3.2, the 81-176 strain has a glycine compared to a serine in the NCTC 11168 strain; in row 2, the 81-176 strain has a serine compared to a proline in the NCTC 11168 strain. In row 4, the 81-176 strain has a glutamic acid compared to a glycine in the NCTC 11168 strain and a proline compared to a serine. In row 5, the 81-176 strain has an asparagine

compared to a serine in the NCTC 11168 strain, a methionine compared to an isoleucine and a valine compared to an alanine. One of these amino acid differences is conserved, three are semi-conserved and three are non-conserved substitutions (Figure 3.2). However, none of the identified amino acid differences is in the conserved fibronectin binding motif.

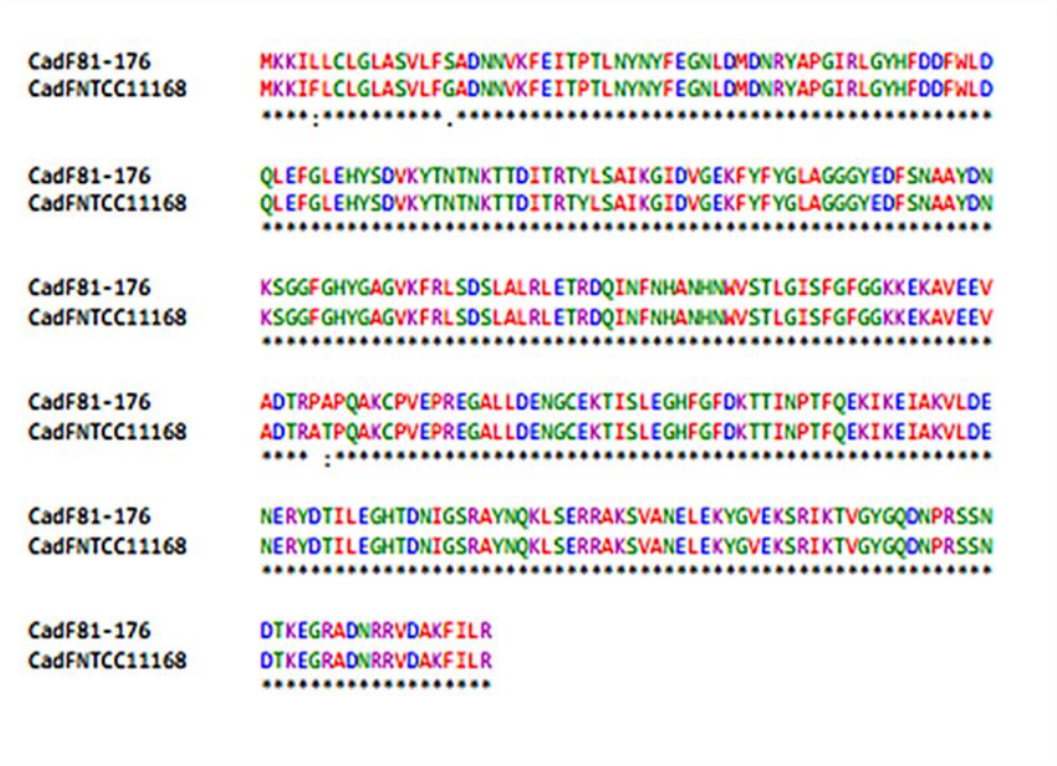

Figure 3.1. ClustalW output showing multiple sequence alignment of CadF from the NCTC 11168 and 81-176 wild-type strains. An "*" indicates a fully conserved amino acid; a ":" indicates conservation between amino acids with strongly similar properties; a "." indicates conservation between amino acids with weakly similar properties.

Figure 3.2. ClustalW output showing multiple sequence alignment of FlpA from the NCTC 11168 and 81-176 wild-type strains. An "*" indicates a fully conserved amino acid; a ":" indicates conservation between amino acids with strongly similar properties; a "." indicates conservation between amino acids with weakly similar properties.

Further pairwise sequence alignments showed there was 98.7% identity and 98.7% similarity for CadF (Figure 3.1) and 98.3% identity and 98.8 similarity for FlpA (Figure 3.2) between strains NCTC 11168 and 81-176. Even though more variation was observed in the FlpA protein sequence compared to the CadF protein sequence, the two proteins are suggested to have almost identical roles in both strains. CadF and FlpA showed binding ability to fibronectin in both the 11168H and 81-176 strains (see Section 3.2.10).

However, for the NCTC 11168 CadF and FlpA proteins sequences, there is only 19.8% identity and 32.2% similarity between them (Figure 3.3). This suggested that although there maybe functional differences between the two proteins, some function might be conserved between different strains, as CadF and FlpA do both function as fibronectin binding proteins in both the 11168H and 81-176 strains.

Figure 3.3. ClustalW output showing multiple sequence alignment of CadF and FlpA from the NCTC 11168. An "*" indicates a fully conserved amino acid; a ":" indicates conservation between amino acids with strongly similar properties; a "." indicates conservation between amino acids with weakly similar properties.

3.2.1.1 Predicted 3-D models of CadF and FlpA

To gain further insights into the structure, function and localisation relationship of CadF and FlpA, the amino acid sequences were submitted to the online tool Phyre (Kelley et al., 2015) and the highest score alignments were selected for comparison of 3-D structures. Predicting a 3-D model structure from an amino acid sequence provides three-dimensional information. A Ribbon diagram or Richardson diagram is the most common method used for representation of protein structures (Richardson, 1985). A ribbon diagram shows the organisation and path of the backbone proteins in a simple, basic molecular structure. Secondary protein structures such as an α-helix are depicted as coiled ribbons, whilst β-strands are depicted as an arrow with a pleat or thin line/tube. The CadF 3-D model was based on template c5wt1B crystal structure of the periplasmic portion of outer membrane protein2 a (ompa) a member of protein-like OmpA from *Capnocytophaga gingivalis*. The FlpA 3-D model was based on template c1zlgA a solution structure of the extracellular matrix protein anosmin1. Both have 100% confidence against the templates but the sequence coverage was 46% for CadF and 95% for FlpA. FlpA has three fibronectin binding motifs, which are simillar to fibronectin found in ECM hence the higher sequence coverage (95%). Cartoon ribbon diagrams were generated from the Phyre2 web portal for protein modeling, prediction and analysis (Kelley et al., 2015). However, limitations with homology detection are; if there is no known structure/template for the sequence to be modelled on, the modelling will be impossible and very unreliable and also the method cannot predict point mutations (Kelley et al., 2015).

Generally, proteins with a similar structure indicates proteins with a similar function, but it is not the case here with the generated 3-D structure models of CadF and FlpA. Although there is an apparent redundancy in *C. jejuni* 11168H between the CadF and FlpA homologues, the amino acid sequences of these two proteins with putatively similar functions are quite divergent (19.8% identity and 32.2% similarity) (see Figure 3.3). These differences are reflected in the 3-D model structure. However, it is unclear whether this sequence diversity reflects differences between their functions.

A

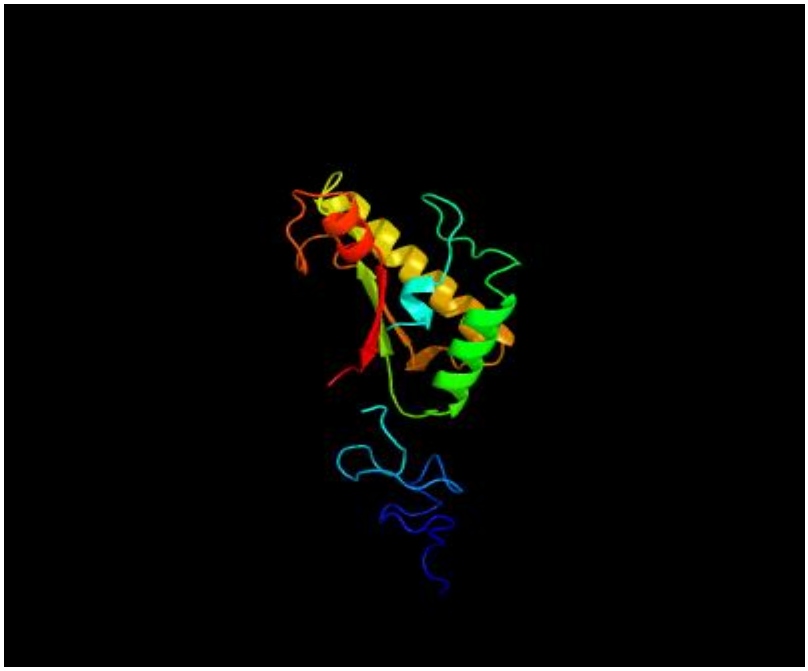

B

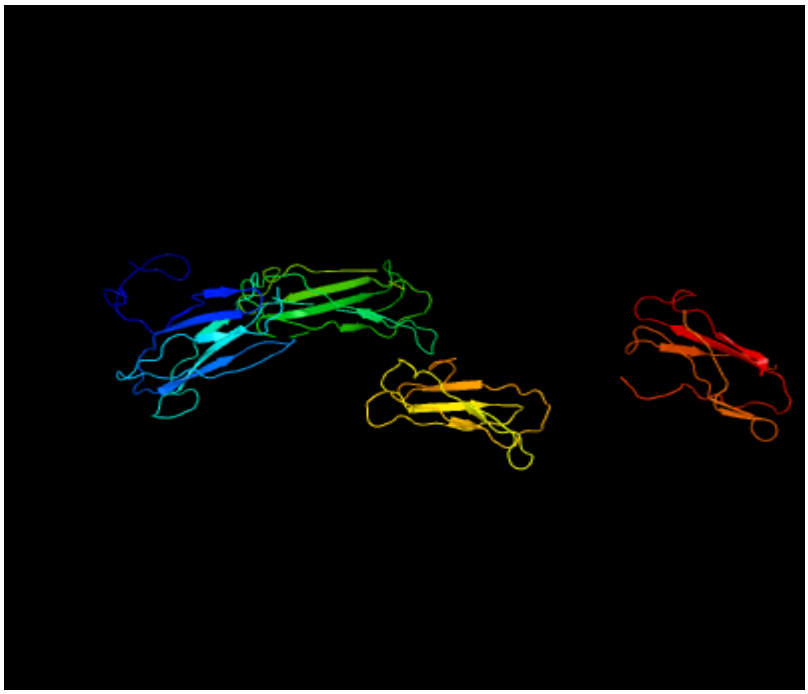

Figure 3.4. Predicted 3-D models of CadF and FlpA. The 3-D structures of CadF (A) and FlpA (B). The models are coloured based on the rainbow colouring scheme showing N-terminus (Blue) and C-terminus (Red). Related proteins have similar length and similar colour in a particular region of related proteins. The structure models were generated by Pyre2 (http://www.phyre).

3.2.2 Construction of a 11168H *cadF* mutant

To investigate the role of CadF in the 11168H wild-type strain, a 11168H *cadF* mutant was constructed via homologous recombination (Karlyshev and Wren, 2005). *cadF* Forward and *cadF* Reverse primers were designed to amplify a *cadF* gene fragment from 11168H genomic DNA (gDNA). A PCR reaction was performed then analysed using agarose gel electrophoresis to confirm the amplification of the correct sized fragment as described in Section 2.3.4. Then a PCR clean up was performed to purify the PCR product prior to ligation into the pGEMT-easy vector. The ligated PI vector was transformed into XL-2 Blue MRF competent cells and plated onto LB agar plates containing ampicillin. After incubation, any resulting blue colonies were indicative of negative transformants, whilst colourless colonies were indicative of positive transformants. Boilates from these positive colonies were screened for the presence of *cadF* by PCR. A kanamycin cassette was then inserted into the cloned *cadF* gene fragment. The resulting construct was pGEMT-easy-*cadF*-11168H-KanR which was transformed into XL-2 Blue MRF competent cells. Plasmid DNA from *E. coli* containing a construct with the kanamycin cassette in the correct orientation was used to electroporate *C. jejuni* 11168H competent cells, which were plated onto a non-selective CBA plate. The plate was incubated for 24 hours under microaerophilic conditions at 37ºC. A bacterial suspension in PBS was made from the resulting growth on the CBA plate. Two hundred microliters of this suspension was spread onto a fresh CBA plate supplemented with kanamycin and incubated under the same conditions for further 3 – 4 days.

gDNA was isolated from the putative 11168H *cadF* mutants and screened for insertion of the kanamycin cassette using gene specific primers (reverse and forward) using a standard PCR reaction. PCR products were analysed by gel electrophoresis. The amplified *cadF* mutant band was 2360 bps in size because of the successful insertion of the 1400 bp kanamycin cassette into the 960 bp *cadF* gene (Figure 3.5). The correct kanamycin cassette orientation was confirmed using kanamycin Forward out and *cadF* gene specific primers (data not shown).

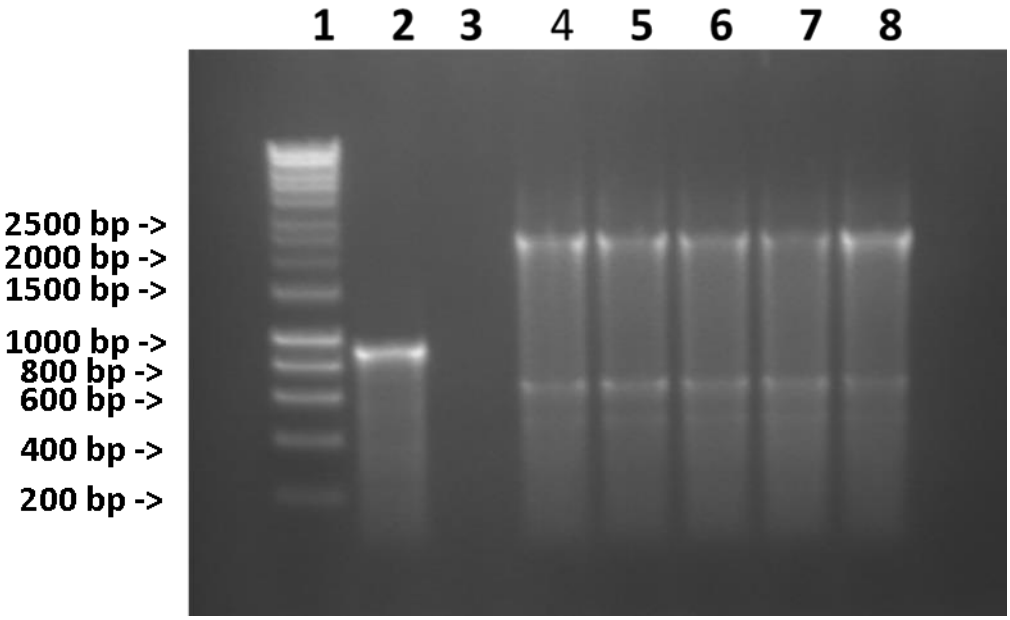

Figure 3.5. PCR verification of the construction of a *C. jejuni* 11168H *cadF* mutant. Lane 1: Ladder; Lane 2: Positive control; Lane 3: Negative control; Lane 4 – Lane 8: 11168H *cadF* mutants (clones 1-5).

3.2.3 Growth kinetics of the 11168H wild-type strain, *cadF* and *flpA* mutants

As an initial phenotypic investigation to assess the effect of the mutation of *cadF* and *flpA* in the 11168H strain, growth rate experiments were performed. Both the 11168H *cadF* and *flpA* mutants exhibited reduced growth rates compared to the wild-type strain during the early and mid log phases of growth. However, towards the late log phase, growth of the *cadF* and *flpA* mutants was similar to the level of wild-type strain. (Figure 3.6).

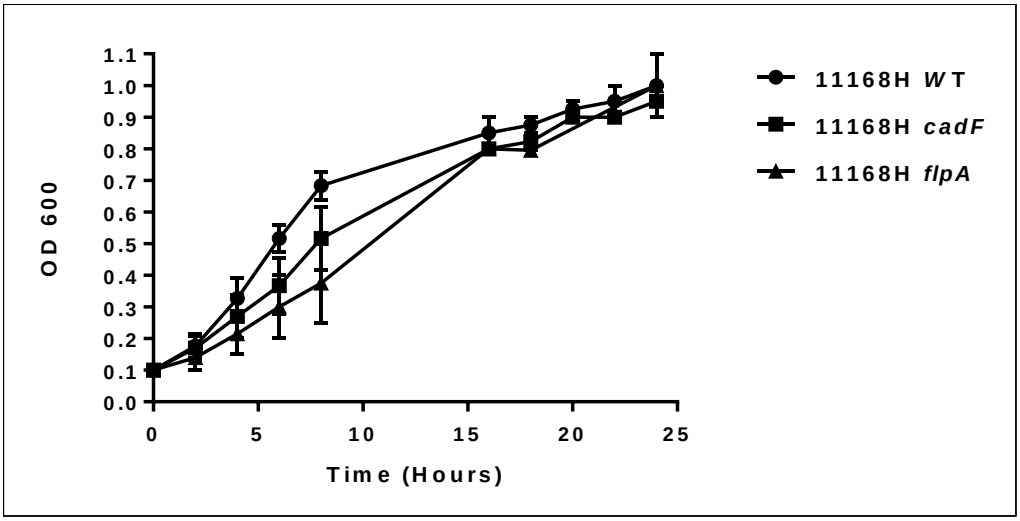

Figure 3.6. Representative growth curves of *C. jejuni* 11168H wild-type strain, *cadF* and *flpA* mutants. Brucella broth was inoculated with *C. jejuni* 11168H wild-type or mutant strains at an OD_{600} of 0.1 and incubated with constant shaking at 75 rpm under microaerobic conditions at 37^{o}C. At intervals of 2 h, 1 ml samples were removed and the OD_{600} recorded. Data shown are representative of three independent experiments.

3.2.4 Motility assay for 11168H wild-type strain, *cadF* and *flpA* mutants

C. jejuni displays rapid and darting motility that enables the bacteria to colonise the intestine of humans, animals and avians (Wassenaar et al., 1991, Black et al., 1988, Poly and Guerry, 2008). Mutation of *cadF* or *flpA* resulted in reduced motility in the 11168H strain (Figure 3.7). Initially at 24 h, both the wild-type strain and the *cadF* mutant exhibited similar motility, but the *flpA* mutant was less motile. At 48 h, the *cadF* mutant exhibited a similar reduction in motility as the *flpA* mutant. However, at 72 h, the *flpA* mutant exhibited a greater reduction in motility compared to the *cadF* mutant.

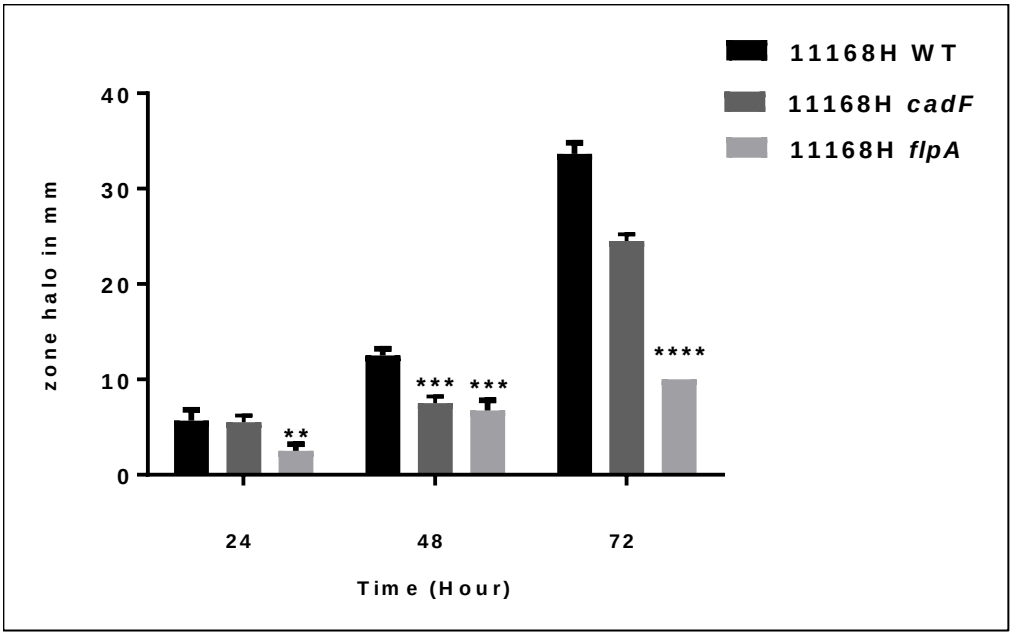

Figure 3.7. Motility assessment of 11168H wild-type strain, *cadF* and *flpA* mutants. Bacteria were grown for 24 h on blood agar plates. A suspension was prepared and adjusted to an OD_{600} of 1.0. 1.5 µl of this suspension was pipetted into the centre of soft agar plates and incubated at 37^{o}C under microaerobic conditions for 72 h. The level of motility was assessed by measuring the diameter of the growth halo at 24 h, 48 h and 72 h.

3.2.5 Growth kinetics of the 81-176 wild-type strain, *cadF* and *flpA* mutants

Both the 81-176 *cadF* and *flpA* mutants exhibited a similar growth rate compared to the wild-type strain. However, the *flpA* mutant exhibited a reduced growth rate during the late logarithmic / early stationary growth phases.

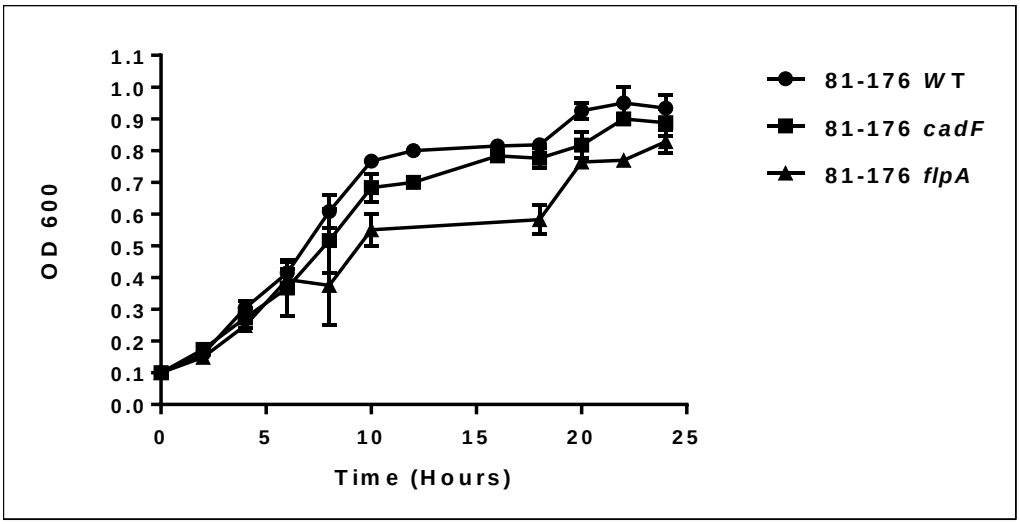

Figure 3.8. Representative growth curves of *C. jejuni* 81-176 wild-type strain, *cadF* and *flpA* mutants. Brucella broth was inoculated with *C. jejuni* 81-176 wild-type or mutant strains at an OD_{600} of 0.1 and incubated with constant shaking at 75 rpm under microaerobic conditions at 37^{o}C. At intervals of 2 h, 1 ml samples were removed and the OD_{600} recorded. Data shown are representative of three independent experiments.

3.2.6 Motility assay for 81-176 wild-type strain, *cadF* and *flpA* mutants

Mutation of *cadF* or *flpA* in the 81-176 wild-type strain reduced motility significantly. In addition, the f*lpA* mutant showed significantly reduced motility compared to the *cadF* mutant.

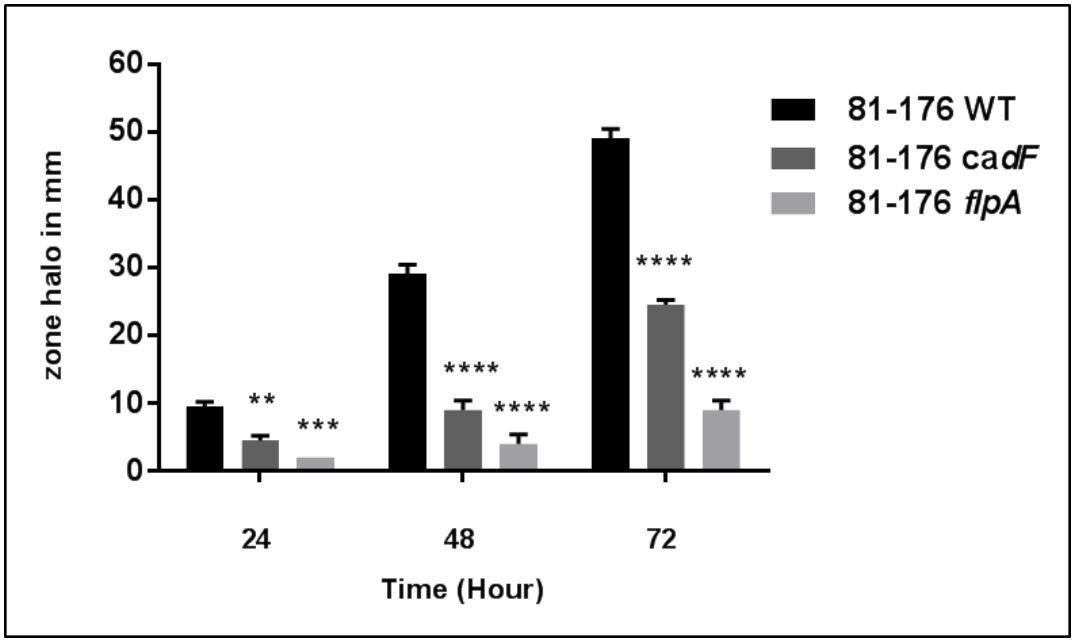

Figure 3.9. Motility assessment of 81-176 wild-type strain, *cadF* and *flpA* mutants. Bacteria were grown for 24 h on blood agar plates. A suspension was prepared and adjusted to an OD_{600} of 1.0. 1.5 µl of this suspension was pipetted into the centre of soft agar plates and incubated at 37°C under microaerobic conditions for 72 h. The level of motility was assessed by measuring the diameter of the growth halo at 24 h, 48 h and 72 h.

3.2.7 Gene expression analysis in the 11168H and 81-176 wild-type strains

A recent study investigating the impact of DNA supercoiling on promoter region activity showed that in both the 11168H and 81-176 wild-type strains, the promoter region of *cadF* exhibited a higher activity than the promoter region of *flpA.*

However, the promoter region of *flpA* in 81-176 was slightly more active than the promoter region of *flpA* in 11168H (Eoin Scanlan, PhD Thesis, UCD, 2014).

Gene expression in both the 11168H and 81-176 strains was analysed to investigate the extent of differences in *cadF* and *flpA* transcription in both strains.

3.2.7.1 RT-PCR analysis of cadF and flpA expression in the 11168H and 81-176 strains

The correlation between promoter region activity and the resulting transcription of genes was investigated to see whether higher promoter region activity resulted in higher levels of transcription. Total RNA was isolated from the 11168H and 81-176 wild-type strains and respective mutants. The mRNA was converted to cDNA using RT-PCR and then used as a template for amplification using standard PCR with either *cadF* or *flpA* primers. PCR products were analysed on an agarose gel. Resulting bands were further analysed using Image J software. Data analysis was performed by comparing the expressed density of the selected peaks (wild-type strain or mutants) relative to a standard peak (*gyrA*). The relative density was calculated by dividing the percentage value for each sample by the percentage value for the standard. The standard used was the *gyrA* primer band. In addition, the relative density for standard is 1 (expression of *gyrA)* (Table 3.1).

Table 3.1 Relative density for each selected Image J peak.

Sample	Area	Percent	Relative Density
11168H WT cDNA with flpA primer	757.406	2.655	0.206534422
11168H WT cDNA with cadF primer	8716.054	30.558	2.377129522
11168H WT cDNA with gyrA primer	3666.569	12.855	1
11168H cadF mutant cDNA with flpA primer	1738.891	6.097	0.47399518
11168H cadF mutant cDNA with gyrA primer	3668.861	12.863	1
11168H flpA mutant cDNA with cadF primer	6673.69	23.398	2.021600138
11168H flpA mutant cDNA with gyrA primer	3301.276	11.574	1

Figure 3.10 is a representative photo of an agarose gel showing that bands amplified from cDNA were less intense and smaller in size compared to bands amplified from gDNA isolated from wild-type strains.

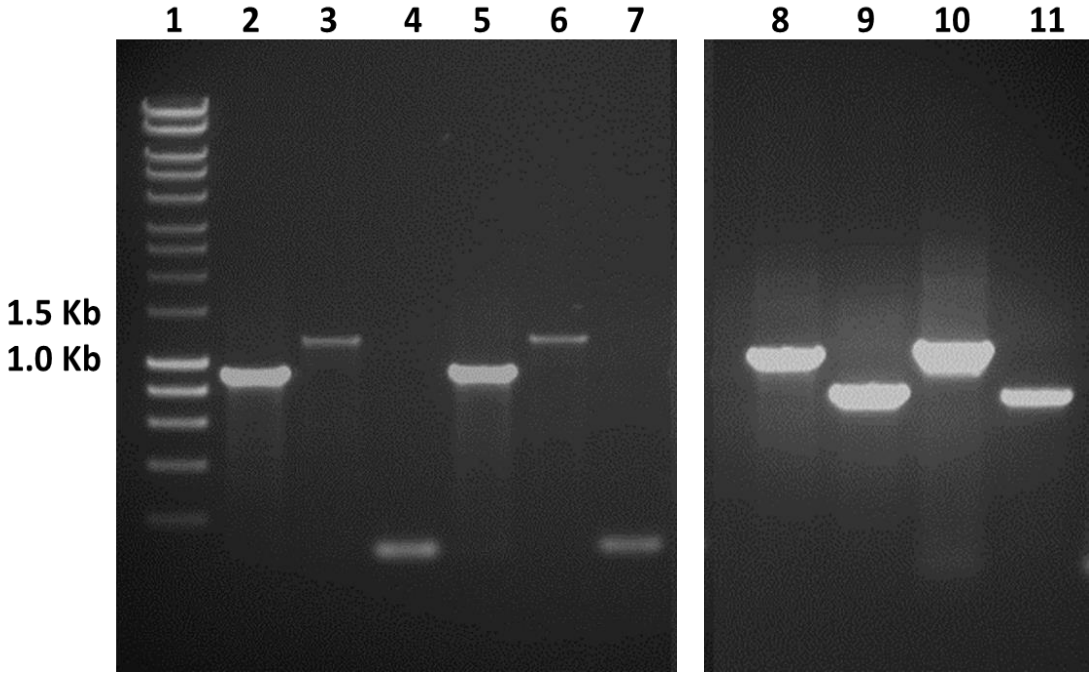

Figure 3.10. Comparison of *cadF* and *flpA* PCR products amplified from either genomic DNA or complementary DNA from the 11168H or 81-176 wild-type strains. Representative agarose gel electrophoresis of PCR products. Lane 1: Ladder; Lane 2: 11168H cDNA / *cadF* primers; Lane 3: 11168H cDNA / *flpA* primers; Lane 4: 11168H cDNA / *gyrA* primers*;* Lane 5: 81-176 cDNA / *cadF* primers; Lane 6: 81-176 cDNA / *flpA* primers; Lane 7: 81-176 cDNA / *gyrA* primers; Lane 8: 11168H gDNA / *flpA* primers; Lane 9: 11168H gDNA / *cadF* primers; Lane 10: 81-176 gDNA / *flpA* primers*;* Lane 11: 81-176 gDNA / *cadF* primers*.*

Both the 11168H and 81-176 wild-type strains were compared for expression of *cadF* and *flpA* (Figure 3.11). *cadF* was expressed at a higher level than *flpA* in both strains. In the 81-176 wild-type strain, *cadF* was expressed at a significantly higher level than in the 11168H wild-type strain ($p < 0.01$). Both 11168H and 81-176 wild-type strains expressed *flpA* at a lower level than *cadF* and at almost the same level with no significance difference between the 11168H and 81-176 strains. This data

supports the promoter region activity data showing that the *cadF* promoter region exhibited higher activity compared to the *flpA* promoter region in both the 11168 and 81-176 strains.

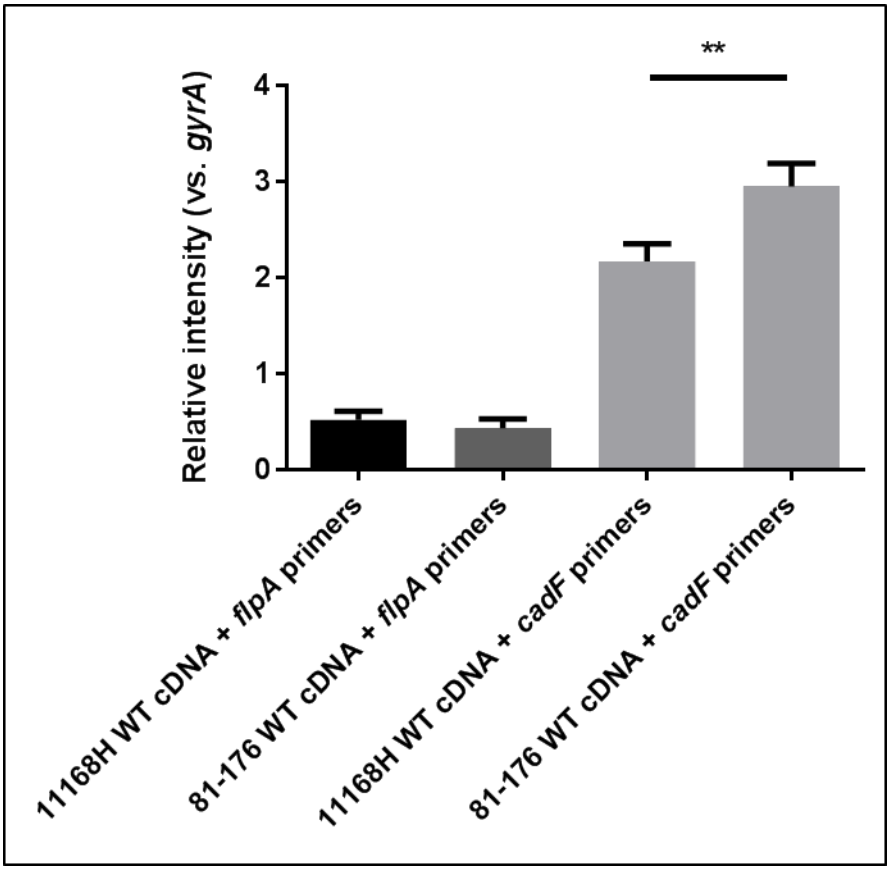

Figure 3.11. Increased expression of *cadF* in both 11168H and 81-176 wild-type strains. RNA from both wild-type strains was isolated and converted to cDNA by RT-PCR. cDNA was used as a PCR template using either *cadF, flpA* or *gyrA* primers. PCR products were analysed by agarose gel electrophoresis. Image J was used to quantify band intensities. *cadF* and *flpA* expression is presented relative to *gyrA* expression and is representative of at least triplicate experiments. ** denotes $p < 0.01$.

3.2.8 RT-PCR analysis of *cadF* and *flpA* expression in the 11168H *cadF* and *flpA* mutants

The expression of *cadF* was increased in the 11168H *flpA* mutant compared to the 11168H wild-type strain, suggesting that *cadF* expression is increased in the absence of FlpA.

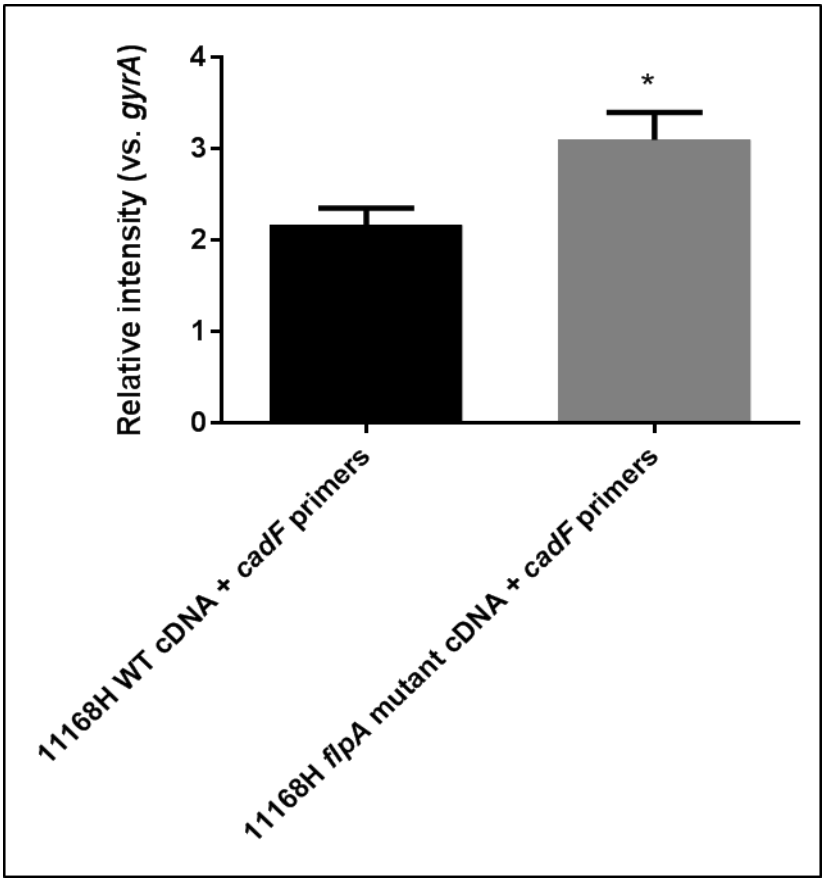

Figure 3.12. RT-PCR analysis of *cadF* expression in the 11168H wild-type strain and *flpA* mutant. RNA from the 11168H wild-type strain and *flpA* mutant were isolated and converted to cDNA by RT-PCR. cDNA was used as PCR template using *cadF* or *gyrA* primers. PCR products were analysed by agarose gel electrophoresis. Image J was used to quantify band intensities. *cadF* expression is presented relative to *gyrA* expression and is representative of at least triplicate experiments. * denotes $p < 0.05$.

In contrast, no significant changes in the expression of *flpA* were observed in the *cadF* mutant compared to the 11168H wild-type strain.

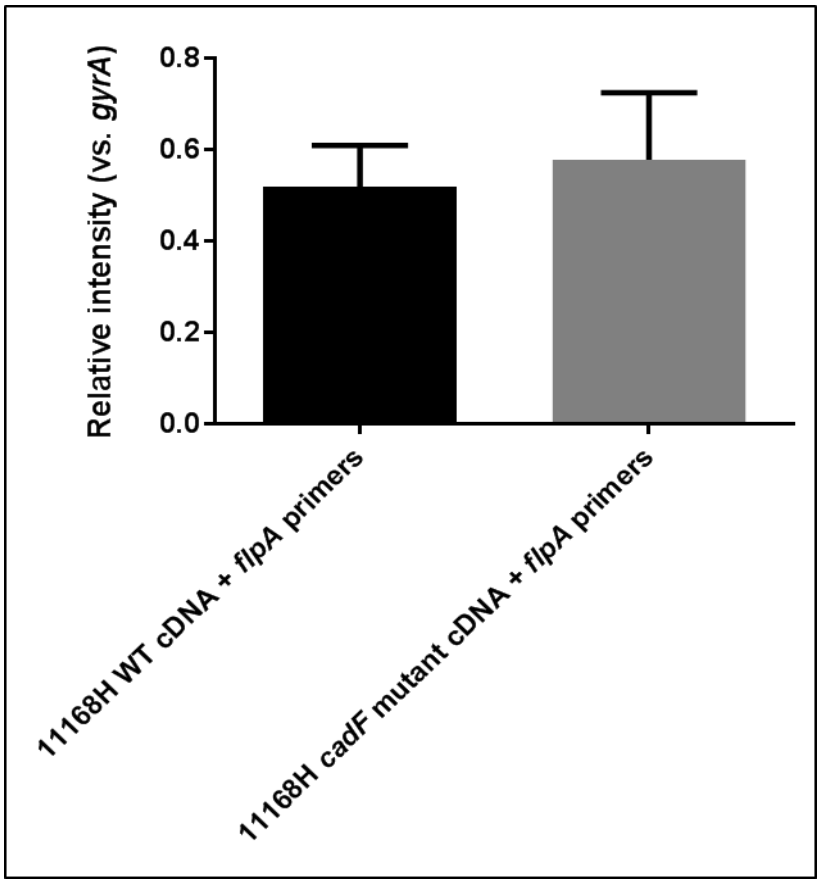

Figure 3.13. RT-PCR analysis of *flpA* expression in the 11168H wild-type strain and *cadF* mutant. RNA from wild-type strain and *cadF* mutant were isolated and converted to cDNA by RT-PCR. cDNA was used as PCR template using *flpA* or *gyrA* primers. PCR products were analysed by agarose gel electrophoresis. Image J was used to quantify band intensities. *flpA* expression is presented relative to *gyrA* expression and is representative of at least triplicate experiments.

3.2.9 RT-PCR analysis of *cadF* and *flpA* expression in the 81-176 *cadF* and *flpA* mutants

No significant changes in the expression of *cadF* were observed in the 81-176 *flpA* mutant compared to the 81-176 wild-type strain.

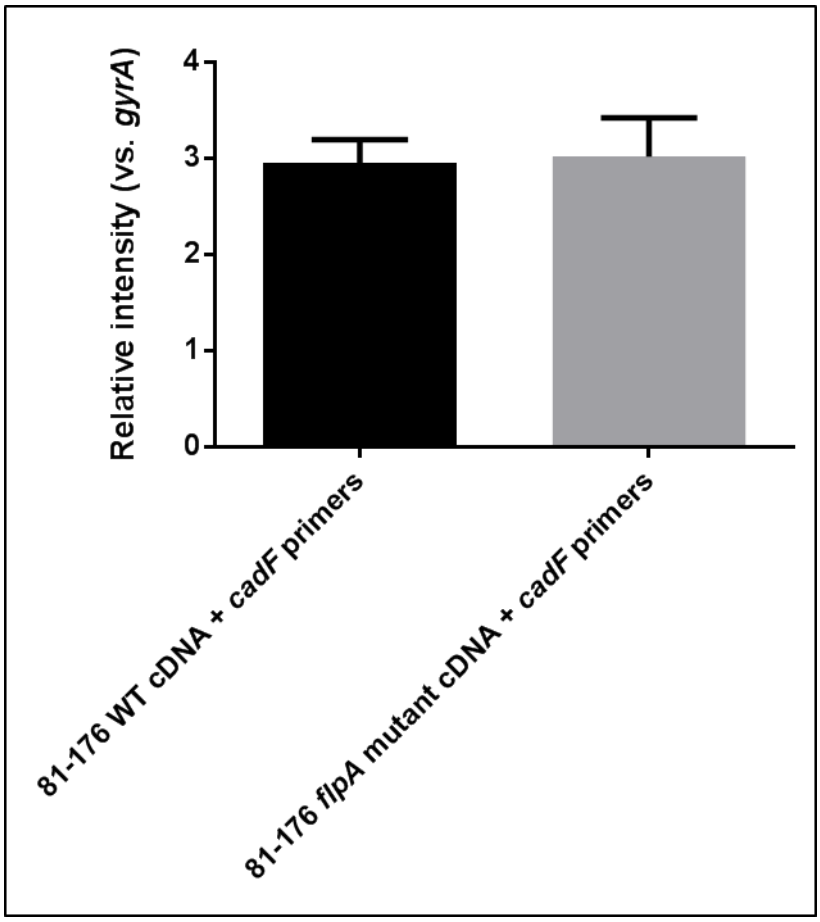

Figure 3.14. RT-PCR analysis of *cadF* expression in the 81-176 wild-type strain and *flpA* mutant. RNA from the 81-176 wild-type strain and *flpA* mutant were isolated and converted to cDNA by RT-PCR. cDNA was used as PCR template using *cadF* or *gyrA* primers. PCR products were analysed by agarose gel electrophoresis. Image J was used to quantify band intensities. *cadF* expression is presented relative to *gyrA* expression and is representative of at least triplicate experiments.

There was a non-significant increase in *flpA* expression observed in the 81-176 *cadF* mutant compared to the 81-176 wild-type strain.

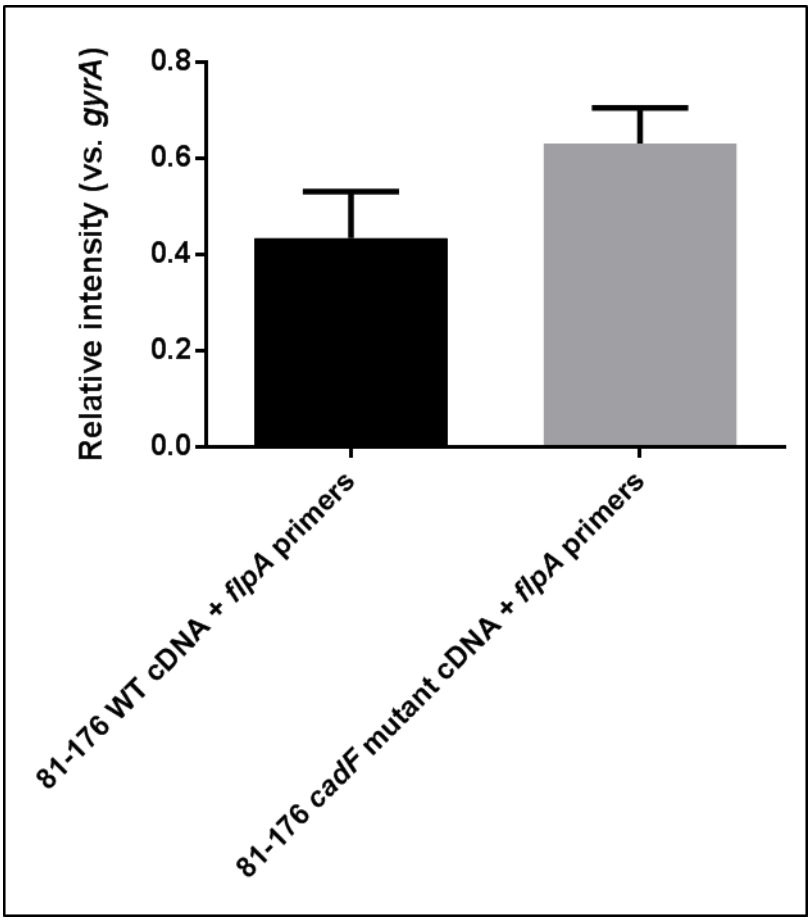

Figure 3.15. RT-PCR analysis of *flpA* expression in the 81-176 wild-type strain and *cadF* mutant. RNA from the 81-176 wild-type strain and *cadF* mutant were isolated and converted to cDNA by RT-PCR. cDNA was used as PCR template using *flpA* or *gyrA* primers. PCR products were analysed by agarose gel electrophoresis. Image J was used to quantify band intensities. *flpA* expression is presented relative to *gyrA* expression and is representative of at least triplicate experiments.

3.2.10 Binding to fibronectin *in vitro* of the 11168H and 81-176 wild-type strains

During colonisation, *C. jejuni* must interact with receptors on human IECs. Numerous *C. jejuni* proteins mediate this interaction with the multiple components of the IEC surface. Fibronectin binding plays an important role in the pathogenesis of many bacteria (Pankov and Yamada, 2002).

Fibronectin and laminin are components of the extracellular matrix of epithelial cells. CadF and FlpA are probably the most studied *C. jejuni* adhesions and are highly conserved amongst *C. jejuni* strains. Experiments were performed to investigate any differences in the binding capabilities of CadF and FlpA in the 11168H and 81-176 wild-type strains.

To determine if the binding capability of the 11168H and 81-176 wild-type strains to fibronectin was the same, fibronectin binding assays were performed. The data showed that the 81-176 wild-type strain binds to immobilised fibronectin at a significantly reduced level compared to the 11168H wild-type strain at both 15 min and 60 min time points. However, at 30 min, there was no significant difference observed in the level of fibronectin binding between 11168H and 81-176 wild-type strain.

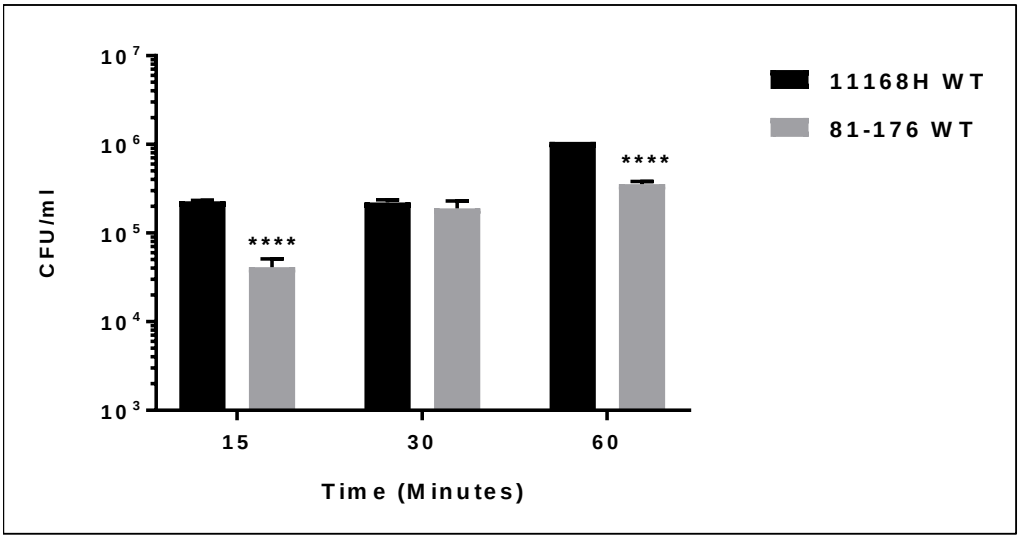

Figure 3.16 Fibronectin binding assays. Immobilised fibronectin in a 96 well plate was infected with inoculums of *C. jejuni* 11168H or 81-176 wild-type strains at OD_{600} of 0.1 (≈10^8 cfu/ml) for 15, 30 or 60 min. At the end of incubation period, wells were washed with PBS. Trypsin EDTA was used to detach adherent bacteria. Suspensions were serially diluted and plated on CBA plates. Data are representative of a minimum of triplicate biological replicates. **** denotes $p < 0.0001$.

3.2.11 Binding to fibronectin *in vitro* of the 11168H wild-type strain, *cadF* and *flpA* mutants

Mutation of either *cadF* or *flpA* in the 11168H strain resulted in reduced binding to immobilised fibronectin at all-time points (Figure 3.17). There was an increase in binding to fibronectin over time for both the 11168H wild-type strain and *cadF* mutant. For the 11168H *cadF* mutant, there was a steady increase in binding from 15 min to 60 min as was the case for the wild-type strain. It interesting to note that the *cadF* mutant could recover to the level of binding similar to that of the wild-type strain after 60 min (Figure 3.17A). However, mutation of *flpA* resulted in significantly reduced binding to immobilised fibronectin compared to the wild-type strain. The *flpA* mutant was not able to recover to the level of binding similar to that of the wild-type strain after 60 min (Figure 3.17B).

A

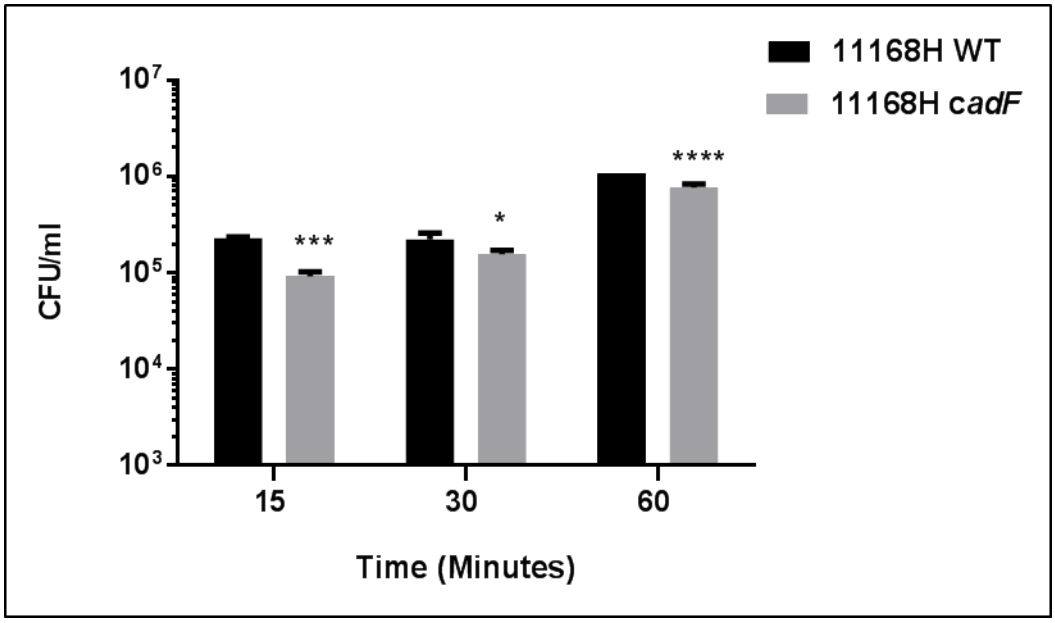

B

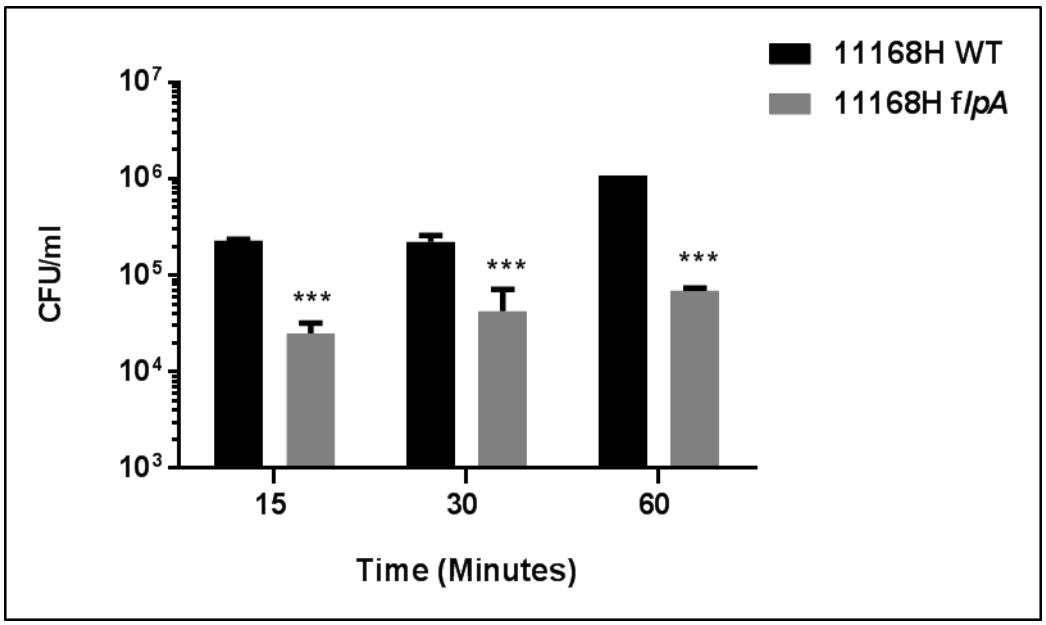

Figure 3.17. Fibronectin binding assays. Immobilised fibronectin in a 96 well plate was infected with inoculums of *C. jejuni* 11168H wild-type strain, *cadF* or *flpA* mutants at OD_{600} of 0.1 (≈10^8 cfu/ml) for 15, 30 or 60 min. At the end of incubation period, wells were washed with PBS. Trypsin EDTA was used to detach adherent bacteria. Suspensions were serially diluted and plated on CBA plates. Data are representative of a minimum of triplicate biological replicates. * denotes $p < 0.05$; *** denotes $p < 0.001$; **** denotes $p < 0.0001$.

3.2.12 Binding to fibronectin *in vitro* of the 81-176 wild-type strain, *cadF* and *flpA* mutants

Mutation of *cadF* or *flpA* in the 81-176 strain produced similar results as with the 11168H strain, with reduced binding to immobilised fibronectin compared to the wild-type strain (Figure 3.18). Both the 81-176 *cadF* and *flpA* mutants showed reduced binding, at both 30 and 60 min. However at 15 min this was not significant. At 60 min both the 81-176 *cadF* and *flpA* mutants showed reduced binding ($p < 0.0001$) compared to the wild-type strain. Also at this time point, the *cadF* mutant bound to fibronectin at a higher level compared to the *flpA* mutant.

A

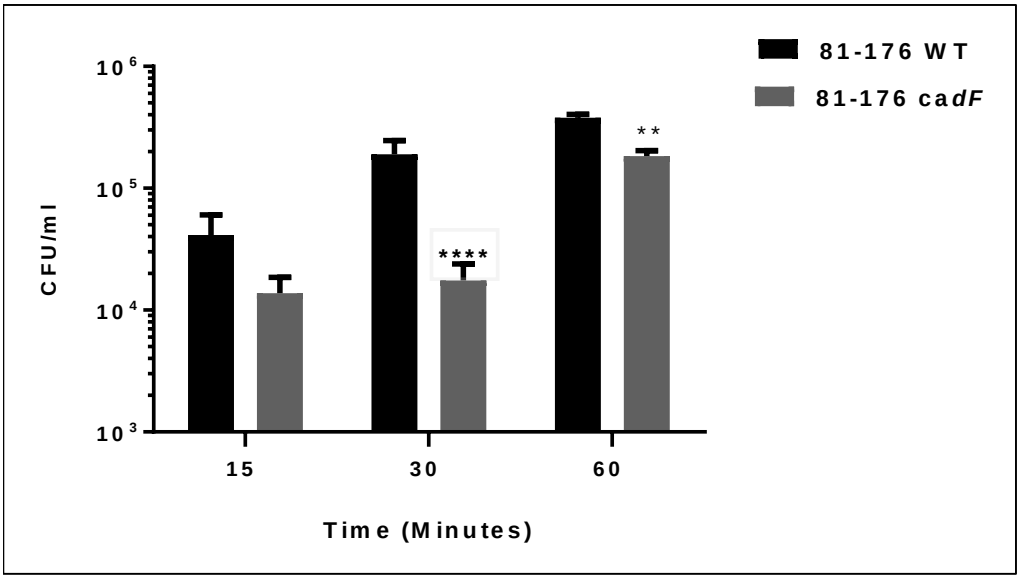

B

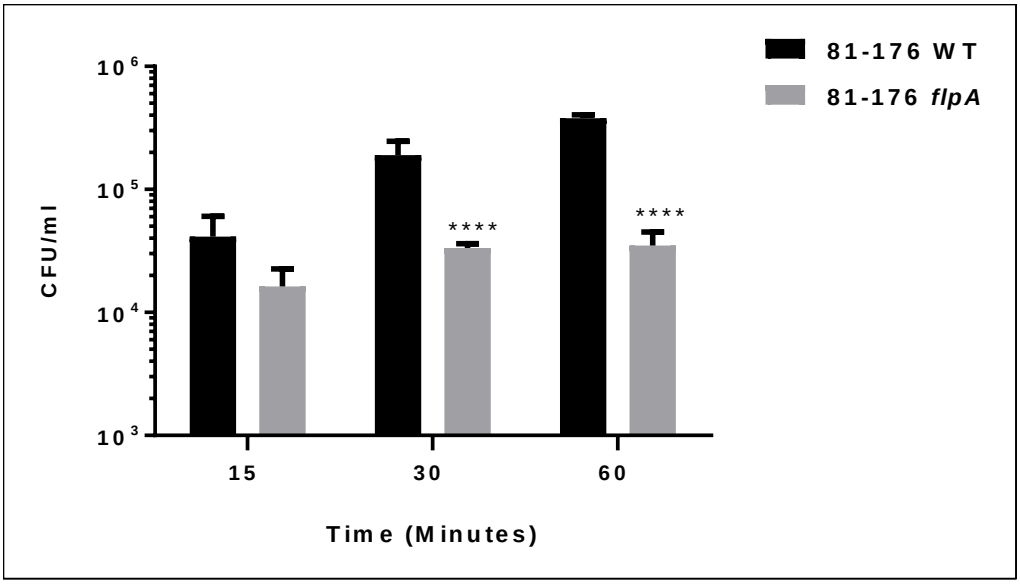

Figure 3.18. Fibronection binding assays. Immobilised fibronectin in a 96 well plate was infected with inoculums of *C. jejuni* 81-176 wild-type strain, *cadF* or *flpA* mutants at OD_{600} of 0.1 (≈10^8 cfu/ml) for 15, 30 or 60 min. At the end of incubation period, wells were washed with PBS. Trypsin EDTA was used to detach adherent bacteria. Suspensions were serially diluted and plated on CBA plates. Data are representative of a minimum of triplicate biological replicates. ** denotes p<0.01;**** denotes p < 0.0001.

3.2.13 Binding to laminin *in vitro* of the 11168H wild-type strain, *cadF* and *flpA* mutants

Laminin is a major component in the basal lamina, a layer of the extracellular matrix secreted by the epithelial cells. Data have shown that all strains of *H. pylori* bind to laminin at a higher affinity compared to *C. jejuni.* This comparison was made to investigate whether *C. jejuni* binds as efficiently to laminin as to fibronectin.

Laminin binding assays showed that the 11168H *cadF* mutant exhibited no significant difference in binding capacity to laminin compared to the 11168H wild-type strain (Figure 3.19). However, the 11168H *flpA* mutant exhibited a significantly reduced binding capacity ($p < 0.05$).

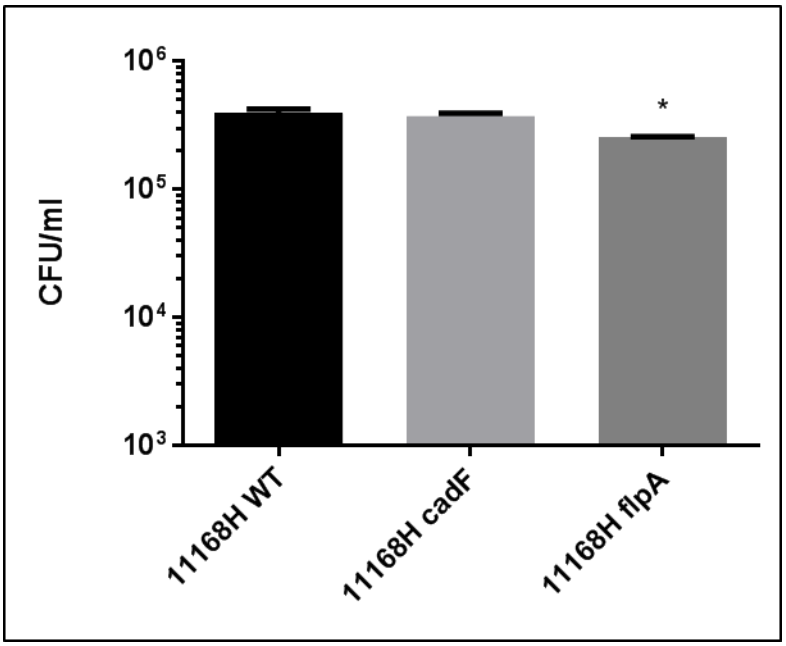

Figure 3.19. Laminin binding assays. Immobilised laminin in a 96 well plate was infected with inoculums of *C. jejuni* 11168H wild-type strain, *cadF* or *flpA* mutants at OD_{600} of 0.1 (≈10^8 cfu/ml) for 15, 30 or 60 min. At the end of incubation period, wells were washed with PBS. Trypsin EDTA was used to detach adherent bacteria. Suspensions were serially diluted and plated on CBA plates. Data are representative of a minimum of triplicate biological replicates. * denotes $p < 0.05$.

3.2.14 Binding to laminin *in vitro* of the 81-176 wild-type strain, *cadF* and *flpA* mutants

Laminin binding assays showed that the 81-176 *cadF* mutant exhibited no significant difference in binding capacity to laminin compared to the wild-type strain (Figure 3.20). However, the 81-176 *flpA* mutant exhibited a significantly reduced binding capacity ($p < 0.05$).

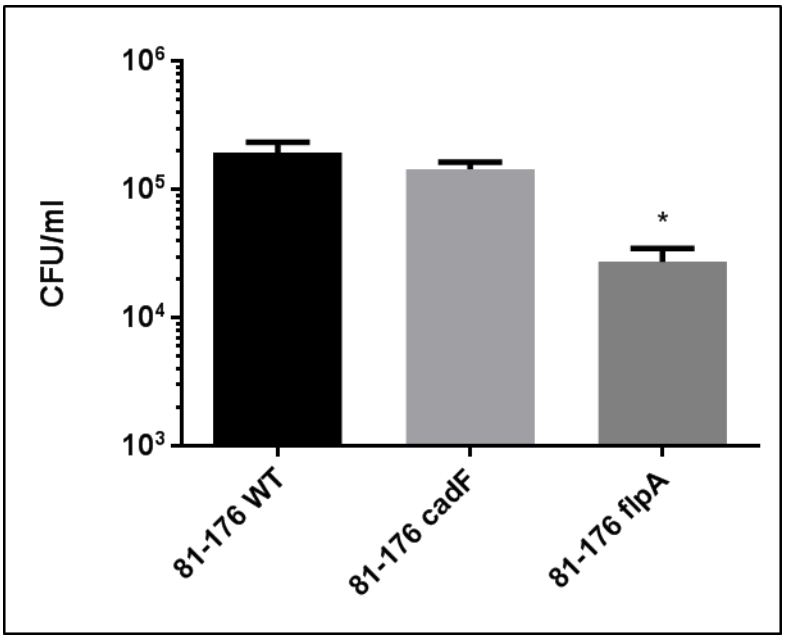

Figure 3.20. Laminin binding assays. Immobilised laminin in a 96 well plate was infected with inoculums of *C. jejuni* 81-176 wild-type strain, *cadF* or *flpA* mutants at OD_{600} of 0.1 (≈10^8 cfu/ml) for 15, 30 or 60 min. At the end of incubation period, wells were washed with PBS. Trypsin EDTA was used to detach adherent bacteria. Suspensions were serially diluted and plated on CBA plates. Data are representative of a minimum of triplicate biological replicates. * denotes $p < 0.05$.

3.2.15 *Galleria mellonella* model of infection for *C. jejuni*

Due to the lack of a convenient small animal model available to study *C. jejuni* pathogenesis, the use of insects as alternative models of infection has been developed. The human and insect immune systems, both humeral and cellular, share many similarities. Even though insects lack an acquired immune system which is mediated by B and T lymphocytes, they have a well-developed innate immune system that reacts rapidly to infectious agents (Harding et al., 2013, Senior et al., 2011). Insects have specialised phagocytic cells known as haemocytes that function to phagocytose pathogens and form aggregates that encapsulate and neutralise bacteria. These cells mimic mammalian phagocytic cells and produce bactericidal compounds such as superoxide (Harding et al., 2013, Senior et al., 2011). Activation of haemocytes triggers a phenol oxidase (PO) which results in melanisation and production of anti-microbial compounds (Lavine and Strand, 2002).

G. mellonella larvae have been widely used as a non-mammalian model for bacterial infection studies (Champion et al., 2009). Larvae can be infected at 37°C and possess haemocytes. To investigate the effect of mutation of *cadF* or *flpA* in the 11168H and 81-176 strains, experiments were performed using *G. mellonella* as a model of infection.

3.2.15.1 Melanisation in *G. mellonella* larvae infected with *C. jejuni*

Previous studies have shown that *G. mellonella* larvae are susceptible to bacterial infections. Haemolymph produces antimicrobials effectors that have been shown to inhibit growth of *L. monocytogenes* in an inhibition zone assay *(Mukherjee et al., 2010)*.

The melanisation reaction occurred when *G. mellonella* haemolymph was added to a lawn of *C. jejuni* (Figure 3.21A). This process was also reflected in the changing colour of larvae following injection of a *C. jejuni* inoculum (10^7 CFU/larvae) (Figure 3.21B). As early as 30 minutes post-infection, larvae colour turned to brown. In addition, these larvae later turned black and died within 48 hours. However, some larvae that turned brown but were still responsive to touch would return to a cream colour after 48 hours (data not shown). Larvae were counted as dead when the cream coloured larvae turned brown or black and were unresponsive to touch. No mortality of larvae was observed when injected with PBS or unchallenged.

A

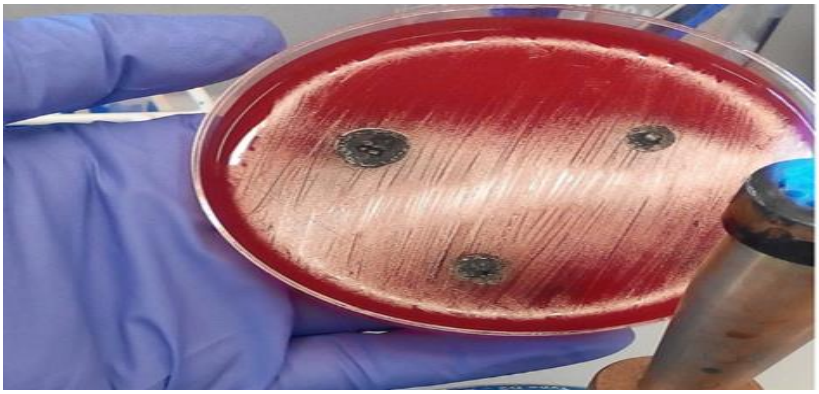

B

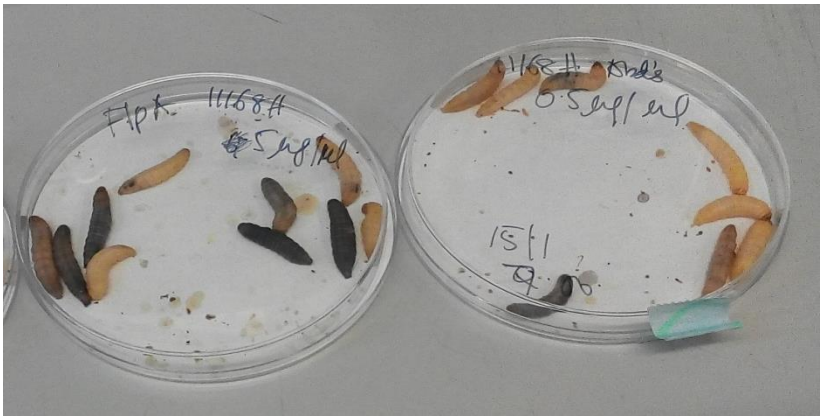

Figure 3.21. *C. jejuni* infection in *G. mellonella* larvae. A. *G. mellonella* melanisation process. Haemolymph from several larvae was collected and added onto a lawn of *C. jejuni* on a CBA plate then incubated at 37^{o}C for 48 hours. Zones of black granulation were observed where the haemolymph had been added. B. Corresponding colour change of larvae from cream to brown or black following infection with *C. jejuni.* 10 µl of OD_{600} 0.1 *C. jejuni* suspension in PBS was injected into a hind leg of each larvae (≈10^{7} CFU/larvae). Larvae were incubated at 37^{o}C for 48 hours. Survival was observed at 24 intervals.

3.2.15.2 *G. mellonella* model of infection with 11168H wild-type strain, cadF and flpA mutants

G. mellonella larvae were infected with the 11168H wild-type strain, *cadF* or *flpA* mutants (10 larvae for each strain). At intervals of 24 hours, survival was recorded. The 11168H wild-type strain was the most cytotoxic with more than 70% larval mortality compared to the 11168H *cadF* and *flpA* mutants, which both produced larval mortality below 50% (Figure 3.22). The 11168H *cadF* mutant killed significantly less larvae than the 11168H *flpA* mutant ($p < 0.01$). These results indicate that the *flpA* mutant is more cytotoxic to *G. mellonella* larvae than the *cadF* mutant in the 11168H strain. No mortality was observed with uninfected larvae, which received no *C. jejuni* inoculum or in larvae infected with only a PBS inoculum.

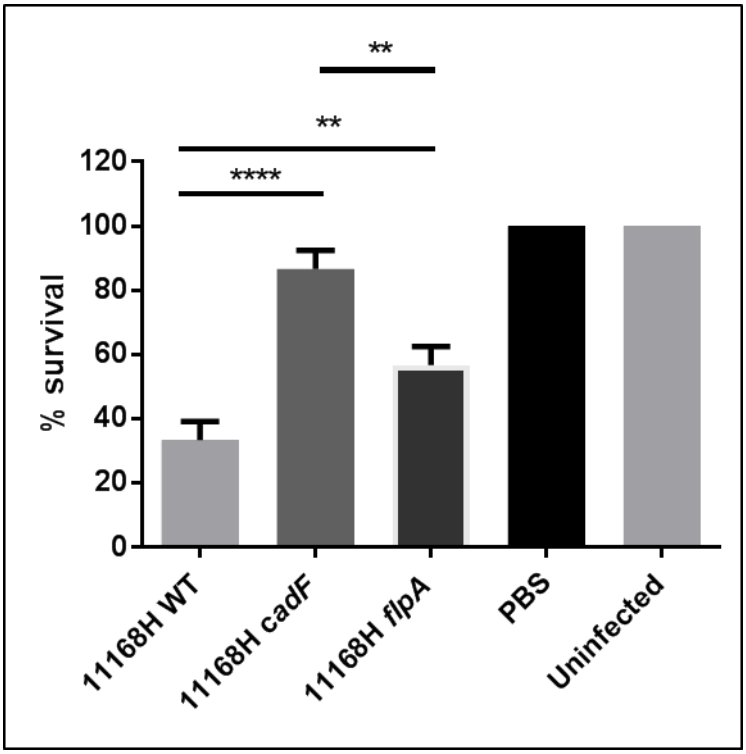

Figure 3.22. *G. mellonella* model of infection. Larvae was inoculated with 10 µl each of 11168H wild-type strain, *cadF* or *flpA* mutants at OD_{600} 0.1, equivalent to ≈10^7 CFU of *C. jejuni,* via the hind leg using a 10-gauge syringe. Larvae were incubated at 37^{o}C for the duration of the experiment. At intervals of 24 h, larvae were inspected for live or death counts. Inoculation with PBS was used as control. 10 larvae were used for every sample and data were from a minimum of three experiments. ** denotes $p < 0.01$ and **** denotes $p < 0.0001$.

3.2.15.3 *G. mellonella* model of infection with 81-176 wild-type strain, cadF and flpA mutants

G. mellonella larvae were infected with the 81-176 wild-type strain, *cadF* or *flpA* mutants (10 larvae for each strain). At intervals of 24 hours, survival was recorded. Mutation of *cadF* or *flpA* in the 81-176 strain reduced cytotoxicity in G*. mellonella* larvae compare to wild-type strain (Figure 3.23). The 81-176 wild-type strain was the most cytotoxic with 70% larval mortality. Moreover, the 81-176 *cadF* mutant

killed significantly less larvae with more than 90% survival than the 81-176 *flpA* mutant with 50% survival. This result also indicated that the *flpA* mutant is more cytotoxic than the *cadF* mutant to *G. mellonella* larvae in the 81-176 strain. Nevertheless, in comparison to the 11168H strain, the difference was not as high as in the 81-176 strain. No mortality was observed with uninfected larvae, which received no *C. jejuni* inoculum or in larvae infected with only a PBS inoculum.

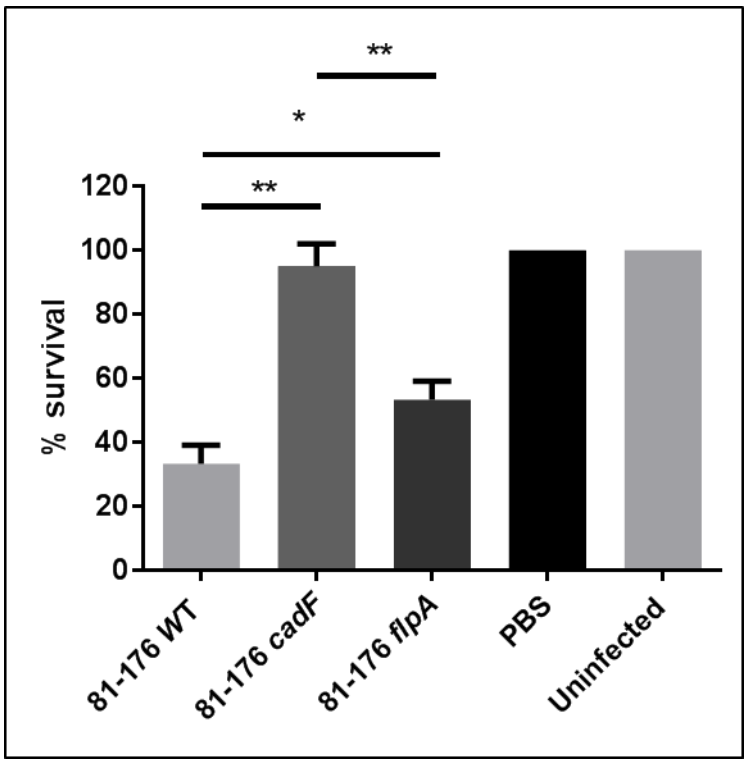

Figure 3.23. *G. mellonella* model of infection. Larvae were inoculated with 10 µl each of 81-176 wild-type strain, *cadF* or *flpA* mutants at OD_{600} 0.1, equivalent to ≈10^7 CFU of *C. jejuni,* via the hind leg using a 10-gauge syringe. Larvae were incubated at 37^{o}C for the duration of the experiment. At intervals of 24 h, larvae were inspected for live or death counts. Inoculation with PBS was used as control. 10 larvae were used for every sample and data were from a minimum of three experiments. * denotes $p < 0.05$ and ** denotes $p < 0.01$.

3.2.16 Interaction of 11168H wild-type strain, *cadF* and *flpA* mutants with T84 intestinal epithelial cells

Bacterial infection of IECs allows the investigation of both *C. jejuni* adhesion and invasion. The 11168H *cadF* mutant exhibited a reduced ability to interact (both adhesion and invasion) with T84 IECs compared to the wild-type strain with numbers of interacting bacteria lower but not significantly so. The increase in interaction between 3 h and 24 h was greater for the 11168H *cadF* mutant than for the wild-type strain (Figure 3.24A). There was a significant difference between the ability of the 11168H *flpA* mutant to interact with T84 IECs in comparison to the wild-type strain. The 11168H *flpA* mutant exhibited a reduced ability to interact with T84 IECs compared to the wild-type strain at 3 h, however this was not significant. The 11168H *flpA mutant* displayed a significant reduction in interaction at 24 h. The increase in interaction between 3 h and 24 h was greater for the 11168H *flpA* mutant than for the wild-type strain (Figure 3.24B).

A

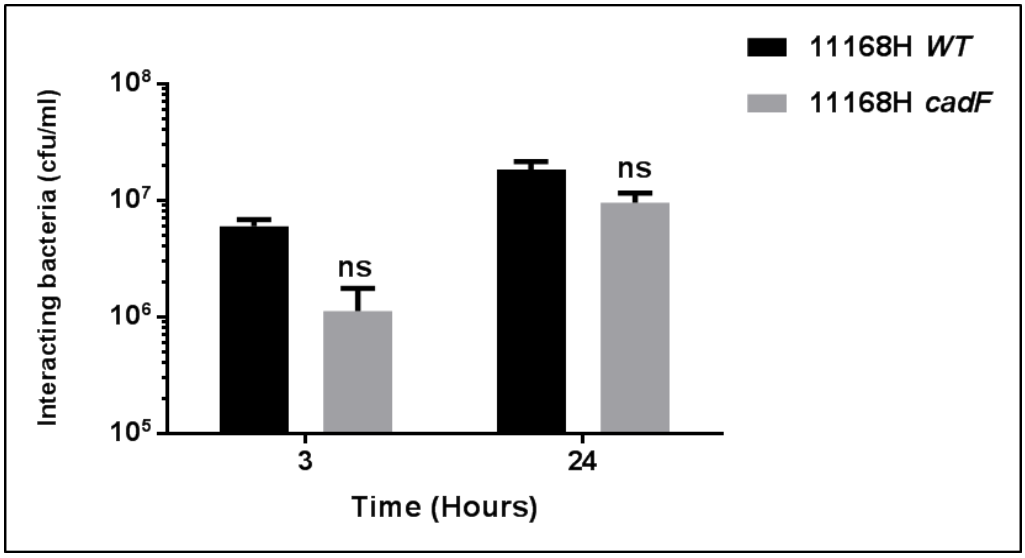

B

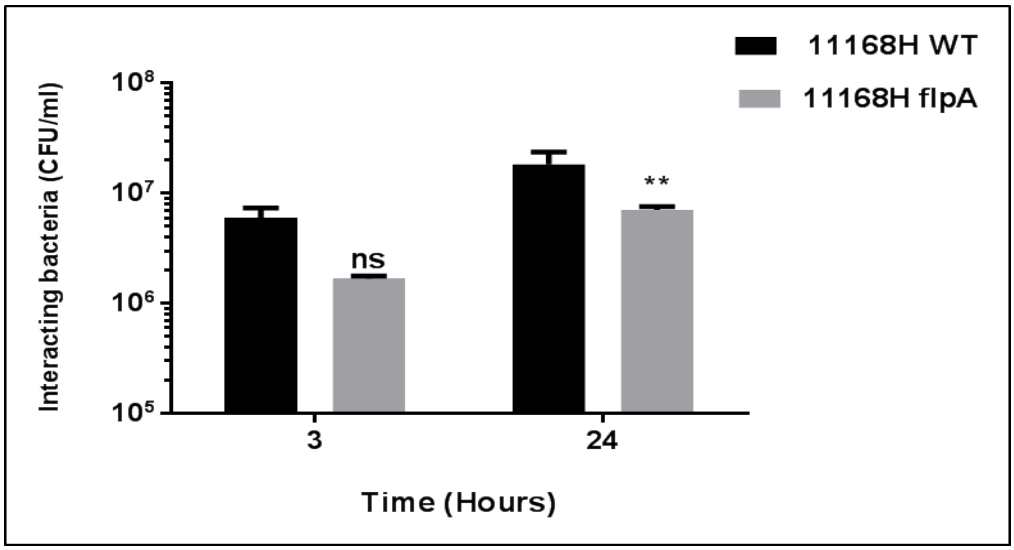

Figure 3.24. Interaction of *C. jejuni* 11168H wild-type strain, *cadF* and *flpA* mutants with T84 IECs. Confluent monolayers were infected with *C. jejuni* 11168H wild-type strain, *cadF* or *flpA* mutants and incubated for 3 h or 24 h. Triton X-100 was added following washes with PBS to lyse the cells. Serial dilutions of lysates were plated on CBA. After 48 h, CFU were counted. Data are representative of a minimum of triplicate biological replicates. ** denotes $p < 0.01$.

3.2.17 Invasion of 11168H wild-type strain, *cadF* and *flpA* mutants with T84 intestinal epithelial cells

Both 11168H *cadF* and *flpA* mutants displayed a significant reduction in invasion of T84 cells compared to the wild-type strain at both 3 h and 24 h time points. However, the invasion numbers for both mutants were still able to increase between 3 h to 24 h (Figure 3.25 A and B).

A

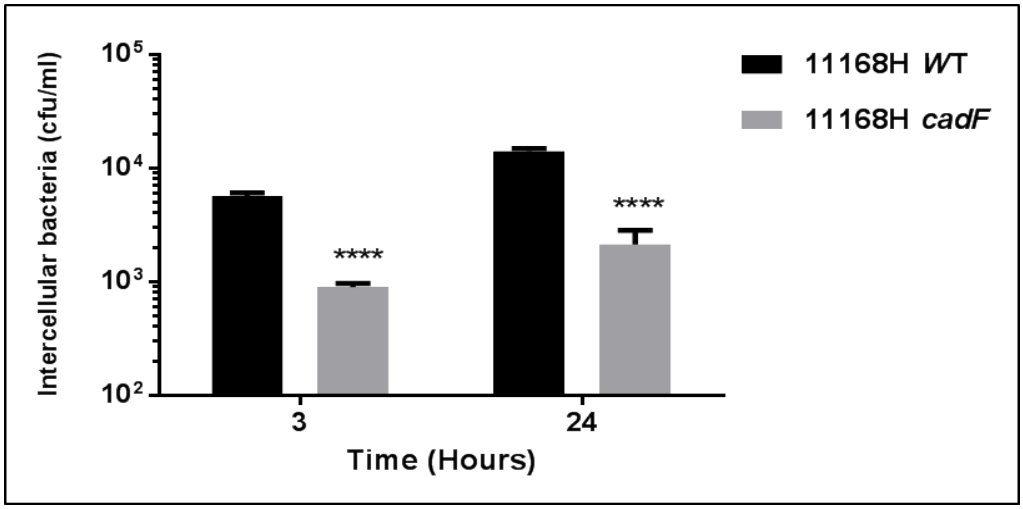

B

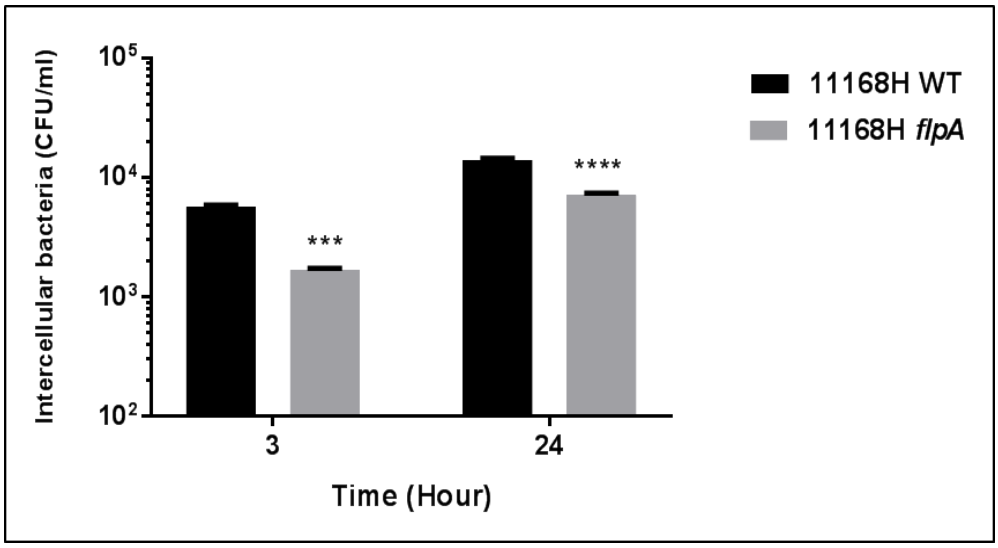

Figure 3.25. Invasion of *C. jejuni* 11168H wild-type strain, *cadF* and *flpA* mutants with T84 IECs. Confluent monolayers were infected with *C. jejuni* 11168H wild-type strain, *cadF* or *flpA* mutants and incubated for 3 h or 24 h. Following PBS washes, cells were further incubated with gentamicin (150 µg/ml) for 2 h to kill extracellular bacteria, then lysed with Triton X-100. Serial dilutions of lysates were plated on CBA. After 48 h, CFU were counted. Data are representative of a minimum of triplicate biological replicates. *** denotes $p < 0.001$; **** denotes $p < 0.0001$.

3.2.18 Interaction of 11168H wild-type strain, *cadF* and *flpA* mutants with Caco-2 intestinal epithelial cells

Caco-2 IECs was chosen to further investigate the interaction and invasion capability of 11168H *cadF* and *flpA* mutants. The 11168H *cadF* mutant exhibited a slightly reduced ability to interact with Caco-2 IECs compared to the wild-type strain with numbers of interacting bacteria lower but not significantly so. The increase in interaction between 3 h and 24 h was slightly greater for the 11168H *cadF* mutant than for the wild-type strain (Figure 3.26A). However, the 11168H *flpA* mutant exhibited a significant reduction in interaction with Caco-2 IECs at 3 h and 24 h compared to that of wild-type strain (Figure 3.26B). In addition, the interaction numbers for both mutants were still able to increase between 3 h to 24 h.

A

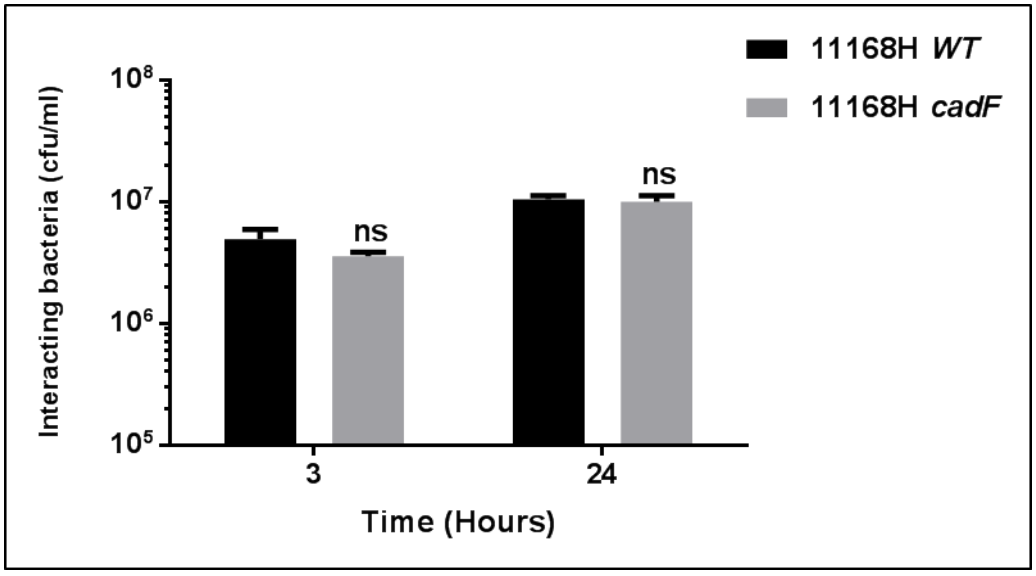

B

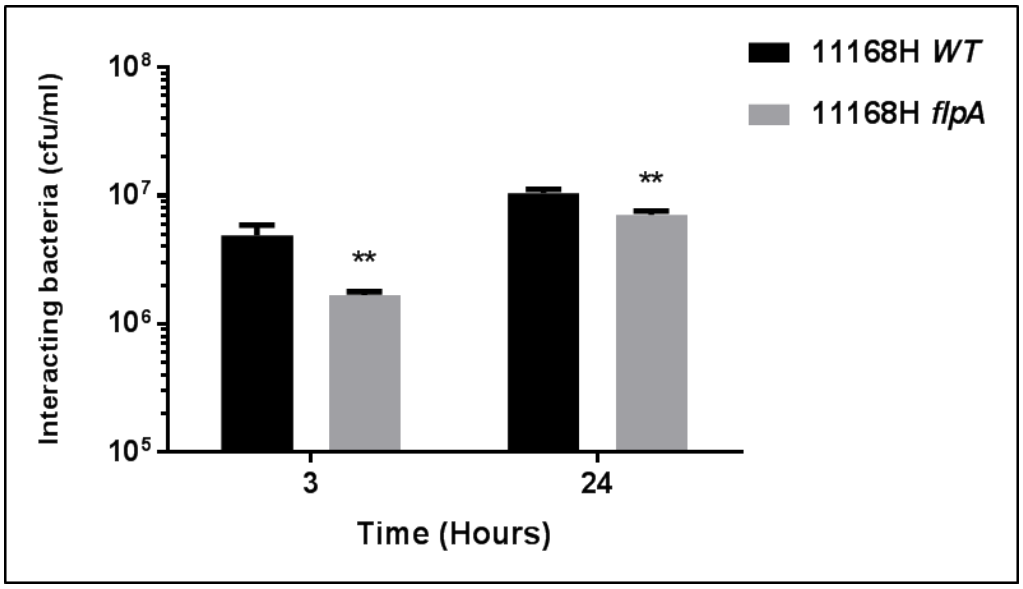

Figure 3.26. Interaction of *C. jejuni* 11168H wild-type strain, *cadF* and *flpA* mutants with Caco-2 IECs. Confluent monolayers were infected with *C. jejuni* 11168H wild-type strain, *cadF* or *flpA* mutants and incubated for 3 h or 24 h. Triton X-100 was added following washes with PBS to lyse the cells. Serial dilutions of lysates were plated on CBA. After 48 h, CFU were counted. Data are representative of a minimum of triplicate biological replicates. ** denotes $p < 0.01$.

3.2.19 Invasion of 11168H wild-type strain, *cadF* and *flpA* mutants with Caco-2 intestinal epithelial cells

Both the 11168H *cadF* and *flpA* mutants displayed a significant reduction in invasion of Caco-2 IECs compared to wild-type strain at both 3 h and 24 h time points. In addition, the invasion numbers were able to increase between 3 h to 24 h (Figure 3.27A and B). The *flpA* mutant exhibited a reduced level of invasion of Caco-2 IECs compared to the *cadF* mutant.

A

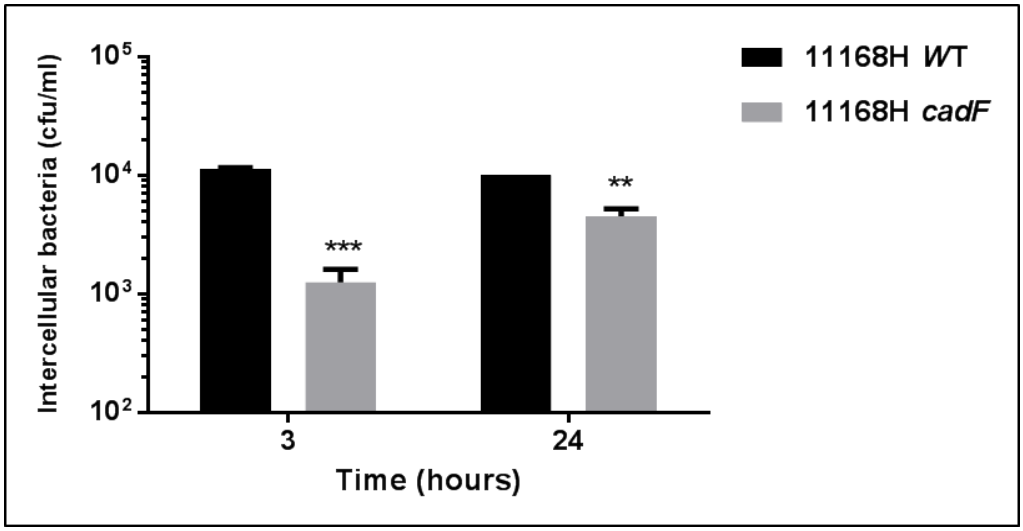

B

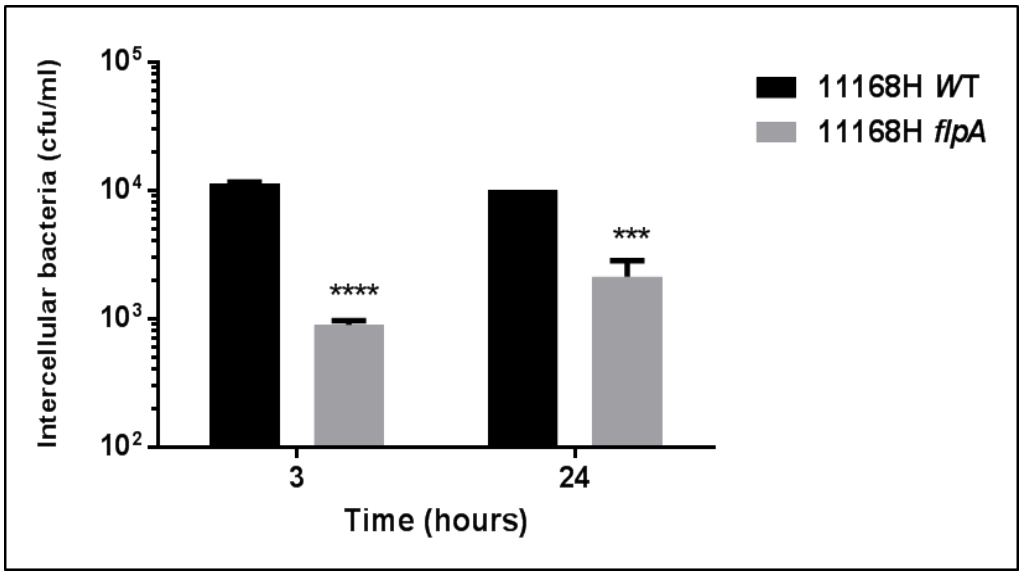

Figure 3.27. Invasion of *C. jejuni* 11168H wild-type strain, *cadF* and *flpA* mutants with Caco-2 IECs. Confluent monolayers were infected with *C. jejuni* 11168H wild-type strain, *cadF* or *flpA* mutants and incubated for 3 h or 24 h. Following the PBS washes, cells were further incubated with gentamicin (150 µg/ml) for 2 h to kill extracellular bacteria, then lysed with Triton X-100. Serial dilutions of lysates were plated on CBA. After 48 h, CFU were counted. Data are representative of a minimum of triplicate biological replicates. ** denotes $p < 0.01$; *** denotes $p < 0.001$; ****denotes $p < 0.0001$.

3.2.20 Comparison of interaction with T84 intestinal epithelial cells of 11168H & 81-176 *cadF* and *flpA* mutants

A previous study performed at the LSHTM showed that both the 81-176 *cadF* and *flpA* mutants had a similar significant reduction in bacterial interactions with intestinal epithelial cells (Neveda Naz, PhD Thesis, LSHTM, 2014). In this study, both 11168H *cadF* and *flpA* mutants exhibited a reduction in interactions with T84 cells compared to the wild-type strain at both 3 h and 24 h time points. However, the interaction numbers were able to increase between 3 h to 24 h. The increase of interaction at 24 h was greater for the 11168H *cadF* mutant than for the 11168H *flpA* mutant (Figure 3.28A). Both 81-176 *cadF* and *flpA* mutants also exhibited a reduction in interactions with T84 cells compared to the wild-type strain at both 3 h and 24 h time points. Again, the interaction numbers were able to increase between 3 h to 24 h. However, interaction of the 81-176 wild-type strain was the highest, the 81-176 *cadF* mutant was intermediate, and the 81-176 *flpA* mutant the lowest (Figure 3.28B).

A

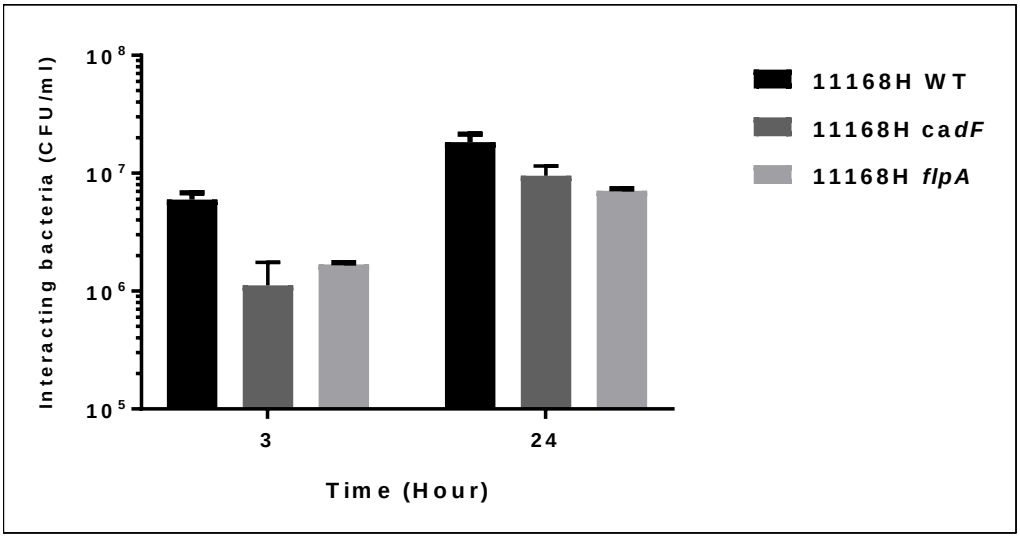

B

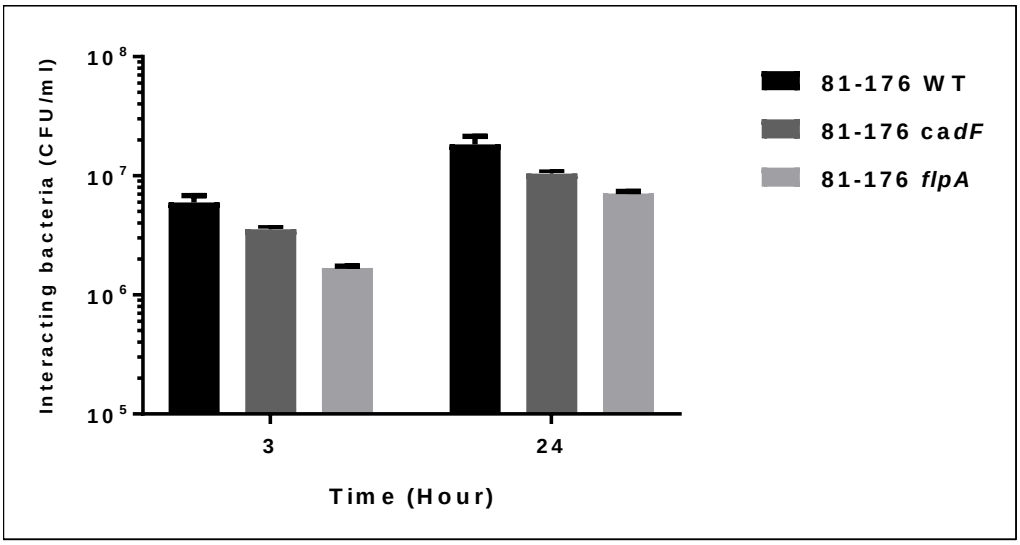

Figure 3.28. Interaction of *C. jejuni* 11168H & 81-176 wild type strains, *cadF* and *flpA* mutants with T84 IECs. Confluent monolayer cells were infected with *C. jejuni* 11168H or 81-176 wild type strains, *cadF* or *flpA* mutants and incubated for 3 h or 24 h. Triton X-100 was added following washes with PBS to lyse the cells. Serial dilutions of lysates were plated on CBA. After 48 h, CFU were counted. Data are representative of a minimum of triplicate biological replicates.

3.2.21 Comparison of invasion of T84 intestinal epithelial cells of 11168H & 81-176 *cadF* and *flpA* mutants

Both the 11168H *cadF* and *flpA* mutants displayed a significant reduction in invasion of T84 IECs compared to the wild-type strain at both 3 h and 24 h time points. However, the invasion numbers were able to increase between 3 h and 24 h. Interestingly, the 11168H *cadF* mutant exhibited a lower level of invasion of T84 IECs compared to the 11168H *flpA* mutant at both 3 h and 24 h (Figure 3.29A). Both the 81-176 *cadF* and *flpA* mutants also displayed a significant reduction in invasion of T84 IECs compared to the wild-type strain at both 3 h and 24 h time points. However, the invasion numbers decreased between 3 h and 24 h for the wild-type strain, whilst the *flpA* mutant showed similar numbers whilst only the *cadF* mutant showed increased numbers (Figure 3.29B).

A

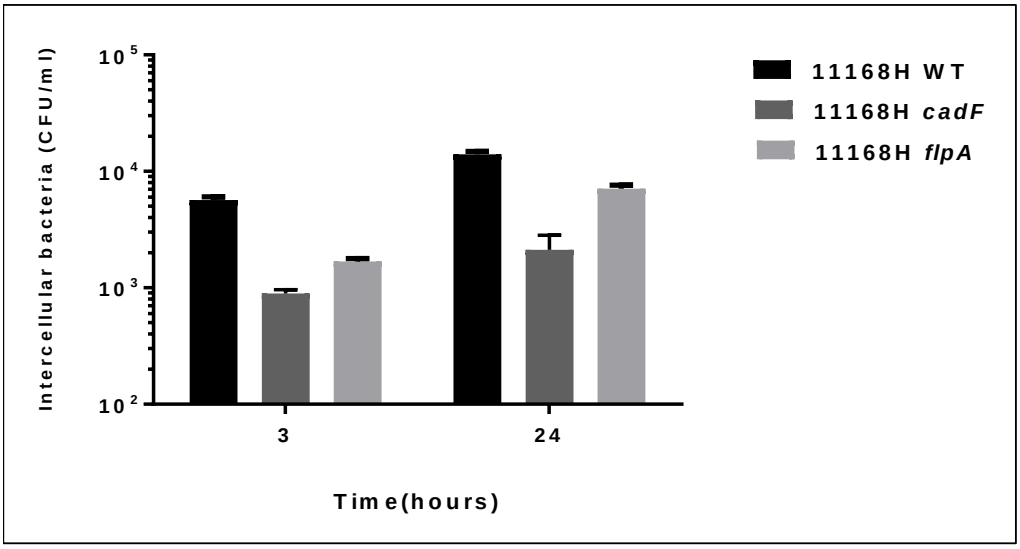

B

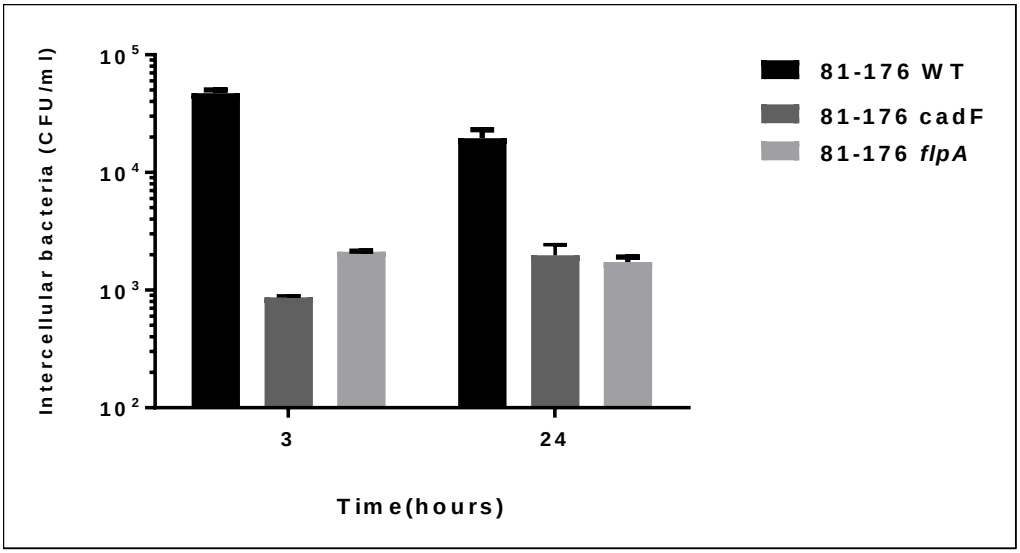

Figure 3.29. Invasion of *C. jejuni* 11168H & 81-176 wild-type strains, *cadF* and *flpA* mutants with T84 IECs. Confluent monolayers were infected with *C. jejuni* 11168H or 81-176 wild-type strains, *cadF* or *flpA* mutants and incubated for 3 h or 24 h. Following the PBS washes, cells were further incubated with gentamicin (150 µg/ml) for 2 h to kill extracellular bacteria, then lysed with Triton X-100. Serial dilutions of lysates were plated on CBA. After 48 h, CFU were counted. Data are representative of a minimum of triplicate biological replicates.

3.3 Discussion

Genomic diversity is widespread in bacteria, particularly in *Campylobacter* species. There is extensive evidence in the literature to support not only genomic but also phenotypic variation in *C. jejun*i (Duong and Konkel, 2009, Esson et al., 2016, Friis et al., 2010, Gundogdu et al., 2016, Hanel et al., 2009, Poly et al., 2005, Wassenaar et al., 1998). The most extensively studied *C. jejuni* 81-176 wild-type strain was isolated from an outbreak in humans (Korlath et al., 1985). The *C. jejuni* 81-176 strain has been used in many studies investigating signal transduction events, adhesion and invasion, intracellular survival, *in vitro* growth kinetics, motility and host immune responses (Monteville and Konkel, 2002, Hu et al., 2008, Wine et al., 2008, Boehm et al., 2012, Watson and Galan, 2008, Nemelka et al., 2009). As such, the majority of our understanding of molecular pathogenesis of *C. jejuni* is derived from the study of this strain and only a small amount from the study of a few other strains that may or may not cause infection in humans. Other *C. jejuni* strains that have been studied include F38011, 81116, 11168, M129, GB11, GB19, and TGH9011. Even though based on just one strain, a study of pathogenesis can be performed, however, for confirmation of pathogenic mechanisms, data from other studies using different strains is preferable especially with *C. jejuni*.

However optimised an assay, still some strains of *C. jejuni* exhibit invasion at a low-level compared to others. This leads to the question whether all *C. jejuni* strains are invasive and may indicate that the invasion phenotype is difficult to maintain when passaging strains in a laboratory. In addition, it is open to debate whether different *C. jejuni* strains use different mechanisms to enter a cell. With all this information in mind, the work in this chapter explored the roles of the two highly conserved adhesion proteins CadF and FlpA in two *C. jejuni* 11168H and 81-176 strains.

Bioinformatics analysis was performed to determine any variation in the amino acids sequences. It was clear that CadF and FlpA are two different proteins because they have only 19.8% identity and 32.2% similarity between them. This suggests that even though both CadF and FlpA are fibronectin binding proteins, they may have different functions. In addition, this is probably why CadF and FlpA work in collaboration and are both required for maximal binding as reported

previously by Konkel *et al.* (Konkel et al., 2010). CadF as a fibronectin binding protein, showed identical function in the 11168 and 81-176 strains; and the same for FlpA as a fibronectin binding protein in both the 11168H and 81-176 strains. This is probably because between the two strains, the identity and similarity are 98.8%. These suggests in terms of individual functions, that CadF and FlpA are highly conserved in the 11168 and 81-176 strains.

Data presented in this chapter indicates that differences exist between strains which can be observed in phenotypic assays as well as in other experiments. In conclusion, the roles of CadF and FlpA are similar in both the 11168H and 81-176 strains but with different functional efficiency.

Flagellum-driven motility is a key requirement for *C. jejuni* interactions with host cells (Poly and Guerry, 2008). Motility is essential for colonisation and non-motile strains exhibit reduced adhesion and invasion to IECs (Wassenaar et al., 1991). Other studies also showed that non-motile strains exhibited reduced invasion *in vitro* (Russell and Blake, 1994, Yao et al., 1994) and invasion in mice (Yanagawa et al., 1994). However, efficient invasion depends on more than motility alone as many fully motile mutants exhibit reduced invasion capabilities. It has been demonstrated that increased bacterial adherence is not sufficient for increased of invasion (Hu and Kopecko, 1999).

Nevertheless, checking the motility of a mutant was suggested as the spontaneous loss of motility can affect invasion capabilities (Gaynor et al., 2004). In addition, it was reported that mutation and genomic variation could cause different morphology in *C. jejuni* (Esson et al., 2016).

The phenotypic characterisation of the two *C. jejuni* 11168H and 81-176 strains in this study identified similarities and differences. The 11168H wild-type strain was more motile than the 11168H *cadF* and *flpA* mutants. Moreover, this result was in agreement with earlier work that showed 81-176 *cadF* and *flpA* mutants also exhibited reduced motility compared to the wild-type strain. However, the 81-176 strain exhibited higher motility at all-time points compared to that of the 11168H strain. Interestingly, in both the 11168H and 81-176 strains, the *cadF* mutants exhibited similar levels of motility, as was also the case for the *flpA* mutants. These suggests that regardless of strain, mutation of *cadF* and *flpA* results in reduced motility in *C. jejuni*.

Bacterial physiology changes successively through growth stages. Typically, cells must stabilise when first introduced into fresh medium. Bacteria then spend some

time in lag phase to adjust to the new environment. Bacteria then grow at a maximal rate after entering the log phase until limiting nutrients cause growth to slow and bacteria then enter the stationery phase. The growth curve data showed that in both the 11168H and 81-176 strains, mutation of *cadF* and *flpA* reduced growth in BB. In the 11168H strain, growth peaked at an $O.D_{600}$ of 1 at 24 h, whereas the 81-176 strain peaked at an $O.D_{600}$ of 0.9 at 22 h. In general, the growth rate experiments showed that *cadF* and *flpA* mutants exhibited reduced growth in comparison to the respective wild-type strains.

In DNA topology, changes are correlated to growth stage. In log phase, DNA is negatively supercoiled, whereas in lag and stationery phases the DNA is in a more relaxed state (Dorman, 2013). DNA in the 81-176 strain is also in a more relaxed state compared to the more supercoiled DNA in the 11168H strain and this results in the 11168 strain been more motile than the 81-176 strain (Shortt et al., 2016). However, in this study the 81-176 strain was more motile than the 11168H strain, which may be due to the LSHTM 81-176 strain used in this study been more supercoiled than the UCD 81-176 strain.

Motility and intact flagella have been shown to impact colonisation of C*. jejuni* to IECs *in vivo* and *in vitro* (Grant et al., 1993, Wassenaar et al., 1993). However, flagella were required for reaching a cell monolayer but not for adhesion (Grant et al., 1993). Hence, there have been studies where centrifugation was included as a step during adhesion and invasion assays to discount motility as a potential factor influencing invasion (Wassenaar et al., 1991, Konkel et al., 2004). However, it is still unclear as to how adhesion proteins such as CadF and FlpA can affect motility and this will require further investigation.

To investigate the differences in levels of *cadF* and *flpA* expression, RT-PCR analysis was performed on the 11168H and 81-176 wild-type strains and the respective mutants. RT-PCR is a semi quantitative method used to measure the relative intensity of *cadF* and *flpA* expression using *gyrA* as reference gene. *gyrA* is a housekeeping gene which encodes DNA gyrase that is expressed constitutively in *C. jejuni* (Joslin and Hendrixson, 2009).

Data from a recent study showed correlation between DNA supercoiling and motility. The more relaxed the supercoiling of DNA, the less motile the strain, as seen with the 81-176 strain. Whereas in the 11168 strain, the more negatively supercoiled DNA results in a more motile strain (Shortt et al., 2016). Another study also reported that the promoter region for *cadF* showed higher activities compared

to the promoter region for *flpA* in both the 11168 and 81-176 strains. However, the level of *flpA* promoter region activity was expressed slightly higher in the 81-176 strain compared to in the 11168 strain (Eoin Scanlan, PhD Thesis, UCD, 2014).

Results from this study showed that the level of expression of *cadF* is higher than that of *flpA* in both the 11168H and 81-176 wild-type strains. In addition, the 81-176 wild-type strain expressed higher levels of *cadF* than the 11168H wild-type strain. Interestingly, no significant differences between the levels of *flpA* expressed in the 11168H or 81-176 strains was observed. In the 11168H strain, mutation of *flpA* increased the level expression of *cadF* to more than that of the wild-type strain, suggesting some form of compensation for the loss of FlpA. However, expression of *flpA* was at the same level in either the 11168H wild-type strain or the 11168H *cadF* mutant. In the 81-176 strain however, both wild-type strain and *cadF* mutant expressed *flpA* at the same level, whilst the *flpA* mutant expressed *cadF* at a higher level than the wild-type strain but not significantly so. This may indicate different compensation mechanisms for the loss of CadF or FlpA in different *C. jejuni* strains, but further work would be required to confirm this.

Fibronectin is a major component of the extracellular matrix (ECM). Fibronectin is a 220 KDa monomer glycoprotein present at regions of cell-to-cell contact in IECs and composed of three types of repeating units (type I, II and III) (Konkel et al., 2010). Fibronectin acts as an adhesion molecule that anchors cells to ECM components. Many cellular interactions including tissue repair, blood clotting, cell migration and adhesion are facilitated by fibronectin. Cells rely on the surface protein fibronectin to interact with the cells surroundings, but many pathogens can also bind to this molecule and hijack the host cell signalling pathways (Henderson et al., 2011). The binding of bacteria to fibronectin will trigger cellular signal pathways and result in subsequent formation of focal adhesion complexes that rearrange the cytoskeleton of the cells, resulting in bacterial uptake by the host cells. *C. jejuni* ability to bind to fibronectin increases the probability of bringing other virulence factors closer to host cells and promotes bacterial internalisation (Konkel et al., 1992c).

Numerous *C. jejuni* proteins mediate the interaction between the multiple components of the IECs including fibronectin. In addition, numerous studies demonstrated the manipulation of host cell behaviour by pathogens binding to a component of the ECM such as fibronectin (van Putten et al., 1998). The two most characterised *C. jejuni* adhesins are CadF (Konkel et al., 2005) and FlpA

(Flanagan et al., 2009, Konkel et al., 2010). As CadF and FlpA are fibronectin binding proteins, the ability of CadF and FlpA to bind to fibronectin was determined using a fibronectin binding assay.

The 11168H wild-type strain bound at higher levels to fibronectin at all time points in comparison to the 81-176 wild-type strain. However, binding capacity to fibronectin was significantly reduced in the 11168H and 81-176 following mutation of *cadF* or *flpA*. This is in agreement with previous studies that showed reduced binding was observed in both F38011 *cadF* and *flpA* mutants (Konkel et al., 2010). In both the 11168H and 81-176 strains, mutation of *flpA* appeared to result in a more significant reduction in the numbers of bacteria binding to fibronectin compared to mutation of *cadF*. This is surprising as the level of *cadF* promoter region activity was higher than that of the level of the *flpA* promoter region activity in both the 11168H and 81-176 strains, which would suggest that mutation of *cadF* should have a more significant effect on binding to fibronectin. However, in the 81-176 strain, at 15 min and 30 min no significant differences between the *cadF* and *flpA* mutants binding capacity compared to the wild-type strain was observed but at 60 mins it was clear that the *cadF* mutant bound more than the *flpA* mutant. The data suggests that in both the 11168H and 81-176 strains, FlpA plays a more important role in binding to fibronectin than CadF. In addition, there were no significant differences in the binding of the 11168H and 81-176 *flpA* mutants to fibronectin whilst there was a slight increase in the 11168H *cadF* mutant binding capacity compared to that of the 81-176 *cadF* mutant.

The theme that can be identified from the fibronectin binding study was that CadF and FlpA have similar roles and similar importance when in the same strain. However, the extent of the binding efficiency of both *cadF* and *flpA* mutants differs between strains. These findings support the data from various studies that showed maximal binding to host cells requires both CadF and FlpA (Konkel et al., 1997, Konkel et al., 2010, Flanagan et al., 2009, Krause-Gruszczynska et al., 2007b, Monteville et al., 2003). In general, it is established that *C. jejuni* strains adhere to IECs but to a different degree and efficiency depending on the strain (Ahmed et al., 2002) and results in this study also are in agreement with those data showing the consistency of the CadF and FlpA role during interactions with IECs.

Non-mammalian models of infection have garnered much popularity and one that is simple, practical and widely used in research to study bacterial infection is the larvae of *G. mellonella* (wax moth) and this model can also can be used as a model

for antibiotic efficacy (Vogel et al., 2011). *G. mellonella* has an immune response similar to humans. The larvae possess innate immune cells called haemocytes that function like macrophages and neutrophils in humans. The haemocytes also produce melanin that result in melanisation. *G. mellonella* larvae have been used as a model of infection due to several advantages over big and small animal models. Studies have used *G. mellonella* with *C. jejuni* (Champion et al., 2009), with *Legionella pneumophila* (Harding et al., 2013), with *Listeria spp* (Mukherjee et al., 2010), with *Pseudomonas aeruginosa* (Jander et al., 2000) and with *Francicisella tularensis* (Aperis et al., 2007).

Some of the advantages of using the larvae are; they are small and easy to handle, inexpensive, no specific food required and survive at 37^{o}C (Champion et al., 2009, Champion et al., 2008, Chang and Miller, 2006, Mukherjee et al., 2010). Study of *C. jejuni rrpA* and *rrpB* mutants (Gundogdu et al., 2015, Gundogdu et al., 2011) and *C. jejuni* OMVs isolated from different mutants showed reduced cytoxicity (Elmi et al., 2012, Elmi et al., 2016). These data confirm that *G. mellonella* is susceptible to *C. jejuni* infection.

Infection with *C. jejuni* caused the melanisation process to occur in *G. mellonella* larvae as exhibited in this study. Hemocytes generate melanin and deposit it in tissues surrounding the pathogen during infection. As a result, the infected larvae change colour from the normal uninfected cream colour to brown or black. The mechanisms and role of melanin in host defence are still unclear, however this result demonstrated and supported evidence that was in the literature about insect immunity against pathogens (Nappi and Christensen, 2005, Nappi and Vass, 2001).

A comparison of the results from the larval cytotoxicity study demonstrated that in both the 11168H and 81-176 wild-type strains mutation of *cadF* and *flpA* reduced cytotoxicity compare to the respective wild-type strain. In addition, in both the 11168H and 81-176 strains, the *cadF* mutant exhibited significantly reduced cytotoxicity compared to the *flpA mutant*. However, the cytotoxicity of the 11168H *cadF* mutant was much less than the 81-176 *cadF* mutant. This is in keeping with the level of *cadF* promoter region activity been higher than that of the level of the *flpA* promoter region activity in both the 11168H and 81-176 strains, suggesting that CadF may play a more significant role in larval cytotoxicity than FlpA in the 11168H and 81-176 strains. Alternatively it could be assumed that CadF and FlpA exhibited similar roles and importance in causing cytotoxicity although with

different efficiency due to different levels of expression. These data also contributed to the growing evidence that *C. jejuni* wild-type strain and mutants are cytotoxic to *G. mellonella.* Moreover, it supported data that *G. mellonella* showed a correlation between pathogen virulence in insect and in mammalian models.

For successful attachment and colonisation, the process required is adhesion to and then invasion into the host cells. With all the numerous published data, the fact is that the invasion process of *C. jejuni* involves a myriad of bacterial and host factors and work in co-operation to mediate optimal adherence to host cells. Many studies showed adherence-defective mutants exhibit only reduced rather than severely abolished interactions with eukaryotic cells wherein the mutants reach adherence levels of about 20% to 50% of the wild-type strain (Backert and Hofreuter, 2013).

The ability of *C. jejuni* to invade human IECs is crucial for the establishment of an infection. *C. jejuni* entrance to IECs is widely reported and some studies have shown *C. jejuni* inside of IECs during mouse infections (Stahl et al., 2014). CadF was characterised as a fibronectin binding protein in 1997 (Konkel et al., 1999a). Following that, many studies have reported the involvement of CadF in *C. jejuni* adhesion to and invasion of host cells. A *cadF* mutant exhibited reduced binding to host cells *in vitro*, such as to INT 407 cells (Moser et al., 1997). Reduced *in vivo* colonisation of broilers was also observed with a F38011 *cadF* mutant (Ziprin et al., 1999). A previous study demonstrated that FlpA plays a role in *C. jejuni* colonisation of chicks and a *flpA* mutant has reduced colonisation in chickens (Flanagan et al., 2009).

IECs cell cultures provide a useful alternative method to study *C. jejuni* interactions *in vitro* (Friis et al., 2005). Both T84 and Caco-2 are cells from human colon adenocarcinoma and colonic carcinoma respectively. These IECs are characterised as polarised cells that display distinct apical and baso-lateral compartments. An earlier study by Kohler *et al.* provided evidence that polarised IECs are suitable for research into bacterial pathogenesis in general and in specific cell adherence and invasion (Kohler et al., 2002). Even though IECs are an established model for intestinal epithelial transport mechanisms, variation in experiments still exists. This is due to cell culturing condition factors such age, batch, density, passage frequency and numbers that have impact on cell line behaviour in the long term (Hidalgo et al., 1989). In these experiments to further explore the roles of CadF and FlpA in the two different 11168H and 81-176 strains,

both T84 and Caco-2 IECs were used. Results from a previous study suggested that FlpA plays a more important role in invasion of Caco-2 cells in the 81-176 strain (Neveda Naz, PhD Thesis, LSHTM, 2014).

Therefore, investigations were performed to confirm whether FlpA had the same more significant role in invasion in a different *C. jejuni* strain. However, in this study, this was not the case. There are a few things to consider here. Firstly, in assays using T84 cells, both the 11168H *cadF* and *flpA* mutants showed a reduction in interaction with and invasion compared to that of the 11168H wild-type strain. Interaction of the 11168H *cadF* mutant was reduced compared to that of the 11168H wild-type strain, but this was not significant. In contrast, interaction of the 11168H *flpA* mutant was significantly reduced compared to that of the 11168H wild-type strain. However, both the 11168H *cadF* and *flpA* mutants exhibited highly significant reduction in invasion of T84 cells compared to that of wild-type strain. Secondly, in assays using Caco-2 cells, only the 11168H *flpA* mutant demonstrated a significant reduction in interactions with Caco-2 cells compared to that of 11168H wild-type strain. Further, both the 11168H *cadF* and *flpA* mutants showed a significant reduction in invasion of Caco-2 cells compared to that of 11168H wild-type strain. However, the 11168H *flpA* mutant ability to invade Caco-2 cells appeared to be more reduced compared to that of the 11168H *cadF* mutant.

Having established the above, looking at the *cadF* and *flpA* mutants in general, both initially displayed a reduction in ability to interact with and invade both T84 and Caco-2 cell types compared to the wild-type strain. However, after 24 h infection, both the *cadF* and *flpA* mutants were able to increase interactions and invasion to a higher level than after 3 h infection, but not to the level of wild-type strain irrespective of the IECs used. Hence, in the 11168H strain, both CadF and FlpA were required for successful invasion of IECs with similar capability level and importance. Even though FlpA has three repeats of the same type 111 domain as Fn (Konkel et al., 1999c), that does not seem to make FlpA bind more strongly to Fn compared to CadF. In general, it is established that *C. jejuni* adhere to IECs but to a different degree and efficiency depending on different strains (Ahmed et al., 2002). In addition, it was also suggested that CadF and FlpA work in co-operation to enable entry into host cells. A previous study reported *C. jejuni* induces IECs membrane ruffling, a phenomenom that was dependent on the CadF and FlpA Fn-binding proteins (Eucker and Konkel, 2012, Backert et al., 2013). This suggests that inactivation of *cadF* and *flpA* is sufficient to disrupt the activation of host signaling pathways.

The pathogenesis of *C. jejuni* has been studied in multiple IECs. To further investigate the roles of CadF and FlpA and to highlight the involvement of *C. jejuni* strain variation, T84 IECs were infected with *C. jejuni* 11168H and 81-176 wild-type strains and respective *cadF* and *flpA* mutants. It was observed that both *cadF* and *flpA* mutants behaved similarly during adhesion to and invasion of T84 and Caco-2 cells. Reduced interaction of both the 11168H and 81-176 *cadF* and *flpA* mutants to T84 and Caco-2 cells was observed. However, in both the 11168H and 81-176 strains, the *flpA* mutant exhibited a statistically significant reduction in binding to both T84 and Caco-2 cells. In contrast with these observation, the numbers of the *cadF* mutant internalised into T84 cells was slightly reduced compared to the *flpA* mutant.

A study showed that *C. jejuni* invasiveness varies between *C. jejuni* strains (Biswas et al., 2000, Harvey et al., 1999). *C. jejuni* invasion into IECs depends on the concentration of bacteria used to infect IECs (Biswas et al., 2004, Biswas et al., 2000). One study has reported that it is best to use a reduced multiplicity of infection (MOI) as this can result in maximum *C. jejuni* invasion (Friis et al., 2005). Furthermore, many subtle variations such as the use of different cell types such as HEP-2, INT 407 or HeLa from non-polarised cells and MDCK (monkey), have been shown to have implications on reaching a concensus on the ability of *C. jejuni* to invade IECs (De Melo et al., 1989, Fauchere et al., 1986, Oelschlaeger et al., 1993). One study has suggested that cell lines originated from human intestinal epithelium are best and most suitable in investigating *C. jejuni* invasion mechanisms (Konkel et al., 1992a). It can be assumed that cell type can potentially influence the experiment outcomes as suggested by Friis *et al.* (Friis et al., 2005).

The next chapter will explore further the roles of CadF and FlpA in *C. jejuni* interactions with host cells.

CHAPTER FOUR: FURTHER INVESTIGATION OF ROLES OF CADF AND FLPA DURING *C. jejuni* INTERACTIONS WITH HUMAN INTESTINAL CELLS

4.1 Introduction

C. jejuni interaction with IECs is a multifactorial process, involving colonisation, followed by adherence to then invasion into IECs (O Croinin and Backert, 2012). The current view is that *C. jejuni* expresses proteins such as CadF and FlpA to interact with IEC receptors, particularly via fibronectin, which is attached to IECs by α5β1 integrins (Konkel et al., 2010). It has been hypothesised that the binding of CadF and FlpA to fibronectin triggers *C. jejuni* uptake via a IEC driven process involving actin remodelling, focal adhesion kinase and Src family kinases (Monteville et al., 2003). *In vitro* studies have suggested that fibronectin on the baso-lateral surface of IECs is sufficient for *C. jejuni*-integrin bridging.

Several IECs types have been used to study the role of CadF and FlpA in various *C. jejuni* wild-type strains (Monteville et al., 2003, Krause-Gruszczynska et al., 2011, Boehm et al., 2011). However, most previous studies have used a *C. jejuni* F38011 wild-type strain with INT 407 cells (Konkel et al., 2010). Although, these studies have elucidated the role of CadF and FlpA in the *C. jejuni* F38011 strain, gaps in our understanding of the roles of CadF and FlpA remain, particularly in the widely studied *C. jejuni* 11168H and 81-176 wild-type strains. There are also conflicting reports on the role of both proteins in *C. jejuni* capacity to interact with different IECs. Furthermore, mutation of either *cadF* or *flpA* partially diminishes the ability of *C. jejuni* F38011 strain to bind to fibronectin *in vitro* and/or interact with INT- 407 cells (Konkel et al., 1997, Monteville et al., 2003, Konkel et al., 2010).

Different enteric pathogens have been shown to interact with and invade IECs by secreting proteins to facilitate interactions with and invasion of IECs (Singamsetty et al., 2008). Studies from different groups (Elmi et al., 2012, Lindmark et al., 2009) have described localisation of both fibronectin binding proteins CadF and FlpA in OMVs isolated from *C. jejuni* 11168H and 81-176 wild-type strains. Hence, the aim of this chapter is to investigate further the roles of CadF and FlpA in both live *C. jejuni* 11168H and 81-176 wild-type strains as well as associated with OMVs during interactions with host IECs.

4.2 Results

4.2.1 TEER measurement in T84 and Caco-2 intestinal epithelial cells

T84 and Caco-2 IECs are human intestinal cell lines that are able to form polarised monolayers (Everest et al., 1992, Monteville and Konkel, 2002). Polarised cells display distinct apical and baso-lateral compartments, form a brush border with microvilli and maintain tight junctions. These junctions function as a paracellular barrier for passage of solutes across Caco-2 monolayers (Hidalgo et al., 1989). A tight junction is a dynamic cell to cell adhesion which forms a continuous barrier around IECs (Yap et al., 1998). Barrier integrity is vital for the physiological activities of the tissue. Development of the membrane integrity of monolayers was assessed before further assays involving translocation of bacteria into IECs were performed. TEER measures tight junction permeability and monolayer integrity based on the resistance that intact monolayers provide. When the monolayers are compromised, the TEER value is reduced.

To determine the role of CadF and FlpA in the ability of C*. jejuni* to breach the polarised IECs, the TEER value of confluent uninfected Caco-2 and T84 polarised monolayers was determined. Both cell types exhibited a different average range of TEER values. Caco-2 monolayers consistently had higher TEER values than T84 monolayers from day 1 to 15 post-seeding. At day 1 until day 6 post-seeding, T84 monolayers showed TEER values similar to the control value, however after day 6 post-seeding, T84 monolayers showed increasing TEER values until a peak at day 15 then reducing until day 21. Control values were from Transwell® inserts without IECs which produced constant TEER values at around 100 ohm (Ω) (Figure 4.1).

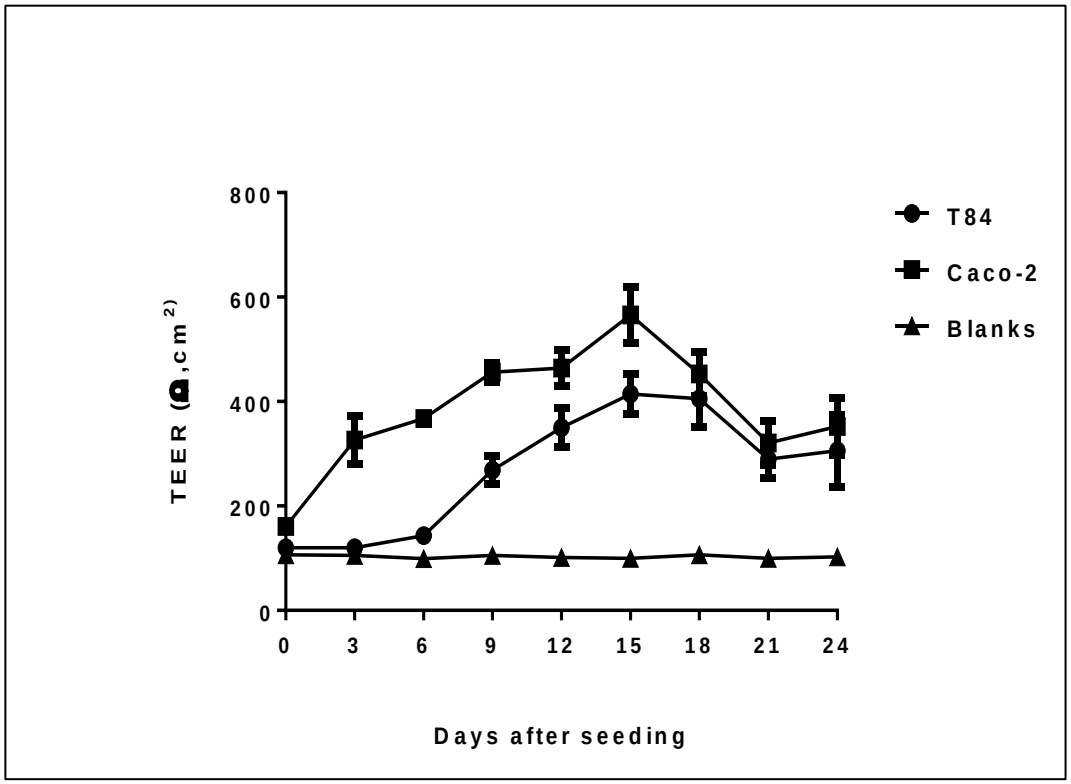

Figure 4.1. TEER values of uninfected T84 and Caco-2 IEC monolayers. T84 and Caco-2 IECs were grown on Transwell® inserts in a 12-well plate. The media was changed every 48 h. The TEER measurements were recorded using EVOM prior to change of media. Blanks were the TEER values recorded from Transwell® inserts without IECs. Data are representative of triplicate independent experiments.

4.2.2 No effect on TEER of T84 intestinal epithelial cells following infection with the 11168H *cadF* or *flpA* mutants

Assays were performed to investigate whether infection with 11168H wild-type strain, *cadF* or *flpA* mutants affected the TEER of T84 IECs differently. There was no significant difference in TEER values in T84 IECs 24 h post-infection with the 11168H wild-type strain, *cadF* or *flpA* mutants compared to the non-infected T84 IECs (control). The 11168H wild-type strain exhibited slightly reduced TEER

values in T84 monolayers compared to both *cadF* and *flpA* mutants, however no significant differences were observed. In addition, the 11168H *cadF* mutant exhibited a slightly higher TEER value compared to the 11168H *flpA* mutant although this was not significant (Figure 4.2).

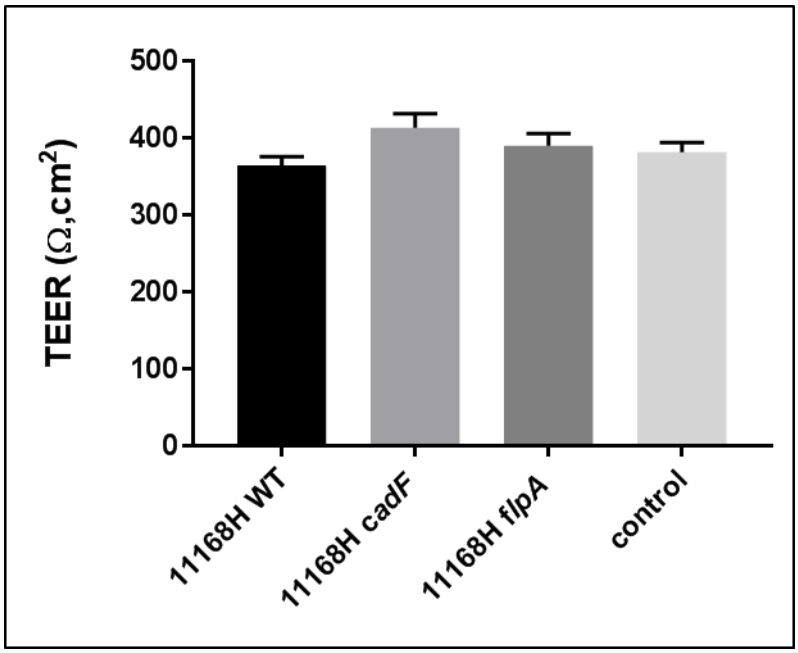

Figure 4.2. Infection with 11168H wild-type strain, *cadF* or *flpA* mutants has no effect on TEER values of T84 IEC monolayers. T84 IECs were seeded and allowed to polarise on Transwell® inserts in a 12- well plate. Monolayers were then infected (MOI 100:1) with the 11168H wild-type strain, *cadF* or *flpA* mutants. TEER measurements were recorded after 24 h infection. Data are representative of triplicate independent experiments.

4.2.3 Translocation of *C. jejuni* 11168H wild-type strain, *cadF* and *flpA* mutants across T84 intestinal epithelial cells

The ability of the 11168H wild-type strain, *cadF* and *flpA* mutants to translocate across a T84 IEC monolayer was investigated. There was no significant difference in the ability to translocate T84 IECs observed between the 11168H wild-type strain and either the 11168H *cadF* or *flpA* mutants. All three strains were able to translocate across the membrane barrier equally efficiently base on the similar level of relative fluorescence unit (RFU) (Figure 4.3 and Figure 4.4).

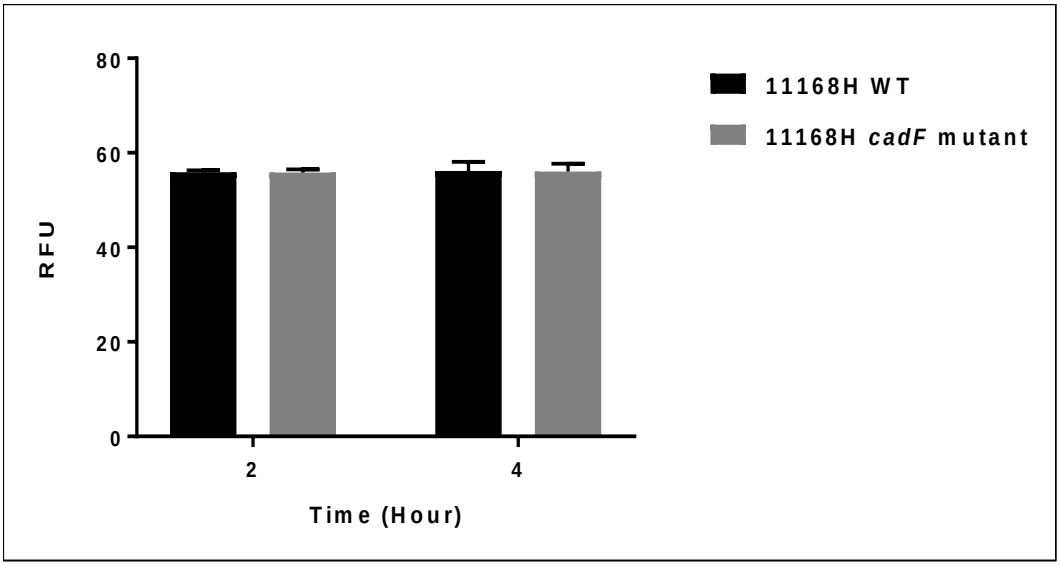

Figure 4.3. 11168H *cadF* mutant translocates across a T84 IEC monolayer at the same rate as 11168H wild-type strain. T84 IECs were seeded and allowed to polarise on Transwell® inserts in a 12-well plate. T84 monolayers were infected (MOI 100:1) with the 11168H wild-type strain expressing GFP or the 11168H *cadF* mutant expressing GFP. At 2 h and 4 h time points, media from the baso-lateral compartment was collected into a 96-well opaque plate and the relative fluorescence units from the GFP expressing bacteria recorded. Data are representative of triplicate independent experiments.

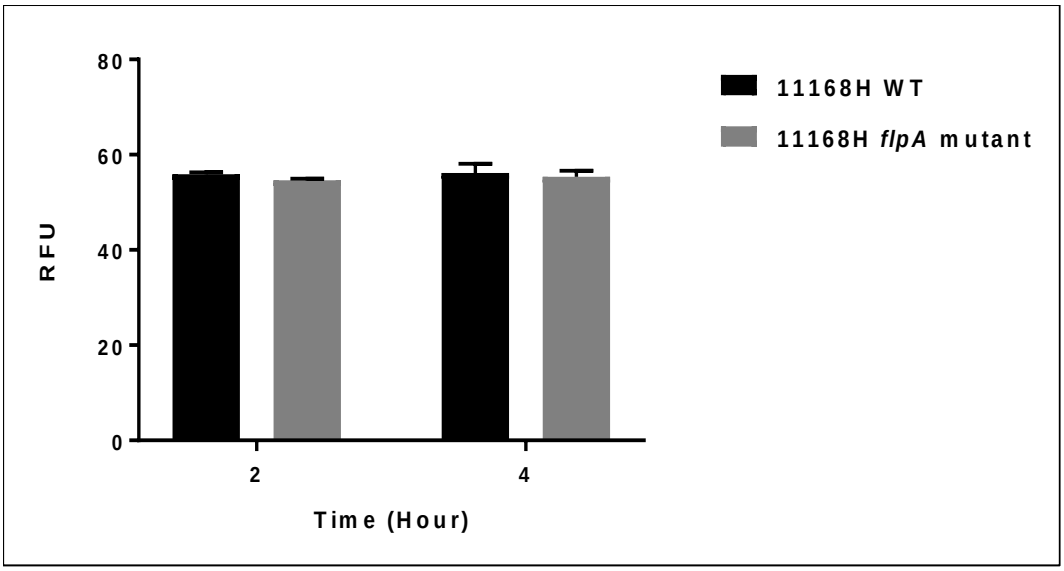

Figure 4.4. 11168H *flpA* mutant translocates across a T84 IEC monolayer at the same rate as 11168H wild-type strain. T84 IECs were seeded and allowed to polarise on Transwell® filter inserts in a 12-well plate. T84 monolayers were infected (MOI 100:1) with the 11168H wild-type strain expressing GFP or the 11168H *flpA* mutant expressing GFP. At 2 h and 4 h time points, media from the baso-lateral compartment was collected into a 96-well opaque plate and the relative fluorescence units from the GFP expressing bacteria recorded. Data are representative of triplicate independent experiments.

4.2.4 Induction of IL-8 from T84 intestinal epithelial cells following infection with 11168H wild-type strain, *cadF* and *flpA* mutants

ELISA was performed to investigate the ability of *C. jejuni* 11168H wild-type strain, *cadF* and *flpA* mutants to induce IL-8 in IECs.

Results from the ELISA showed that no significant difference was observed in the ability of the 11168H wild-type strain, *cadF* or *flpA* mutants to induce IL-8 from T84 IECs. All strains induced IL-8 at a similar level after 24 h infection.

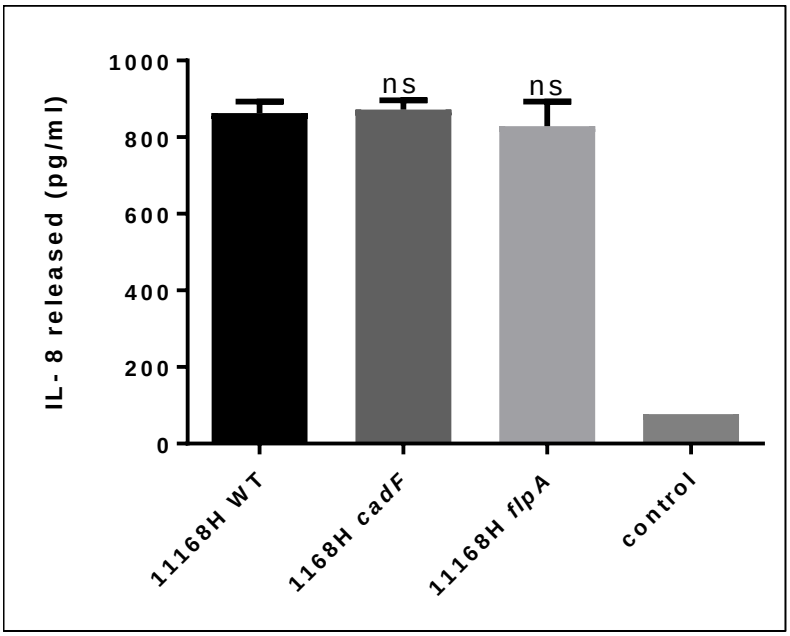

Figure 4.5. IL-8 induction from T84 IECs following infection with 11168H wild-type strain, *cadF* or *flpA* mutants. T84 IECs were infected (MOI 100:1) with 11168H wild-type strain, *cadF* or *flpA* mutants. Supernatants were collected after 24 h infection and the levels of IL-8 induced from T84 IECs quantified using a human IL-8 ELISA. Data are representative of triplicate independent experiments.

4.2.5 Induction of IL-8 from T84 intestinal epithelial cells following infection with 81-176 wild-type strain, *cadF* or *flpA* mutants

A reduction in IL-8 induced from infected T84 IECs was observed with the 81-178 *cadF* or *flpA* mutant in comparison to the 81-176 wild-type strain. Infection with the 81-176 *cadF* mutant resulted in a small reduction in induction of IL-8 from T84 IECs compared to wild-type strain, however this was not significant. In contrast, infection with the 81-176 *flpA* mutant resulted in a significant reduction in IL-8 induction compared to that of the wild-type strain (Figure 4.6). The 81-176 wild-type strain induced IL-8 to a similar level as the 11168H wild-type strain.

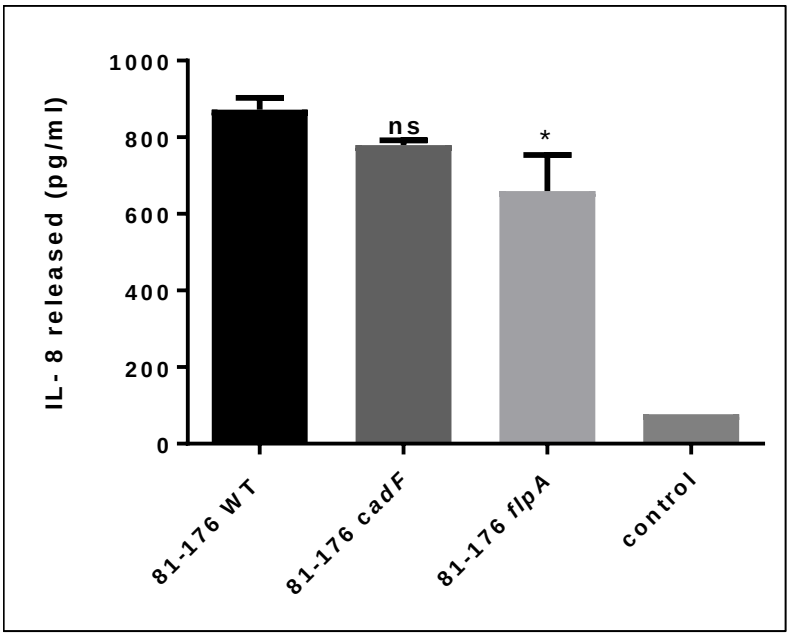

Figure 4.6. IL-8 induction from T84 IECs following infection with 81-176 wild-type strain, *cadF* or *flpA* mutants. T84 IECs were infected (MOI 100:1) with 81-176 wild-type strain, *cadF* or *flpA* mutants. Supernatants were collected after 24 h infection and the levels of IL-8 induced from T84 IECs quantified using a human IL-8 ELISA. Data are representative of triplicate independent experiments. * denotes $p < 0.05$.

4.2.6 Rac1 activation in Caco-2 intestinal epithelial cells following infection with 11168H wild-type strain, *cadF* or *flpA* mutants

Rac1 is a member of the Rho family of small GTPases and acts as a switch to activate signalling events that modulate cytoskeleton reorganisation resulting in bacterial uptake. Rac1 regulates the cycle between active GTP-bound to inactive GDP- bound status. In the GTP-bound active state, the GTPases transmits a signal and activates a series of intracellular events (Caron and Hall, 1998). It has been reported that *C. jejuni* internalisation into INT 407 IECs involved time-dependent activation of Rac1 and Cdc42 (Boehm et al., 2012, Krause-Gruszczynska et al., 2007a, Eucker and Konkel, 2012).

To investigate if the mutation of *cadF* or *flpA* has an impact on the activation of Rac1, a G-LISA assay was performed. Results showed that there was a significant difference observed in the activation of Rac1 between the 11168H wild-type strain and the *cadF* or *flpA* mutants (Figure 4.7). The activity of Rac1 following infection with the 11168H wild-type strain was set as 100%. Mutation of *cadF* or *flpA* induced Rac1 activation to a similar level at 66% or 65% respectively of the Rac1 activity following wild-type strain infection.

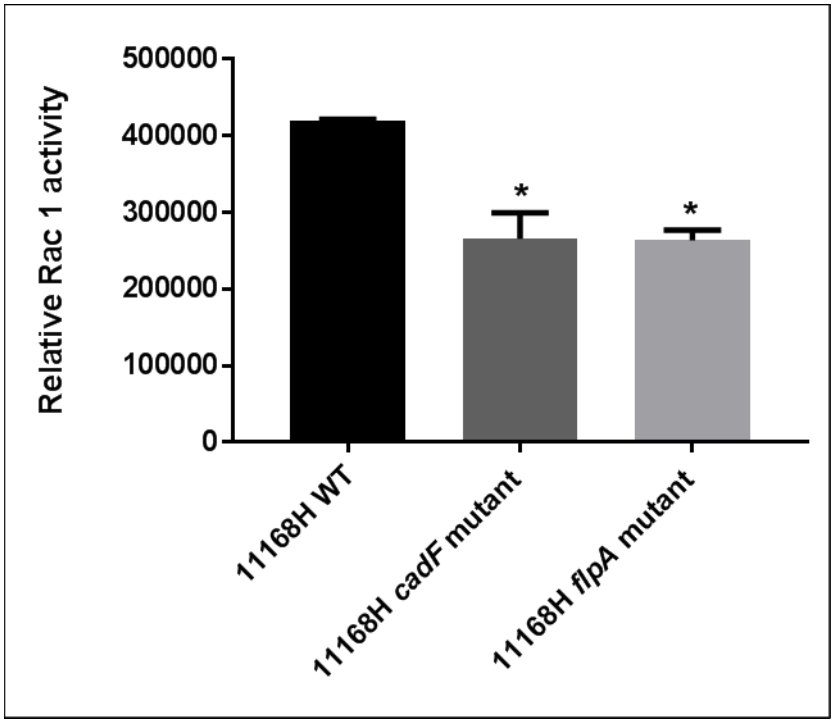

Figure 4.7. Activation of Rac1 in serum starved Caco-2 IECs following infection with 11168H wild-type strain, *cadF* or *flpA* mutants. Caco-2 monolayers were infected (MOI 100:1) with the 11168H wild-type strain, *cadF* or *flpA* mutants. After 20 minutes incubation, cells were lysed and the total protein concentration was determined. Whole cell lysates were processed and analysed for activated Rac1 by G-LISA™. Total active Rac1 was indicated in relative optical density. Data are representative of triplicate independent experiments. * denotes $p < 0.05$.

4.2.7 Determination of protein concentration of OMVs isolated from 11168H or 81-176 wild-type strains and the respective *cadF* or *flpA* mutants

OMVs are an important bacterial virulence factor, playing a major role in bacterial pathogenesis (Kuehn and Kesty, 2005, Kulp and Kuehn, 2010). A study by Elmi *et*

al. here at the LSHTM, identified both CadF and FlpA associated with *C. jejuni* 11168H OMVs. Bacteria use OMVs to deliver virulence factors into host cells (Ellis and Kuehn, 2010). It was hypothesised that *C. jejuni* may use OMVs to deliver bacterial virulence factors to host cells which then promote bacterial interactions with and invasion of IECs, as well as the modulation of the host response (Elmi et al., 2012).

Following OMV isolation from the 11168H or 81-176 wild-type strains and the respective *cadF* or *flpA* mutants, the protein concentration of these isolated OMVs was quantified using a BCA assay. The OMV protein concentration was determined using a standard curve of a known absorbance from varying concentrations of BSA (Figure 4.8A). Approximately 200 µg OMVs by protein content were isolated from 100 ml of culture supernatant. There was no significant difference ($p > 0.05$) between the protein concentrations of OMV isolated from the 11168H or 81-176 wild-type strains and the respective *cadF* or *flpA* mutants (Figure 4.8B).

.

A

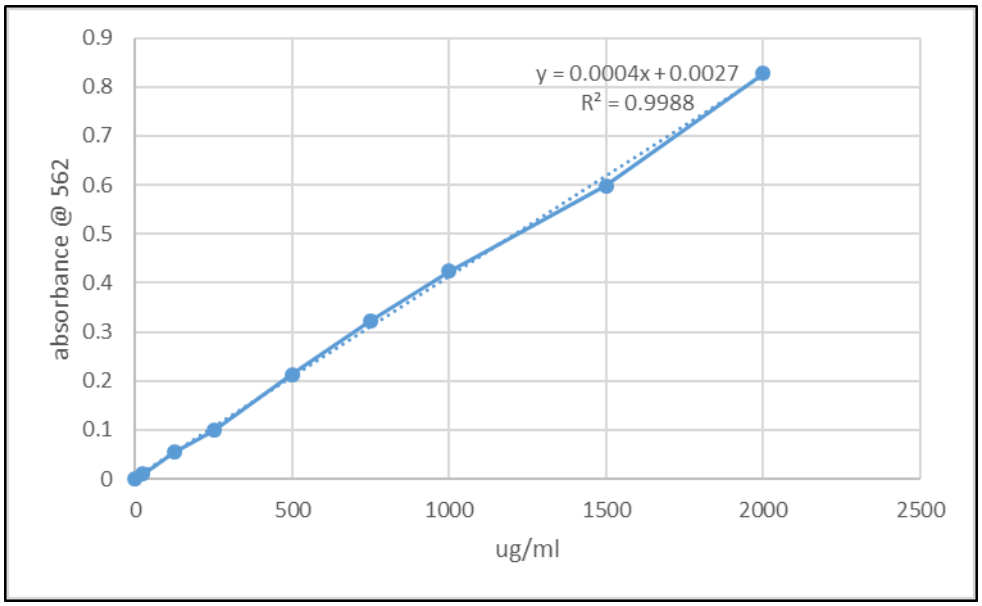

B

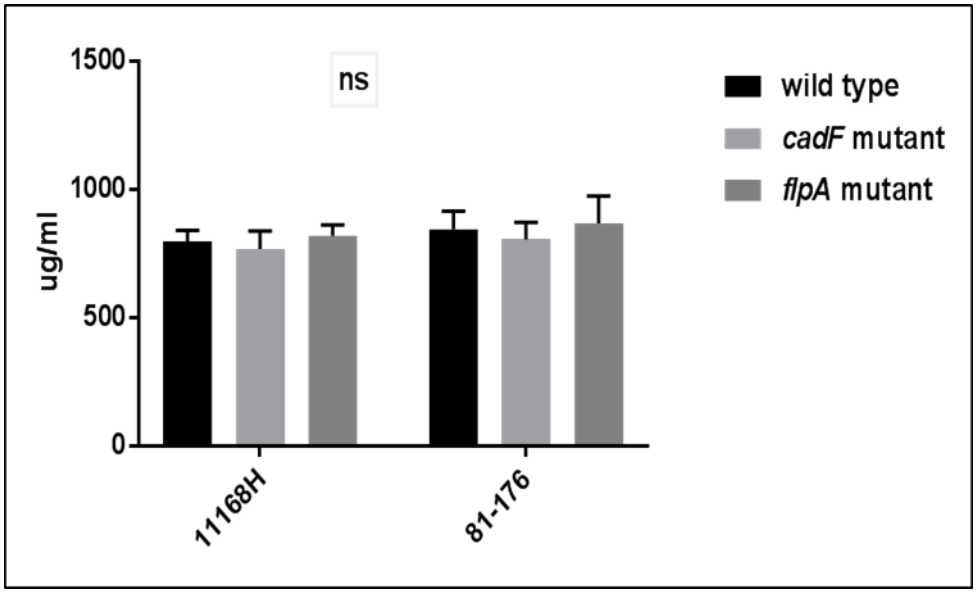

Figure 4.8. Protein concentration of OMVs isolated from the 11168H or 81-176 wild-type strains and the respective *cadF* or *flpA* mutants. A. Standard curve for a BCA assay. Samples of known concentrations of BSA were added in triplicates to a 96-microtiter plate and incubated at room temperature. The line derived is from a linear regression analysis of the data. B. 50 ml of Brucella broth was inoculated with the 11168H or 81-176 wild-type strains, *cadF* or *flpA* mutants at an OD_{600} of 0.1 and grown for 16 h. OMVs were isolated then protein concentrations determined using a BCA assay. Data are representative of triplicate independent experiments.

4.2.8 Pre-treatment of fibronectin binding assay with OMVs isolated from 11168H wild-type strain, *cadF* or *flpA* mutants

It has been shown that pre-treatment of T84 IECs with OMVs enhanced 11168H wild-type strain invasion (Elmi et al., 2016). When immobilised fibronectin was pre-treated with 10 µg of OMVs isolated from the 11168H wild-type strain, the 11168H wild-type strain exhibited reduced binding to fibronectin. This is probably due to binding site competition by OMVs that block the live bacteria from binding to

fibronectin. When immobilised fibronectin was pre-treated with 10 µg of OMVs isolated from either the *cadF* or *flpA* mutants, no significant difference in reduction of binding of the 11168H wild-type strain was observed.

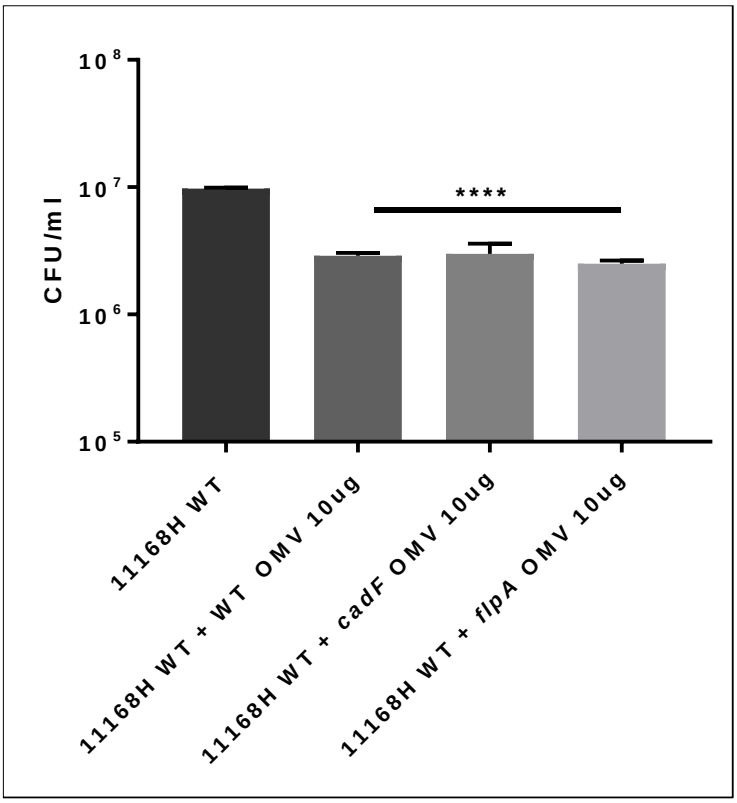

Figure 4.9. Pre-treatment of immobilised fibronectin with OMVs prior to incubation with *C. jejuni.* Immobilised fibronectin was pre-treated with OMVs (10 µg) isolated from either the 11168H wild-type strain, *cadF* or *flpA* mutants for 1 h at 37^{o}C before co-incubation with the 11168H wild-type strain. At the end of the incubation period, wells were washed with PBS. Trypsin EDTA was used to detach adherent bacteria. Suspensions were serially diluted and plated on CBA plates. Data are representative of triplicate independent experiments. **** denotes $p < 0.0001$.

4.2.9 Cytotoxicity assay (LDH) with OMVs isolated from 11168H wild-type strain, *cadF* or *flpA* mutants

OMV cytotoxicity towards Caco-2 IECs was investigated by quantifying the release of cytosolic lactate dehydrogenase (LDH) as a measure of cellular damage. OMVs isolated from the 11168H *cadF* mutant showed no significant difference in cytotoxicity compared to OMVs isolated from the wild-type strain. However, OMVs isolated from the 11168H *flpA* mutant showed a significant increase ($p < 0.001$) in cytotoxicity compared to OMVs isolated from the 11168H wild-type strain. Total lysis of Caco-2 IECs following treatment with 1% (v/v) Triton X-100 represented 100% cytotoxicity. Cells treated with PBS represented the negative control.

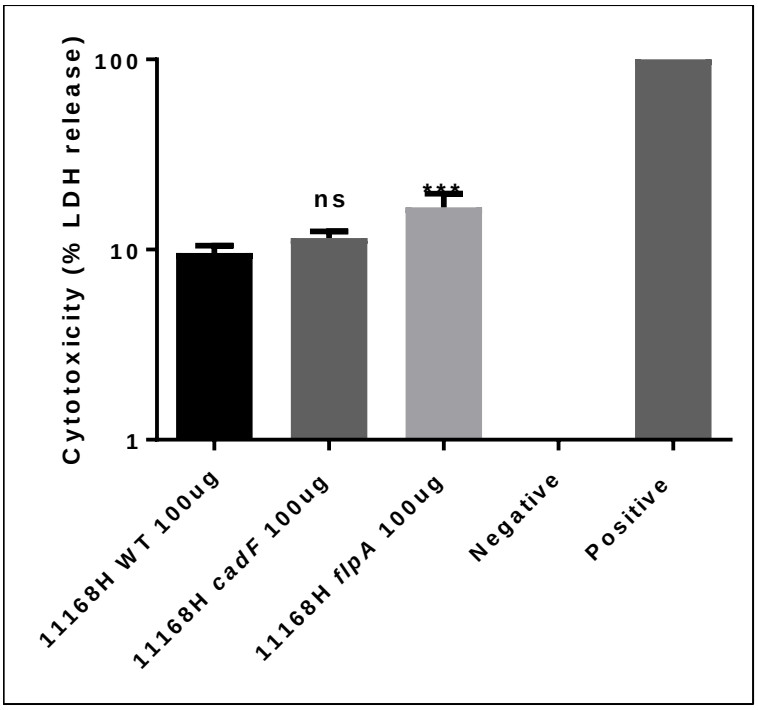

Figure 4.10. Cytotoxic effects of OMVs on Caco-2 IECs. OMVs (100 µg) isolated from 11168H wild-type strain, *cadF* or *flpA* mutants were co-incubated with Caco-2 IECs for 24 h. Supernatants were collected and analyse for the released of lactate dehydrogenase (LDH.) Positive control was Caco-2 cells lysed with 1% (v/v) Triton X-100. Negative control was Caco-2 cells co-incubated with PBS. Data are representative of triplicate independent experiments. *** denotes $p < 0.01$; ns denotes no significant difference.

4.2.10 Cytotoxicity assay (LDH) with OMVs isolated from 81-176 wild-type strain, *cadF* or *flpA* mutants

OMVs isolated from the 81-176 *cadF* or *flpA* mutants showed significantly increased cytotoxicity towards Caco-2 IECs compared to OMVs isolated from the 81-176 wild-type strain. There was a small increase in LDH released by OMVs from the 81-176 *cadF* mutant compared to OMVs from the 81-176 *flpA* mutant.

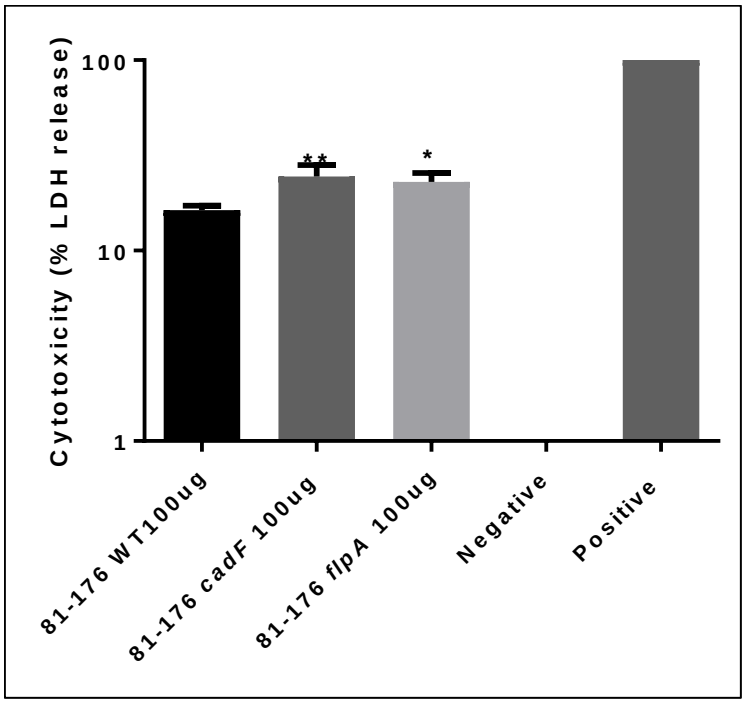

Figure 4.11. Cytotoxic effects of OMVs on Caco-2 IECs. OMVs (100 µg) isolated from 81-176 wild-type strain, *cadF* or *flpA* mutants were co-incubated with Caco-2 IECs for 24 h. Supernatants were collected and subjected to LDH assay. Positive control was Caco-2 cells lyse with 1% (v/v) Triton X-100. Negative control was Caco-2 cells co-incubated with PBS. Data are representative of triplicate independent experiments. * denotes $p < 0.5$; ** denotes $p < 0.01$; ns denotes no significant difference.

4.2.11 Cytotoxicity of OMVs isolated from 11168H wild-type strain, *cadF* and *flpA* mutants in the *Galleria mellonella* model of infection

Further investigations were performed to see whether the mutation of *cadF* or *flpA* had any effect on the cytotoxic potential of *C. jejuni* OMVs in the *G. mellonella* larvae model of infection. This invertebrate model has been widely used to investigate pathogenesis of various pathogens including *C. jejuni* (Champion et al., 2010). *G. mellonella* larvae were injected with OMVs (5 µg) isolated from the 11168H wild-type strain, *cadF* or *flpA* mutants. After 24 h infection, larvae were inspected for mortality. Results showed that mutation of *cadF* or *flpA* in the 11168H strain significantly reduced the cytotoxicity of OMVs to *G. mellonella* compared to OMVs isolated from the 11168H wild-type strain. OMVs isolated from the 11168H *flpA* mutant were slightly less cytotoxic than OMVs isolated from the 11168H *cadF* mutant (Figure 4.12). No further mortality was observed at 48 h and 72 h post-infection (data not shown).

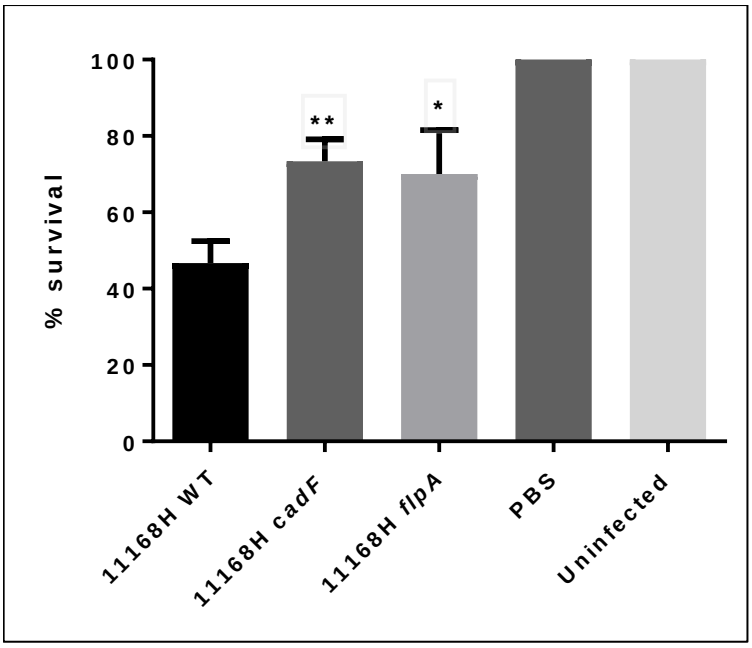

Figure 4.12. Cytotoxicity of OMVs isolated from 11168H wild-type strain, *cadF* or *flpA* mutants in *G. mellonella* model of infection. Larvae was inoculated with 5 µg of OMVs isolated from the 11168H wild-type strain, *cadF* or *flpA* mutants, injected into the hind leg using a 10-gauge syringe. Larvae were incubated at 37°C for the duration of the experiment. At 24 h, larvae were inspected for live and deed counts. Inoculation with PBS was used as control. 10 larvae were used for every sample. Data are representative of triplicate independent experiments. * denotes $p < 0.05$; ** denotes $p < 0.01$.

4.2.12 Cytotoxicity of OMVs isolated from 81-176 wild-type strain, *cadF* and *flpA* mutants in the *Galleria mellonella* model of infection

OMVs isolated from the 81-176 *flpA* mutant showed significantly less cytotoxicity compared to OMVs isolated from the 81-176 *cadF* mutant or the 81-176 wild-type strain. This was demonstrated by highest survival of larvae infected with OMVs isolated from the *flpA* mutant. OMVs isolated from the *cadF* mutant caused a slight increase in *G. mellonella* larvae mortality compared to wild-type strain OMVs, however this was not significant (Figure 4.13).

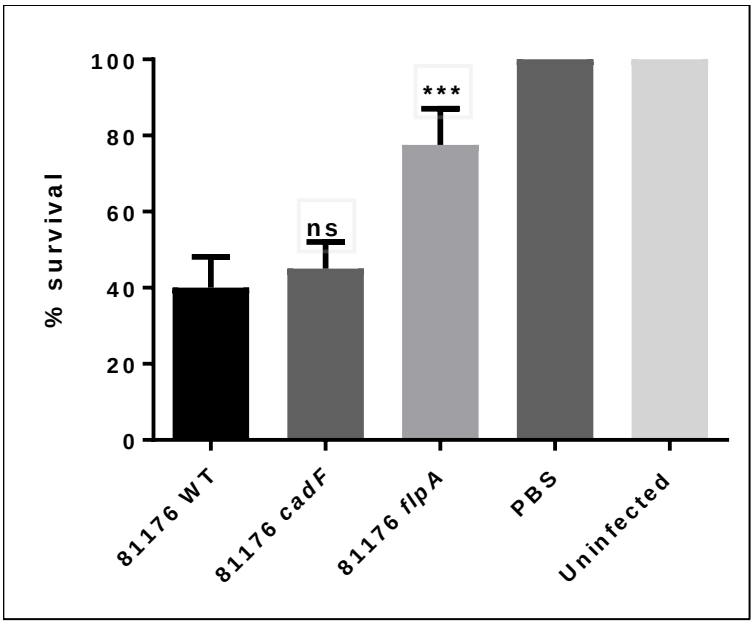

Figure 4.13. Cytotoxicity of OMVs isolated from 81-176 wild-type strain, *cadF* or *flpA* mutants in *G. mellonella* model of infection. Larvae was inoculated with 5 µg of OMVs isolated from the 81-176 wild-type strain, *cadF* or *flpA* mutants, injected into the hind leg using a 10-gauge syringe. Larvae were incubated at 37°C for the duration of the experiment. At 24 h, larvae were inspected for live and dead counts. Inoculation with PBS was used as control. 10 larvae were used for every sample. Data are representative of triplicate independent experiments. *** denotes $p < 0.001$; ns denotes no significant difference.

4.2.13 Induction of IL-8 from T84 intestinal epithelial cells following co-incubation with OMVs isolated from 11168H wild-type strain, *cadF* or *flpA* mutants

Both OMVs isolated from 11168H *cadF* or *flpA* mutants induced slightly lower levels of IL-8 in comparison to OMVs isolated from wild-type strain, however this was not significant. As previously observed with IL-8 induced from T84 cells infected with live 11168H wild-type strain, *cadF* or *flpA* mutants, similar results were observed with OMVs isolated from the respective strains. Interestingly, the level of IL-8 induced by live *C. jejuni* (≈10^8 cfu/ml) was more than double the IL-8 level induced by the respective OMV samples (100 □g) at 800 pg/ml and 300 pg/ml

respectively (compare Figure 4.5 with Figure 4.14). These results suggest that *C. jejuni* 11168H OMVs induce IL-8 from T84 IECs via a CadF / FlpA independent mechanism.

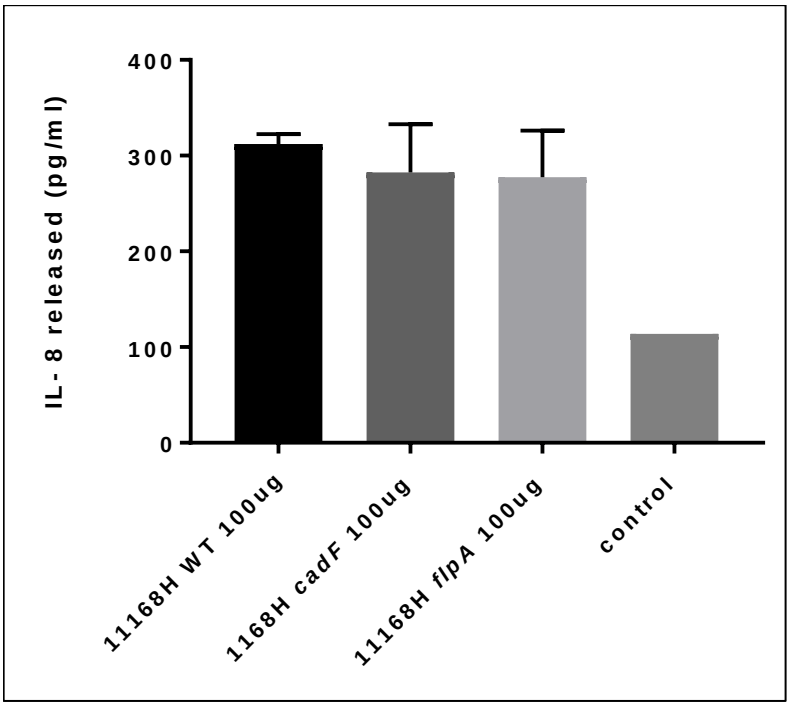

Figure 4.14. Induction of IL-8 from T84 IECs following co-incubation with OMVs isolated from 11168H wild-type strain, *cadF* or *flpA* mutants. T84 IECs were co-incubated with 100 µg OMVs isolated from 11168H wild type strain, *cadF* or *flpA* mutants for 24 h. Supernatants were collected and the levels of IL-8 quantified using a human IL-8 ELISA. Data are representative of triplicate independent experiments.

4.2.14 Induction of IL-8 from T84 intestinal epithelial cells following co-incubation with OMVs isolated from 81-176 wild-type strain, *cadF* and *flpA* mutants

OMVs isolated from 81-176 *cadF* or *flpA* mutants induced significantly lower levels of IL-8 compared to OMVs isolated from the wild-type strain. However, the difference level induced by *cadF* and *flpA* mutants was not significant. It was also observed that IL-8 induction following co-incubation with OMVs was around half that induced following infection with live *C. jejuni* strains (compare Figure 4.6 with Figure 4.15).

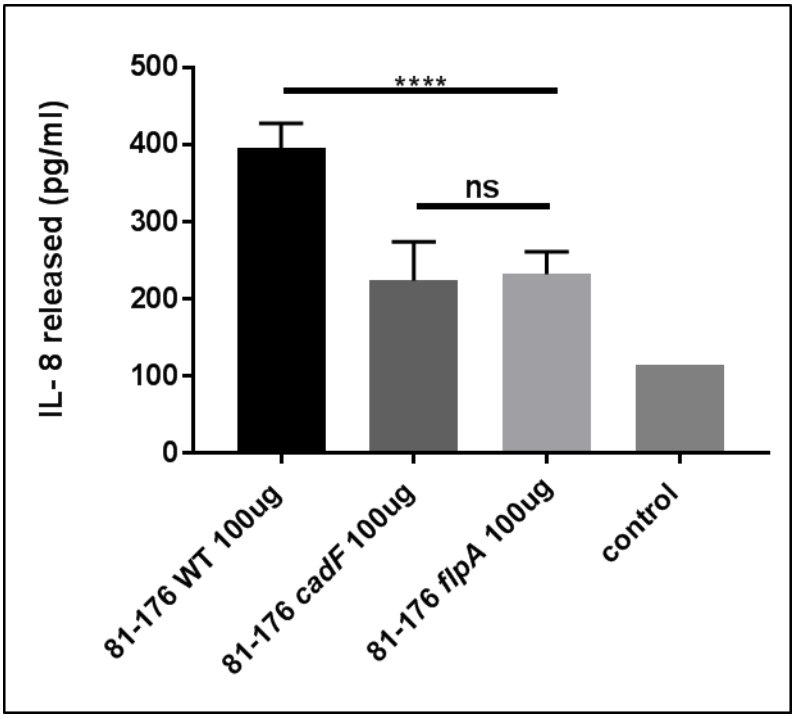

Figure 4.15. Induction of IL-8 from T84 IECs following co-incubation with OMVs isolated from the 81-176 wild-type strain, *cadF* or *flpA* mutants. T84 IECs were co-incubated with 100 µg OMVs isolated from 81-176 wild type strain, *cadF* or *flpA* mutants. Supernatants were collected and the levels of IL-8 quantified using a human IL-8 ELISA. Data are representative of triplicate independent experiments. **** denotes $p < 0.0001$; ns denotes no significant difference.

4.2.15 Methyl-beta-cyclodextrin inhibition of 11168H wild-type strain, *cadF* or *flpA* mutants invasion of T84 intestinal epithelial cells

The epithelial cell plasma membrane contains microdomains termed lipid rafts composed of cholesterol. Fusion of bacteria within the microdomain enables an invasion pathway via caveolin-mediated endocytosis. This is because the lipid rafts invaginate into a caveolae with bacteria inside it. Methyl-beta-cyclodextrin (MβCD) depletes the cholesterol in the lipid rafts, thus inhibiting this particular pathway (Simons and Toomre, 2000). Disruption of lipid rafts by pre-treating T84 IECs with MβCD reduced the invasion of the 11168H wild-type strain and also both the *cadF* and *flpA* mutants (Figure 4.16). The wild-type strain exhibited a similar level of invasion of T84 IECs after the cells were treated with MβCD as the *cadF* or *flpA* mutants.

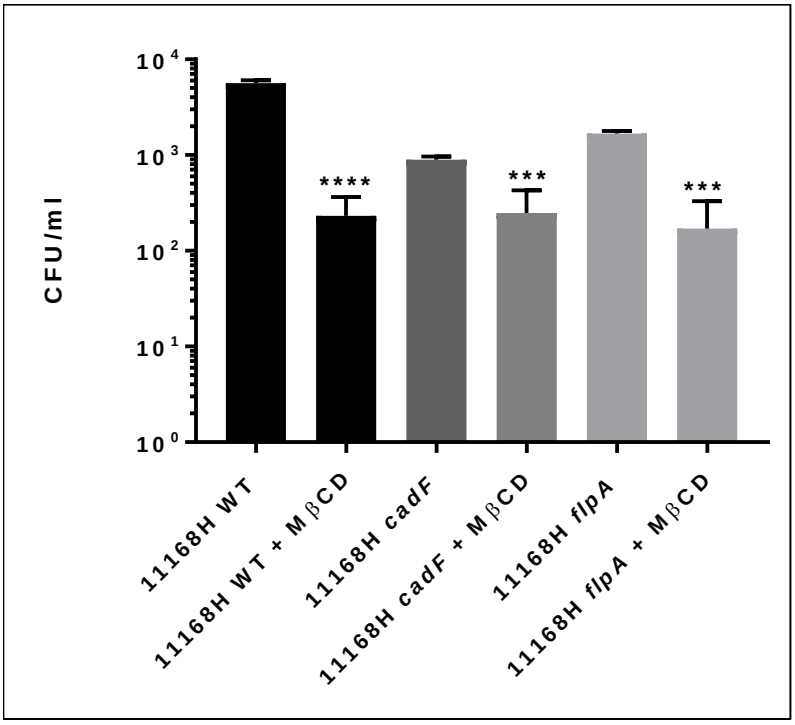

Figure 4.16. Methyl-beta-cyclodextrin (MβCD) inhibition of bacterial invasion. T84 IECs were pre-treated with 5 μM MβCD for 1 h prior to infection. *C. jejuni* 11168H wild-type strain, *cadF* or *flpA* mutants were co-incubated with T84 IECs that were pre-treated with MβCD or a control with no inhibitor treatment, for 3 h. After incubation, T84 IECs were lysed with 0.2% (v/v) Triton X-100 and interacting bacteria enumerated. Comparison was made between treated and non-treated T84 IECs. Data are representative of triplicate independent experiments. *** denotes $p < 0.001$ and **** denotes $p < 0.0001$.

4.2.16 Cytochalasin D inhibition of 11168H wild-type strain, *cadF* or *flpA* mutants invasion of T84 intestinal epithelial cells

Pathogens use the host cell cytoskeleton to mediate or trigger bacterial internalisation. The host cell cytoskeleton consists of microfilaments that are smaller than microtubules. Many studies have shown that disruption of microfilaments by cytochalasin D (Cyto D) inhibites the entry of many pathogens including *Listeria monocytogenes* (Cossart, 1995), EPEC *E. coli* (Sanger et al., 1996) and *Shigella flexneri (Mounier et al., 1997)*. Inhibition of microfilament polymerisation by pre-treating T84 IECs with Cyto D reduced the invasion of the 11168H wild-type strain and also both the *cadF* and *flpA* mutants (Figure 4.17). In addition, the *cadF* and *flpA* mutants showed a further reduction in invasion compared to the wild-type strain in pre-treated cells. Depolymerisation of microfilaments affected the invasion of the 11168H *flpA* mutant more significantly than the 11168H *cadF* mutant.

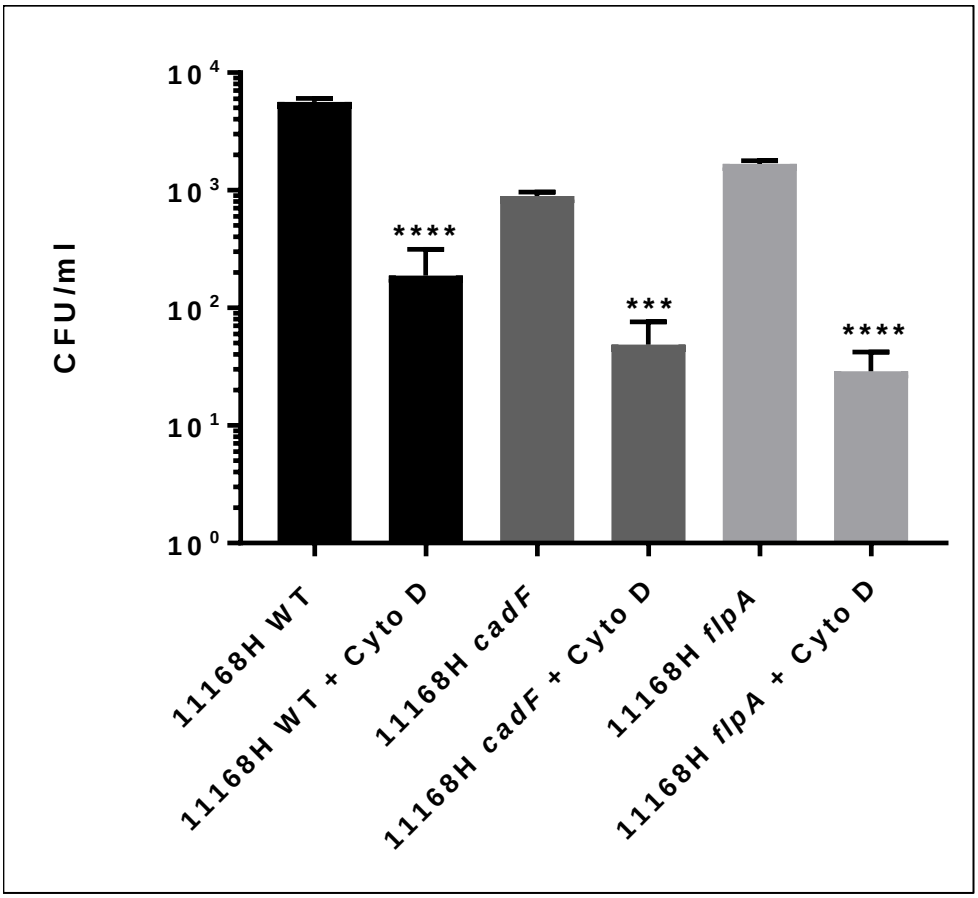

Figure 4.17. Cytochalasin D inhibition of bacterial invasion. T84 IECs were pre-treated with 3 μM cytochalasin D (Cyto D) for 1 h prior to infection. *C. jejuni* 11168H wild-type strain, *cadF* or *flpA* mutants were co-incubated with T84 IECs that were pre-treated with Cyto D or with a control with no inhibitor treatment, for 3 h. After incubation, T84 IECs were lysed with 0.2% (v/v) Triton X-100 and interacting bacteria enumerated. Comparison was made between treated and non-treated T84 IECs. Data are representative of triplicate independent experiments. *** denotes $p < 0.001$ and **** denotes $p < 0.0001$

4.2.17 Colchicine inhibition of 11168H wild-type strain, *cadF* or *flpA* mutants invasion of T84 intestinal epithelial cells

In order to establish the involvement of MTs in the invasion mechanisms of *C. jejuni*, colchicine, an inhibitor that causes MT depolymerisation, was used in the invasion assay. Tubulin is pivotal for microtubules, and depolymerisation of microtubulin impacts on the cytoskeleton (Wei et al., 2013). Inhibition of MT polymerisation by pre-treating T84 IECs with colchicine reduced the invasion of the 11168H wild-type strain and *cadF* mutant. The wild-type strain exhibited a similar level of invasion of T84 IECs after the cells were pre-treated with colchicine as the *cadF* mutant. However, no significant reduction in invasion of the 11168H *flpA* mutant was observed with cells pre-treated with colchicine compared to non-treated cells. Interestingly with T84 IECs pre-treated with colchicine, the 11168H *flpA* mutant exhibited a significantly higher level of invasion compared to the 11168H wild-type strain.

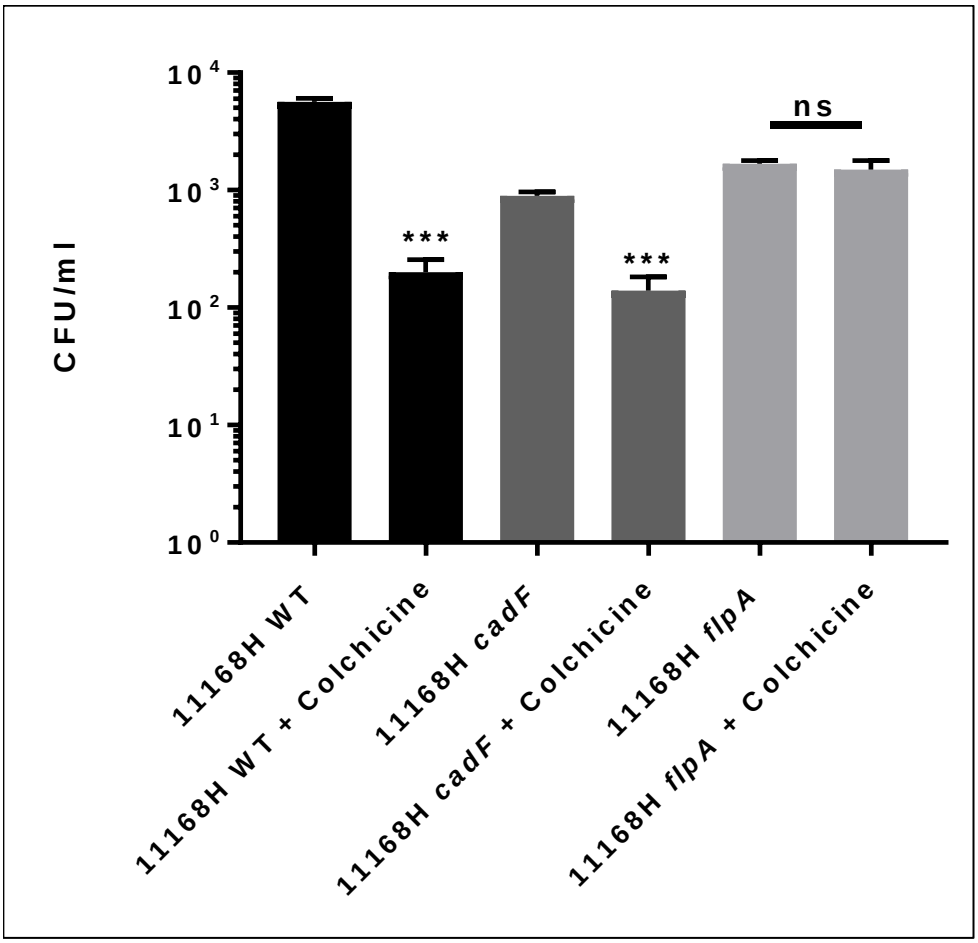

Figure 4.18. Colchicine inhibition of bacterial invasion. T84 IECs were pre-treated with 10 μM colchicine for 1 h prior to infection. *C. jejuni* 11168H wild-type strain, *cadF* or *flpA* mutants were co-incubated with T84 IECs that were pre-treated with colchicine or a control with no inhibitor treatment, for 3 h. After incubation, T84 IECs were lysed with 0.2% (v/v) Triton X-100 and interacting bacteria enumerated. Data are representative of triplicate independent experiments. Comparison was made between treated and non-treated T84 IECs. *** denotes $p < 0.001$.

4.2.18 Wortmannin inhibition of 11168H wild-type strain, *cadF* and *flpA* mutants invasion of T84 intestinal epithelial cells

PI3-K is a signal transducer enzyme involved in many basic cell functions, including cell proliferation, differentiation, motility growth and intracellular trafficking. Wortmannin inhibits the activity of PI3-K (Biswas et al., 2000), was not required for invasion of T84 IECs by the 11168H *cadF* mutant. Inhibition of PI3-K activation by pre-treating T84 IECs with wortmannin reduced the invasion of the 11168H wild-type strain and *flpA* mutant. However, no significant reduction in invasion of the 11168H *cadF* mutant was observed with cells pre-treated with wortmannin compared to non-treated cells. The wild-type strain exhibited a similar level of invasion of T84 IECs after the cells were pre-treated with wortmannin as the *cadF* mutant, whilst the *flpA* mutant showed a further reduction in invasion compared to the wild-type strain.

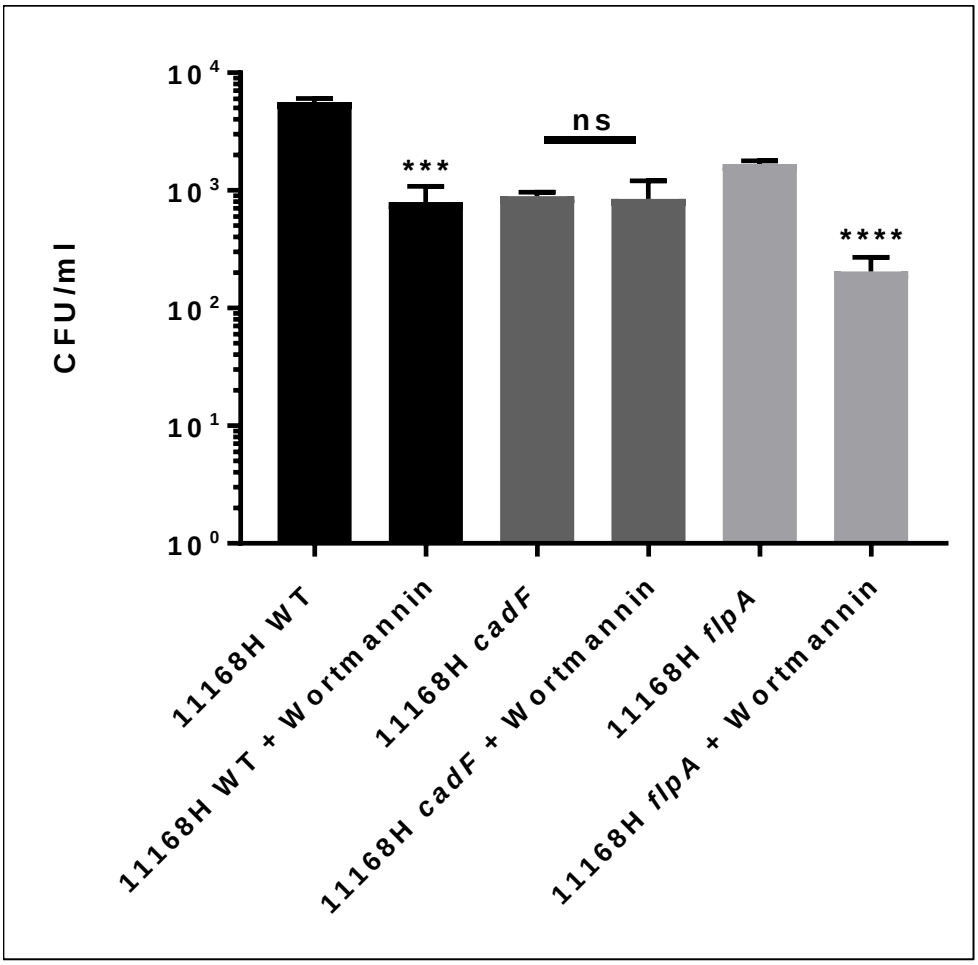

Figure 4.19. Wortmannin inhibition of bacterial invasion. T84 IECs were pre-treated with 1 μM wortmannin for 1 h prior to infection. *C. jejuni* 11168H wild-type strain, *cadF* or *flpA* mutants were co-incubated with T84 IECs that were pre-treated with wortmannin or a control with no inhibitor treatment, for 3 h. After incubation, T84 IECs were lysed with 0.2% (v/v) Triton X-100 and interacting bacteria enumerated. Data are representative of triplicate independent experiments. Comparison was made between treated and non-treated T84 IECs. *** denotes $p < 0.001$ and ****denote $p < 0.0001$.

4.2.19 Comparison of the inhibition of 11168H wild-type strain, *cadF* or *flpA* mutant invasion of T84 intestinal epithelial cells

The inhibitors used in this study all affected the ability of *C. jejuni* to invade T84 IECs. Figure 4.20 shows the effect of each inhibitor on the invasion of T84 IECs by *C. jejuni* 11168H wild-type strain, *cadF* or *flpA* mutants. Invasion by the 11168H wild-type strain was reduced by all inhibitors. However, whilst the reduction in invasion caused by pre-treatment with MβCD, Cyto D and colchicine was at a similar same level, pre-treatment with wortmannin appeared to have less of an impact on wild-type invasion of T84 IECs. Invasion by the 11168H *cadF* mutant was also reduced by pre-treatment with MβCD, Cyto D and colchicine. However pre-treatment with wortmannin had no impact on invasion by the *cadF* mutant. Invasion by the 11168H *flpA* mutant was reduced by pre-treatment with MβCD, Cyto D and wortmannin. However pre-treatment with colchicine increased the level of invasion by the *flpA* mutant.

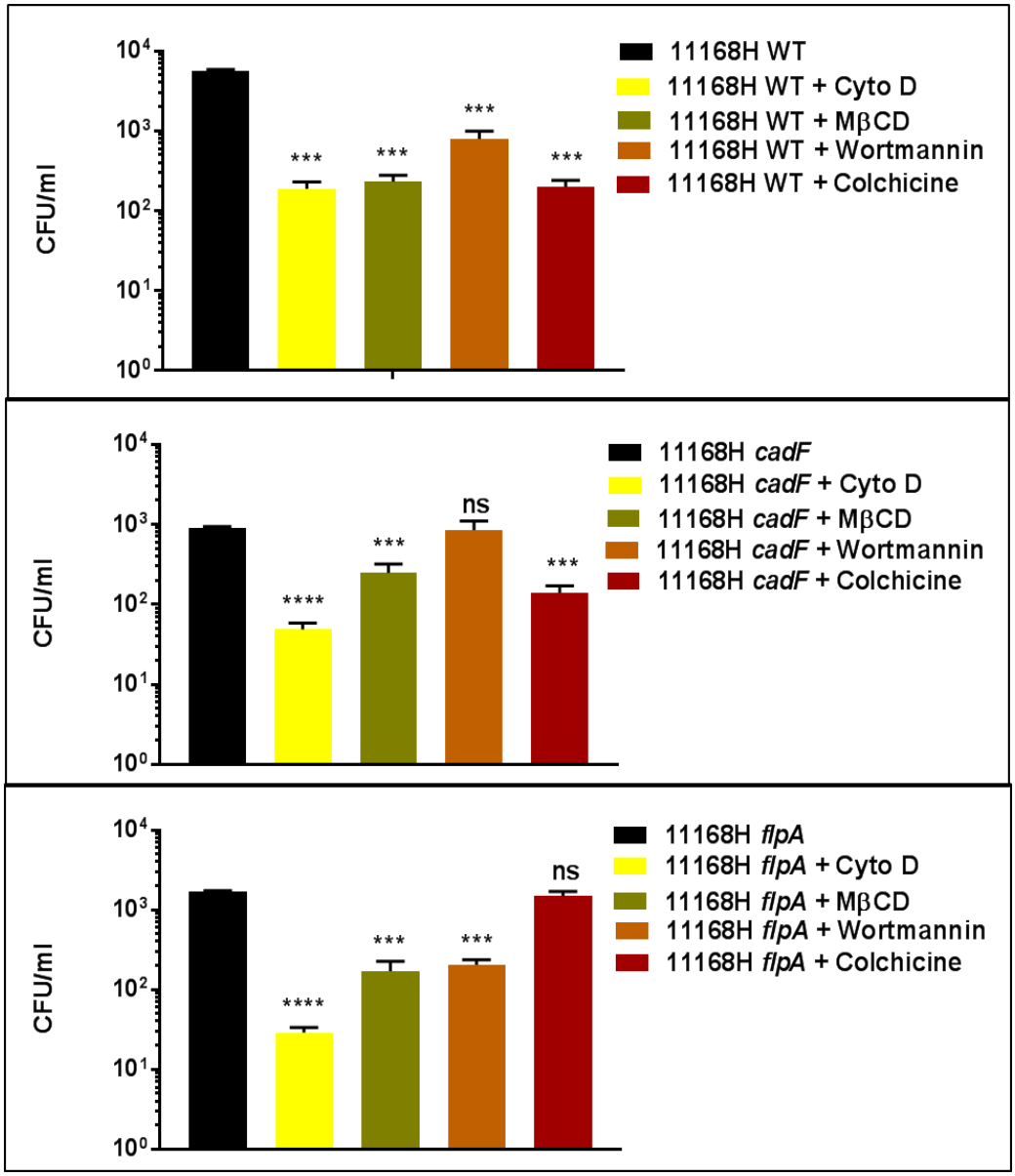

Figure 4.20. Comparison of the effect of eukaryotic inhibitors on the invasion of T84 IECs by 11168H wild-type strain, *cadF* or *flpA* mutants. T84 IECs that were pre-treated with an inhibitor or a control with no inhibitor treatment were infected (MOI 100:1) with *C. jejuni* 11168H wild-type strain, *cadF* or *flpA* mutants for 3 h. After incubation, T84 IECs were lysed with 0.2% (v/v) Triton X-100 and interacting bacteria enumerated. Data are representative of triplicate independent experiments. Comparison was made between treated and non-treated T84 IECs. *** denotes $p < 0.001$ and ****denote $p < 0.0001$. ns denotes no significant difference.

4.2.20 Summary of effects of inhibitors on 11168H and 81-176 wild-type strains, *cadF* and *flpA* mutants invasion into T84 intestinal epithelial cells.

Many studies that have investigated the pathways that *C. jejuni* utilises to invade intestinal epithelial cells have used pharmacological inhibitors that block the function or specific components in the invasion pathways that *C. jejuni* are hypothesised to use.

Table 4.1. Effect of eukaryotic inhibitors on the invasion of T84 IECs by 11168H or 81-176 wild-type strains and 11168H *cadF* or *flpA* mutants.

Inhibitors	Actions	Mechanisms	11168H wild-type strain	11168H *cadF* mutant	11168H *flpA* mutant	81-176 wild-type
Cytochalasin D	Depolymerises actin	Depolymerises actin units that assemble into microfilaments and inhibits membrane fusion with bacteria	√ (inhibited)	√	√	× (not inhibited)
Methyl-beta cyclodextrin	Depletes cholesterol	Depletes cholesterol in the microdomain of the plasma membrane that form the lipid rafts	√	√	√	√
Colchicine	Depolymerises tubulin	Depolymerises tubulin units that assemble into microtubules	√	√	×	√
Wortmannin	Inhibits PI3K for protein synthesis	Binds directly and irreversibly to the catalytic protein (110kDa) of PI3K	√	×	√	√

4.3 Discussion

The human IEC lines and methodologies used to study the pathogenesis mechanisms of enteric bacteria *in vitro* attempt to mimic the cells found in the intestine and the intestinal environment *in vivo*. Much of what is known about *C. jejuni* adhesion to and invasion of human IECs *in vitro* has been generated using non-polarised cell lines, such as Hep-2, HeLa, INT 407, Caco-2 or T84 cells (Wine et al., 2008, Monteville et al., 2003, Monteville and Konkel, 2002, Fauchere et al., 1986). While these studies have provided important insights into aspects of *C. jejuni* infection of non-polarised IECs, all are inherently limited by the significant differences that exist between cell lines as well as the difference between *in vitro* cell culture conditions (De Melo et al., 1989, Fauchere et al., 1986, Konkel and Joens, 1989). Non-polarised IECs lack key morphological phenotypes and do not completely reflect the IECs *in vivo*. Previous studies have reported that human IECs grown on permeable Transwell® filters can form a highly polarised IEC monolayer with a characteristic apical plasma membrane domain and baso-lateral surface. These cells more closely resemble and serve as a better model to investigate pathogen infections or toxin exposure (Kohler et al., 2007, Hurley and McCormick, 2003, Berkes et al., 2003).

The mechanisms of *C. jejuni* adhesion to and invasion of IECs have been studied in some detail using polarised T84 (human colonic carcinoma) and Caco-2 (small intestine epithelial cell) cell lines (Grant et al., 1993, Pignata et al., 1994, Nataro et al., 1996). As polarised monolayers, these IECs cells exhibit normal microvilli and brush borders, and more closely resemble IECs *in vivo* (Finlay and Falkow, 1990, Everest et al., 1992). The integrity of the polarised IECs is sustained through cell-cell sealing mediated by tight junctions, adherens junctions and desmosomes, which act as barriers to prevent invasion of *C. jejuni* (Boehm et al., 2012).The tight junction is the most lumenal cell-cell junction and completely surrounds IECs. The tight junction is also composed of scaffolding proteins, including zonula occludens (ZO)-1, junctional adhesion molecule (JAM)-1, claudin, and occludin.

The integrity of polarised IECs monolayers *in vitro* before and after infection with *C. jejuni* can be determined by measuring TEER. TEER measurement is a sensitive indicator for barrier integrity of electrical resistance between the apical

and baso-lateral compartments. The IECs Transwell® filter insert model has been used to investigate the impact of *C. jejuni* infection on IEC barrier integrity (Boehm et al., 2012, Bras and Ketley, 1999, MacCallum et al., 2005b).

In this chapter, around 14 days after seeding in 12-well inserts (0.3 µm pore size), the T84 and Caco-2 IECs reached peak levels of TEER. This supports the data from previous studies (Bras and Ketley, 1999, Konkel et al., 1992c, Grant et al., 1993, Mills et al., 2012). TEER levels reflect retention of barrier function. However, other studies have shown that only 7 days were required for Caco-2 IECs to form a polarised monolayer (Hu et al., 2008, Harvey et al., 1999). Weekly feeding (change of fresh culture medium) has been shown to maintain the peak TEER for a month, while a lack of feeding will lower the TEER quickly after 14 days (Hurley et al., 2016). In this study, Caco-2 and T84 IECs showed a peak TEER of 500 Ω cm^2 and 400 Ω cm^2 respectively. A previous study also reported that the TEER value for T84 IECs averages 400 Ω cm^2 whilst non-infected Caco-2 IECs showed a peak TEER of between 300-500 Ω cm^2 (Konkel et al., 1992c). Having established the polarised state of the IECs, the monolayers were infected 14 days after seeding. Any IECs which showed a TEER value less than or equal 100 Ω cm^2 were excluded in this study because the blank Transwell® insert (baseline TEER) without cells produced TEER values around 100 Ω cm^2. In contrast, some studies have reported the opposite (Hurley et al., 2016). The variable TEER value results were probably due to different methods and lab settings employed. Despite these limitations, polarised human IEC models are a useful model for investigation of enteric pathogen interactions with host cells. These IECs cultured on Transwell® filters offer numerous advantages compared to laboratory animal studies.

The TEER assay was used to determine the impact of bacterial infection on IECs monolayers, while *C. jejuni* translocation from apical to baso-lateral compartment was studied to provide evidence of disruption of IECs monolayer integrity. Generally, the degree of pathogen invasion correlates with the reduced integrity of the host cell plasma membrane, because loss of membrane integrity results in increased permeability hence more bacterial translocation across the membrane barrier.

A decrease of TEER in IECs may be because of increased paracellular permeability, local cell lysis within the monolayer or a change of ion flux across the monolayer (Madi et al., 2010). *S. Typhimurium* translocates across

polarised human IECs with the complete loss of TEER after 6 h (Finlay and Falkow, 1990). The same effect was observed with *Vibrio parahaemolyticus* (Lynch et al., 2005) and *E. coli* (Puthenedam et al., 2007). Bacteria such as *P. fluorescens* were found to decrease the TEER of Caco-2/TC7 monolayers, which was associated with increased paracellular permeability and the rearrangement of F-actin microfilaments in the cytoskeleton (Madi et al., 2010).

However, the results from this study showed that translocation of the *C. jejuni* 11168H wild-type strain, *cadF* and *flpA* mutants were not associated with a reduction in TEER of T84 cells. These results suggest that barrier integrity was not disrupted following infection with either the 11168H wild-type strain, *cadF* or *flpA* mutants. This is consistent with previous studies that have showed *C. jejuni* wild-type strains M129, 81116 and 81-176 were able to translocate across Caco-2 monolayers without a reduction of TEER after between 6 h to 72 h post infection (Konkel et al., 1992c, Grant et al., 1993, Louwen et al., 2012). In addition, it was also reported that an increase of inoculum (1000 fold) still had no impact on TEER even after 6 h infection. However in another study, infection with clinical isolates *C. jejuni* over 24 h reduced TEER in Caco-2 cells (Bras and Ketley, 1999).

C. jejuni has been reported to translocate via M cells, transcellularly across cells and paracellularly between cells (Bras and Ketley, 1999, Walker et al., 1988, Everest et al., 1999, Konkel and Cieplak, 1992, Harvey et al., 1999). *C. jejuni* M129, F38011 and 81116 strains translocate across Caco-2 IECs in a time-dependent manner. However, translocation reached a peak 4 h post-infection (Konkel et al., 1992c). In this study, the ability of the 11168H wild-type strain, *cadF* and *flpA* mutants to translocate across T84 cells was assessed. Instead of counting the CFUs, a 11168 wild-type strain, *cadF* and *flpA* mutants expressing GFP were used. After a period of incubation, the baso-lateral media was collected and fluorescence intensity quantified. The *cadF* GFP and *flpA* GFP mutants were both observed to translocate across T84 IECs as efficiently as the 11168H GFP wild-type strain, based on the fluorescence intensity. This suggests that CadF and FlpA are not involved in the transmigration of *C. jejuni* across IECs.

The mechanisms by which *C. jejuni* transmigrate across IECs are poorly defined. Previous studies reported that *C. jejuni* can translocate across polarised cell monolayers via the paracellular route without reduction of TEER

(Konkel and Cieplak, 1992, Everest et al., 1992, Harvey et al., 1999, Bras and Ketley, 1999). In contrast, other studies observed the opposite that *C. jejuni* infection caused a reduction in TEER (Pogacar et al., 2010, Wine et al., 2008, Chen et al., 2006).

In previous studies, the loss of TEER in Caco-2 IECs after 24 h infection was observed using a high MOI of 10^5:1 (MacCallum et al., 2005b) and similarly in T84 IECs (Chen et al., 2006). Both events were associated with reorganisation of TJ proteins such as occludin. OMVs isolated from the 11168H wild-type strain were able to cleave E-cadherin and occludin in T84 IECs (Elmi et al., 2016). Another suggested entry mechanism that has been described is a paracellular pathway called subvasion. *C. jejuni* invade non-polarised Chang epithelial cells from the baso-lateral surface (van Alphen et al., 2008). Without evidence of a decrease in monolayer integrity, it is still inconclusive to confirm whether the translocation occurred transcellularly or paracellularly. *C. jejuni* probably employ both or either pathways at the same time or at different times depending on strain and IECs. One study has suggested that *C. jejuni* enters the host cell by HtrA mediated-cleaving E-cadherin, without a reduce in TEER (Boehm et al., 2012). Alternatively epithelial cells of human origin could reseal after penetration as has been observed in guinea pig epithelial cells (Takeuchi, 1967).

Numerous studies have reported that breaches in IEC barrier integrity following paracellular invasion results in penetration of luminal antigens and microbes, stimulating pro-inflammatory responses (Larson et al., 2008). Mutation of *cadF* and *flpA* in the 81-176 strain reduced the level of IL-8 released by T84 IECs, in contrast no significant reduction in IL-8 induction was observed by the 11168H *cadF* and *flpA* mutants. Previous studies have shown that *C. jejuni* interactions with IECs induces innate immune responses, such as production of IL-6 (Friis et al., 2009), IL-8 (MacCallum et al., 2006) and TNFα (Al-Salloom et al., 2003). The MacCallum *et al.* study also reported that *C. jejuni* infection induces more IL-8 from T84 IECs than from Caco-2 IECs (MacCallum et al., 2006). However, in another study, the 81-176 wild-type strain was observed to induce IL-8 more than the 11168H wild-type strain in Caco-2 and Hep-2 cells (Zilbauer et al., 2005). Several studies also have reported a link between *C. jejuni* 11168H virulence factors and the induction of the innate immune response (Black et al., 1988, Russell et al., 1989). There are several *C. jejuni* virulence factors that play a role in the activation of host cell innate immune responses, nevertheless

the bigger picture is still unclear (Hickey, et al. 2000). Production of IL-8 from host cells is an important immune response against infection and may also result in inflammatory diarrhoea during *C. jejuni* infection (Watson and Galan, 2005, Hu and Hickey, 2005). IL-8 induced by *Shigella* and *Salmonella* involved signalling via Nuclear factor kappaB (NF-κB) (Hobbie et al., 1997, Philpott et al., 2000). The same impact was also observed in HeLa cells infected with *C. jejuni* NCTC 11168 (Mellits et al., 2002). Infection of *C. jejuni* 81-176 wild-type strain in NF-κB deficient mice results in the mice chronically colonised and developing gastritis compared to wild-type mice (Fox et al., 2004). Furthermore, another study reported that *C. jejuni* induction of IL-8 from IECs was both independent and dependent on CDT (Hickey et al., 2000).

The cellular mechanisms that allow *C. jejuni* adhesion to and invasion into IECs are not well understood (O Croinin and Backert, 2012, Cossart and Sansonetti, 2004). The debate regarding the zipper and/or trigger mechanisms of bacterial invasion is still ongoing (O Croinin and Backert, 2012) *C. jejuni* interacts with IECs in a very specific manner preferably via Rac1 and Cdc42. Many aspects of actin dynamics are regulated by activation of Rac1 (Albertson et al., 2008) such as lamellipodia formation and protrusion of actin networks. Rho and Rac regulate the polymerisation of actin to produce stress fibres and lamellipodia respectively (Nobes and Hall, 1995a). *C. jejuni* 81-176, 84-25 and F38011 wild-type strains were all shown to induce Rac1 in INT 407 cells (Krause-Gruszczynska et al., 2007a). The activation of Rac1 was attributed to the recruitment of lipid rafts (Boehm et al., 2011).

Based on these observations, the ability of *cadF* and *flpA* mutants to activate Rac1 in IECs was investigated. Both *cadF* and *flpA* mutants exhibit a similar significant reduction in the ability to induce Rac1 activation in serum-starved T84 IECs compared to wild-type strain. This suggests that both CadF and FlpA are involved in Rac1 activation, demonstrating a further role of these fibronectin binding protein in *C. jejuni* pathogenesis. Activation of Rac1 leads to actin cytoskeleton reorganisation, such as membrane ruffling and formation of lamellipodia (Nobes and Hall, 1995a). These have been shown to play a role in the zipper or trigger entry pathway mechanism (Cossart and Sansonetti, 2004). However, it also suggests that other *C. jeuni* virulence factors must be involved, since *cadF* and *flpA* mutants were still able to activate Rac1 in T84 IECs.

Consistent with this hypothesis, a recent study of Rac1 in fibroblast cells provides further evidence. Boehm *et al.* proposed that the pathway of fibronectin→integrin beta 1→FAK involved Rac1 activation. This study used fibroblast cells which knockout fibronectin and integrin beta 1. This study used C*. jejuni* wild-type strains 81–176, 84–25 and F38011 with the respective isogenic *cadF, flaAB* and *flhA* mutants, and the IECs used were INT 407 cells. The results showed that fibronectin, integrins and FAK were involved during efficient uptake of *C. jejuni*. In this study, the role of the second fibronectin binding protein FlpA (Flanagan et al., 2009) as well as CadF was investigated.

Rac1 is a member of the Rho superfamily of small GTPases (Tran Van Nhieu et al., 1999, Hall, 1990, Cossart and Sansonetti, 2004), which also includes Cdc42 and RhoA (Caron and Hall, 1998, Nobes and Hall, 1995a). GTPases act as a molecular switch in the active state to transmit signals in many cellular pathways. The collective events in turn will control many cellular functions including cytoskeleton rearrangements in host cells such as membrane ruffles (lamellipodia) and microprojections (filopodia) (Nobes et al., 1995). Rac1 activation in host cells results in formation of membrane ruffling (Nobes et al., 1995, Nobes and Hall, 1995b). Rac1 was shown to be a central regulator in *C. jejuni* 81-176 internalisation into host cells (Krause-Gruszczynska et al., 2007a). In other pathogens such as *S. Enterica* and *S. flexneri,* invasion into host cells was observed to be heavily associated with membrane ruffles (Hardt et al., 1998, Cossart and Sansonetti, 2004, Tran Van Nhieu et al., 1999). In this study, in the Rac1 activation assay, both *cadF* and *flpA* mutants were able to induce Rac1 activation but at a reduced level compared to wild-type strain, suggesting that in *C. jejuni* 11168H, both CadF and FlpA work synergistically to facilitate *C. jejuni* entry into host intestinal epithelial cells. This finding also supports the previous data that showed bacterial fibronectin-binding proteins acted together and with secreted proteins to promote maximal *C. jejuni* invasion of host cells by stimulating membrane ruffling (Eucker and Konkel, 2012). A F38011 *cadF* mutant has also been shown to play a role in Rac1 and Cdc42 activation in INT 407 cells. It was also suggested that CadF might not function independently and that other bacterial factors were involved (Krause-Gruszczynska et al., 2007a). However, even when only one of the fibronectin binding proteins is present as in the case with either of the *cadF* or *flpA* mutants, both these mutants were still able to induce Rac1 activation. This suggested that both CadF and FlpA act in tandem to activate Rac1 for efficient *C. jejuni* invasion.

C. jejuni produces OMVs that contain many proteins (Lindmark et al., 2009, Elmi et al., 2012, Jang et al., 2014). *C. jejuni* 11168H OMVs have been reported to contain 151 proteins (Elmi et al., 2012). *C. jejuni* virulence proteins identified in OMVs include all three components of CDT (CdtA, CdtB and CdtC), the HtrA and Cj0511 proteases, 16 *N*-linked glycoproteins, major antigenic protein Peb3 and both fibronectin binding proteins CadF and FlpA (Elmi et al., 2012).

C. jejuni OMVs have been shown to be cytotoxic to human IECs (Lindmark et al., 2009, Elmi et al., 2012). Mutation of *cadF* or *flpA* in both the 11168H and 81-176 strains resulted in the OMVs isolated from either mutant exhibiting reduced cytotoxicity in the *G. mellonella* larvae model of infection. In Chapter 3, it was shown that infection with either the *cadF* or *flpA* mutant increased the survival of *G. mellonella* larvae compared to infection with a wild-type strain. OMVs were less cytotoxic compared to live bacteria when injected into *G. mellonella* larvae. This indicates that CadF and FlpA play a role in pathogenesis in the *G. mellonella* larvae model of infection. These results support previous data that showed OMVs isolated from either a *htrA* mutant or a *Cj1365c* mutant exhibited reduced cytotoxicity in *G. mellonella* larvae (Elmi et al., 2016). In contrast, OMVs isolated from a *cdtA* mutant showed cytotoxicity levels similar to OMVs isolated from the 11168H wild-type strain (Elmi et al., 2012). In this study, the cytotoxicity of OMVs from *C. jejuni* wild-type strains and from respective *cadF* or *flpA* mutants to Caco-2 cells was investigated. OMVs isolated from either the *cadF* or *flpA* mutants showed reduced cytotoxicity against Caco-2 IECs.

C. jejuni OMVs have also been reported to induced immune responses much like live bacteria that results in production of IL-8 from intestinal epithelial cells (Elmi et al., 2012) In this study OMVs isolated from the 11168H wild-type strain, *cadF* or *flpA* mutants were able to induce production of IL-8 from T84 IECs similar to live bacteria. In addition, there was also no significant difference between IL-8 production by the *cadF* and *flpA* mutants compared to the wild-type strain, both with live bacterial cells or OMVs. However the level of IL-8 production was much lower after co-incubation with OMVs (300 pg/ml) compared to infection with live bacterial cells (800 pg/ml). However OMVs isolated from the 81-176 *cadF* or *flpA* mutants showed a significant reduction in IL-8 production by T84 IECs compared to OMVs isolated from the wild-type strain. The level of IL-8 induced by the 81-176 wild-type strain OMVs was lower by 50% than the level induced by live wild-type bacterial cells at 400 pg/ml and

800 pg/ml respectively. Also the level of IL-8 induced by the 81-176 *cadF* or *flpA* mutant OMVs was reduced compared to the respective live bacterial cells at 200 pg/ml to 600 pg/ml respectively. These conflicting results could be explained by differences in protein expression between the *C. jejuni* 11168H and 81-176 strains, including size of OMV release and production (Lindmark et al., 2009, Elmi et al., 2012). A study reported that OMV protein contents from *Pseudomonas aeruginosa* are strain dependent (Bauman and Kuehn, 2006). In the same study, it was also shown that different composition in OMVs protein cause variations in OMVs morphology.

Bacterial invasion into IECs allow pathogens to establish a niche inside the host cells. Certain pathogens utilise more than one invasion pathway to not only maximise the chance to successfully invade IECs, but also to survive the defence by varieties of immune weaponry mounted by the IECs (Cossart and Sansonetti, 2004). *C. jejuni* invasion into IECs is considered as one of the hallmarks for *C. jejuni*-caused tissue damage, however the molecular mechanism of *C. jejuni* invasion is widely unclear. Pharmacological inhibitor studies can identify cellular pathways used by pathogens to enter host cells (Backert and Hofreuter, 2013). In this study, specific pharmacological inhibitors were used to investigate whether *C. jejuni* invasion into IECs involved caveolae-mediated endocytosis, microfilaments, microtubules and/or the PI3 Kinase host signalling pathways.

The plasma membrane of IECs contains a special region termed lipid rafts. Lipid microdomains are enriched with cholesterol and sphingolipids. Functions of lipid rafts include polarised secretion, membrane transport and the generation of cell polarity. Lipid rafts are also enriched in many signal transduction molecules and play a role in sensing the extracellular environment. Caveolae are a subset of lipid rafts with a caveolin filament component which is a cholesterol binding protein (Rothberg et al., 1992). Many pathogens including bacteria, viruses and parasites have been reported to target the lipid rafts function to their advantage. *E.coli* has been shown to enter mast cells through lipid rafts (Shin et al., 2000) as has *Mycobacterium bovis* uptake by mouse macrophages (Gatfield and Pieters, 2000). *Plasmodium falciparum* surrounding membrane was reported to be enveloped in a caveolae-like structure (Olliaro and Castelli, 1997). In the case of viruses, measles and influenza virus assembly were both observed at this domain. In addition, components of mature virion were also found associated with the lipid rafts (Manie et al., 2000, Scheiffele et al., 1999). Other

studies showed that entry of virus particles was inhibited by caveolae - disrupting drugs (Parton and Lindsay, 1999, Norkin, 1999). Many studies have shown that caveolae-mediated endocytosis plays a role in *C. jejuni* internalisation into IECs. Drugs that inhibit lipid rafts also inhibit *C. jejuni* invasion of Caco-2, T84 and INT 407 cells (Wooldridge et al., 1996, Watson and Galan, 2008, Krause-Gruszczynska et al., 2007b, Hu et al., 2006). However a study by Konkel *et al.* demonstrated that *C. jejuni* invasion was not dependent on caveolae (Konkel et al., 2013).

Treatment of IECs with MβCD reduces the cholesterol content in lipid raft fractions and resulted in a significant reduction of *C. jejuni* invasion of T84 IECs by the 11168H wild-type strain, *cadF* mutant and *flpA* mutant to similar levels. This suggests that *C. jejuni* invasive ability is in part dependent on intact lipid rafts in the plasma membrane of IECs, but that neither CadF nor FlpA are involved in this invasion pathway. These findings are in agreement with a study reported by Watson & Galan that showed with T84 cells treated with MβCD, *C. jejuni* invasion was blocked in a dose-dependent manner (Watson and Galan, 2008). Moreover, upon depletion and sequestration of plasma membrane cholesterol, the invasion ability of the *C. jejuni* 81-176 wild-type strain was reduced (Watson and Galan, 2008).

Lipid rafts are thought to be involved in cell signalling pathways. *C. jejuni* OMVs induced a reduced level of IL-8 from lipid raft depleted T84 cells (Elmi et al., 2012). Since lipid rafts are highly ordered structures enriched in sphingolipids and glycosylphosphatidylinositol-anchored proteins (GPI-Aps), the reduced levels of IL-8 from IECs treated with *cadF* and *flpA* mutants OMVs may be correlated with the reduced ability of *cadF* and *flpA* mutants to interact with fibronectin. Similar results were reported for other enteropathogens in which depleted lipid rafts from IECs accounted for a reduced entry or internalisation into host cell (Kohler et al., 2002, de Souza Santos and Orth, 2014, Steele-Mortimer, 2008). It was also reported that treatment of IECs with cholesterol-sequestering agent flippin III reduced the levels of *Salmonella* interacting with IECs (Lim et al., 2010).

MF depolymerisation by cyto D has been used to study the involvement of MFs in *C. jejuni* invasion into IECs (De Melo et al., 1989, Konkel and Joens, 1989). The rapidly growing ends of actin filaments were inhibited and shortened by cyto D. This has been used to establish that most intracellular bacterial

pathogens including *S. Typhimurium* use pathways that involved MF elements to enter host epithelial cells (Finlay and Falkow, 1988, Elsinghorst et al., 1989). However, diverse results have been reported. *C. jejuni* internalisation was markedly reduced in Hep-2 cells that were treated with cytochalasin B, another inhibitor that depolymerises actin and inhibits endocytosis (De Melo et al., 1989). In contrast, one study showed increased invasion (Bouwman et al., 2013), while another observed reduced invasion into IECs that were pre-treated with cyto D (Monteville et al., 2003). Yet another study showed no inhibition of invasion as observed with the 81-176 strain in Caco-2 cells (Russell and Blake, 1994). The results in this study are in agreement to that of Monteville *et al.* who used the F38011 and 81-176 strains with INT 407 cells. Depolymerisation of MFs significantly reduced the invasion of the 11168H wild-type strain, the *cadF* mutant as well as the *flpA* mutant. Moreover, the *cadF* and *flpA* mutants were both further reduced in invasion into T84 IECs compared to that of the 11168H wild-type strain. However, the reduction of invasion between the *cadF* and the *flpA* mutants was not significant. This indicates that *C. jejuni* invasion into T84 IECs is dependent on MFs and that both CadF and FlpA play a role in this invasion pathway. In contrast, a previous study here at the LSHTM had shown that the 81-176 wild-type strain increased invasion into Caco-2 IECs pre-treated with cyto D (Neveda Naz, PhD Thesis, LSHTM, 2014) in agreement with the Bouwman *et al.* study. This also supported the evidence that *C. jejuni* 81-176 invasion into INT 407 and T84 IECs was increased and did not required MFs when the cells were pre-treated with cytochalasin D (Oelschlaeger et al., 1993). These contrasting results are probably due to a combination of both strain- and cell line-dependent effects (Oelschlaeger et al., 1993).

Colchicine is a tubulin inhibitor that blocks polymerisation of MTs (Dalbeth et al., 2014). The use of colchicine as an inhibitor showed reduced invasion of *C. jejuni*, *Citrobacter freunddi* and enterohemorrhagic *E. coli* (EHEC) (Biswas et al., 2003, Hu and Kopecko, 1999, Oelschlaeger et al., 1993) in Caco-2 IECs, however not in T84 IECs (Wine et al., 2008). A previous study, using the 81-176 wild-type strain also showed a reduction in invasion of Caco-2 IECs (Neveda Naz, PhD Thesis, LSHTM, 2014). In this study, invasion of T84 IECs by both the 11168H wild-type strain and *cadF* mutant was reduced significantly when T84 IECs were pre-treated with colchicine compared to the non-treated cells. However, the *flpA* mutant showed no significant reduction in invasion when T84 IECs were pre-treated with colchicine compared to the non-treated

cells. In addition, the *flpA* mutant invasion was increased compared to the wild-type invasion in T84 IECs pre-treated with colchicine. This may be due to the higher levels of *cadF* expressed in the 11168H *flpA* mutant compared to the wild-type strain (see Chapter 3). These results indicate that *C. jejuni* invasion into T84 IECs is dependent on MTs and that FlpA plays a role in this invasion pathway.

However, the data published regarding the involvement of MTs and MFs during *C. jejuni* invasion again varies. Specifically, this falls into four groups. The first group of studies report that *C. jejuni* required MTs and MFs. In this group, *C. jejuni* 81-176, F38011 and M129 strains were observed to reduce invasion in cells treated with cyto D (depolymerise MFs), mycalolide B (depolymerise F-actin) and nocodazole (MT inhibitor) (Konkel and Joens, 1989, Biswas et al., 2000, Bacon et al., 2000, Oelschlaeger et al., 1993, Hu and Kopecko, 1999, Monteville and Konkel, 2002, Monteville et al., 2003). In the second group*, C. jejuni* invasion requires MTs only. In this study, 81-176 wild-type strain entry into INT 407 cells was inhibited as much as 90% when the cells were treated with many MT depolymerising inhibitors that included colchicine, demecolcine, vincristine or vinblastine as well as nocodazole (Oelschlaeger et al., 1993, Hu and Kopecko, 1999). In addition, invasion was increased in the presence of inhibitors of MFs by around 200%. In the third group, *C. jejuni* invasion requires MFs only. A study reported that in the 81-176 and F38011 strains that CadF plays an important role in invasion of host cells. Since CadF mediates binding to fibronectin, which is found at the basal side of epithelial cells, it was suggested that MFs are required for internalisation (Monteville and Konkel, 2002, De Melo et al., 1989, Konkel and Joens, 1989). Whilst in the fourth group, *C. jejuni* internalisation into Caco-2 cells required neither MTs nor MFs (Russell and Blake, 1994). However in this study, the 11168H wild-type strain and *cadF* mutant fall into group one as for both invasion of T84 IECs was significantly reduced when MTs or MFs were inhibited by colchicine or cyto D respectively. In contrast, the *flpA* mutant falls into group three as inhibition of MTs resulted in no significant reduction of invasion into T84 IECs. In this study, a slight modification was made to the protocol used with the inhibitor removed after 1 h incubation prior to infection, whilst in other studies the inhibitor was left for the entire duration of infection. What clear from those studies are the strains and cells used as well as methods employed in each study was different, hence the results.

Protein kinases are key regulator for many cell functions thus have many membrane receptors. Interaction between receptors and ligands result in activation or phosphorylation of certain set of proteins in host cells. Phosphoinositol kinase (PI3-K) activity can be inhibited by wortmannin. A study reported that *C. jejuni* 81-176 invasion was reduced in wortmannin treated Caco-2 IECs (Hu et al., 2006). Other kinases inhibitors such as stauroporine for general kinase and genistein for tyrosine kinase were also shown to inhibit invasion of the 81-176 strain (Kopecko et al., 2001) and also the 81116 strain (Biswas et al., 2004, Wooldridge et al., 1996). Treatment with wortmannin was shown to reduce invasion of *C. jejuni* and inhibit the activation of GTPase in INT 407 cells (Krause-Gruszczynska et al., 2011). Activation will trigger Rac1 and be followed by cascading events, cytoskeleton reorganisations and membrane ruffling (Cossart and Sansonetti, 2004, Cossart, 2004, Hawkins et al., 1995). Euker *et al.* reported that wortmannin inhibited the invasion of *C. jejuni* F38011 into INT 407 cells in a dose-dependent manner (Eucker and Konkel, 2012). In this study, the 11168H wild-type strain and *flpA* mutant showed a reduction in invasion of T84 IECs pre-treated with wortmannin compared to cells not treated with wortmannin. However, the 11168H *cadF* mutant showed no significant reduction in invasion between treated and non-treated cells. Previous data showed that the 81-176 wild-type strain exhibited reduced invasion of Caco-2 IECs pre-treated with wortmannin. This indicates that *C. jejuni* invasion into T84 IECs is dependent on the involvement of protein kinase activity, specifically in this case PI3K activation and that CadF plays a role in this invasion pathway. Other evidence of the involvement of protein kinases was reported with the mitogen-activated protein kinase (MAPK) which regulates nuclear transcription events that result in bacterial uptake via rearrangement of cytoskeleton in host cells (Biswas et al., 2004, MacCallum et al., 2005a). Inhibitors for p38MAPK were shown to reduce 81-176 invasion into INT 407 cells (Hu et al., 2006, Hu and Kopecko, 1999) .

Studies have clearly demonstrated that the cellular events during *C. jejuni* interactions (adhesion and invasion) with IECs are multifactorial processes (Hu and Kopecko, 1999, Ketley, 1997, Wassenaar and Blaser, 1999). Therefore, looking at the individual *C. jejuni* strain findings in this study in some ways explain and support the above statements, as well as the variation of data previously published. The invasion pathways used by the 11168H wild-type strain, *cadF* or *flpA* mutants can be partially deduced from the inhibitors assays.

With the 11168H wild-type strain, all inhibitors used significantly reduced invasion of T84 IECs. All inhibitors reduced invasion of the 11168H wild-type strain to a similar level except wortmannin that resulted in a slightly higher level of invasion. Reduction in invasion was similar to that of *cadF* and *flpA* mutants in T84 IECs treated with MβCD. In T84 IECs treated with colchicine and wortmannin, the wild-type strain also exhibited similar levels of invasion to the *cadF* mutant. Therefore, the results indicate that 11168H wild-type strain invasion into T84 IECs is dependent of MFs, MTs, intact lipid rafts as well as PI3 kinases. However the *C. jejuni* invasion pathways mediated by CadF and FlpA appear to be different. Invasion of the 11168H *cadF* mutant is reduced by cyto D and colchicine, but not by wortmannin. This suggests that CadF-mediated invasion involves PI3 activation. Invasion of 11168H *flpA* mutant is reduced by cyto D and wortmannin, but not by colchicine. This suggests that FlpA-mediated invasion involves a MT-dependent pathway. CadF and FlpA are different fibronectin-binding proteins and share less than 20% identity and around 32% similarity. This supports the hypothesis that CadF and FlpA play a role in different invasion pathways utilised by *C. jejuni* to enter IECs. Thus, it also may explain and reflect the involvement of many pathways with different mechanisms that *C. jejuni* in general exhibit regarding interactions with host IECs. However, further investigations using different strains will be required to see the true picture of pathogenesis in *C. jejuni*.

CHAPTER FIVE: VISUALISATION OF INTERACTIONS OF GFP EXPRESSING *C. jejuni* STRAINS WITH HUMAN INTESTINAL EPITHLIAL CELLS

5.1 Introduction

In order to escape the host immune defence, bacteria often invade host cells as a means of survival. *C. jejuni* interactions with human intestinal epithelial cells have been investigated *in vitro* using polarised Caco-2 and T84 cell lines. The stable expression of GFP in 11168H strains will provide an important tool for studying *C. jejuni* interactions with different cell types *in vitro*. In addition, studies involving animal models of infection will benefit from a *C. jejuni* strain stably expressing GFP to follow intracellular bacteria *in vivo* for the further investigation of *C. jejuni* mechanisms of pathogenesis.

The GFP plasmid (pCJC4) was provided by Dr Dennis Linton (University of Manchester). Plasmid pCJC4 contains a chloramphenicol resistance cassette (*cat*) with upstream and downstream restriction sites, flanked by regions of the *C. jejuni* NCTC 11168H pseudogene *Cj0223*. The *porA* promoter region, a strong promoter from *C. jejuni* NCTC 11168 is located upstream of a green fluorescent reporter gene (*gfp*), inserted upstream of the *cat* gene. *C. jejuni* cells that conjugated with pCJC4 were observed internalised following bacterial invasion of HeLa cells by fluorescent microscopy (Jervis et al., 2015). Competent cells of *C. jejuni* 11168H wild-type strain, *cadF* and *flpA* mutants were prepared and 1 ug of purified GFP plasmid DNA was used to transform the wild-type strain, *cadF* and *flpA* mutants as described in Section 2.3.15. pCJC4 was successfully transformed into the 11168H wild-type strain, *cadF* and *flpA* mutants, resulting in stable expression of GFP in all strains based on confocal fluorescent microscopy images. These strains were used to visualise *C. jejuni* interactions with human intestinal epithelial cells.

5.2 Results

5.2.1 Growth kinetics of 11168H wild-type strain, *cadF* and *flpA* mutants expressing GFP

Growth assays were performed to assess the impact of expressing GFP. The growth kinetics of the 11168H wild-type strain, *cadF* and *flpA* mutants expressing GFP exhibited a similar pattern compared to the respective non-GFP expressing strains. Initially the 11168H wild-type strain growth was slightly reduced compared to the *cadF* and *flpA* mutants, however after 15 h, the wild-type strain growth was highest followed by *cadF* mutant with the *flpA* mutant lowest (compare Figure 5.1 with Figure 3.6). This indicated that GFP expression does not impact significantly on the growth of these *C. jejuni* strains.

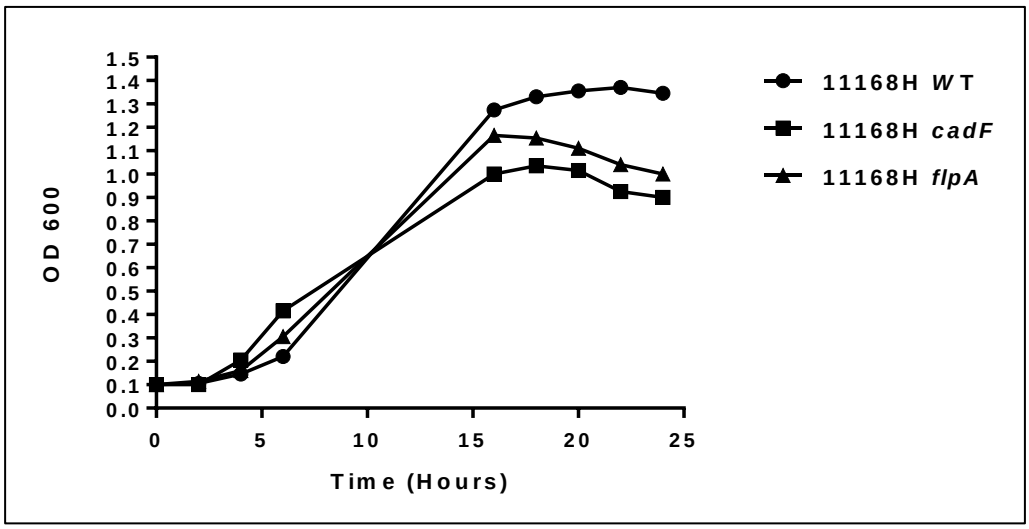

Figure 5.1. Representative growth curves of *C. jejuni* 11168H wild-type strain, *cadF* and *flpA* mutants expressing GFP. Brucella broth was inoculated with *C. jejuni* 11168H wild-type strain, *cadF* or *flpA* mutants at an OD_{600} of 0.1 and incubated with constant shaking at 75 rpm under microaerobic conditions at 37ºC. At intervals of 2 h, 1 ml samples were removed and the OD_{600} recorded. Data shown are representative of three independent experiments.

5.2.2 Motility assays for 11168H wild-type strain, *cadF* and *flpA* mutants expressing GFP

Motility assays were performed to assess the impact of expressing GFP. Both the 11168H *cadF* and *flpA* mutants showed reduced motility compared to wild-type strain and the same phenotypes were observed in the respective non-GFP expressing strains. In addition, *cadF* and *flpA* mutants expressing GFP showed similar motility to the *cadF* and *flpA* non-GFP expressing mutants. However, in comparison to the non-GFP expressing wild-type strain, the 11168H wild-type strain expressing GFP exhibited increased motility (compare Figure 5.2 with Figure 3.7).

A

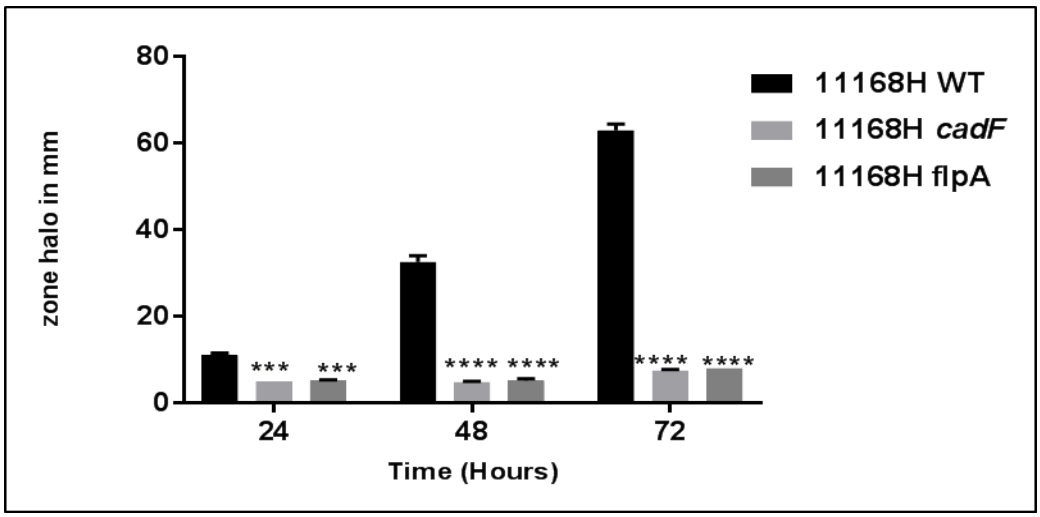

B

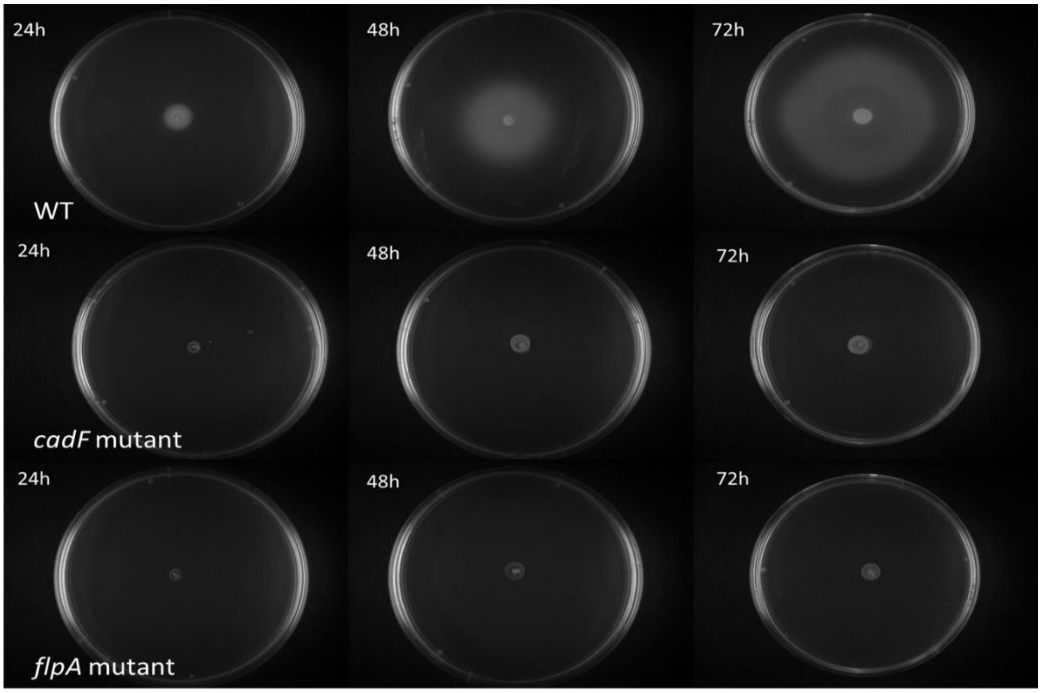

Figure 5.2. Motility assessment of 11168H wild-type strain, *cadF* and *flpA* mutants expressing GFP. Bacteria were grown for 24 h on blood agar plates. A suspension was prepared and adjusted to an OD_{600} of 1.0. 1.5 µl of this suspension was pipetted into the centre of soft agar plates and incubated at 37ºC under microaerobic conditions for 72 h. The level of motility was assessed by measuring the diameter of the growth halo at 24 h, 48 h and 72 h. A. Differences of motility observed in 11168H wild-type, *cadF* mutant and *flpA* mutant expressing GFP. B. Representative images showing motility assay plates of 11168H wild-type, *cadF* mutant or *flpA* mutant expressing GFP at 24, 48 and 72 h. *** denotes p< 0.001 and **** denotes p<0.0001. Data is representative of three independent experiments.

5.2.3 Interactions with and invasion of Caco-2 IECs by the 11168H wild-type strain, *cadF* and *flpA* mutants expressing GFP

In comparison to the non-GFP expressing strains (see Chapter 3), the strains expressing GFP exhibited similar patterns of interaction and invasion with Caco-2 cells.

As with the non-GFP expressing strains, both the 11168H *cadF* and *flpA* mutants expressing GFP exhibited a reduction in interactions with Caco-2 cells compared to the wild-type strain at both 3 h and 24 h time points. However, the interaction numbers increased between 3 h to 24 h (compare Figure 5.3 A with Figure 3.26 A and Figure 3.26 B).

No significant reduction in invasion was observed at 3 h time points for both the 11168H *cadF* and *flpA* mutants expressing GFP. However, both the 11168H *cadF* and *flpA* mutants expressing GFP displayed a significant reduction in invasion of Caco-2 IECs compared to wild-type strain at 24 h time points. In addition, there was no significant increased from 3 h to 24 h on both the 11168H *cadF* and *flpA* mutants expressing GFP invasion, compared to the non-GFP expressing strains (compare Figure 5.3 B with Figure 3. 27A and Figure 3.7 B).

A

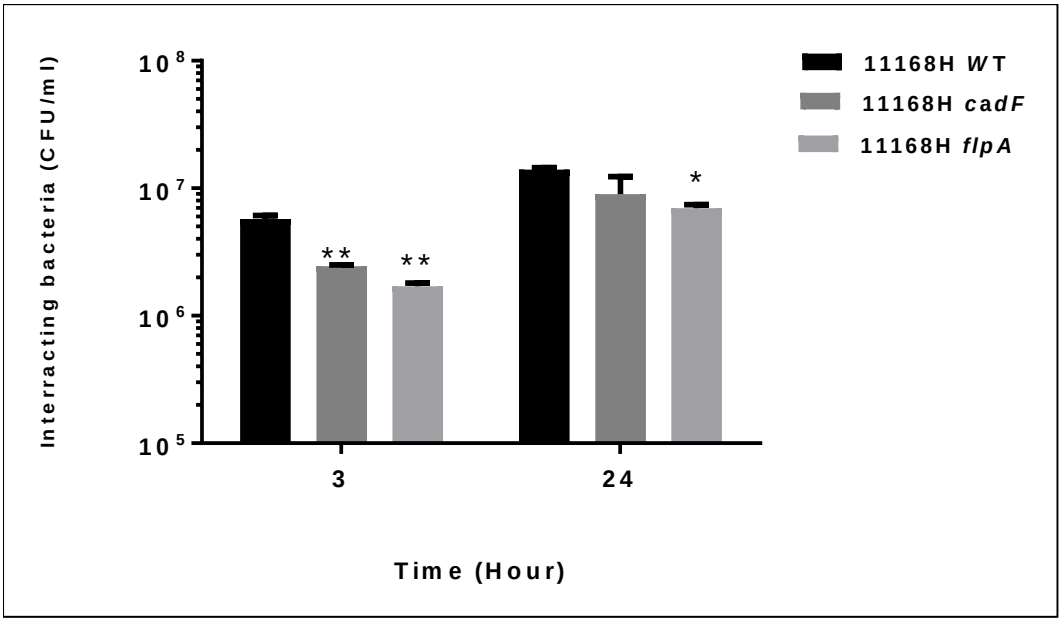

B

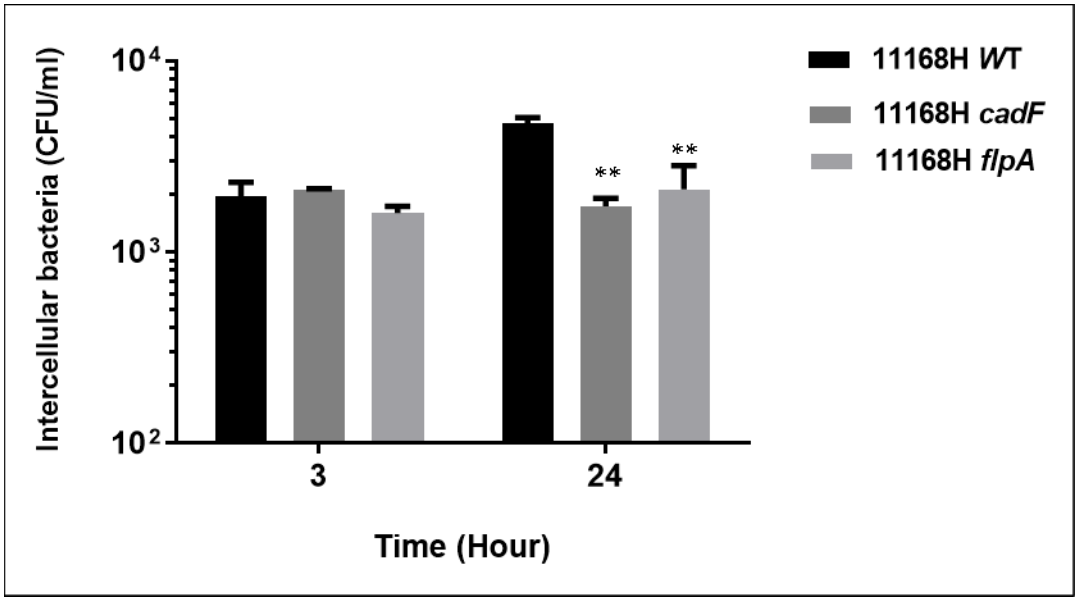

Figure 5.3. Interactions and invasion of *C. jejuni* 11168H wild-type strain, *cadF* and *flpA* mutants expressing GFP with T84 IECs. Confluent monolayers were infected (MOI 100:1) with *C. jejuni* 11168H wild-type strain, *cadF* or *flpA* mutants expressing GFP and incubated for 3 h or 24 h. A. For interaction assays, Triton X-100 was added following washes with PBS to lyse the cells; B. For invasion assays, cells were further incubated with gentamicin (150 µg/ml) for 2 h to kill extracellular bacteria, then lysed with Triton X-100. Serial dilution of lysates were plated on CBA plates. After 48 h, CFU were counted. Data are representative of a minimum of triplicate biological replicates. * denotes $p < 0.05$; ** denotes $p < 0.01$.

5.2.4 *C. jejuni* 11168 wild-type strain expressing GFP invades Caco-2 IECs

In the pathogenesis of many intestinal infections, it appears that adherence to surface mucosa is a pre-requisite for bacterial invasion into host cells. Therefore, initial experiments were performed to investigate the visualisation of *C. jejuni* interactions with Caco-2 IECs using the 11168H wild-type strain expressing GFP. At 30 min post-infection, bacteria were observed

extracellularly surrounding the Caco-2 cells (Figure 5.4). At 60 min post-infection, bacteria were observed at the periphery of cells (Figure 5.5). At both 2 h and 24 h post-infection, many bacteria were observed intracellularly adjacent to the nucleus (Figure 5.6 and Figure 5.7).

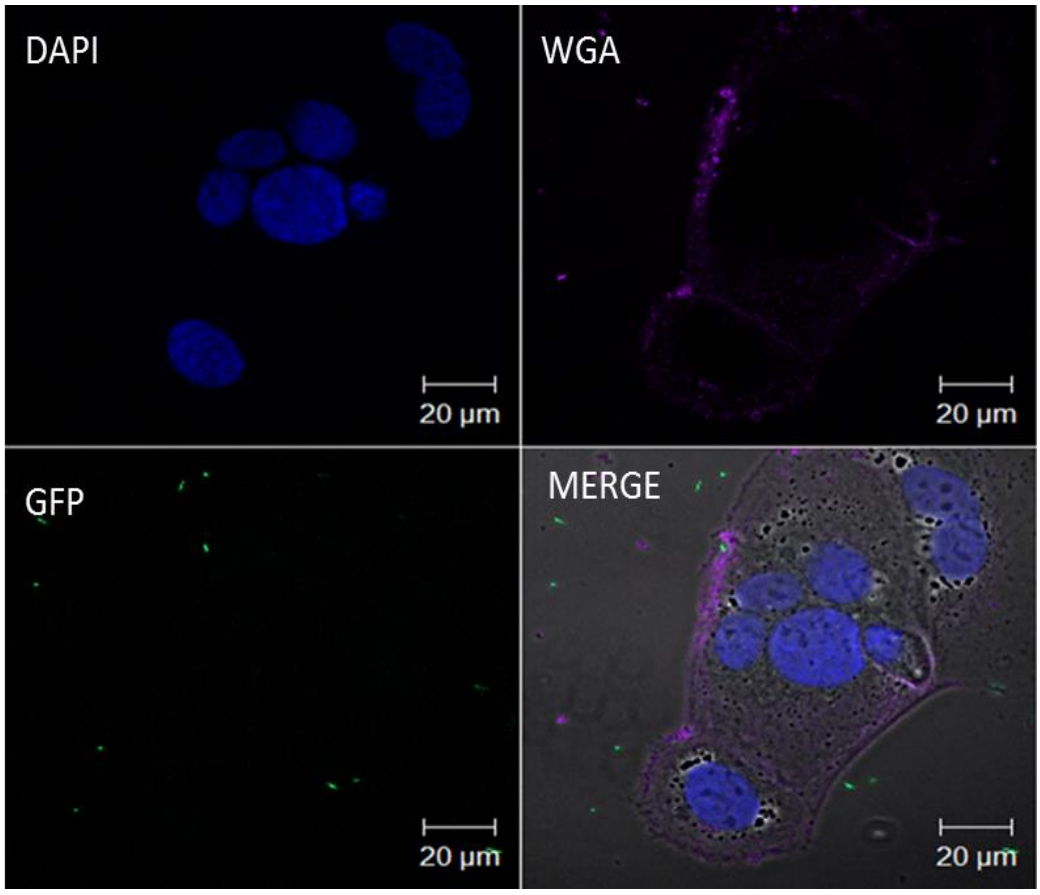

Figure 5.4. Representative confocal micrograph of Caco-2 cells infected with GFP expressing 11168H wild-type strain showing the position of bacteria 30 minutes post-infection. Caco-2 cells infected (MOI 100:1) with GFP expressing 11168H wild-type strain were prepared and stained using DAPI (Blue) for nucleus and WGA (Red) for plasma membrane. Combined confocal fluorescence images of Caco-2 cells infected with GFP expressing 11168H wild-type strain (Green) for 30 min, showing extracellular bacteria close to the Caco-2 cells. The majority of bacteria was observed outside of the cells.

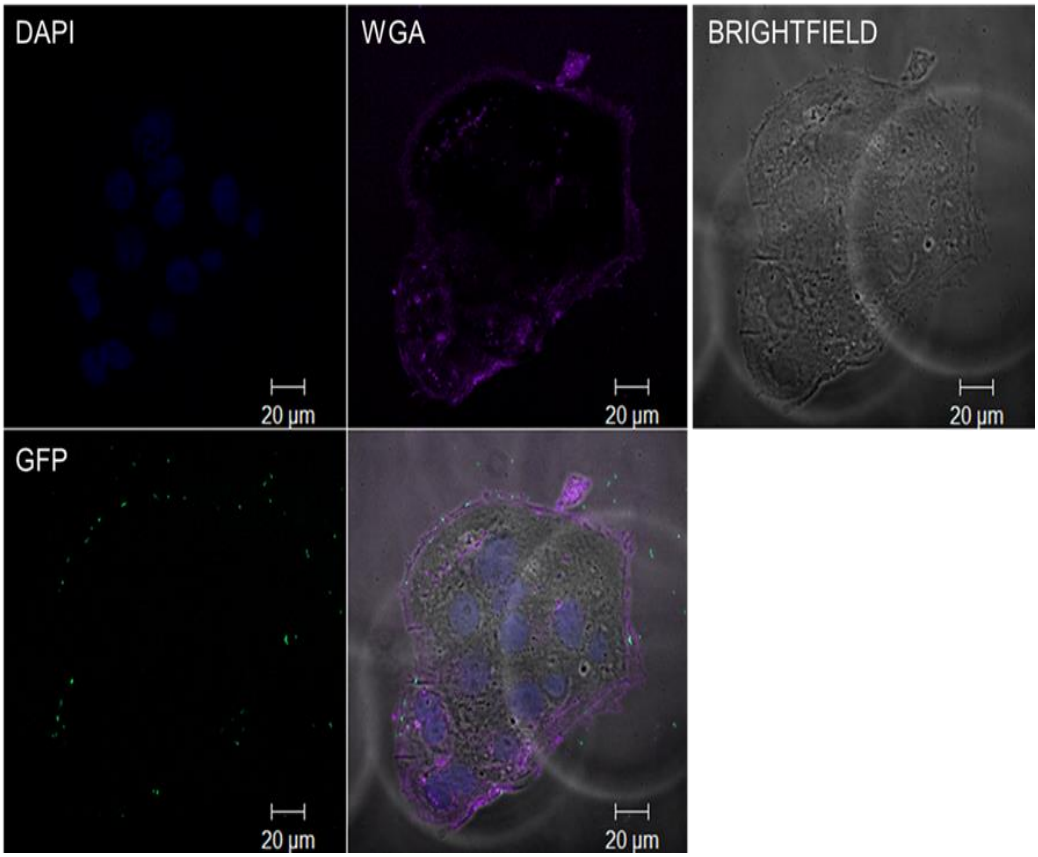

Figure 5.5. Representative confocal micrograph of Caco-2 cells infected with GFP expressing 11168H wild-type strain showing the position of bacteria 60 minutes post-infection. Caco-2 cells infected (MOI 100:1) with GFP expressing 11168H wild-type strain were prepared and stained using DAPI (Blue) for nucleus and WGA (Red) for plasma membrane. Combined confocal fluorescence images of Caco-2 cells infected with GFP expressing 11168H wild-type strain (Green) for 60 min, showing majority of bacteria at the periphery of the cells and internalised within plasma membrane of cells.

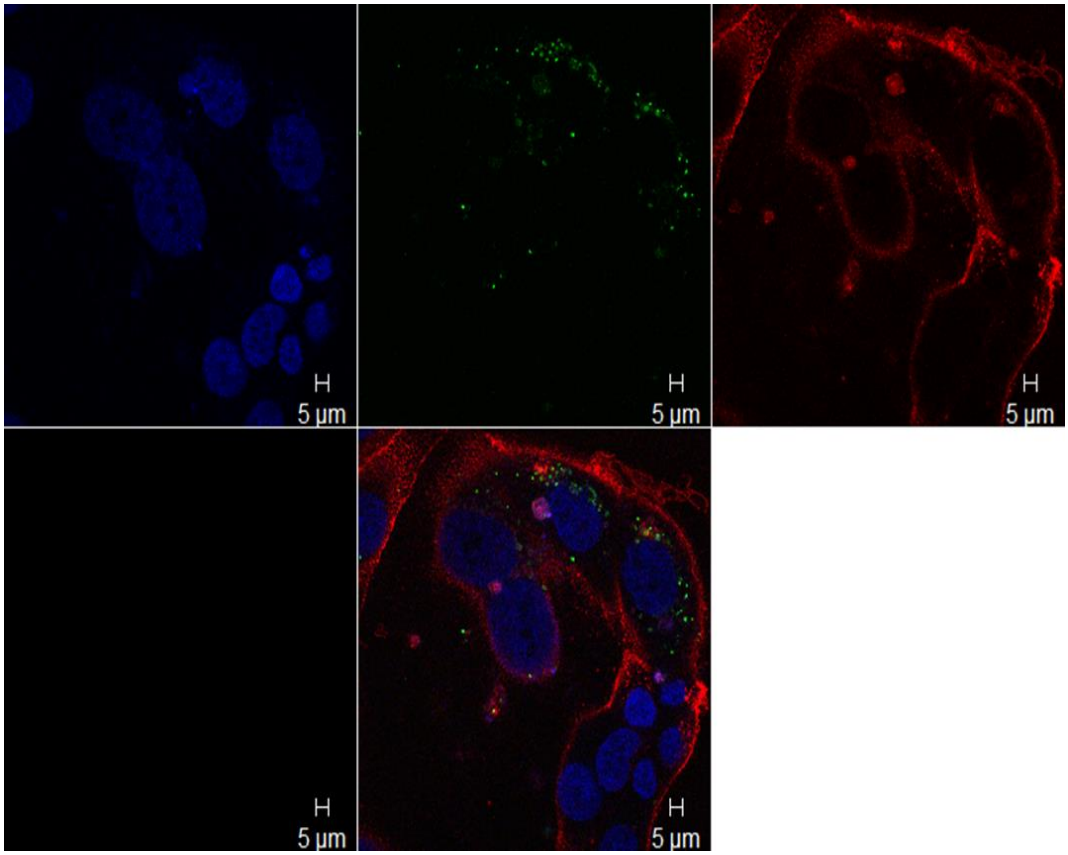

Figure 5.6. Representative confocal micrograph of Caco-2 cells infected with GFP expressing 11168H wild-type strain showing the position of bacteria 2 h post-infection. Caco-2 cells infected (MOI 100:1) with GFP expressing 11168H wild-type strain were prepared and stained using DAPI (Blue) for nucleus and WGA (Red) for plasma membrane. Combined confocal fluorescence images of Caco-2 cells infected with GFP expressing 11168H wild-type strain (Green) for 2 h, showing majority of bacteria were internalised. Most bacteria were observed inside the cytoplasm of the cells and some aligned just inside the plasma membrane of cells. Some bacterial were membrane-associated with the cytoskeleton appeared yellow.

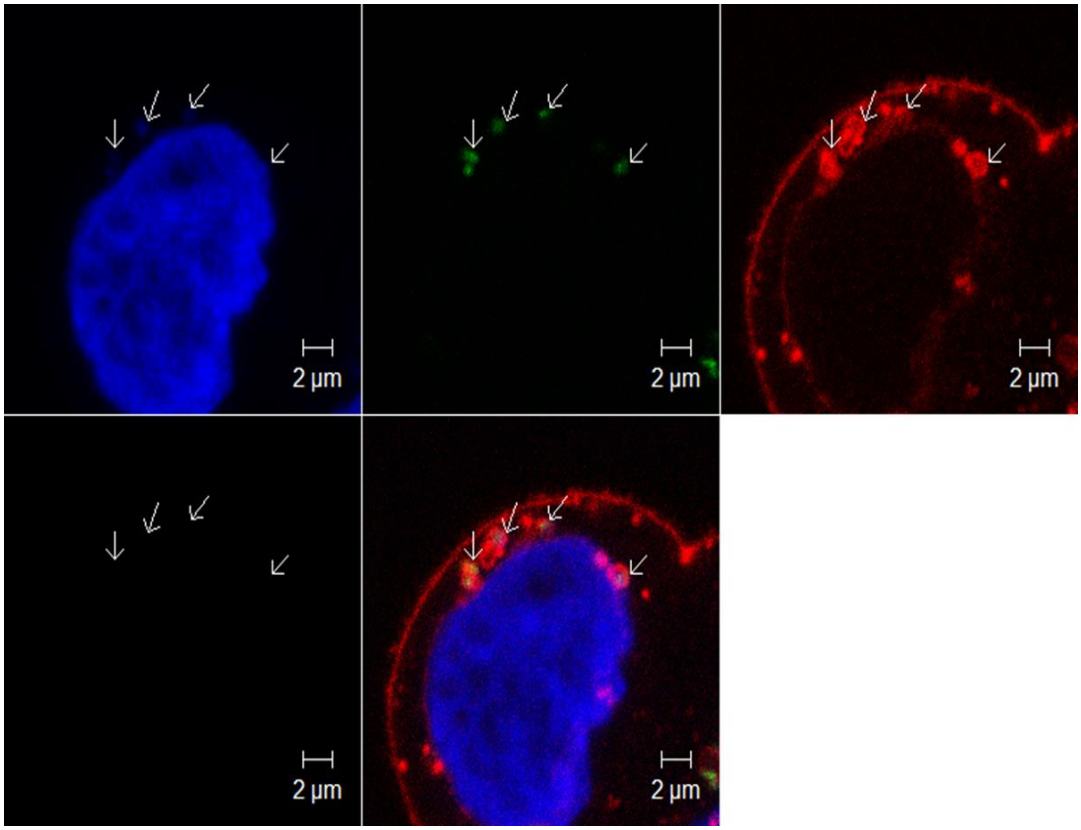

Figure 5.7. Representative confocal micrograph of Caco-2 cells infected with GFP expressing 11168H wild-type strain showing the position of bacteria 24 h post-infection. Caco-2 cells infected (MOI 100:1) with GFP expressing 11168H wild-type strain were prepared and stained using DAPI (Blue) for nucleus and WGA (Red) for plasma membrane. Combined confocal fluorescence images of Caco-2 cells infected with GFP expressing 11168H wild-type strain (Green) for 24 h, showing bacteria close to the nucleus. Some bacteria that were membrane-associated with the cytoskeleton appeared yellow.

5.2.5 *C. jejuni* 11168H wild-type strain expressing GFP invades T84 IECs

Further experiments were performed to investigate the visualisation of *C. jejuni* interactions with T84 IECs using the 11168H wild-type strain expressing GFP. Confocal microscopy of T84 cells confirm the association of *C. jejuni* 11168H with T84 IECs. Bacteria were readily observed internalised in T84 IECs 24 h post-infection in various stages simultaneously (Figure 5.8 A and B). At the initial stage, some bacteria were seen adhering to the outside of the cell at the plasma membrane, whilst others were already internalised inside the cells (Panel A). In the same micrograph, the ruffling of the membrane surrounding the T84 cell was also observed. Entering the cell results in *C. jejuni* being enveloped in the plasma membrane (Red) as observed in Panel B. Thus some internalised *C. jejuni* were seen as yellow in colour as these bacteria were associated with the host cell plasma membrane. However, bacteria were also observed without any association with the plasma membrane (Green).

A

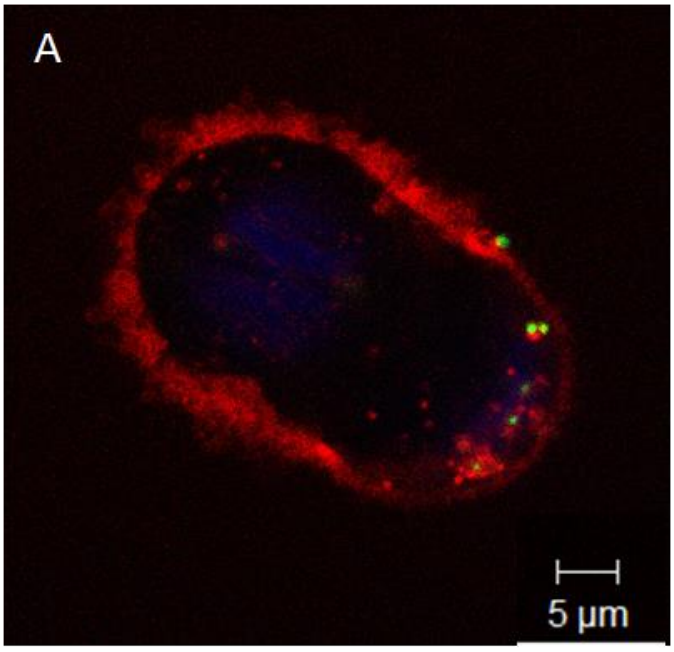

B

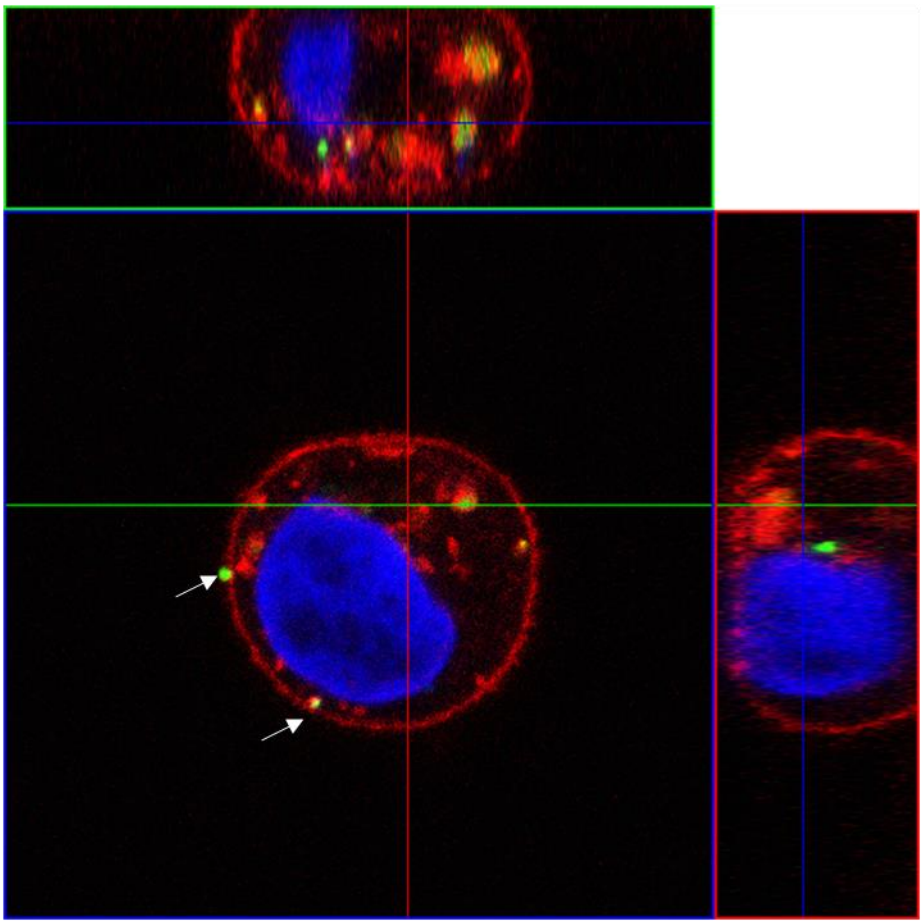

Figure 5.8. Cellular association of *C. jejuni* in T84 IECs. Representative confocal micrograph of T84 cells infected with GFP expressing 11168H wild-type strain showing the position of bacteria 24 h post-infection. T84 cells infected (MOI 100:1) with GFP expressing 11168H wild-type strain for 24 h. Cells were prepared and stained using DAPI (Blue) for nucleus and WGA (Red) for plasma membrane. Panel A shows C*. jejuni* adhered at the plasma membrane outside cells and internalised inside the plasma membrane inside cells. Panel B shows a Z stack-combined confocal fluorescence images of T84 cells infected with GFP expressing 11168H wild-type strain (Green), showing bacteria about to enter the cell has no plasma membrane around it, whilst another bacteria almost inside the cell, was enclosed with the plasma membrane (Red) around it. Another bacteria already inside the cell can be observed close to the cell nucleus. Bacterial which were membrane-associated with the cytoskeleton appeared yellow.

5.2.6 Control untreated and uninfected Caco-2 IECs

Comparison was made in untreated and uninfected Caco-2 cells to visualise and establish *C. jejuni* invasion prior performing further experiments. Caco-2 cells were grown on cover slips as described in Section 2.19. As a control, cells untreated with inhibitors and uninfected with *C. jejuni* were stained either with WGA to show the plasma membrane or with rhodamine-phalloidin to highlight the actin cytoskeleton (Figure 5.9). Caco-2 cells were stained showing the plasma membrane (Red) in uninfected Caco-2 cells (Panel A) and infected with *C. jejuni* (Green) (Panel B). Caco-2 cells were stained showing actin filaments (Red) in uninfected Caco-2 cells (Panel C) and infected with *C. jejuni* (Green) (Panel D).

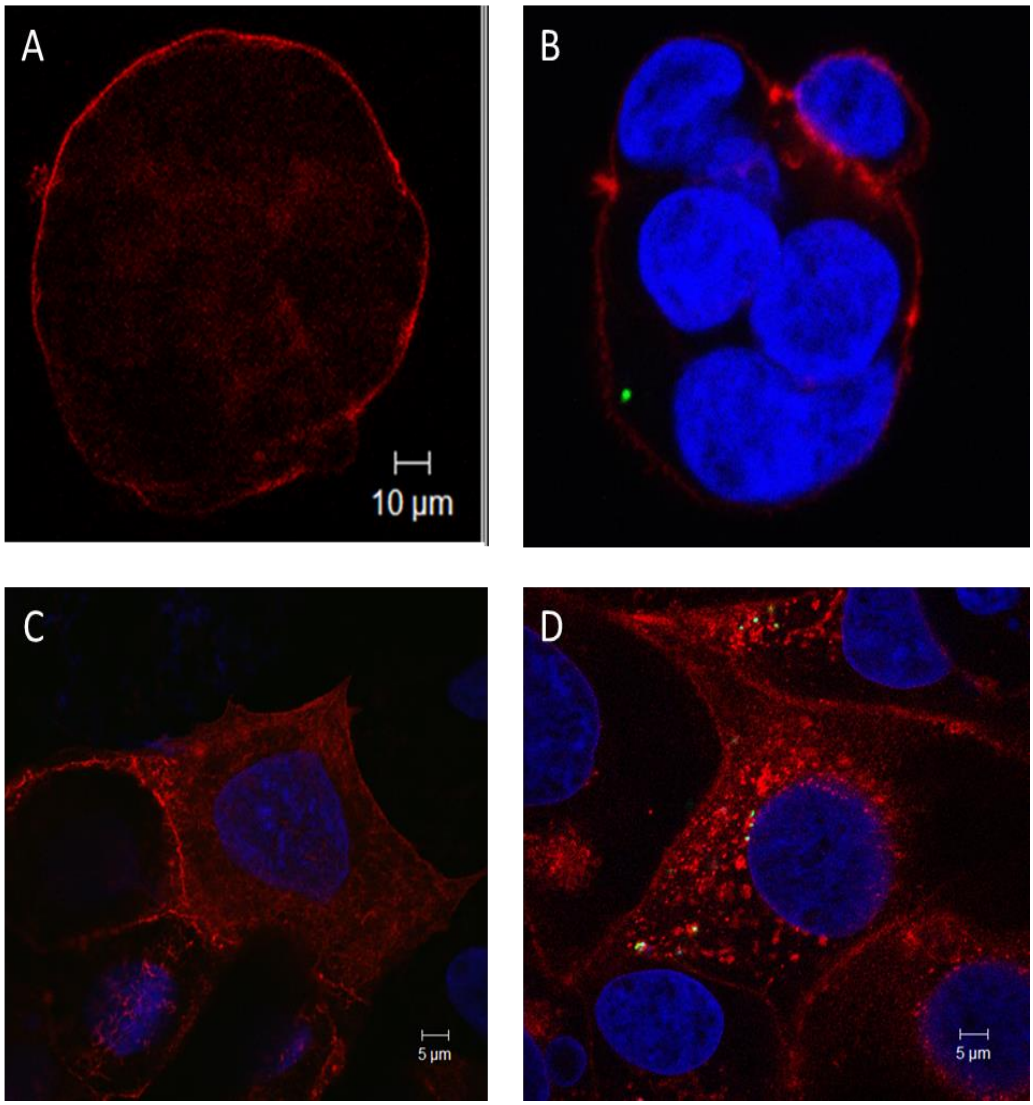

Figure 5. 9. Uninfected and infected Caco-2 IECs. A and C are uninfected IECs whilst B and D are IECs infected (MOI 100:1) with *C. jejuni* 11168H wild-type strain expressing GFP (Green). IECs were grown on coverslips and co-incubated with or without bacteria for 2 h. Following incubation cells were fixed, washed and stained using DAPI (Blue) for nucleus, WGA (Red) for plasma membrane (in A and B) or rhodamine-phalloidin (Red) for actin filaments (in C and D). Panel A. Uninfected Caco-2 cell stained with WGA (Red) showing the presence of plasma membrane; Panel B. Infected Caco-2 cell stained with WGA (Red) showing the presence of plasma membrane and *C. jejuni* (Green); Panel C. Uninfected Caco-2 cell stained with rhodamine-phalloidin (Red) showing the presence of actin filaments; Panel D. Infected Caco-2 cells stained with rhodamine-phalloidin (Red) showing the presence of actin filaments and *C. jejuni* (Green).

5.2.7 Reorganisation of actin cytoskeleton showing membrane ruffling in Caco-2 IECs

C. jejuni infection results in reorganisation of the actin cytoskeleton in both Caco-2 and T84 IECS. The *S. flexneri* IpaABCD secreted proteins have been reported to play an important role in the bacterial entry process (Menard et al., 1993) by inducing actin polymerisation and formation of filopodia and lamellipodia upon entry into epithelial cells . These structures were triggered by the *S. flexneri* IpaC protein and were dependent on Cdc42 and Rac GTPases (Tran Van Nhieu et al., 1999). Cytoskeleton assembly in cells is a result of activated small GTPases (Russell and Blake, 1994).

A study by Hall *et al.* showed that small GTPases such as Rho, Rac and Cdc42 control the assembly and organisation of the actin cytoskeleton in epithelial cells (Nobes and Hall, 1995b). Among the effects observed following Rho, Rac or Cdc42 activation in these cells were the formation of stress fibres and lamellipodia (Ridley and Hall, 1992, Ridley et al., 1992). In line with these observations, experiments were performed to visualise the effects of infection with the 11168H wild-type strain expressing GFP on Caco-2 cells.

Following bacterial infection of Caco-2 cells, membrane ruffling was observed. The different formations observed were protrusion finger-like filopodia (Figure 5.10 A), lamellipodia (Figure 5.11 A) and stress fibres (Figure 5.12 A). Filopodia appear like microspikes of actin protrusions and very motile. Filopodia grow by extension up to 25 µm in length. Filopodia and lamellipodia are highly motile with ‘wave’ movement because the structures are able to detach, reattach and fold back upon themselves. Filopodia were closely associated to lamellipodia and the highly motile dynamic structures were observed to be co-ordinated forming one after another and to produce membrane ruffles (Nobes et al., 1995, Nobes and Hall, 1995a).

5.2.7.1 Filopodia formation in Caco-2 cells

Data has been published that activation of Rac1 results in induction of membrane ruffles in epithelial cells. Filopodia and lamellipodia are examples of membrane ruffles (Caron and Hall, 1998, Ridley and Hall, 1992). To determine whether changes in the actin cytoskeleton were mediated by *C. jejuni* infection as a result of the activation Rac GTPases, experiments were performed whereby Caco-2 cells were infected with 11168H and confocal microscopy images were analysed.

Following infection with the 11168H wild-type strain, formations such as filopodia and lamellipodia were observed in Caco-2 cells (Figure 5.10). A structure of filopodia that resemble micro spikes and also protrusions of actin filaments were observed (see panel B and C). In panel D, similar structures were also observed in association with *C. jejuni* (Green). These observations are similar to the structures observed in a previous study (panel A) (Nobes and Hall, 1995b).

A

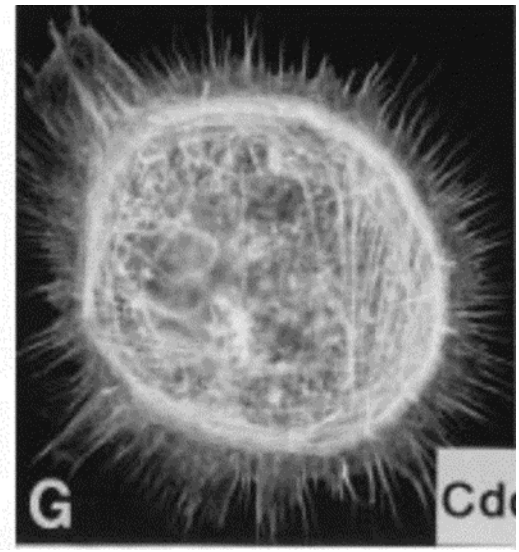

B

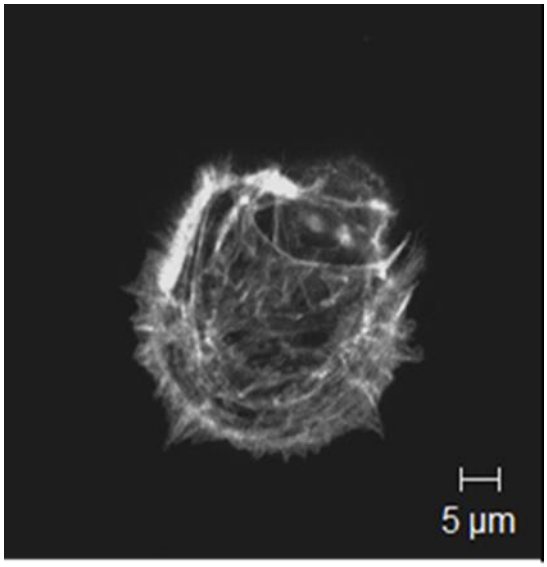

C

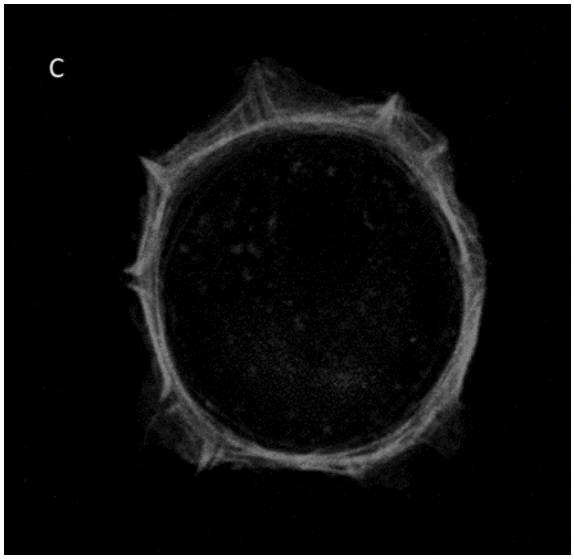

D

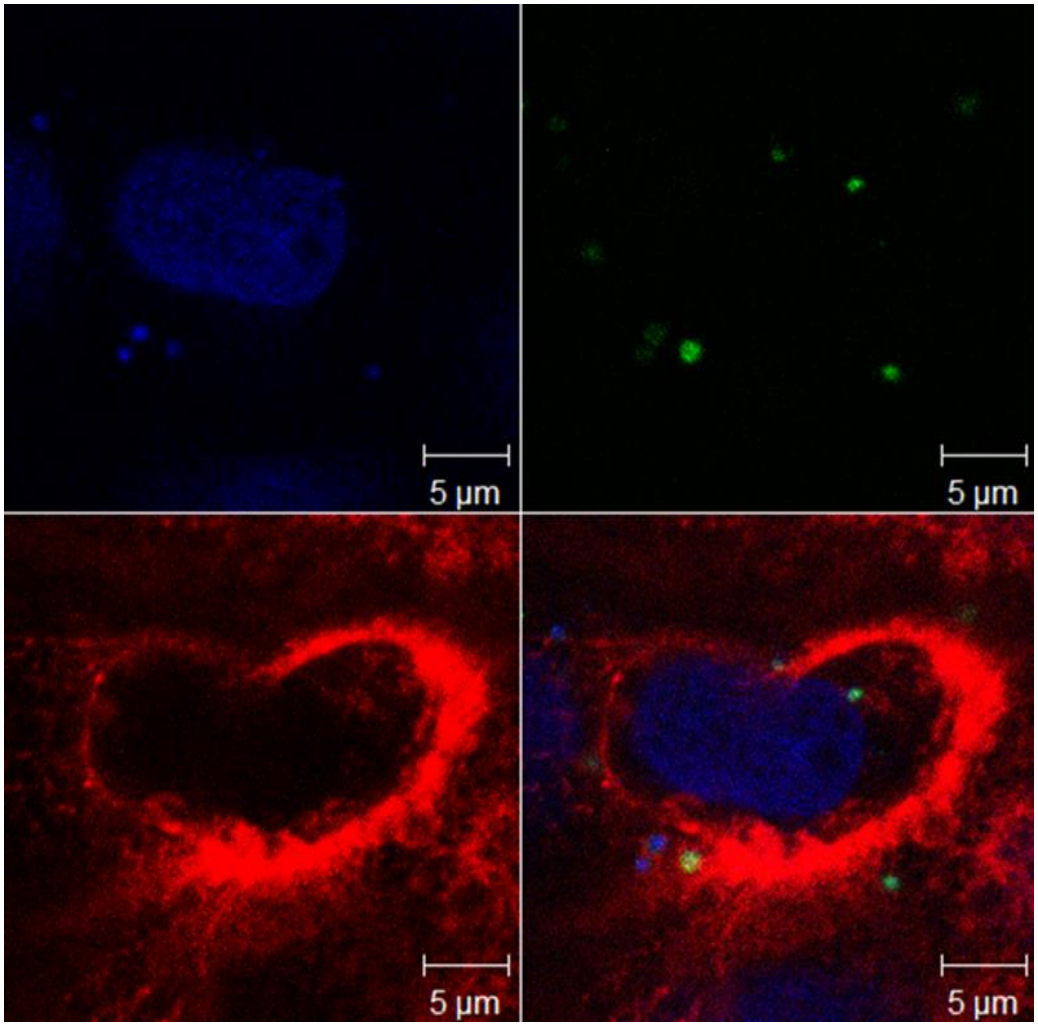

Figure 5.10. Representative confocal micrographs of Caco-2 cells infected with GFP expressing 11168H wild-type strain showing the formation of filopodia. Caco-2 cells infected with GFP expressing 11168H wild-type strain (MOI 100:1) were prepared and stained using (DAPI) (Blue) for nucleus and rhodamine phalloidin (Red) for actin filament. Panel A. Image showing formation of filopodia in Swiss 3T3 fibroblast cells (Nobes and Hall, 1995a). Panel B and C. Structures of filopodia observed in Caco-2 cells infected with *C. jejuni* 11168H wild-type strain. Panel D. Representative confocal fluorescence images of Caco-2 cells infected with 11168H wild-type strain showing actin filaments as protrusion like formations (filopodia) (Red) and some internalised *C. jejuni* (Green).

5.2.7.2 Lamellipodia formation in Caco-2 cells

Studies have reported that lamellipodia and membrane ruffles were produced at the cell periphery as a result of Rac activation that regulates polymerisation of actin (Nobes and Hall, 1995b, Caron and Hall, 1998, Ridley et al., 1992).

Following infection with the 11168H wild-type strain, formation of lamellipodia were observed in Caco-2 cells (Figure 5.11). In panel B, formation of lamellipodia was observed as a membrane protrusion induced by actin polymerisation at the cell periphery following infection with *C. jejuni* 11168H. In panel C, the similar structure was observed along with some internalised *C. jejuni* (Green). This is in agreement with observation (panel A) from a previous study (Ridley et al., 1992).

A

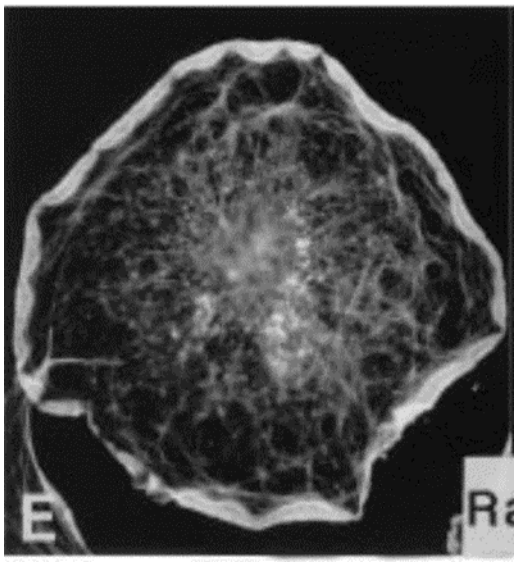

B

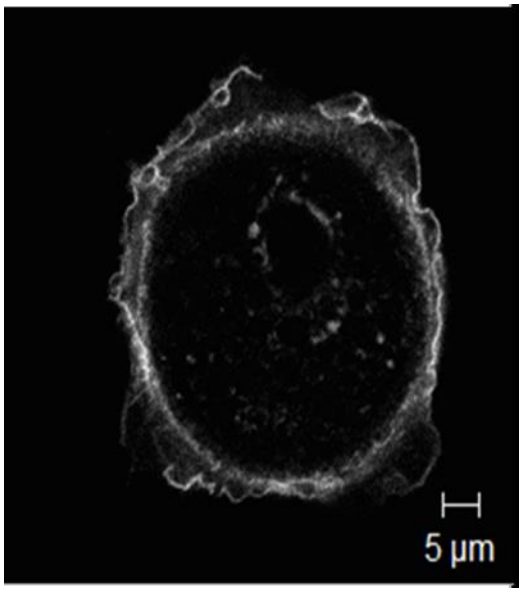

C

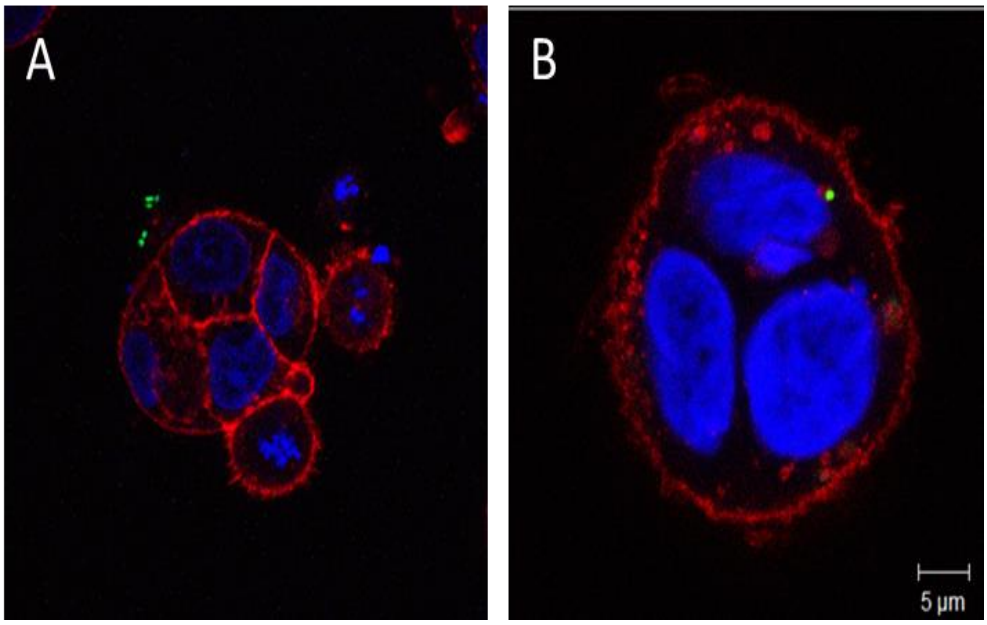

Figure 5.11. Representative confocal micrograph of Caco-2 cells infected with GFP expressing 11168H wild-type strain showing the formation of lamellipodia. Caco-2 cells infected with GFP expressing 11168H wild-type strain (MOI 100:1) were prepared and stained using (DAPI) (Blue) for nucleus and rhodamine phalloidin (Red) for actin filament. Panel A. Image showing lamellipodia in Swiss 3T3 fibroblast cells (Hall, 1999). Panel B. Representative confocal fluorescence images of Caco-2 cells infected with GFP expressing 11168H wild-type strain, showing membrane ruffles as ribbon-like formation (lamellipodia) (Red). Panel C. Both Figure A and B are infected Caco-2 cells showing membrane ruffles and lamellipodia with some internalised *C. jejuni* (Green).

5.2.7.3 Stress fibre formation in Caco-2 cells

Infection with *C. jejuni* activated Rac1 member of small GTPases, results in cytoskeleton rearrangements including stress fibres (Nobes and Hall, 1995a)

During infection with the 11168H wild-type strain (Green), formation of stress fibres (Red) were observed in Caco-2 cells (Figure 5.12). In panel B, stress fibres were observed and panel C, some internalised *C. jejuni* (Green) were also seen in close contact with the stress fibres. This observation was similar to the one reported (panel A) where Swiss 3T3 fibroblast cells were injected with recombinant Rac protein (V12rac) for GTPases activation (Hall and Nobes, 2000).

A

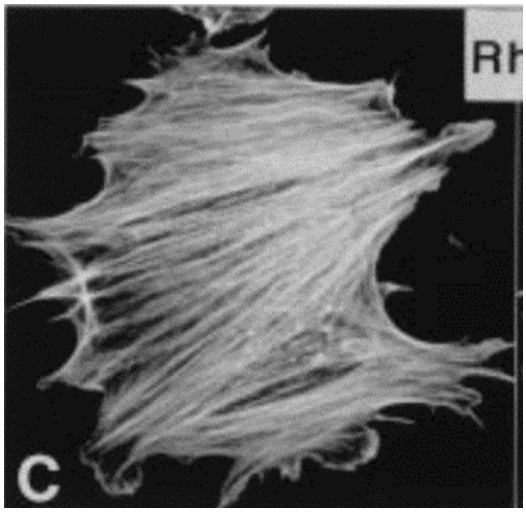

B

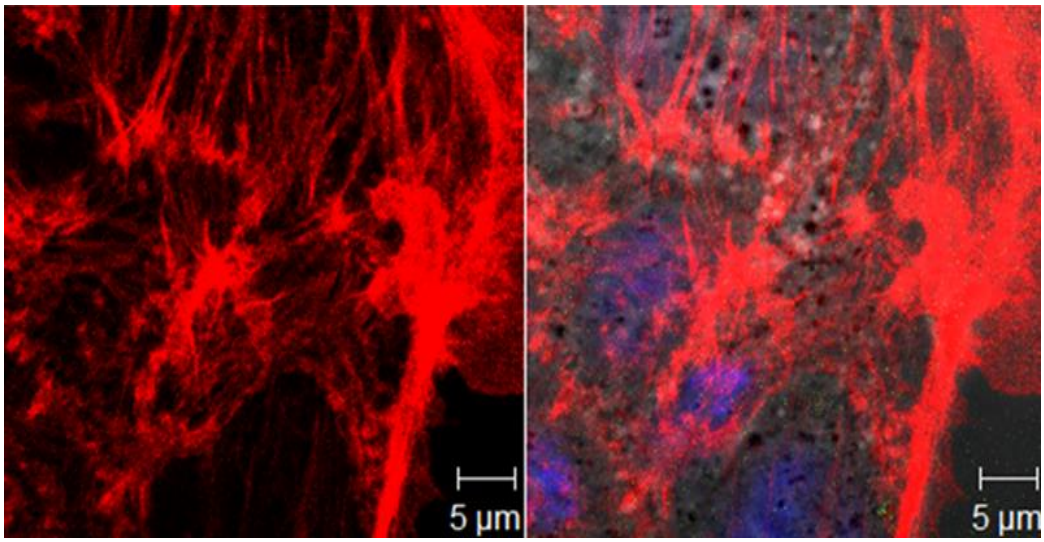

C

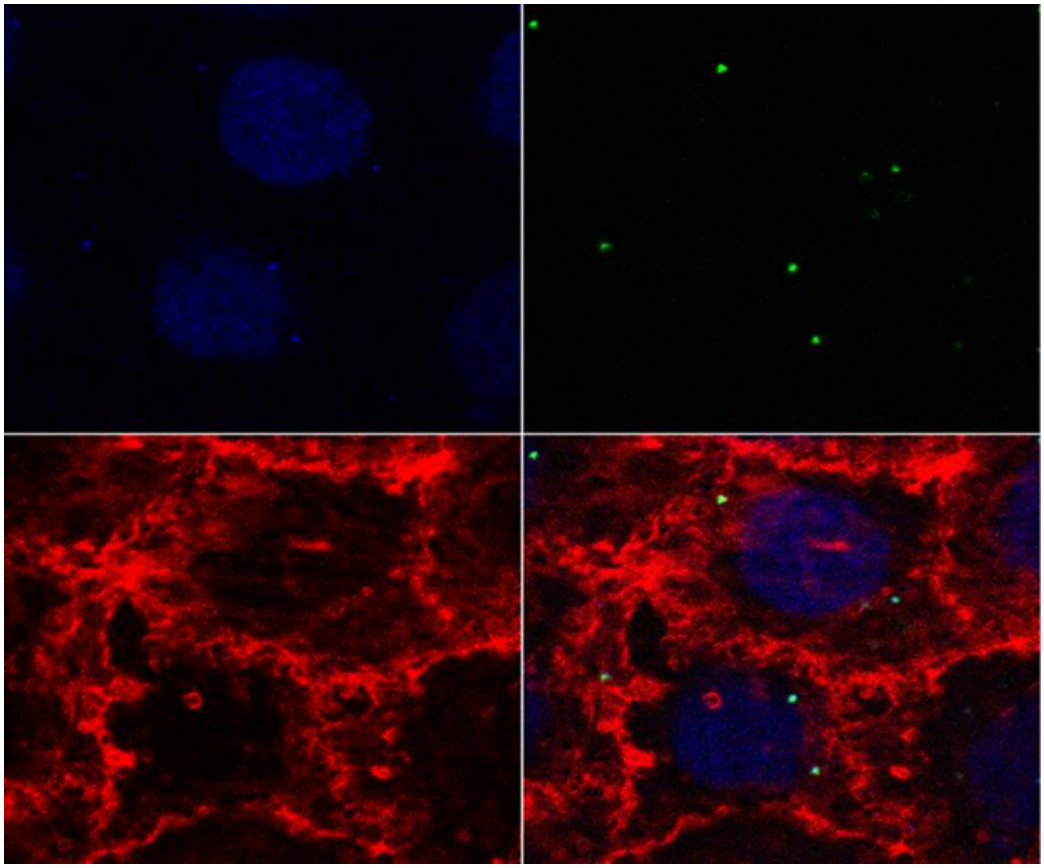

Figure 5.12. Representative confocal micrograph of Caco-2 cells infected with GFP expressing 11168H wild-type strain showing the formation of stress fibres. Caco-2 cells infected with GFP expressing 11168H wild-type strain (MOI 100:1) were prepared and stained using (DAPI) (Blue) for nucleus and rhodamine phalloidin (Red) for actin filament. Panel A. Image showing stress fibres in Swiss 3T3 fibroblast cells (Nobes and Hall, 1995a). Panel B. Representative confocal micrograph of Caco-2 cells infected with 11168H wild-type strain showing the actin stress fibres within the cells. Panel C. Combined confocal fluorescence images showing stress fibres as a result of interaction with *C. jejuni* (Green) and some internalised *C. jejuni.*

5.2.8 Intracellular *C. jejuni* 11168H wild-type strain expressing GFP associated with actin cytoskeleton

After internalisation into the host cell, *C. jejuni* appears closely associated with the actin cytoskeleton structure. Therefore experiments were performed to visualise the association of *C. jejuni* 11168H with the actin cytoskeletal following the invasion of IECs. The position of *C. jejuni* and actin cytoskeleton accumulation were observed 1 h post-infection (Figure 5.13). The results showed *C. jejuni* clearly associated with the actin cytoskeleton. Highly fluorescent intracellular *C. jejuni* expressing GFP were readily visualised within the actin cytoskeleton network inside the cells.

A

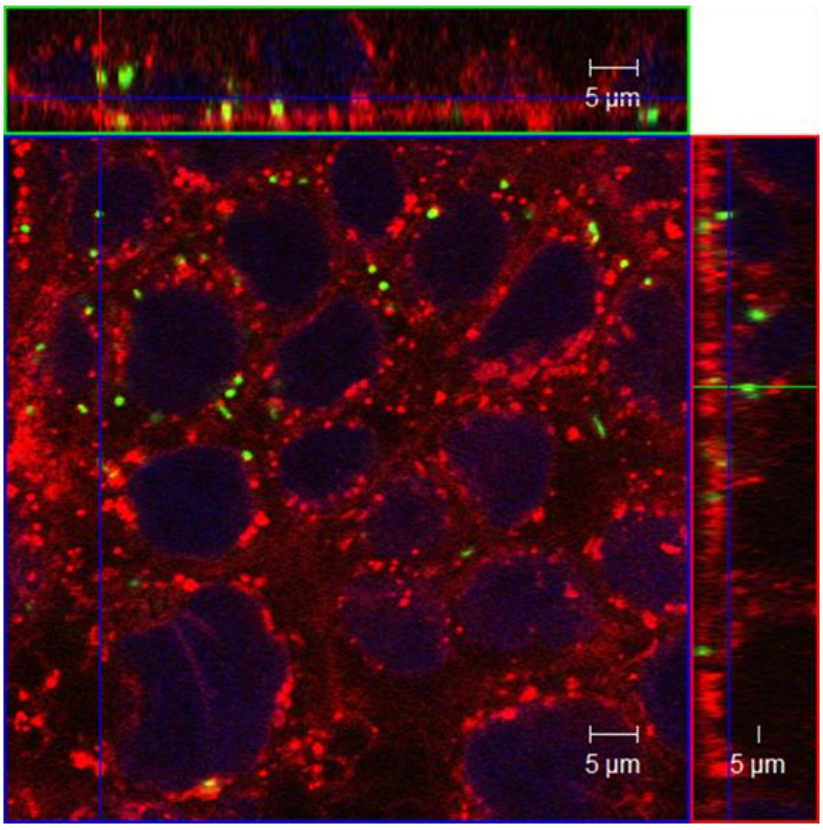

B

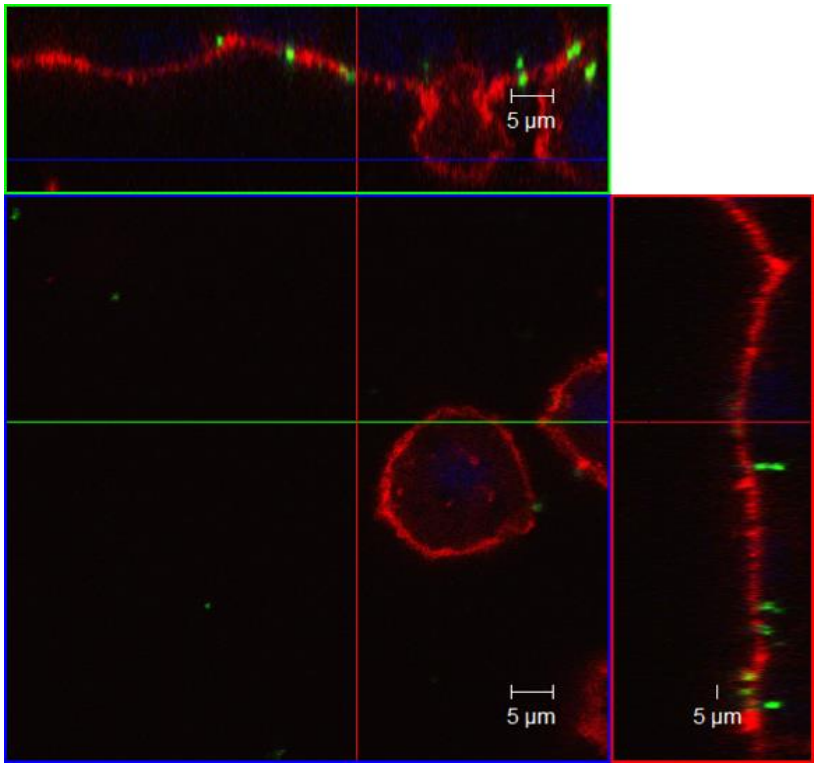

C

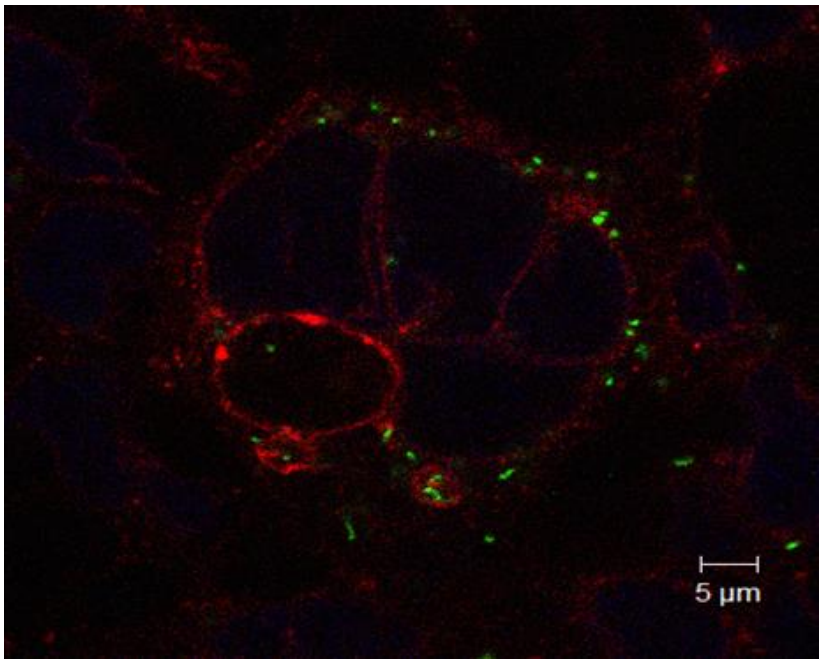

D

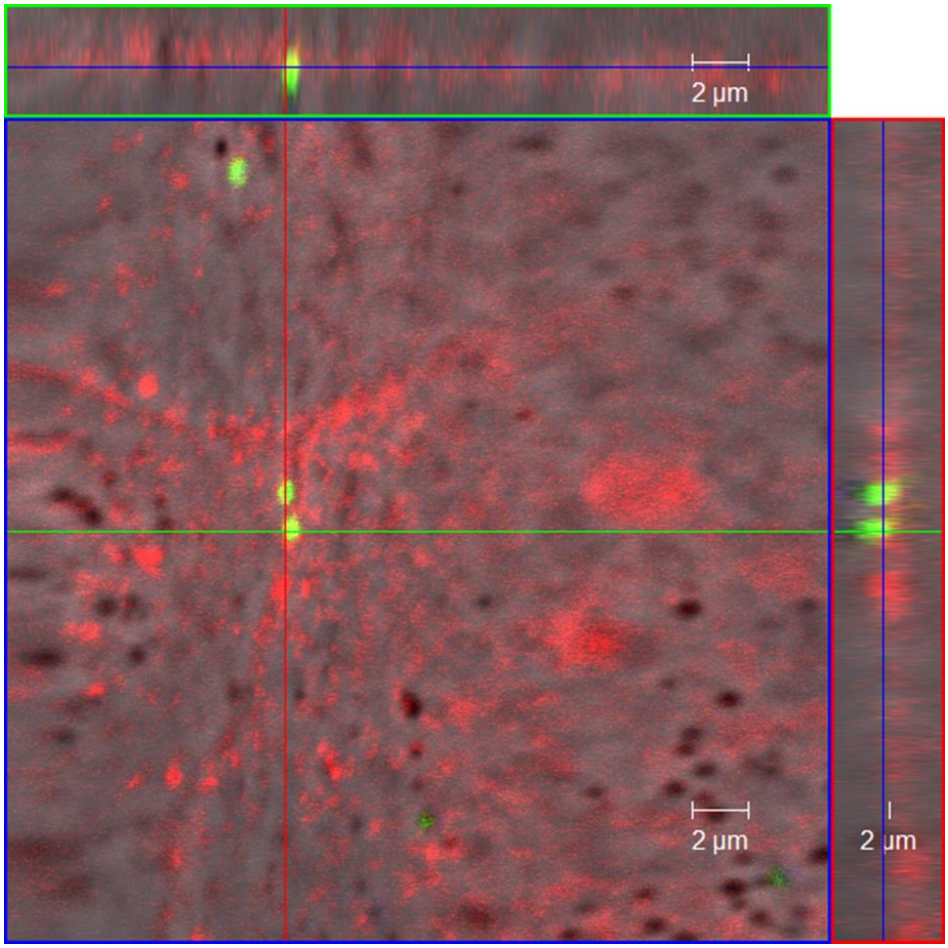

Figure 5. 13. Representative confocal micrograph of Caco-2 cells infected with GFP expressing 11168H wild-type strain showing internalised bacteria at the proximity of actin cytoskeleton. Caco-2 cells infected with GFP expressing 11168H wild-type strain (MOI 100:1) were prepared and stained using DAPI (Blue) for nucleus and rhodamine pallodine (Red) for actin filaments. Panel A, B and C show position of *C. jejuni* clearly associated with actin accumulation. Panel D shows an enlarged image and transversal optical sections to the side of panels for the location of the bacteria relative to the cells basis.

5.2.9 Intracellular *C. jejuni* 11168H wild-type strain expressing GFP is not associated with actin cytoskeleton

In a previous study, infection of HeLa cells with *C. jejuni* showed various stages of penetration. Some of the internalised bacteria appeared to be co-localised with vacuoles, some partially lysed, some associated with actin structures and some retain the size and S shaped (Fauchere et al., 1986).

From confocal microscopy images following bacterial invasion of Caco-2 cells, internalised *C. jejuni* can be observed inside the cytoplasm (Figure 5.14). The GFP expressing 11168H wild-type strain (Green) was observed internalised in Caco-2 cells but also with no apparent association with the actin cytoskeleton (Red). Some bacteria also appeared singly showing the characteristic spiral shape (arrow). This result is also consistent with a previous study showing *C. jejuni* internalised in INT 407 cells with no apparent association with actin (Hu and Kopecko, 1999).

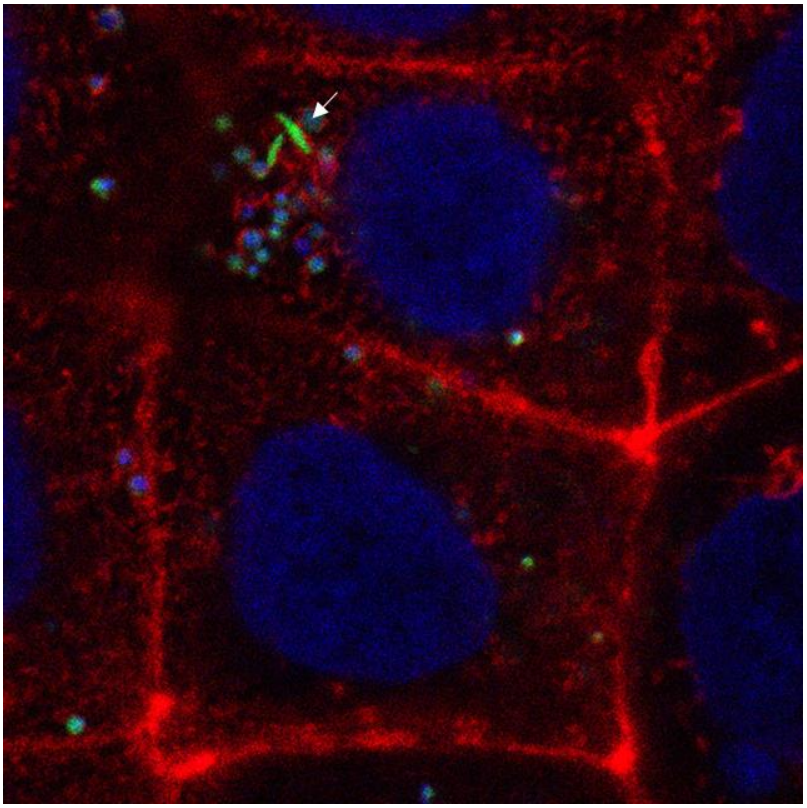

Figure 5.14. Internalised GFP expressing 11168H wild-type strain showed non-association with actin cytoskeleton in Caco-2 IECs. Representative confocal micrograph of Caco-2 cells infected with GFP expressing 11168H wild-type strain (MOI 100:1) (Green) for 1 h. Caco-2 cells infected with GFP expressing 11168H wild-type strain were prepared and stained using DAPI (Blue) for nucleus and rhodamine phalloidin for actin filaments (Red). GFP expressing 11168H wild-type strain bacteria (arrow) were observed in cell cytoplasm, showing no apparent specific association with the actin cytoskeleton.

5.2.10 Co-localisation of intracellular 11168H wild-type strain expressing GFP with a vacuole in Caco-2 IECs

Based on previous observations, *C. jejuni* has been shown to invade IECs then reside either free within the cytoplasm, associated with actin or in close proximity to the nucleus (Fauchere et al., 1986). In this study, *C. jejuni* was observed to reside within a membrane vacuole and form tight co-localisation, which resulted in yellow fusion structures (Figure 5.15). This suggests that GFP expressing 11168H wild-type strain resides within a membrane-bound vacuole in Caco-2 cells.

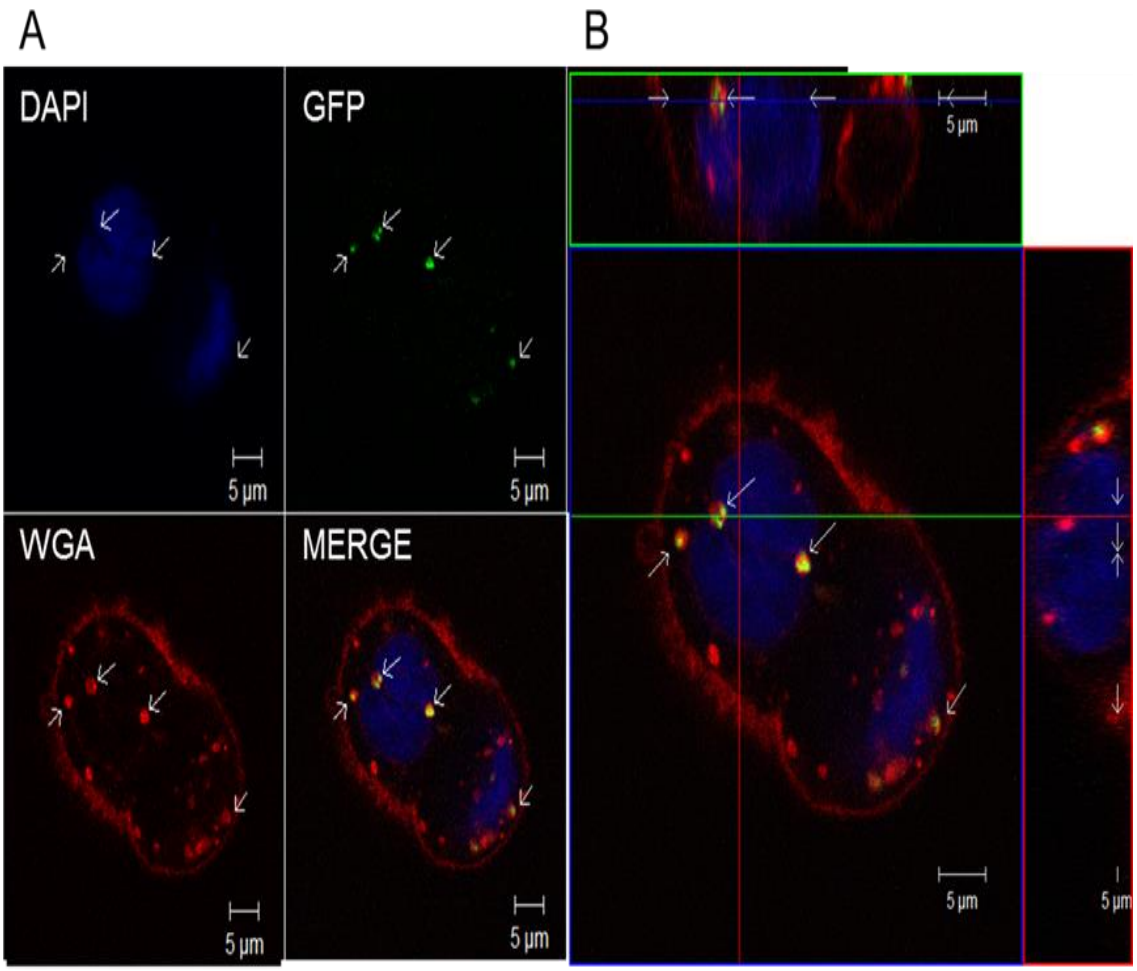

C

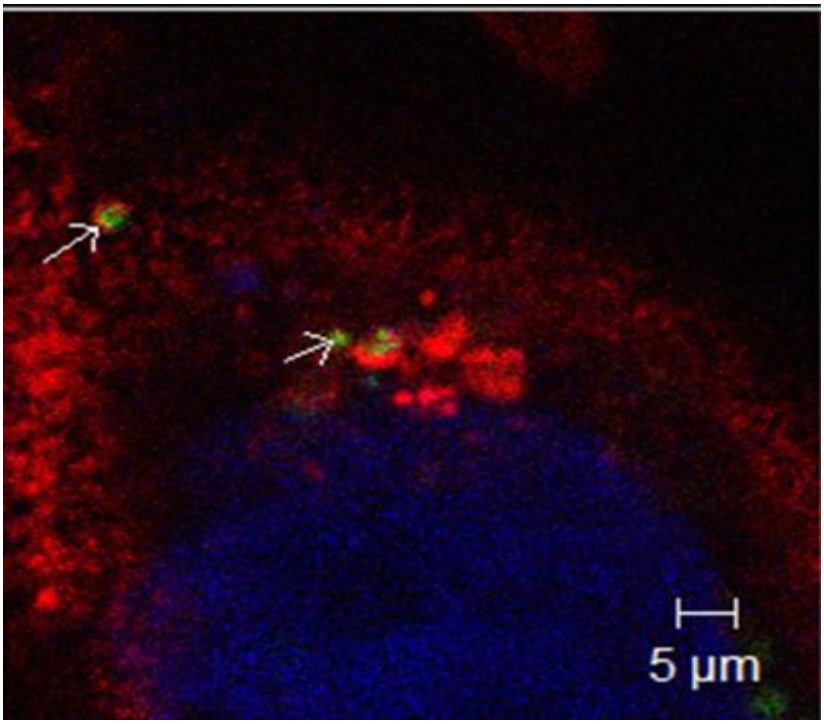

Figure 5.15. Representative confocal micrograph of Caco-2 cells infected with 11168H wild-type strain expressing GFP showing specific co-localisation with plasma membrane. Caco-2 cells infected with GFP expressing 11168H wild-type strain (MOI 100:1) were prepared and stained using DAPI (Blue) for nucleus and WGA (Red) for plasma membrane. Panel A. Combined confocal fluorescence images of Caco-2 cells infected with GFP expressing 11168H wild-type strain for 1 h, showing bacteria internalised and co-localised with plasma membrane. Yellow fusion colour represented tight co-localisation of *C. jejuni* 11168H wild-type strain (Green) with plasma membrane (Red) and could be seen to various degrees with bacteria throughout the cells (arrowhead). Panel B. Z-stack showing relative position of bacteria with plasma membrane in the cells. Panel C. One confocal image plane showing two bacteria residing in vacoules that are co-localised tightly with plasma membrane which appeared as a yellow fusion colour.

5.2 11 Internalisation of *C. jejuni* 11168H wild-type strain expressing GFP into Caco-2 IECs

It has been shown that that the initiation of invasion by *C. jejuni* involves cytoskeleton rearrangements (Konkel et al., 2013). Studies have reported that *C. jejuni* was observed interacting with finger-like protrusions of the host cell membrane during invasion (Biswas et al., 2003, Biswas et al., 2004). Membrane ruffles were shown engulfing *C. jejuni* F3801 wild-type strain into INT 407 cells (Eucker and Konkel, 2012). Confocal microscopy images were analysed after Caco-2 cells were infected with the 11168H wild-type strain expressing GFP (Figure 5.16). *C. jejuni* (Green) was observed engulfed by membrane ruffles formations (Red) during actin cytoskeleton rearrangements.

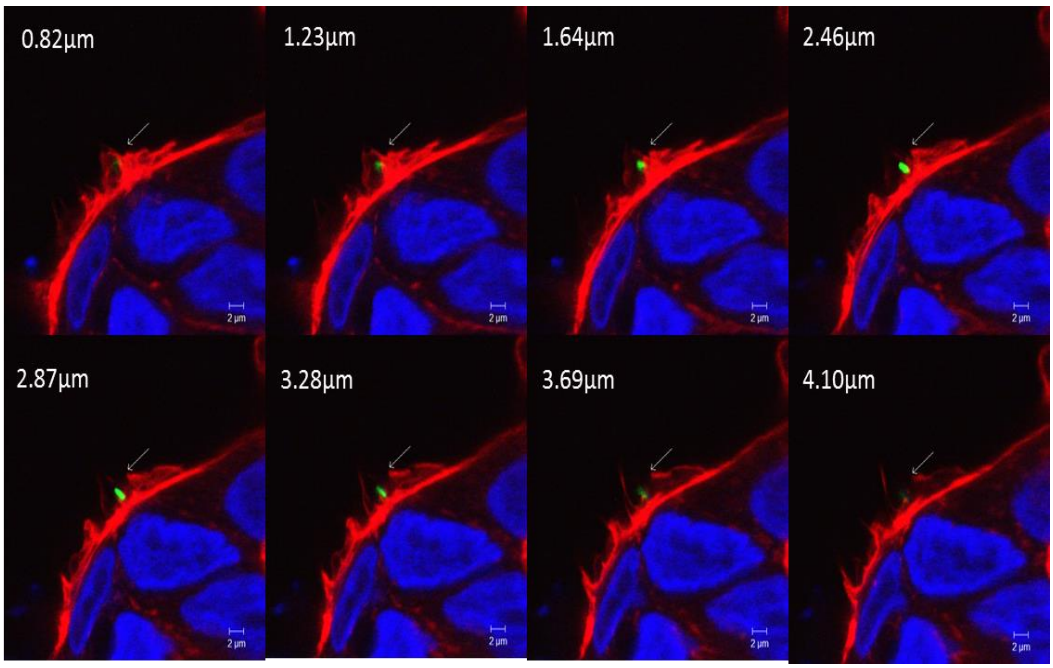

Figure 5.16. Membrane ruffles engulfing *C. jejuni* during invasion into Caco-2 IECs. Representative confocal micrograph of Caco-2 cells infected with GFP expressing 11168H wild-type strain showing internalisation of bacteria into the cell via membrane ruffles. Caco-2 cells infected with GFP expressing 11168H wild-type strain (MOI 100:1) for 1h. Cells were prepared and stained using DAPI (Blue) for nucleus and WGA (Red) for plasma membrane. Scale in µm showing the depth and position of bacterial.

5.2.12 Intracellular 11168H wild-type strain expressing GFP co-localises with late endosomal compartments

Following the observation that intracellular 11168H wild-type strain resides within the Caco-2 cell cytoplasm and also co-localised with actin, further investigations were performed to see whether the CCV co-localises with the late endocytic lysosome–associated membrane protein 1 (Lamp-1). As judged by confocal microscopy, the majority of intracellular bacteria were not co-localised with the late endosomal marker Lamp-1. However, a small number of bacteria were shown to co-localise with late endosomal compartments.

A

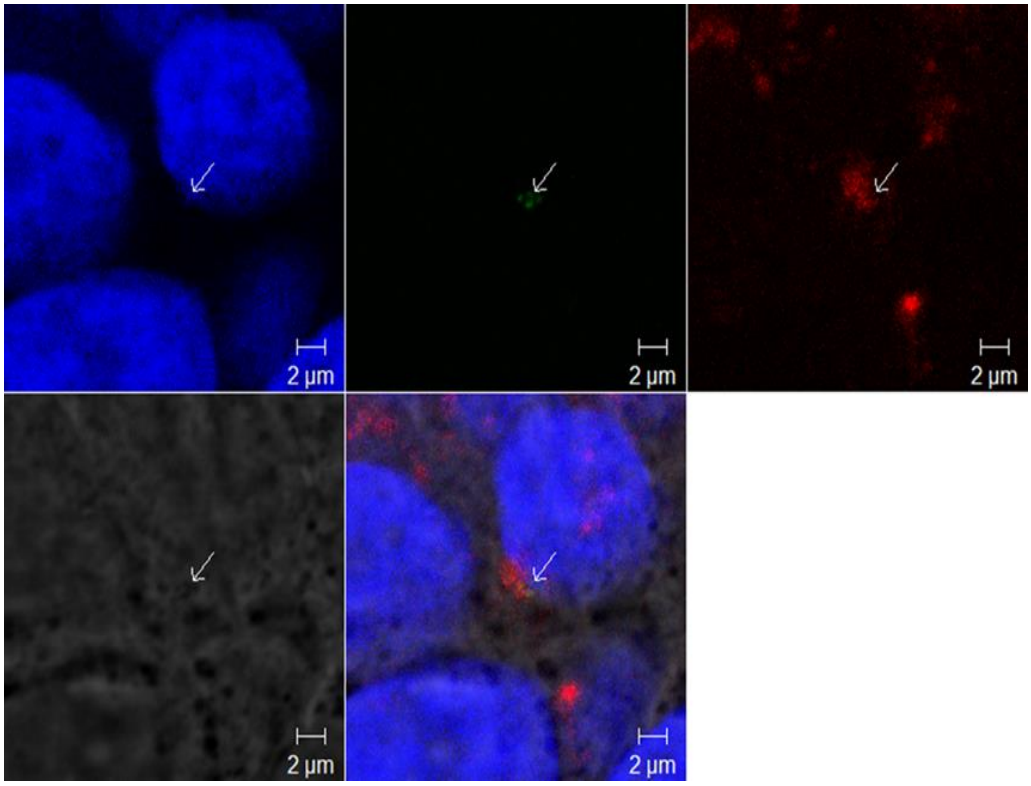

B C

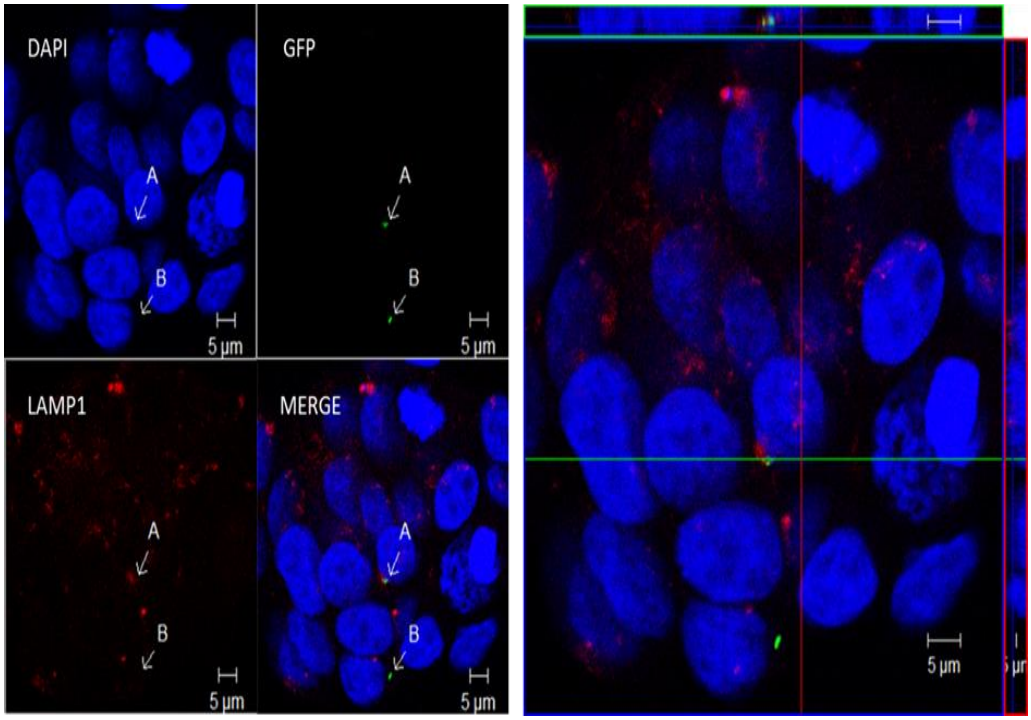

Figure 5.17. Representative confocal micrograph of Caco-2 IECs infected with GFP expressing 11168H wild-type strain for 1 h. Caco-2 IECs infected with GFP expressing 11168H wild-type strain (MOI 100:1) (Green) were prepared and stained using DAPI (Blue) for nucleus and late endosome with (Lamp-1 (H4A3): sc-20011) (Red). Panel A. Combined confocal fluorescence images of Caco-2 cells infected with GFP expressing 11168H wild-type strain for 1 h, showing bacteria co-localised with lamp-1. A slight tinge of yellow fusion colour represents co-localisation of *C. jejuni* 11168H wild-type strain with late endosomal vacoule (arrowhead). Panel B. One confocal image plane showing two bacteria residing in a vacoule that has co-localised with lamp-1 which appears as a yellow fusion colour. Panel C. Z-stack showing relative position of bacteria with actin cytoskeleton in the cells.

5.2.13 Extracellular and intracellular *C. jejuni* wild-type strain expressing GFP in Caco-2 IECs

Dual staining of extracellular bacteria was used to differentiate between extracellular and intracellular bacteria. *C. jejuni* 11168H wild-type strain expressing GFP was used to visualise intracellular bacteria. Caco-2 IECs were seeded and grown overnight on glass coverslips in 24 well plate. Cells were infected with GFP expressing 11168H at MOI of 100:1 for 2 h. Cells were then fixed with 2% (v/v) paraformaldehyde. Polyclonal rabbit anti-campylobacter antibody was added for 30 mins and then cells were washed three times with PBS. After that, anti-rabbit antibody rhodamine conjugated was added for 30 min, and the cells were finally washed again with PBS. Since the cells were not permeabilised, only extracellular bacteria were labelled red with the anti-campylobacter antibody, while intracellular bacteria were free of antibody and remain GFP green. Hence, intracellular 11168H GFP was observed expressing green fluorescence.

A

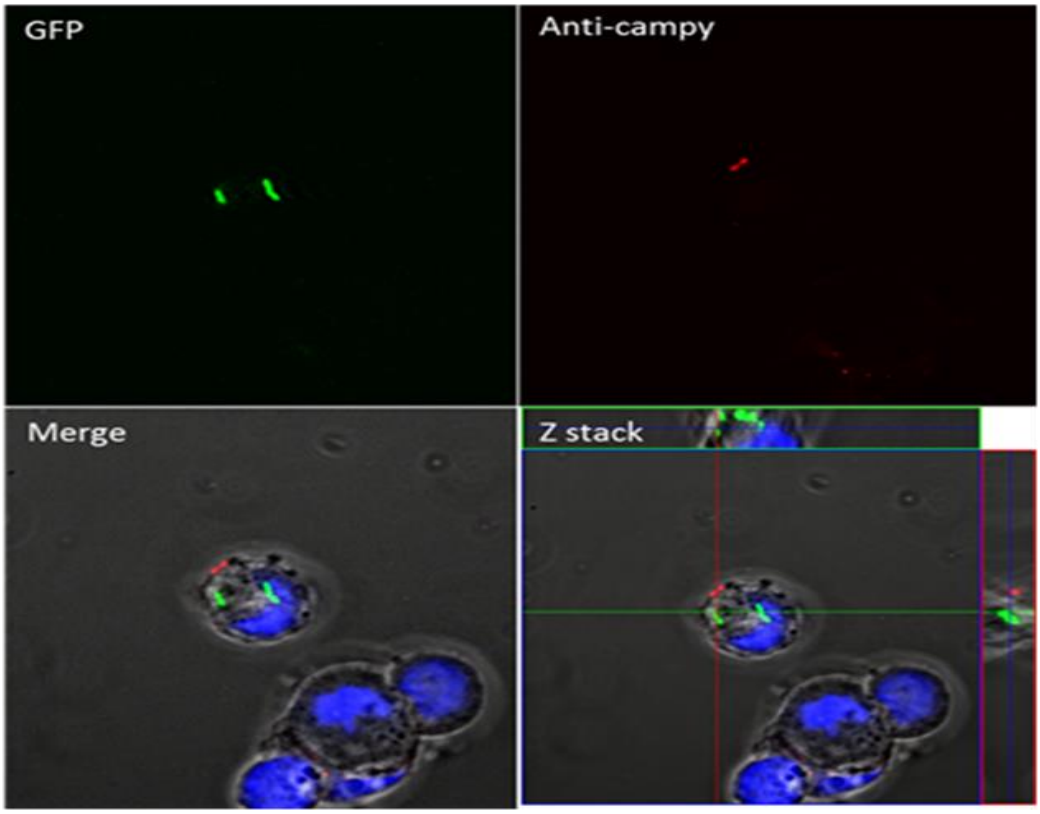

B

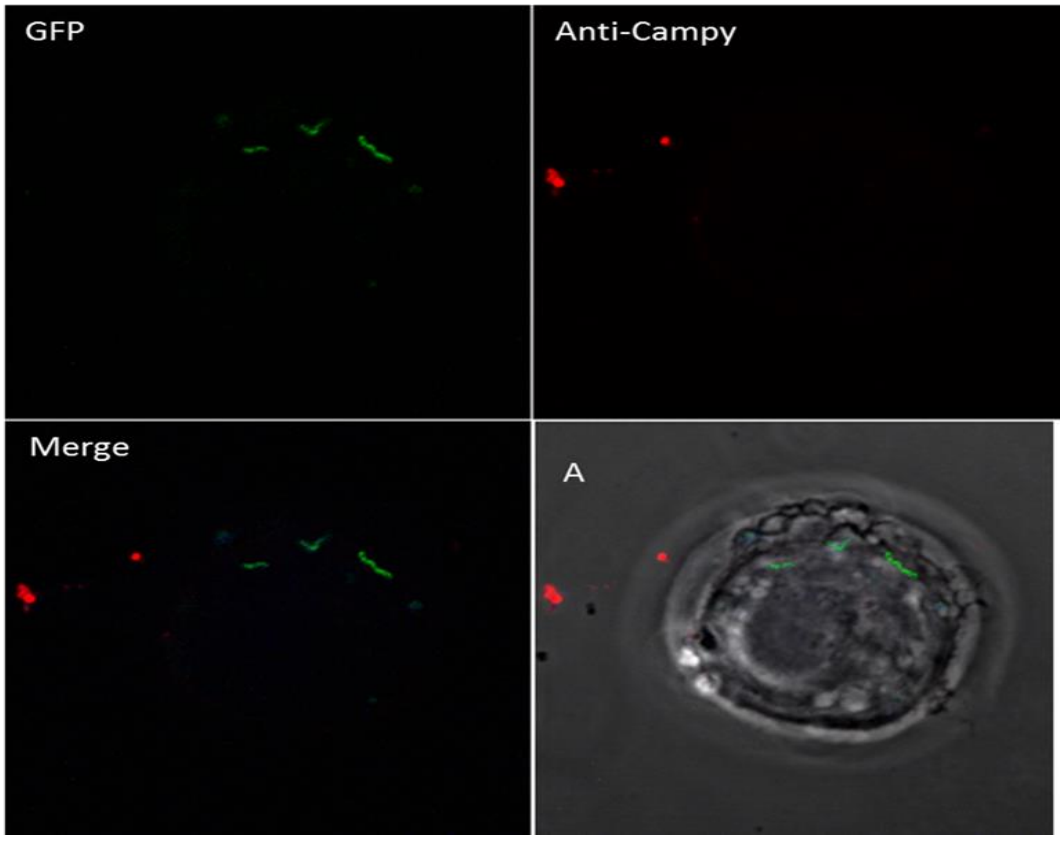

C

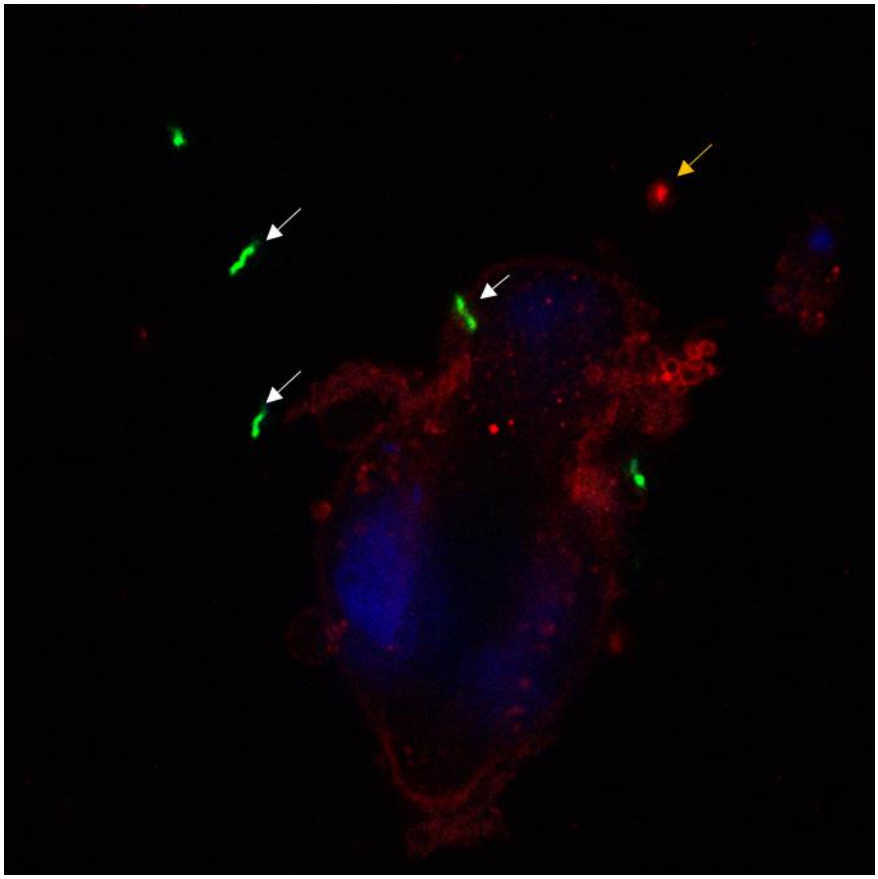

Figure 5.18. Representative confocal micrograph of Caco-2 cells infected with GFP expressing 11168H wild-type strain for 1 h. Caco-2 cells infected with GFP expressing 11168H wild-type strain (MOI 100:1) were prepared and stained using DAPI (Blue) for nucleus and anti-campy (Red). Panels A and B show combined confocal fluorescence images of Caco-2 cells infected with GFP expressing 11168H wild-type strain for 1 h, showing extracellular bacteria (Red) and intracellular bacteria (Green). Panel C. Some intracellular *C. jejuni* 11168H wild-type strain expressing GFP (Green) was observed outside and released from Caco-2 cells, which appeared to be lysed.

5.2.14 Disruption of actin cytoskeleton by eukaryotic inhibitor Cytochalasin D in Caco-2 IECs

C. jejuni invasion into host cells involves interaction with IEC signalling pathways as shown in Chapter 4. A common feature of signalling pathways is the regulation of actin cytoskeleton polymerisation and re-organisation that results in *C. jejuni* internalisation into into host cells. To visualise the effects of the eukaryotic inhibitors on actin cytoskeletal architecture, IECs treated with inhibitors were investigated using confocal microscopy.

Caco-2 IECs were treated with the eukaryotic inhibitors as described in Section 2.2.9. In cells treated with cyto D, actin filaments (Red) were greatly disorganised compared to the non-treated cells (Figure 5.19)

A

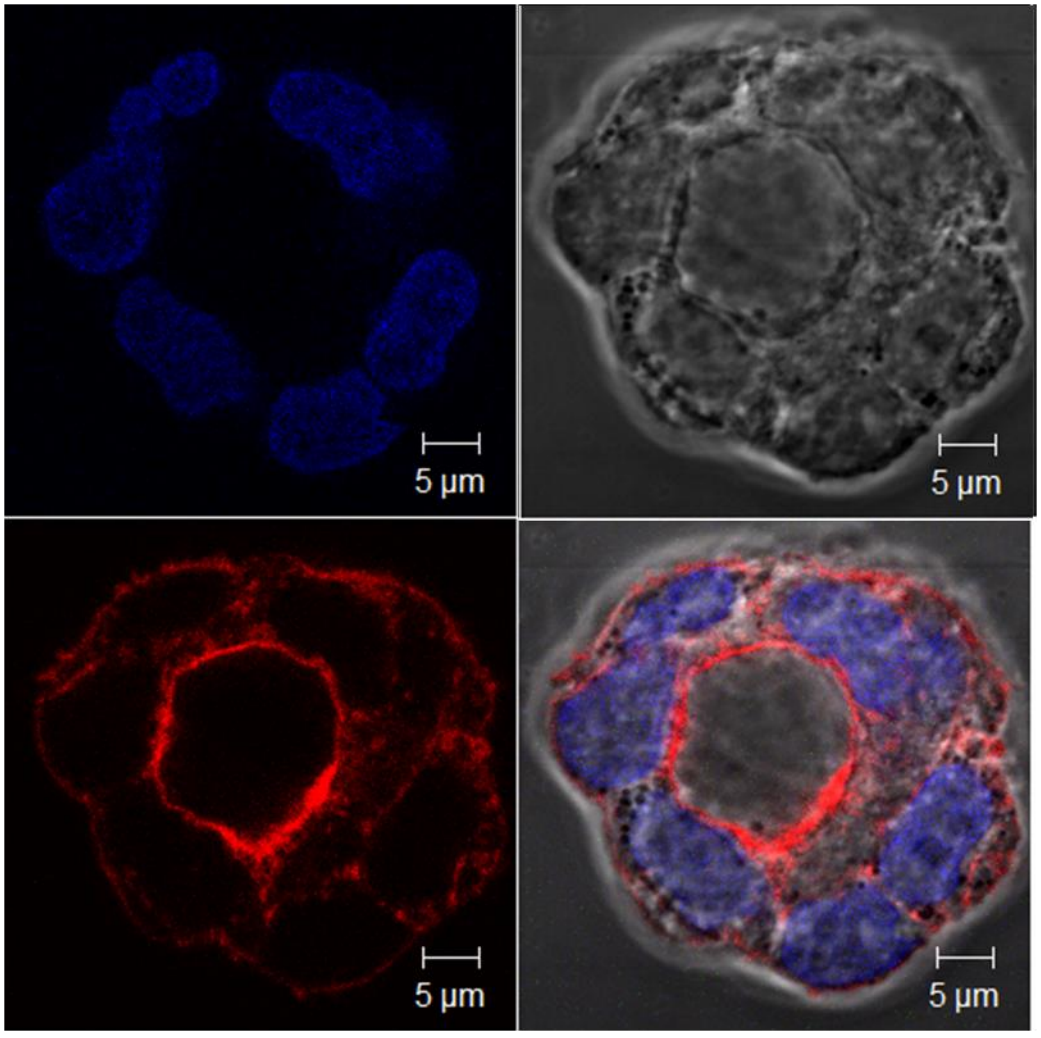

B

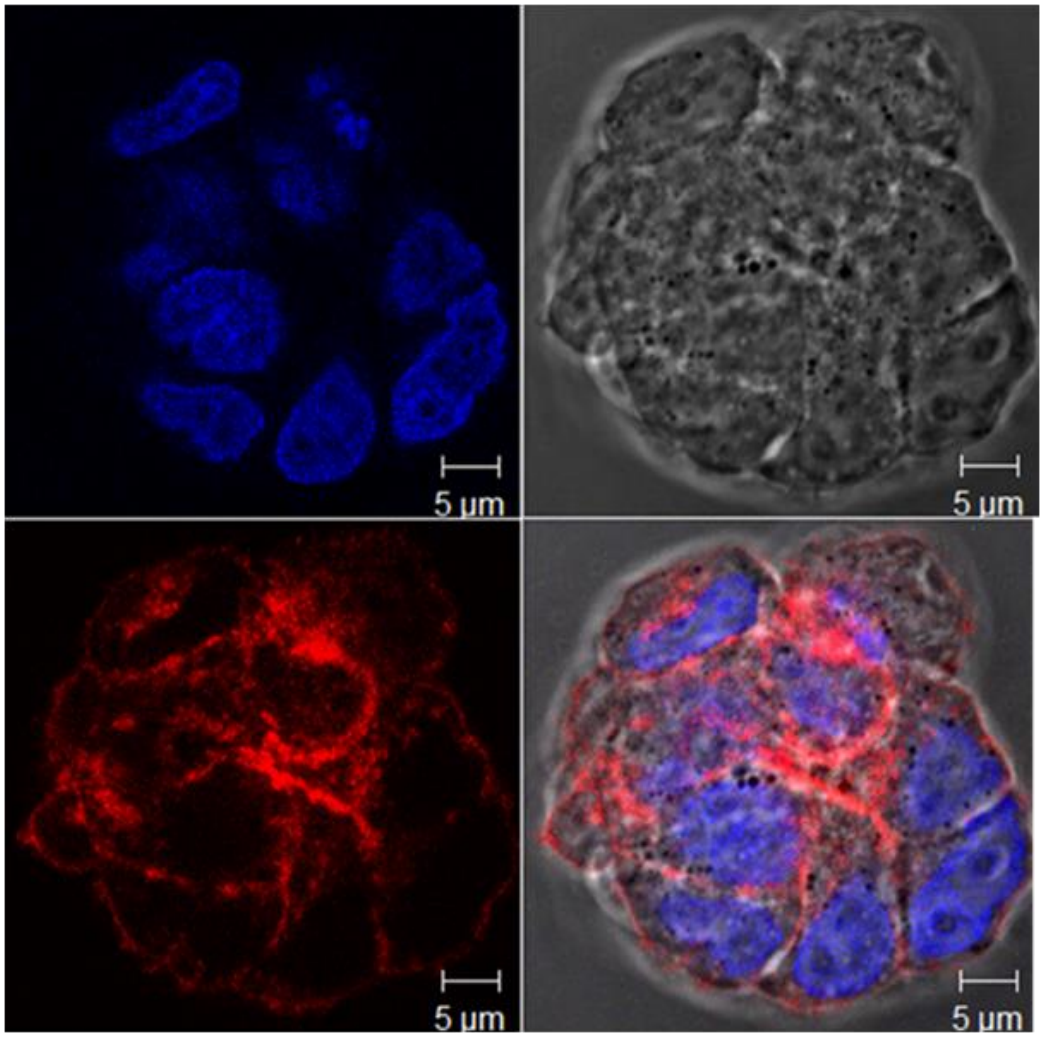

Figure 5.19. Disruption of actin cytoskeleton in Caco-2 IECs. Islands of polarised Caco-2 cells were treated with 3 µM cyto D. Cells were incubated with the inhibitor for 1 h. Following washes with PBS, cells were then fixed with paraformaldehyde and stained with rhodamine phalloidin (Red) for actin and DAPI (Blue) for nucleus. Panel A shows untreated Caco-2 cells and panel B shows Caco-2 cells treated with cyto D.

5.2.15 Disruption of actin cytoskeleton by eukaryotic inhibitor methyl-beta cyclodextrin in Caco-2 IECs

Caco-2 cells treated with MβCD showed significantly damaged actin cytoskeleton compared to the non-treated cells (Figure 5.20).

A

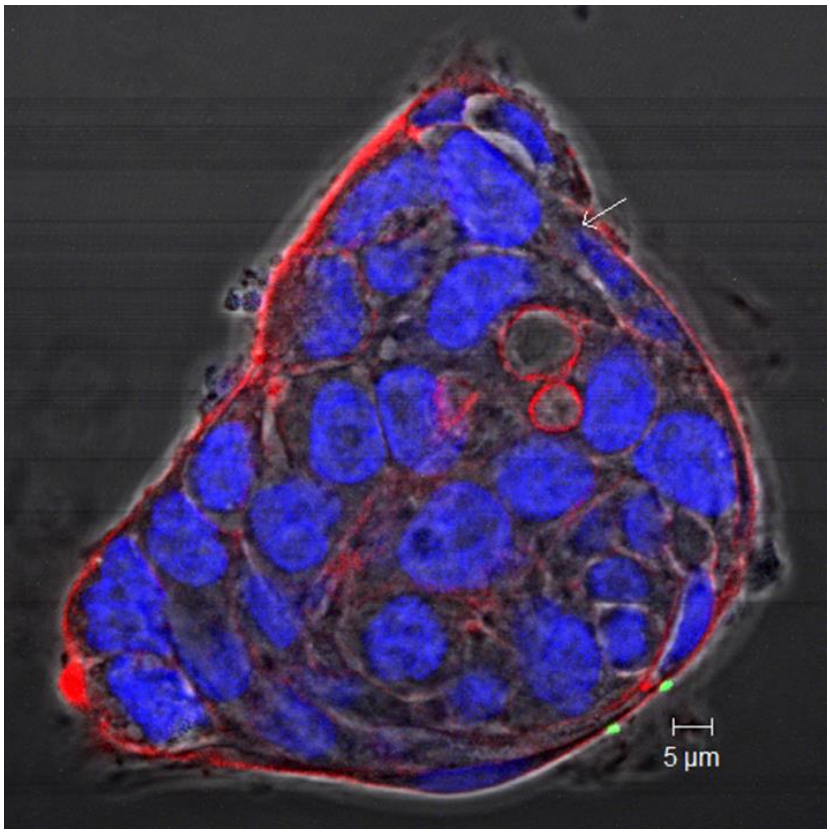

B

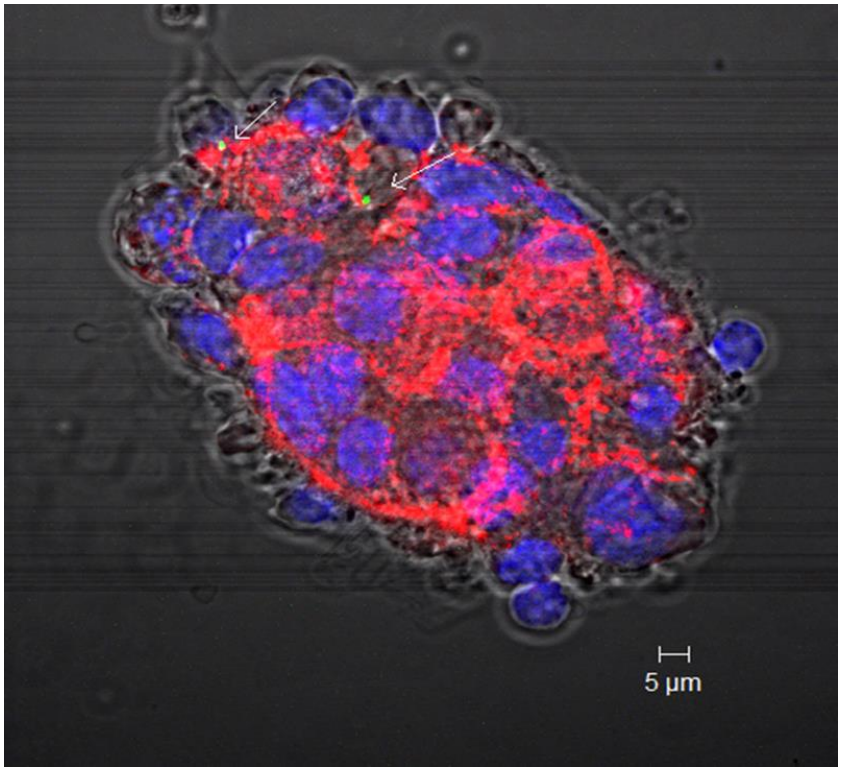

Figure 5.20. Disruption of actin cytoskeleton in Caco-2 IECs. Islands of polarised Caco-2 IECs were treated with 5 µM MβCD. Cells were incubated with the inhibitor for 1 h. Following washes with PBS, cells were then fixed with paraformaldehyde and stained with rhodamine phalloidin (Red) for actin and DAPI (Blue) for nucleus. Panel A shows untreated Caco-2 cells and panel B shows Caco-2 cells treated with MβCD.

5.2.16 Infection of cytochalasin D pre-treated Caco-2 IECs with 11168H wild-type strain expressing GFP

An investigation was performed to attempt to correlate the reduction in invasion caused by the eukaryotic inhibitors as seen with the CFU method in the previous chapter with the effect of the same inhibitor on the cells. Treated and untreated IECs infected with *C. jejuni* strains were compared.

Experiments were performed to determine the role of actin microfilaments in *C. jejuni* 1116H invasion with Caco-2 cell. No difference in the invasion ability was observed from confocal fluorescence microscopy images between the untreated (Panel A) and treated (Panel B) Caco-2 cells infected with 11168H wild-type expressing GFP (Figure 5.21).

A

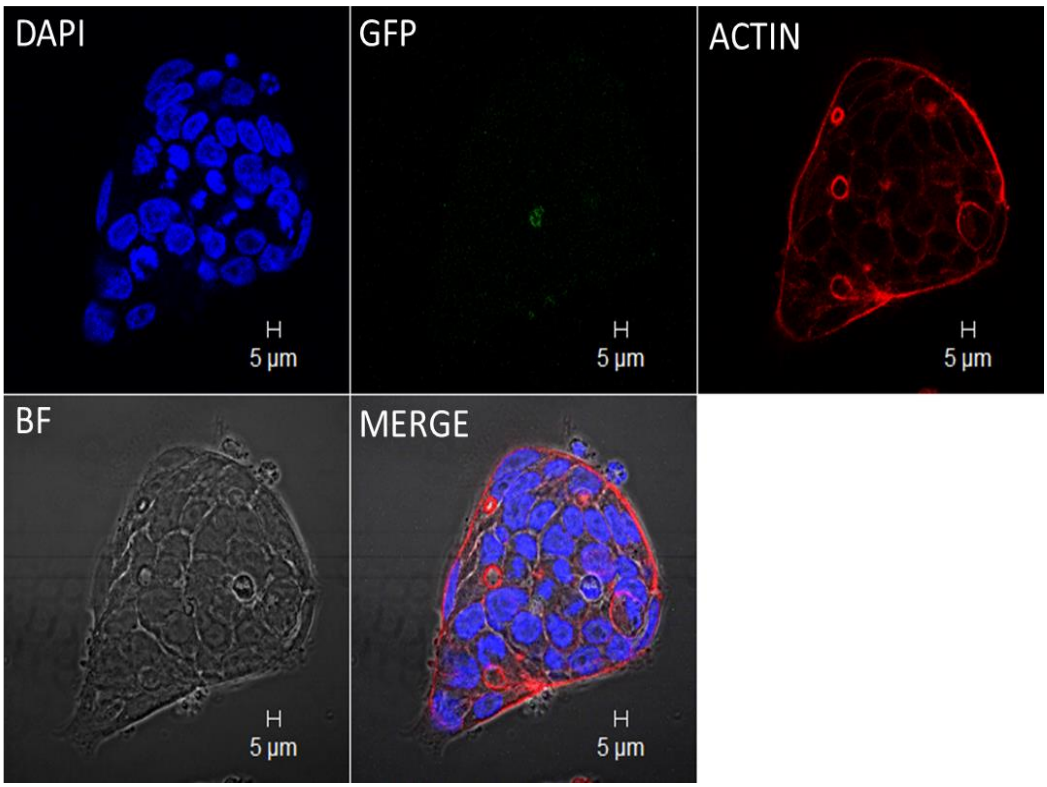

B

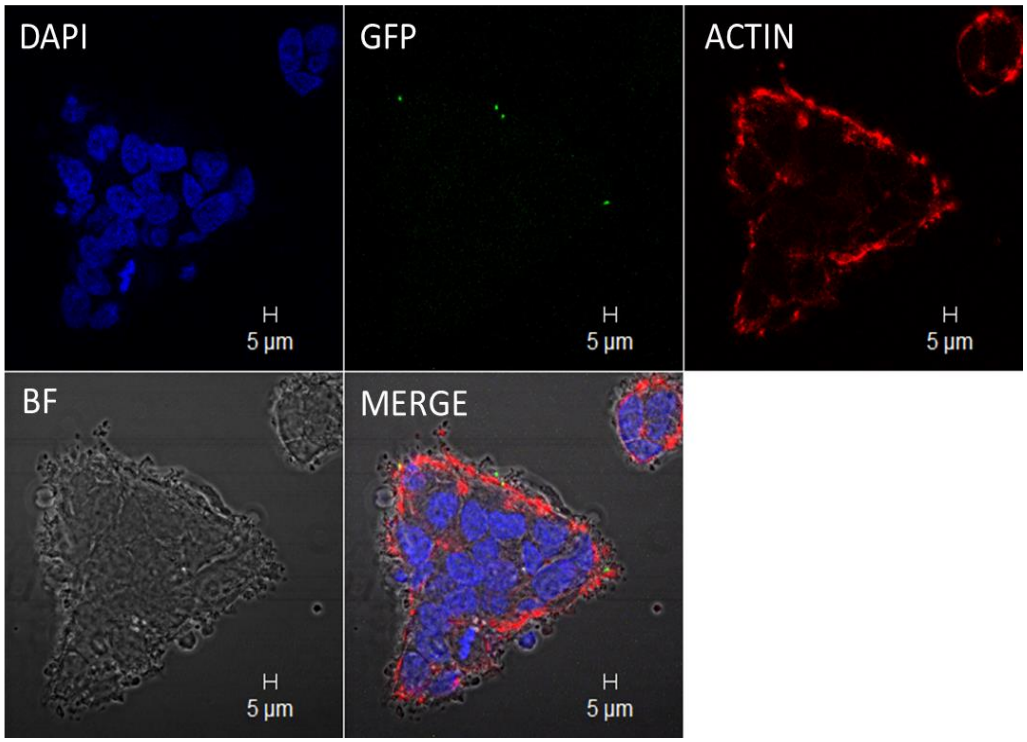

Figure 5.21. Representative confocal micrograph of Caco-2 cells infected with GFP expressing 11168H wild-type strain. Caco-2 cells were A. untreated and B. pre-treated with 3 µM cyto D for 1 h and infected with GFP expressing 11168H wild-type strain (MOI 100:1) for 1 h. Cells were fixed and stained using (DAPI) (Blue) for nucleus and rhodamine phalloidin (Red) for actin filaments.

5.2.17 Infection of cytochalasin D pre-treated Caco-2 IECs with the 11168H *cadF* mutant expressing GFP

Following construction of GFP expressing 11168H *cadF* and *flpA* mutants, invasion assays was performed and analysed using confocal microscopy as described in Section 2.4 and Section 2.6. Further experiments were performed to determine the role of actin microfilaments in *C. jejuni* 1116H *cadF* mutant invasion with Caco-2 cell. As observed from confocal microscopy image, a small number of 11168H *cadF* mutants were observed inside the cells which were not treated with cyto D (panel A). Whilst one *C. jejuni* was observed associated with actin filament (arrow) and some other *C. jejuni* appeared to be in closed contact with the membrane ruffles at the outside of Caco-2 cells

A

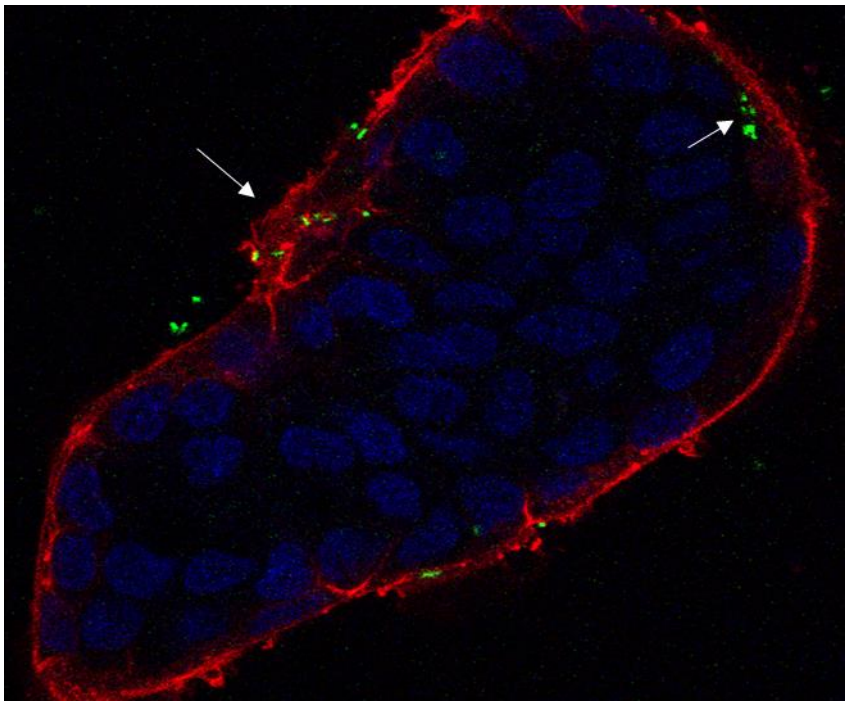

B

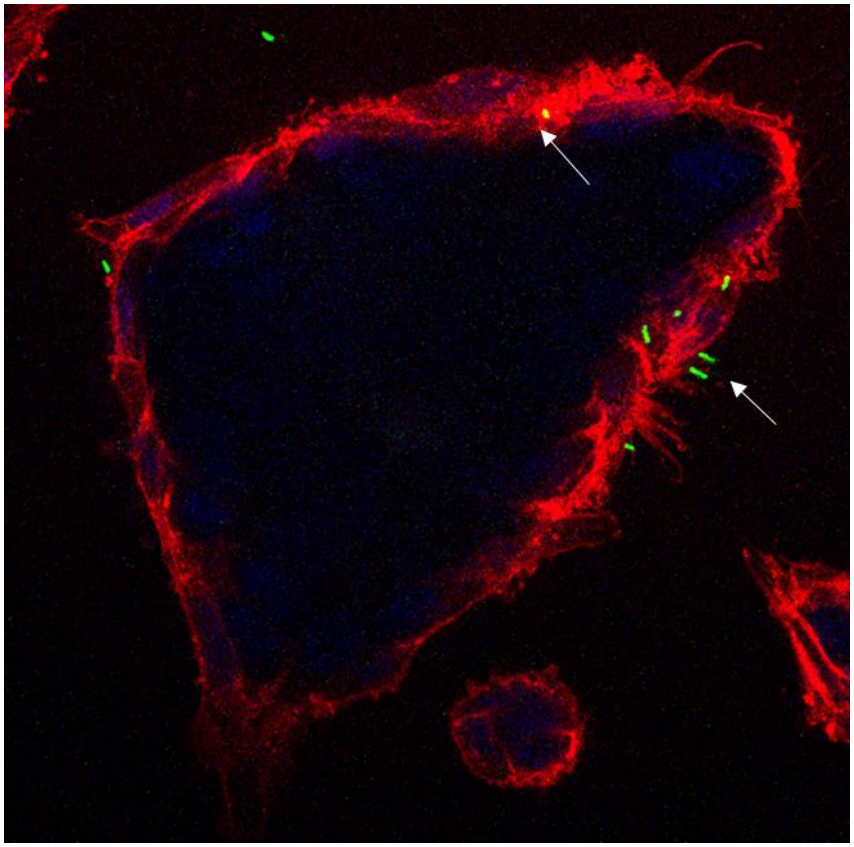

Figure 5.22. Representative confocal micrograph of Caco-2 cells infected with 11168H *cadF* mutant expressing GFP. Caco-2 cells were A. untreated and B. pre-treated with 3 µM cyto D for 1 h and infected with GFP expressing 11168H *cadF* mutant (MOI 100:1) for 1 h. Cells were prepared and stained using DAPI (Blue) for nucleus and rhodamine phalloidin (Red) for actin filaments.

5.2.18 Infection of cytochalasin D pre-treated Caco-2 IECs with the 11168H *flpA* mutant expressing GFP

As with the *C. jejuni* 11168H *cadF* mutant, experiments were also performed to determine the role of actin microfilaments in *C. jejuni* 1116H *flpA* mutant invasion of Caco-2 cell. Both in Caco-2 cells untreated with cyto D (panel A) and treated with cyto D (panel B) the *C. jejuni* 1116H *flpA* mutant was not observed able to invade Caco-2. However, the infection with *C. jejuni* 11168H *flpA* mutant appeared to induce membrane ruffles around the infected Caco-2 cells. Note heavy ruffling surrounding untreated Caco-2 cells (panel A).

A

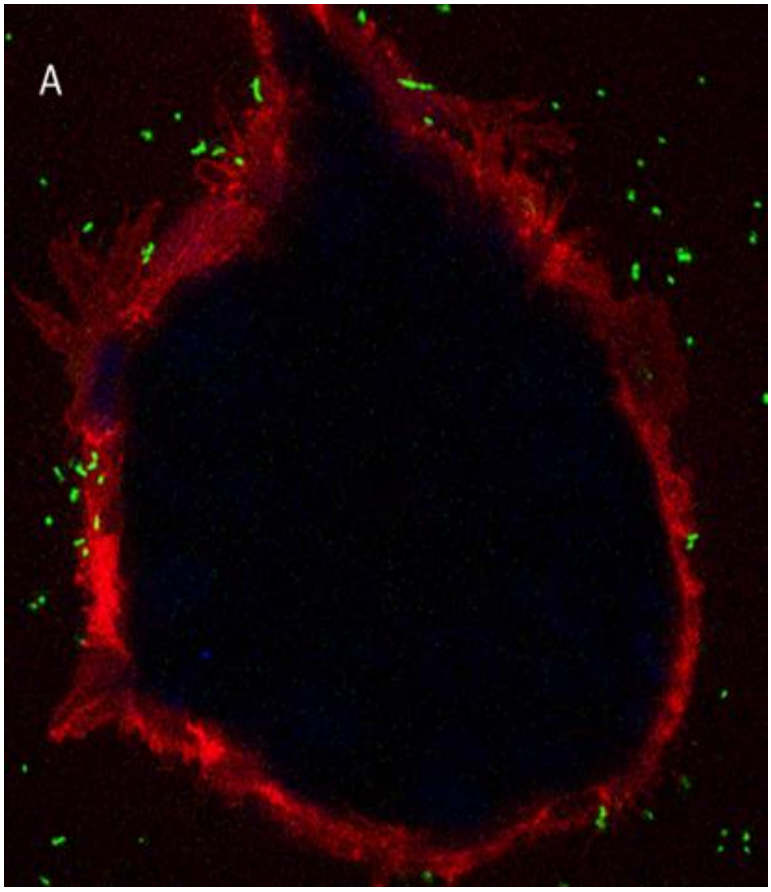

B

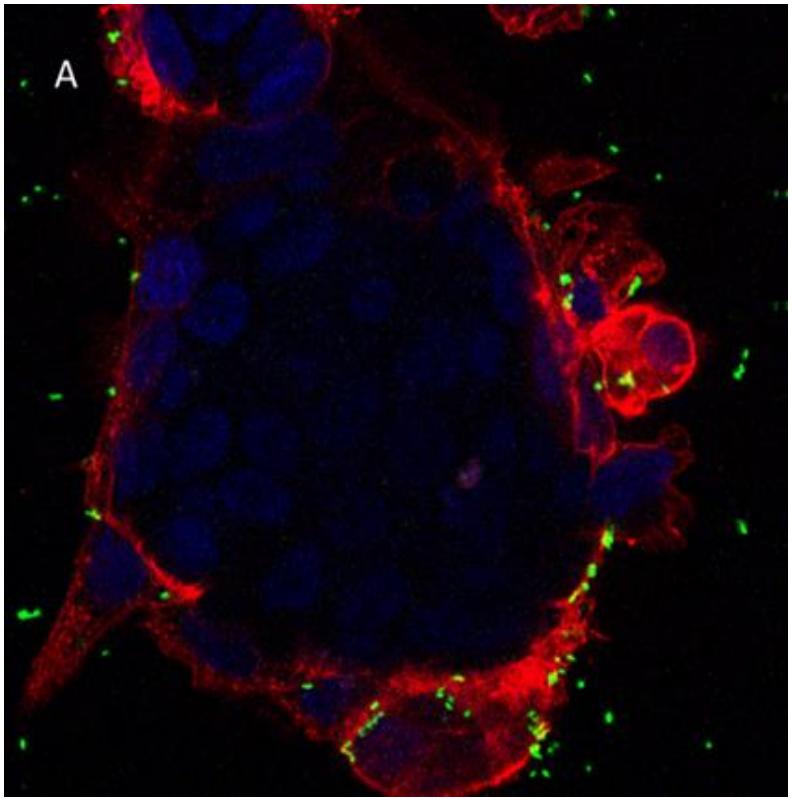

Figure 5. 23. Representative confocal micrograph of Caco-2 cells infected with 11168H *flpA* mutant expressing GFP. Caco-2 cells were A. untreated and B. pre-treated with 3 µM cyto D for 1 h and infected with GFP expressing 11168H *flpA* mutant (MOI 100:1) for 1 h. Cells were fixed and stained using DAPI (Blue) for nucleus and rhodamine phalloidin (Red) for actin filaments. No invasion was observed by *C. jejuni flpA* mutant into both untreated and treated (panel A and panel B respectively). However, the infection caused formation of membrane ruffles around the infected cells.

5.3 Discussion

Successful application of the use of the recombinant green fluorescent protein (GFP) from the jellyfish *A. victoria* to monitor bacterial interactions with eukaryotic cells was first demonstrated in 1994 (Chalfie et al., 1994). The use of recombinant GFP protein to image bacterial interactions with eukaryotic cells has many advantages including the none requirement for any extrinsic factors except blue or UV light. Monitoring of GFP fluorescence is also compatible with various detection technologies, such as simple UV light visualisation, fluorescence microscopy and fluorescence plate readers for *in vitro* and *in vivo* imaging (Errampalli et al., 1999, Tombolini et al., 1999). In addition, the use of recombinant GFP has been shown to have no toxic effects on cells (Chalfie et al., 1994). Recombinant GFP has been widely used to track and visualise bacterial cells localisation within eukaryotic cells and tissue. The attempts to visualise GFP expressing bacteria interacting with eukaryotic cells has promoted the advancement of our understanding of pathogenesis and intracellular survival mechanisms.

The use of GFP to investigate *C. jejuni* interactions with IECs is not widely used due to problems with bacterial expression of GFP in the intracellular environment. In this chapter, the availability of the new *C. jejuni* GFP construct with a highly fluorescent recombinant GFP protein under the control of the strong *C. jejuni porA* promoter that has recently been reported was exploited (Jervis et al., 2015). *C. jejuni* 11168H wild-type strain, *cadF* and *flpA* mutants expressing a bright fluorescence GFP protein were constructed and used to investigate the localisation of these *C. jejuni* strains during interactions with and invasion of both Caco-2 and T84 cells *in vitro*. These experiments have confirmed the invasion pathways of the *C. jejuni* 11168H wild-type strain expressing fluorescence GFP in both Caco-2 and T84 cells. This is the first study, which used a *C. jejuni* 11168H wild-type strain expressing a GFP to characterise the interactions, invasion and intracellular survival of 11168H in IECs. Since IECs are non-phagocytic in nature, *C. jejuni* must actively induce entry into IECs. Traditionally *C. jejuni* 11168H interactions with IECs have been visualised either using immunofluorescence, where antibodies bound to fluorescent dyes are used to target *C. jejuni* (Hu and Kopecko, 1999) or by live/dead staining (Watson and Galan, 2008).

Expression of GFP was confirmed not to impact significantly growth or motility (Clark et al., 2009, Kadioglu et al., 2001). For all the experiments conducted, GFP-expressing *C. jejuni* strains maintained the ability to constitutively express GFP. Initially, comparisons were made between the growth kinetics of the wild-type GFP-expressing strain and GFP-expressing mutants. In all instances, the growth curves were virtually identical to the respective non-GFP expressing strains and no significant differences in growth rate were observed. These observations suggested that recombinant GFP expression in these *C. jejuni* 11168H strains did not significantly affect bacterial growth rate and are in agreement with previous studies (Chalfie et al. 1994; Skillman et al. 1998). However, there was a slight change in motility, where the *C. jejuni* 11168H wild-type strain expressing GFP exhibited increased motility compared to non-GFP expressing wild-type strain, but still within the range of other *C. jejuni* wild-type strains and similar to the level of the highly invasive 81-176 wild-type strain (see Section 3.2.5). As growth rate and motility are known modulators of *C. jejuni* physiology and virulence potential, it was important to eliminate attenuation of these virulence traits as a possible effect of recombinant GFP expression.

A study by Clark *et al.* showed that expression of GFP has no impact on *S. Typhimirium* invasiveness during optimal growth (Clark et al., 2009). Previously, it was also reported that the ability of *Streptococcus pneumoniae* D39 to invade and grow within the infected host was not impacted by carriage of a GFP plasmid (Kadioglu et al., 2001). The *S. pneumoniae* pGFP1 and wild-type strain showed no difference in growth in lung tissue or blood over 48 h of infection. In an earlier study, it was reported that GFP expression did not compromise bacterial activities of *S*. *Typhimirium, Yersinia pseudotuberculosis* or *Mycobacterium marium* either *in vitro* or *in vivo* (Valdivia et al., 1996).

C. jejuni interactions with and invasion into IECs are the initial steps of the pathway taken during *C. jejuni* infection (van Spreeuwel et al., 1985). The confocal microscopy analysis of the 11168H wild-type strain expressing GFP confirmed that *C. jejuni* is readily internalised into T84 and Caco-2 IECs in a time-dependent manner. The results agreed with previous reports which demonstrated immediate interactions of *C. jejuni* with IECs (Hu and Kopecko, 1999). In another study, Hu *et al.* also reported that *C. jejuni* 81-176 was seen at the periphery of INT 407 cells 30 min post-infection (Hu et al., 2008). In this study, bacterial interactions were observed very early on 30 min after infection of IECs, as bacteria were observed surrounding cells at the plasma membrane

outside the cell. At 2 hours post-infection, bacteria were already observed internalised inside cells with the cell monolayer and nuclei appearing to be intact despite the presence of intracellular bacteria.

C. jejuni enters IECs cells via largely uncharacterised mechanisms (Backert et al., 2013). Various studies using specific inhibitors such as MβCD and cyto D have revealed *C. jejuni* to enter IECs by a microtubule-dependent (actin-filament-independent) and/or actin-filament-dependent (microtubule-independent) mechanism (De Melo et al. 1989; Konkel and Joens 1989; Oelschlaeger et al. 1993; Russell and Blake 1994; Hu and Kopecko 1999; Biswas et al. 2003; Monteville et al. 2003). Interestingly, *C. jejuni* requirements for MTs and/or MFs to enter IECs is in contrast to the invasion pathways of other enteric pathogens such as the highly invasive *Salmonella* or *Shigella* species (Galan, 2001, Sansonetti, 2001). C*. jejuni* 81-176 has been reported to enter IECs cells via a mechanism involving MTs but not MFs, while other studies have reported *C. coli* VC167 and other strains of *C. jejuni* that enter cells via a mechanism involving MFs but not MTs. The implications of *C. jejuni* wild-type strains differing in IEC invasion pathways supports the hypothesis that different *C. jejuni* strains have different host cytoskeletal requirements for invasion, depending on both the bacterial strain and IEC line.

Various steps precede the invasion of *C. jejuni* into IECs leading to membrane and cytoskeletal rearrangements. These include binding to IECs, delivery of bacterial virulence factors into the IECs and re-programming of intracellular IECs signalling cascades. These processes commonly involve the activation of small Rho family GTPases such as RhoA, Cdc42 and Rac1, which act as guanine nucleotide-regulated switches and induce various responses during the bacterial infection processes. The three GTPases are linked in actions and to each other, because activation of Cdc42 results in formation of filopodia that leads to Rac activation which in turn induces formation of lamellipodia (Nobes and Hall, 1995b, Nobes et al., 1995). Rac subsequently activates Rho and the resulting focal complexes formation. As suggested by Hall *et al.*, Rho, Rac and Cdc42 work in co-ordination to cause the spatial and temporal actin cytoskeleton reorganisation that leads to cell movement and bacterial internalisation (Hall, 1990). However, while the internalisation of *C. jejuni* strains such 81-176 and F38011 has typically been observed to induce rearrangement of the host actin-cytoskeletal structure, the invasion characteristics of a GFP expressing *C. jejuni* 11168H wild-type has not been investigated yet.

The actin cytoskeleton maintains cell shape and plays a pivotal role in cell motility, phagocytosis and cytokinesis. Small GTPases such as Rho, Rac and Cdc42 have been shown to produce stress fibres, lamellipodia and filopodia respectively by regulating the polymerisation of actin in host cells (Mackay et al., 1995, Nobes and Hall, 1995b). Swiss 3T3 cells were serum starved and microinjected with proteins such as V12rac (Rac 1 isotype) and V14rho (RhoA isotypes) as well as V12cdc42. From between 50-100 cells microinjected, more than 90% exhibited the various forms of membrane ruffles such as stress fibres, lamellipodia and filopodia. In addition, the cells also exhibited the formation of focal adhesions and other adhesion complexes.

Activation of Rac1 is an important event for many invasive pathogens (van Triest et al., 2001, Hardt et al., 1998). Lafont *et al.* reported that GFP-tagged *S. flexneri* upon entering HeLa cells induced membrane ruffles which had lipid raft components (Lafont and van der Goot, 2005). Activated Rac1 induced intensive ruffling of the membrane, as has been observed frequently (Ridley et al., 1992, Obermeier et al., 1998). When serum starved confluent Swiss 3T3 fibroblasts were injected with Cdc42, filopodia were observed 5 min post-injection. In addition to activated Rac1, the cells were then observed to form lamellipodia and spreading rapidly between projection of spikes to form a web that looked like a 'veil' (Nobes and Hall, 1995b). Rho and Rac were shown to control actin polymerisation that leads to formation of stress fibres and membrane ruffle lamellipodia (Ridley and Hall, 1992).

C. jejuni 81-176 wild-type strain induces profound membrane ruffling in INT 407 cells but not in fibronectin, integrin or FAK knockout cells (Boehm et al., 2011). In this study, formation of membrane ruffles was also observed in the Caco-2 serum starved cells infected with 11168H expressing GFP. In addition, infection with the wild-type strain, *cadF* or *flpA* mutants not expressing GFP were shown to induce activation of Rac1 (see Section 4.2.6). Observations from this study were consistent with reports from previous studies which suggested that the *C. jejuni* 81-176 wild-type strain was able to induce membrane ruffling in Caco-2 cells as the result of Rac-1 activation as seen in the formation of lamellipodia (Biswas et al., 2003, Biswas et al., 2004, Hu and Kopecko, 1999). This indicates that *C. jejuni* 11168H wild-type strain activates Cdc42, as well as Rho, as suggested by the observed filopodia and stress fibres respectively.

Having established that the *C. jejuni* 11168H wild-type GFP strain could invade T84 and Caco-2 efficiently, experiments were performed to investigate the intracellular fate of *C. jejuni*. Intracellular pathogens have adapted a variety of survival mechanisms to be able to replicate and survive within host cells. *L. monocytogenes* (Goebel and Kuhn, 2000), S. *flexneri* (Cossart, 2004, Ogawa and Sasakawa, 2006), and *Trypanosoma cruzi* (Brener, 1973) were able to replicate in the cytosol after breaking free from lysosome. Others such as *M. tuberculosis* (Deretic et al., 2006) or *S.* Typhimurium (Knodler and Steele-Mortimer, 2003) reside and survive in compartments that deviate from being fused into lysosomes. In this study, fluorescence confocal micrographs showed that the 11168H wild-type expressing GFP was efficiently internalised within T84 monolayers. Once internalised within T84 cells, *C. jejuni* either co-localised with actin filaments or remained free from any actin filament association. Not all internalised *C. jejuni* bacteria (stained Green) appeared yellow in colour which would suggest association with actin filaments (stained Red). Some bacteria were observed as only a green stain that suggests no association with actin filaments.

This data supports the study published by Galan's group who previously reported that following internalisation, the *C. jejuni* 81-176 wild-type strain resides in a CCV (Watson and Galan, 2008). In addition, other studies have reported that upon infection with IECs, *C. jejuni* co-localises in vacuole or membrane bound compartment (Russell and Blake, 1994, Humphrey et al., 1986, Kiehlbauch et al., 1985, Hickey et al., 2005). In one study, *C. jejuni* 81-176 wild-type strain was observed and even appeared to be motile and able to replicate in a vacuole within human monocytes (Hickey et al., 2005).

Following internalisation into IECs, the CCV was not shown to follow the pathway that usually deliver these vacuole compartments to the conventional cellular lysosomes. This was confirmed when endocytic dextran tracer was not found within the CCV (Watson and Galan, 2008). However, in macrophages, *C. jejuni* found in the CCV cannot avoid the endocytic pathway and is lysed by lysosomes (Watson and Galan, 2008). These data indicate that CCVs were separated from following the endocytic pathway and fusion with lysosomes in cytoplasm. In the endocytic pathway, early and late endosomal markers such as Rab5 and Rab7 respectively could be stained with immunofluorescence antibodies. Once again the CCVs were not accessible to those markers. The mechanisms used by *C. jejuni* to deviate from the classical endocytic pathway

and block fusion with lysosomes remain unknown. Other enteric pathogens utilise virulence effectors that target the regulatory machinery that controls endomembrane transport and fusion, to block and disrupt the function of the Rab proteins (Knodler and Steele-Mortimer, 2003, Meresse et al., 1999).

In order to investigate which endosomal marker the matured CCVs acquired to prevent fusion with lysosomes, an antibody for the late endosomal marker Lamp-1 was used to stain the CCVs. Not many bacteria were observed co-localised with Lamp-1 even though the majority of the intracellular bacteria resided within vacoules as judged by yellow colour fusion in the cells. One study reported that co-localisation with Lamp-1 is transient even though most 81-176 wild-type CCVs were all stained with Lamp-1 2 h post-infection (Watson and Galan, 2008). It was also shown that the CCV was not co-localised with cathepsin B, a lysosomal protein marker. Hence, the data now indicates that *C. jejuni* 81-176 (Watson and Galan, 2008) and 11168H (this study) would reside intracellularly within a vacuole and progress towards the Golgi to allow survival in cytoplasm. The CCV acquires Lamp1, but not Rab 5 and Rab 7, similar to *S. Typimurium* with the exception of Rab 7 that is needed in the case of *S. Typimurium.* This appears to render the bacteria protected or separated from the lysosome pathways.

Cytoskeletal requirements for *C. jejuni* entry into host cells until now have not been finalised, but it is agreed different *C. jejuni* strains adapt to and employ different pathways that suit the environments, cells or assays used. Because of that, data from many different studies showed pathways dependent of both MFs and MTs (Biswas et al., 2003), others showed pathways dependent only on MFs (Monteville et al., 2003) or only on MTs (Oelschlaeger et al., 1993, Kopecko et al., 2001, Hu and Kopecko, 1999) whilst another showed pathways independent of both MFs and MTs (Biswas et al., 2003).

In this chapter, the mechanisms employed by the 11168H wild-type, *cadF* mutant and *flpA* mutants expressing GFP to enter IECs appeared to be both MF- and lipid raft-dependent. However, confocal micrographs did not clearly show any reduction in invasion by the inhibitors cyto D, which inhibits G-actin polymerisation and disrupts F-actin actin filaments, or MβCD, which inhibits lipid rafts in the plasma membrane. In addition, in the same inhibitor treatment, no significant reduction of invasion was observed between treated IECs or non-

treated IECs. For every assay on each strain, minimum of 50 to 100 cells were observed for every field.

GFP allowed the visualisation of the association of *C. jejuni* with actin polymerisation specifically and with the actin cytoskeleton generally. This is because the host cytoskeleton structure is partly made of polymerised actin filaments, which are responsible for many active cell processes including cell movement, membrane ruffling and phagocytosis. In this study, internalised *C. jejuni* was observed demonstrating localised adherence. At the site of adherence, accumulation of actin was observed and it has previously been reported that infection of INT 407 monolayers with *C. jejuni* M21 produced the same effects (Konkel et al., 1992a)

All the *C. jejuni* 11168H expressing GFP strains investigated in this study adhered to and invaded Caco-2 and T84 cells. Each strain also appeared to invade at the same rate judged by the micrographs observed. A previous study has also reported that there was no significant difference observed between the ability of slightly invasive and highly invasive *C. jejuni* strains to adhere to IECs (Biswas et al., 2000). Stimulation of membrane ruffling as a result of *C. jejuni* adhering to IECs proved to be a common phenomenon, although invasiveness may be *C. jejuni* strain specific (Biswas et al., 2000). Data from this study using confocal microscopy supports previous studies whereby the occurrence of pseudopod formation is stimulated by *C. jejuni* and this may play a key role in adherence to the target cell membrane (Konkel et al., 1992a).

CHAPTER SIX: FINAL DISCUSSION

The aim of this study was to further investigate the roles played by the two highly conserved *C. jejuni* fibronectin binding proteins CadF and FlpA during bacterial interactions with IECs. Two *C. jejuni* 11168H and 81-176 strains were used for comparison to initially identify whether the functions of CadF and FlpA are species or strain specific. The two strains 11168 and 81-176 belong to specific MLST clonal complexes of ST-21 and ST-42 respectively. ST-21 represents livestock-associated linages whilst ST-42 represents livestock and water and wildlife-associated linages (Gundogdu et al., 2016).

Although both *cadF* and *flpA* are highly conserved genes in *C. jejuni* strains, differences were identified in the transcription of both genes between the 11168H and 81-176 wild-type strains. *cadF* is transcribed at a higher level (around 4-fold) in both wild-type strains compared to *flpA* (see Figure 3.11). However, transcription of *cadF* in the 81-176 wild-type strain is at a higher level than in the 11168H wild-type strain, under the growth conditions used in this study. In contrast, transcription of *flpA* was at the same level in both 81-176 and 11168H. Bearing this information in mind, results from the different assays used in this study can be interpreted in relation to the predicted levels of CadF or FlpA in the particular strain. Bioinformatic analysis showed that CadF in NCTC 11168 is similar to CadF in 81-176 (see Figure 3.1) and that FlpA in NCTC 11168 is similar to FlpA in 81-176 (see Figure 3.2). This suggests that CadF function will be identical in both 11168H and 81-176 strains and FlpA function will be identical in both strains as well. However, the amino acid sequences of CadF and FlpA are quite divergent as shown by the amino acid alignments (see Figure 3.3) as well as by the 3-D ribbon diagrams (see Figure 3.4). This suggests that CadF and FlpA probably have some differences in function in *C. jejuni*.

6.1 The role of CadF

Studies with the 11168H and 81-176 *cadF* mutants indicated that *C. jejuni* uses CadF to bind to the IEC extracellular matrix protein fibronectin. The binding to fibronectin facilitates the adhesion of *C. jejuni* to IECs and the activation of downstream signal transduction pathways involving small Rho GTPases. The

hypothesises was that inactivation of *cadF* in *C. jejuni* would lead to a reduced level of binding to and invasion into IECs, which could also affect the activation of the IECs signal transduction pathways involving small Rho GTPases including the Rac1 pathway, which involves the initiation of signalling pathways such as integrin signalling for membrane ruffling and for focal adhesion.

The inactivation of *cadF* in both the 11168H and 81-176 wild-type strains resulted in a reduction of adhesion to Caco-2 and T84 IECs. However, the binding of the *cadF* mutants to immobilised fibronectin *in vitro* was not dramatically reduced. This somewhat counter-intuitive result suggests that fibronectin is not the only extracellular receptor that *C. jejuni* binds to on the surface of IECs. The influence of other IECs factors, such as the presence of putative receptors in lipid rafts which *C. jejuni* uses to gain access to IECs to allow subsequent invasion to occur must also be considered. This finding is also in contrast to a study by Konkel *et al.* who reported that CadF has a higher binding affinity to immobilised fibronectin compared to FlpA in the F38011 strain (Konkel et al., 2010). The *cadF* mutants were less cytotoxic than the *flpA* mutants in the *G. mellonella* model of infection. This would suggest that higher levels of CadF have a more severe impact on host cells. Results from other assays demonstrated that CadF in 11168H is required for and played a role in the invasion of IECs, in translocating across IECs, in inducing IL-8 and in activating Rac1. However, the impact of CadF showed no significant difference to that of FlpA on those assays.

While inactivation of *cadF* in both the 11168H and 81-176 wild-type strains is responsible for the reduced adhesion to IECs, it was evident that this is not statistically significant. This may be due to up-regulation of *flpA* as a redundant response as part of a compensation mechanism must also be considered. In addition, both the 11168H and 81-176 c*adF* mutant exhibited higher numbers of interacting bacteria than the respective *flpA* mutant. In contrast, in the invasion assays, the 11168H *cadF* mutant invades less than the 11168H *flpA* mutant. However, the 81-176 *cadF* and *flpA* mutants exhibited similar invasion abilities. These results may indicate that CadF has a more important role in invasion than in interaction with IECs compared to FlpA and also this may be strain-dependent.

The use of inhibitors to investigate the pathways employed by *C. jejuni* to enter IECs has indicated that not all inhibitors have the same impact on the ability of

the 11168H *cadF* mutant to invade IECs. A reduction in the invasion ability of the 11168H *cadF* mutant was evident when IECs were pre-treated with MβCD, cyto D or colchicine. However, pre-treatment of IECs with wortmanin had less impact on the ability of 11168H *cadF* mutant to invade IECs compared to the other three inhibitors. Therefore, the invasion pathway of the 11168H *cadF* mutant involves components such as lipid rafts, MFs and MTs and is independent of PI3-kinases. This suggests that CadF is involved in *C. jejuni* binding to fibronectin which leads to subsequent IECs processes involving PI3 activation to induce internalisation.

6.2 The role of FlpA

FlpA contains three domains similar to that of fibronectin type III binding domains (Konkel et al., 2010). In this study, both 11168H and 81-176 *flpA* mutants were shown to bind less to fibronectin *in vitro* compared to the respective *cadF* mutants. In the interaction assays with IECs, both 11168H and 81-176 *flpA* mutants showed a reduction compared to the respective *cadF* mutants. This suggests that having three FnIII binding domains allows FlpA to play a more important role in binding to fibronectin *in vitro* and in adherence to IECs than CadF. FlpA was also shown to play A role in translocation across IECs, induction of IL-8 and activation of Rac1. In addition, FlpA showed a similar ability and efficiency compared to CadF in translocating across IECs. FlpA also able to induce IL-8 and Rac1 to a similar level compared to CadF.

The ability of the 11168H *flpA* mutant to invade T84 cells was inhibited by MβCD, cytochalasin D and wortmannin. However, colchicine not only did not inhibit invasion by the 11168H *flpA* mutant, but the invasion ability of the 11168H *flpA* mutant was increased to a higher level than that of the 11168H wild-type strain when T84 IECs were pre-treated with colchicine. The 11168H *flpA* mutant expressed higher levels of *cadF* compared to the wild-type strain. The CadF-invasion pathway appears to involve PI3 activation and is independent of MFs and MTs, highlighting the multiple and the complex invasion mechanisms that *C. jejuni* employs to enter IECs. Cytochalasin D depolymerises IECs MFs whilst colchicine inhibits formation MTs. These results

indicate that the FlpA-invasion pathway may involve MTs. This finding also provides novel evidence that while both CadF and FlpA are required for *C. jejuni* invasion to IECs, *C. jejuni* induced MT depolymerisation reduced the invasion ability of *cadF* mutant while in *flpA* mutant MT depolymerisation of IECs was shown to increase the invasion to IECs.

6.3 Roles of CadF and FlpA in *C. jejuni* pathogenesis

This study has identified some similarities and some differences in the roles of CadF and FlpA in *C. jejuni* and provided preliminary evidence as to why *C. jejuni* strains possesses two fibronectin binding adhesins. This can be discussed in relation to progressive steps during *C. jejuni* interactions with host cells.

First step: Pathogenesis of *C. jejuni* begins with adherence. Both CadF and FlpA are able to bind to fibronectin *in vitro*. However, the binding ability of a *flpA* mutant to IECs is reduced significantly compared to a *cadF* mutant. However, it was evident that both proteins play an important role in *C. jejuni* adherence to IECs. FlpA appears to have a more significant role in *C. jejuni* binding as the numbers of the *flpA* mutants binding to IECs were significantly reduced compared to the *cadF* mutants. This could be attributed to the fundamental difference between CadF and FlpA, particularly the presence of three FnIII domains in FlpA compared to CadF. However, both FlpA and CadF are known to bind to the same integrin α5β1 receptors.

Second step: Both CadF and FlpA also play a role in *C. jejuni* invasion of IECs. However, the invasion ability of a *cadF* mutant is reduced significantly compared to a *flpA* mutant with T84 IECs but similar in Caco-2 IECs. Also invasion of both *cadF* and *flpA* mutants is dependent on lipid rafts while there is preferential difference to engage invasion pathways that are either MT- or MF-specific. This suggests that the invasion by *cadF* and *flpA* mutants involve the caveolin-mediated endocytosis pathway. Also that CadF plays a more important role in invasion of IECs compared to FlpA, supported by the higher transcription levels of *cadF* compared to *flpA*.

Third step: Once *C. jejuni* adheres to IECs, CadF and FlpA use separate and different pathways. Entry mediated via CadF is MT- and MF-dependent. In contrast, entry mediated via FlpA is MT-independent. This difference between CadF and FlpA involvement with MTs is probably responsible for the different roles of MFs and MTs during *C. jejuni* invasion as reported in many published studies. *C. jejuni* presumably is able to switch between entry mediated via CadF and entry mediated via FlpA resulting in invasion mechanisms requiring both MFs and MTs or either MFs or MTs.

Fourth step: The end result however is similar, as evidenced by the fact that CadF and FlpA showed similar ability in activating Rac1, a member of small GTPases. Mutation of either *cadF* or *flpA* results in a decrease in Rac1 activation compared to the wild-type strain. This suggests that both CadF and FlpA play a role in Rac1 activation. Rac1activation is a switch that turns on the chain of events such as the formation of focal adhesions, recruitment of other signalling molecules and relaying signals to cytoskeleton components such as MFs and MTs. As a result of this reaction, the host cell cytoskeleton will reorganise and induce membrane ruffles at the site of *C. jejuni* attachment. Actin cytoskeleton rearrangements include the formation of pseudopodia such as lamellipodia and filopodia and can be observed as actin concentration localised with *C. jejuni* internalisation.

Collectively, the results from this study are in agreement to the invasion model proposed by O'Croinin & Backert (O Croinin and Backert, 2012). In relation to this invasion model, this demonstrates that CadF and FlpA work in co-operation through zipper or/and trigger mechanisms. Both CadF and FlpA mediate adherence and invasion through unique mechanisms and activate members of the small GTPases which play central roles in rearranging MFs and MTs in the host cytoskeleton. Thus through CadF and FlpA, C *jejuni* is fully equipped to trigger and activate signalling events that lead to the bacteria being internalised by the host cells.

All taken into consideration, as with any other successful pathogen, *C. jejuni* demonstrates the complex and intricate pathogenesis mechanisms which are different from other enteric pathogens. These involve multiple factors with various and co-operative actions or independent and separate pathways that *C. jejuni* employ for any given cells line, to mediate successful interaction/s that

result in campylobacteriosis and establishing *C. jejuni* as one of the most successful human enteropathogens to date.

Further investigation needs to be performed as a clearer understanding of the pathogenesis mechanisms will contribute to the development of innovative strategies for prevention and therapy in the future.

6.4 Future work

Future gene expression analysis should use RNA seq. Gene expression studies will benefit from RNA seq techniques because this method is excellent to investigate changes in gene expression under different conditions. The next study should investigate the expression of CadF and FlpA in media supplemented with bile salts. In the intestine, the presence of bile salts serves as a protection to host cells by bactericidal activity against pathogens (Urdaneta and Casadesus, 2017). However, it was reported that pathogens are able to survive and establish infection in the presence of bile salts in the intestine. This is because bile salts can activate different bacterial mechanisms for resistance, damage repair and protection (Urdaneta and Casadesus, 2017, Schubert et al., 2017). In another study, bile salts were shown to increase resistance to antimicrobials and change gene expression in *C. jejuni* (Lertpiriyapong et al., 2012). Further, it was reported that bile salts induced Cia expression in *C. jejuni* which enhanced the ability of *C. jejuni* to invade IECs (Rivera-Amill et al., 2001, Malik-Kale et al., 2008). Sodium taurocholate (ST) is a constituent of the bile salts in the caecum (Hamilton et al., 2007). Recently, bile salts have been shown to facilitate germination of *Clostridium difficile* (Kochan et al., 2017). This study will no doubt bring it closer to the natural niche of *C. jejuni* as in the gut environment which makes the result more relevant. Changes in the expression of CadF and FlpA under conditions that more closely mimic those in the human intestine may cast further light of the role of these two fibronectin binding proteins during *C. jejuni* infection.

In this study, the assays were performed at two different time points. In the next study, the adhesion and invasion assay should be performed which include

more time points and longer time points so as to provide a complete picture of *C. jejuni* interaction with IECs. Attempts have been made to construct complements of *cadF* and *flpA* mutants, however with no success. It was noted by Konkel that in his group the construction of *cadF* and *flpA* complements posed significant challenges. However, without doubt, the availability of complementation will be useful to answer and clear any controversial results as complementation should restore the phenotypic changes. Construction of a double *cadF flpA* mutant may also show more clearly the role of CadF and FlpA. A double mutant could show whether CadF and FlpA function independently and/or different mechanisms and pathways are involved. Construction of complements and double mutants should be included in further studies. As with the cell lines employed, it will be also relevant to include cells that produce mucus such as HT29 MTXE-12, and an Homo sapiens colon ileocecal carcinoma cells (HCT8) (Alemka et al., 2010, Lindmark et al., 2009). Previously, a vertical diffusion chamber (VDC) model system was used to more closely mimic the human intestinal microenvironment in *C. jejuni* study. The VDC has two chambers, one, microaerobic environment to mimic apical surface of IECs and second, an aerobic environment to mimic the baso-lateral surfaced of cultured IECs (Mills et al., 2012, Naz et al., 2013). This system potentially will create a better condition for *in vitro C. jejuni* study compared to standard tissue culture methods. Various assays can be performed comparing different strains, different cell lines and gene expression studies, which would all benefit from using the VDC model system. Stem cell research could also be attempted as one of the technique to investigate pathogenesis, as an option has available to use a 'miniguts'. The miniguts grow from a single stem cell isolated from the intestine that is able to form a complex organoid structure and has a similar identity with their original organ (Sato and Clevers, 2013).

GFP expressing *C. jejuni* strains have contributed to following up interaction studies *in vivo*. As a fusion tag, the GFP can be utilised in many ways including protein localisation, movement and the dynamic of the compartments where the bacteria or protein targeted (Gerdes and Kaether, 1996). During visualisation with confocal microscopy, *C. jejuni* can be observed both in vacuoles and free in the cytoplasm. Therefore, further work is needed to clarify the different compartments where *C. jejuni* can be found, especially during infection *in vivo*. Defining the respective roles of these compartments will identify new routes as some usually represent dead-ends in pathogenesis. The interaction of the *cadF*

and *flpA* mutants expressing GFP also can be followed and tracked *in vivo*. As a visual marker, the GFP will allow not only enumeration of the bacteria but also the impact and the fate of the bacteria in the natural environment. A previous study has reported that expression of GFP has no impact on the interaction of pathogens with host cells (Valdivia et al., 1996). However, a recent study has reported that GFP may induce oxidative stress to cells, and this will have an impact on the results obtained in the study where the bacteria is tagged with GFP (Kalyanaraman and Zielonka, 2017).

CadF and FlpA have also been identified among the proteins found in *C. jejuni* OMVs (Elmi et al., 2012). HtrA is also found in *C. jejuni* OMVs and has been shown to play a role in *C. jejuni* invasion through the ability to cleave E-cadherin (Elmi et al., 2016). Further studies are required to demonstrate the effect of *C. jejuni* OMVs in general and OMVs isolated from *cadF* and *flpA* mutants in specific, on damage to host cells such as on epithelial cells and immune cells in order to identify the role of CadF and FlpA in OMV interactions with host cells. As with live bacteria, OMVs entry mechanisms, intracellular localisation and activities will also require further studies. Investigations involving OMVs will result in a greater understanding of *C. jejuni* pathogenesis in humans.

7. References

AHMED, I. H., MANNING, G., WASSENAAR, T. M., CAWTHRAW, S. & NEWELL, D. G. 2002. Identification of genetic differences between two Campylobacter jejuni strains with different colonization potentials. *Microbiology,* 148**,** 1203-12.

AL-SALLOOM, F. S., AL MAHMEED, A., ISMAEEL, A., BOTTA, G. A. & BAKHIET, M. 2003. Campylobacter-stimulated INT407 cells produce dissociated cytokine profiles. *J Infect,* 47**,** 217-24.

ALBERTSON, R., CAO, J., HSIEH, T. S. & SULLIVAN, W. 2008. Vesicles and actin are targeted to the cleavage furrow via furrow microtubules and the central spindle. *J Cell Biol,* 181**,** 777-90.

ALEMKA, A., CLYNE, M., SHANAHAN, F., TOMPKINS, T., CORCIONIVOSCHI, N. & BOURKE, B. 2010. Probiotic colonization of the adherent mucus layer of HT29MTXE12 cells attenuates Campylobacter jejuni virulence properties. *Infect Immun,* 78**,** 2812-22.

ALLEN, V. M., BULL, S. A., CORRY, J. E., DOMINGUE, G., JORGENSEN, F., FROST, J. A., WHYTE, R., GONZALEZ, A., ELVISS, N. & HUMPHREY, T. J. 2007. Campylobacter spp. contamination of chicken carcasses during processing in relation to flock colonisation. *Int J Food Microbiol,* 113**,** 54-61.

ALLOS, B. M. 2001. Campylobacter jejuni Infections: update on emerging issues and trends. *Clin Infect Dis,* 32**,** 1201-6.

ALTER, T., BERESWILL, S., GLUNDER, G., HAAG, L. M., HANEL, I., HEIMESAAT, M. M., LUGERT, R., RAUTENSCHLEIN, S., WEBER, R. M., ZAUTNER, A. E. & GROSS, U. 2011. [Campylobacteriosis of man : livestock as reservoir for Campylobacter species]. *Bundesgesundheitsblatt Gesundheitsforschung Gesundheitsschutz,* 54**,** 728-34.

APERIS, G., FUCHS, B. B., ANDERSON, C. A., WARNER, J. E., CALDERWOOD, S. B. & MYLONAKIS, E. 2007. Galleria mellonella as a model host to study infection by the Francisella tularensis live vaccine strain. *Microbes Infect,* 9**,** 729-34.

ASAKURA, H., YAMASAKI, M., YAMAMOTO, S. & IGIMI, S. 2007. Deletion of peb4 gene impairs cell adhesion and biofilm formation in Campylobacter jejuni. *FEMS Microbiol Lett,* 275**,** 278-85.

ASHGAR, S. S., OLDFIELD, N. J., WOOLDRIDGE, K. G., JONES, M. A., IRVING, G. J., TURNER, D. P. & ALA'ALDEEN, D. A. 2007. CapA, an autotransporter protein of Campylobacter jejuni, mediates association with human epithelial cells and colonization of the chicken gut. *J Bacteriol,* 189**,** 1856-65.

ASHKENAZI, S., DANZIGER, Y., VARSANO, Y., PEILAN, J. & MIMOUNI, M. 1987. Treatment of Campylobacter gastroenteritis. *Arch Dis Child,* 62**,** 84-5.

AWAD, W. A., DUBLECZ, F., HESS, C., DUBLECZ, K., KHAYAL, B., ASCHENBACH, J. R. & HESS, M. 2016. Campylobacter jejuni colonization promotes the translocation of Escherichia coli to extra-intestinal organs and disturbs the short-chain fatty acids profiles in the chicken gut. *Poult Sci,* 95**,** 2259-65.

BABAKHANI, F. K. & JOENS, L. A. 1993. Primary swine intestinal cells as a model for studying Campylobacter jejuni invasiveness. *Infect Immun,* 61**,** 2723-6.

BACKERT, S., BOEHM, M., WESSLER, S. & TEGTMEYER, N. 2013. Transmigration route of Campylobacter jejuni across polarized intestinal epithelial cells: paracellular, transcellular or both? *Cell Commun Signal,* 11**,** 72.

BACKERT, S. & HOFREUTER, D. 2013. Molecular methods to investigate adhesion, transmigration, invasion and intracellular survival of the foodborne pathogen Campylobacter jejuni. *J Microbiol Methods,* 95**,** 8-23.

BACON, D. J., ALM, R. A., BURR, D. H., HU, L., KOPECKO, D. J., EWING, C. P., TRUST, T. J. & GUERRY, P. 2000. Involvement of a plasmid in virulence of Campylobacter jejuni 81-176. *Infect Immun,* 68**,** 4384-90.

BAE, J., OH, E. & JEON, B. 2014. Enhanced transmission of antibiotic resistance in Campylobacter jejuni biofilms by natural transformation. *Antimicrob Agents Chemother,* 58**,** 7573-5.

BAEK, K. T., VEGGE, C. S. & BRONDSTED, L. 2011. HtrA chaperone activity contributes to host cell binding in Campylobacter jejuni. *Gut Pathog,* 3**,** 13.

BARNOY, S., GANCZ, H., ZHU, Y., HONNOLD, C. L., ZURAWSKI, D. V. & VENKATESAN, M. M. 2017. The Galleria mellonella larvae as an in vivo model for evaluation of Shigella virulence. *Gut Microbes,* 8**,** 335-350.

BATCHELOR, R. A., PEARSON, B. M., FRIIS, L. M., GUERRY, P. & WELLS, J. M. 2004. Nucleotide sequences and comparison of two large conjugative plasmids from different Campylobacter species. *Microbiology,* 150**,** 3507-17.

BATISSON, I., GUIMOND, M. P., GIRARD, F., AN, H., ZHU, C., OSWALD, E., FAIRBROTHER, J. M., JACQUES, M. & HAREL, J. 2003. Characterization of the novel factor paa involved in the early steps of the adhesion mechanism of attaching and effacing Escherichia coli. *Infect Immun,* 71**,** 4516-25.

BAUMAN, S. J. & KUEHN, M. J. 2006. Purification of outer membrane vesicles from Pseudomonas aeruginosa and their activation of an IL-8 response. *Microbes Infect,* 8**,** 2400-8.

BAUMAN, S. J. & KUEHN, M. J. 2009. Pseudomonas aeruginosa vesicles associate with and are internalized by human lung epithelial cells. *BMC Microbiol,* 9**,** 26.

BERKES, J., VISWANATHAN, V. K., SAVKOVIC, S. D. & HECHT, G. 2003. Intestinal epithelial responses to enteric pathogens: effects on the tight junction barrier, ion transport, and inflammation. *Gut,* 52**,** 439-51.

BISWAS, D., ITOH, K. & SASAKAWA, C. 2000. Uptake pathways of clinical and healthy animal isolates of Campylobacter jejuni into INT-407 cells. *FEMS Immunol Med Microbiol,* 29**,** 203-11.

BISWAS, D., ITOH, K. & SASAKAWA, C. 2003. Role of microfilaments and microtubules in the invasion of INT-407 cells by Campylobacter jejuni. *Microbiol Immunol,* 47**,** 469-73.

BISWAS, D., NIWA, H. & ITOH, K. 2004. Infection with Campylobacter jejuni induces tyrosine-phosphorylated proteins into INT-407 cells. *Microbiol Immunol,* 48**,** 221-8.

BJERRE, A., BRUSLETTO, B., MOLLNES, T. E., FRITZSONN, E., ROSENQVIST, E., WEDEGE, E., NAMORK, E., KIERULF, P. & BRANDTZAEG, P. 2002. Complement activation induced by purified Neisseria meningitidis lipopolysaccharide (LPS), outer membrane vesicles, whole bacteria, and an LPS-free mutant. *J Infect Dis,* 185**,** 220-8.

BLACK, R. E., LEVINE, M. M., CLEMENTS, M. L., HUGHES, T. P. & BLASER, M. J. 1988. Experimental Campylobacter jejuni infection in humans. *J Infect Dis,* 157**,** 472-9.

BLASER, M. J., BERKOWITZ, I. D., LAFORCE, F. M., CRAVENS, J., RELLER, L. B. & WANG, W. L. 1979. Campylobacter enteritis: clinical and epidemiologic features. *Ann Intern Med,* 91**,** 179-85.

BLASER, M. J., CHECKO, P., BOPP, C., BRUCE, A. & HUGHES, J. M. 1982. Campylobacter enteritis associated with foodborne transmission. *Am J Epidemiol,* 116**,** 886-94.

BLASER, M. J., DUNCAN, D. J., WARREN, G. H. & WANG, W. L. 1983. Experimental Campylobacter jejuni infection of adult mice. *Infect Immun,* 39**,** 908-16.

BLASER, M. J., HARDESTY, H. L., POWERS, B. & WANG, W. L. 1980. Survival of Campylobacter fetus subsp. jejuni in biological milieus. *J Clin Microbiol,* 11**,** 309-13.

BLASER, M. J., WALDMAN, R. J., BARRETT, T. & ERLANDSON, A. L. 1981. Outbreaks of Campylobacter enteritis in two extended families: evidence for person-to-person transmission. *J Pediatr,* 98**,** 254-7.

BLASER, M. J. & WANG, W. L. 1980. Campylobacter infections in human beings. *J Pediatr,* 96**,** 343.

BOEHM, M., HOY, B., ROHDE, M., TEGTMEYER, N., BAEK, K. T., OYARZABAL, O. A., BRONDSTED, L., WESSLER, S. & BACKERT, S. 2012. Rapid paracellular transmigration of Campylobacter jejuni across polarized epithelial cells without affecting TER: role of proteolytic-active HtrA cleaving E-cadherin but not fibronectin. *Gut Pathog,* 4**,** 3.

BOEHM, M., KRAUSE-GRUSZCZYNSKA, M., ROHDE, M., TEGTMEYER, N., TAKAHASHI, S., OYARZABAL, O. A. & BACKERT, S. 2011. Major host factors involved in epithelial cell invasion of Campylobacter jejuni: role of fibronectin, integrin beta1, FAK, Tiam-1, and DOCK180 in activating Rho GTPase Rac1. *Front Cell Infect Microbiol,* 1**,** 17.

BOLTON, D. J. 2015. Campylobacter virulence and survival factors. *Food Microbiol,* 48**,** 99-108.

BOMBERGER, J. M., MACEACHRAN, D. P., COUTERMARSH, B. A., YE, S., O'TOOLE, G. A. & STANTON, B. A. 2009. Long-distance delivery of bacterial virulence factors by Pseudomonas aeruginosa outer membrane vesicles. *PLoS Pathog,* 5**,** e1000382.

BOUWMAN, L. I., NIEWOLD, P. & VAN PUTTEN, J. P. 2013. Basolateral invasion and trafficking of Campylobacter jejuni in polarized epithelial cells. *PLoS One,* 8**,** e54759.

BRAS, A. M. & KETLEY, J. M. 1999. Transcellular translocation of Campylobacter jejuni across human polarised epithelial monolayers. *FEMS Microbiol Lett,* 179**,** 209-15.

BRENER, Z. 1973. Biology of Trypanosoma cruzi. *Annu Rev Microbiol,* 27**,** 347-82.

BUELOW, D. R., CHRISTENSEN, J. E., NEAL-MCKINNEY, J. M. & KONKEL, M. E. 2011. Campylobacter jejuni survival within human epithelial cells is enhanced by the secreted protein CiaI. *Mol Microbiol,* 80**,** 1296-312.

BURGOS-PORTUGAL, J. A., MITCHELL, H. M., CASTANO-RODRIGUEZ, N. & KAAKOUSH, N. O. 2014. The role of autophagy in the intracellular survival of Campylobacter concisus. *FEBS Open Bio,* 4**,** 301-9.

BUTZLER, J. P. & LAUWERS, S. 1979. Campylobacter fetus infection in children. *J Pediatr,* 94**,** 340-1.

BUTZLER, J. P. & SKIRROW, M. B. 1979a. Campylobacter enteritis. *Acta Paediatr Belg,* 32**,** 89-94.

BUTZLER, J. P. & SKIRROW, M. B. 1979b. Campylobacter enteritis. *Clin Gastroenterol,* 8**,** 737-65.

CALLICOTT, K. A., FRIETHRIKSDOTTIR, V., REIERSEN, J., LOWMAN, R., BISAILLON, J. R., GUNNARSSON, E., BERNDTSON, E., HIETT, K. L., NEEDLEMAN, D. S. & STERN,

N. J. 2006. Lack of evidence for vertical transmission of Campylobacter spp. in chickens. *Appl Environ Microbiol,* 72**,** 5794-8.

CARON, E. & HALL, A. 1998. Identification of two distinct mechanisms of phagocytosis controlled by different Rho GTPases. *Science,* 282**,** 1717-21.

CARRILLO, C. D., TABOADA, E., NASH, J. H., LANTHIER, P., KELLY, J., LAU, P. C., VERHULP, R., MYKYTCZUK, O., SY, J., FINDLAY, W. A., AMOAKO, K., GOMIS, S., WILLSON, P., AUSTIN, J. W., POTTER, A., BABIUK, L., ALLAN, B. & SZYMANSKI, C. M. 2004. Genome-wide expression analyses of Campylobacter jejuni NCTC11168 reveals coordinate regulation of motility and virulence by flhA. *J Biol Chem,* 279**,** 20327-38.

CASEY, E., FITZGERALD, E. & LUCEY, B. 2017. Towards understanding clinical campylobacter infection and its transmission: time for a different approach? *Br J Biomed Sci,* 74**,** 53-64.

CASPER, S. J. & HOLT, C. A. 1996. Expression of the green fluorescent protein-encoding gene from a tobacco mosaic virus-based vector. *Gene,* 173**,** 69-73.

CAWTHRAW, S. A., WASSENAAR, T. M., AYLING, R. & NEWELL, D. G. 1996. Increased colonization potential of Campylobacter jejuni strain 81116 after passage through chickens and its implication on the rate of transmission within flocks. *Epidemiol Infect,* 117**,** 213-5.

CDC 2015. <FoodNet-Annual-Report-2015-508c.pdf>.

CHALFIE, M., TU, Y., EUSKIRCHEN, G., WARD, W. W. & PRASHER, D. C. 1994. Green fluorescent protein as a marker for gene expression. *Science,* 263**,** 802-5.

CHAMPION, O. L., COOPER, I. A., JAMES, S. L., FORD, D., KARLYSHEV, A., WREN, B. W., DUFFIELD, M., OYSTON, P. C. & TITBALL, R. W. 2009. Galleria mellonella as an alternative infection model for Yersinia pseudotuberculosis. *Microbiology,* 155**,** 1516-22.

CHAMPION, O. L., KARLYSHEV, A. V., SENIOR, N. J., WOODWARD, M., LA RAGIONE, R., HOWARD, S. L., WREN, B. W. & TITBALL, R. W. 2010. Insect infection model for Campylobacter jejuni reveals that O-methyl phosphoramidate has insecticidal activity. *J Infect Dis,* 201**,** 776-82.

CHAMPION, O. L., VALDEZ, Y., THORSON, L., GUTTMAN, J. A., MENENDEZ, A., GAYNOR, E. C. & FINLAY, B. B. 2008. A murine intraperitoneal infection model reveals that host resistance to Campylobacter jejuni is Nramp1 dependent. *Microbes Infect,* 10**,** 922-7.

CHANG, C. & MILLER, J. F. 2006. Campylobacter jejuni colonization of mice with limited enteric flora. *Infect Immun,* 74**,** 5261-71.

CHATTERJEE, D. & CHAUDHURI, K. 2011. Association of cholera toxin with Vibrio cholerae outer membrane vesicles which are internalized by human intestinal epithelial cells. *FEBS Lett,* 585**,** 1357-62.

CHEN, M. L., GE, Z., FOX, J. G. & SCHAUER, D. B. 2006. Disruption of tight junctions and induction of proinflammatory cytokine responses in colonic epithelial cells by Campylobacter jejuni. *Infect Immun,* 74**,** 6581-9.

CLARK, L., MARTINEZ-ARGUDO, I., HUMPHREY, T. J. & JEPSON, M. A. 2009. GFP plasmid-induced defects in Salmonella invasion depend on plasmid architecture, not protein expression. *Microbiology,* 155**,** 461-7.

CODY, A. J., MCCARTHY, N. M., WIMALARATHNA, H. L., COLLES, F. M., CLARK, L., BOWLER, I. C., MAIDEN, M. C. & DINGLE, K. E. 2012. A longitudinal 6-year study of the molecular epidemiology of clinical campylobacter isolates in Oxfordshire, United kingdom. *J Clin Microbiol,* 50**,** 3193-201.

CODY, C. W., PRASHER, D. C., WESTLER, W. M., PRENDERGAST, F. G. & WARD, W. W. 1993. Chemical structure of the hexapeptide chromophore of the Aequorea green-fluorescent protein. *Biochemistry,* 32**,** 1212-8.

COLLINS, B. S. 2011. Gram-negative outer membrane vesicles in vaccine development. *Discov Med,* 12**,** 7-15.

CORCIONIVOSCHI, N., CLYNE, M., LYONS, A., ELMI, A., GUNDOGDU, O., WREN, B. W., DORRELL, N., KARLYSHEV, A. V. & BOURKE, B. 2009. Campylobacter jejuni cocultured with epithelial cells reduces surface capsular polysaccharide expression. *Infect Immun,* 77**,** 1959-67.

COSSART, P. 1995. Actin-based bacterial motility. *Curr Opin Cell Biol,* 7**,** 94-101.

COSSART, P. 2004. Bacterial invasion: a new strategy to dominate cytoskeleton plasticity. *Dev Cell,* 6**,** 314-5.

COSSART, P. & SANSONETTI, P. J. 2004. Bacterial invasion: the paradigms of enteroinvasive pathogens. *Science,* 304**,** 242-8.

COX, N. A., RICHARDSON, L. J., MAURER, J. J., BERRANG, M. E., FEDORKA-CRAY, P. J., BUHR, R. J., BYRD, J. A., LEE, M. D., HOFACRE, C. L., O'KANE, P. M., LAMMERDING, A. M., CLARK, A. G., THAYER, S. G. & DOYLE, M. P. 2012. Evidence for horizontal and vertical transmission in Campylobacter passage from hen to her progeny. *J Food Prot,* 75**,** 1896-902.

CUBITT, A. B., HEIM, R., ADAMS, S. R., BOYD, A. E., GROSS, L. A. & TSIEN, R. Y. 1995. Understanding, improving and using green fluorescent proteins. *Trends Biochem Sci,* 20**,** 448-55.

CUNNINGHAM, C. & LEE, C. H. 2003. Myocarditis related to Campylobacter jejuni infection: a case report. *BMC Infect Dis,* 3**,** 16.

DALBETH, N., LAUTERIO, T. J. & WOLFE, H. R. 2014. Mechanism of action of colchicine in the treatment of gout. *Clin Ther,* 36**,** 1465-79.

DASTI, J. I., TAREEN, A. M., LUGERT, R., ZAUTNER, A. E. & GROSS, U. 2010. Campylobacter jejuni: a brief overview on pathogenicity-associated factors and disease-mediating mechanisms. *Int J Med Microbiol,* 300**,** 205-11.

DAY, W. A., JR., SAJECKI, J. L., PITTS, T. M. & JOENS, L. A. 2000. Role of catalase in Campylobacter jejuni intracellular survival. *Infect Immun,* 68**,** 6337-45.

DE CESARE, A., SHELDON, B. W., SMITH, K. S. & JAYKUS, L. A. 2003. Survival and persistence of Campylobacter and Salmonella species under various organic loads on food contact surfaces. *J Food Prot,* 66**,** 1587-94.

DE MELO, M. A., GABBIANI, G. & PECHERE, J. C. 1989. Cellular events and intracellular survival of Campylobacter jejuni during infection of HEp-2 cells. *Infect Immun,* 57**,** 2214-22.

DE SOUZA SANTOS, M. & ORTH, K. 2014. Intracellular Vibrio parahaemolyticus escapes the vacuole and establishes a replicative niche in the cytosol of epithelial cells. *MBio,* 5**,** e01506-14.

DEKKER, N. 2000. Outer-membrane phospholipase A: known structure, unknown biological function. *Mol Microbiol,* 35**,** 711-7.

DERETIC, V., SINGH, S., MASTER, S., HARRIS, J., ROBERTS, E., KYEI, G., DAVIS, A., DE HARO, S., NAYLOR, J., LEE, H. H. & VERGNE, I. 2006. Mycobacterium tuberculosis inhibition of phagolysosome biogenesis and autophagy as a host defence mechanism. *Cell Microbiol,* 8**,** 719-27.

DINGLE, K. E., VAN DEN BRAAK, N., COLLES, F. M., PRICE, L. J., WOODWARD, D. L., RODGERS, F. G., ENDTZ, H. P., VAN BELKUM, A. & MAIDEN, M. C. 2001. Sequence typing confirms that Campylobacter jejuni strains associated with Guillain-Barre and Miller-Fisher syndromes are of diverse genetic lineage, serotype, and flagella type. *J Clin Microbiol,* 39**,** 3346-9.

DORMAN, C. J. 2013. Co-operative roles for DNA supercoiling and nucleoid-associated proteins in the regulation of bacterial transcription. *Biochem Soc Trans,* 41**,** 542-7.

DORRELL, N., MANGAN, J. A., LAING, K. G., HINDS, J., LINTON, D., AL-GHUSEIN, H., BARRELL, B. G., PARKHILL, J., STOKER, N. G., KARLYSHEV, A. V., BUTCHER, P. D. & WREN, B. W. 2001. Whole genome comparison of Campylobacter jejuni human isolates using a low-cost microarray reveals extensive genetic diversity. *Genome Res,* 11**,** 1706-15.

DOYLE, M. P. & ROMAN, D. J. 1982a. Prevalence and survival of Campylobacter jejuni in unpasteurized milk. *Appl Environ Microbiol,* 44**,** 1154-8.

DOYLE, M. P. & ROMAN, D. J. 1982b. Response of Campylobacter jejuni to sodium chloride. *Appl Environ Microbiol,* 43**,** 561-5.

DUONG, T. & KONKEL, M. E. 2009. Comparative studies of Campylobacter jejuni genomic diversity reveal the importance of core and dispensable genes in the biology of this enigmatic food-borne pathogen. *Curr Opin Biotechnol,* 20**,** 158-65.

EBI 2018. Institute EB. Genomes Pages - Bacteria 2018 [cited 2018 05 February]. Available from: https://www.ebi.ac.uk/genomes/bacteria.html.

EDDY, J. L., GIELDA, L. M., CAULFIELD, A. J., RANGEL, S. M. & LATHEM, W. W. 2014. Production of outer membrane vesicles by the plague pathogen Yersinia pestis. *PLoS One,* 9**,** e107002.

EFSA 2011. Scientific Opinion onCampylobacterin broiler meat production: control options and performance objectives and/or targets at different stages of the food chain. *EFSA Journal,* 9.

EFSA 2015. The European Union summary report on trends and sources of zoonoses, zoonotic agents and food-borne outbreaks in 2013. *EFSA Journal,* 13.

ELHENAWY, W., BORDING-JORGENSEN, M., VALGUARNERA, E., HAURAT, M. F., WINE, E. & FELDMAN, M. F. 2016. LPS Remodeling Triggers Formation of Outer Membrane Vesicles in Salmonella. *MBio,* 7.

ELLIS, T. N. & KUEHN, M. J. 2010. Virulence and immunomodulatory roles of bacterial outer membrane vesicles. *Microbiol Mol Biol Rev,* 74**,** 81-94.

ELMI, A., NASHER, F., JAGATIA, H., GUNDOGDU, O., BAJAJ-ELLIOTT, M., WREN, B. & DORRELL, N. 2016. Campylobacter jejuni outer membrane vesicle-associated proteolytic activity promotes bacterial invasion by mediating cleavage of intestinal epithelial cell E-cadherin and occludin. *Cell Microbiol,* 18**,** 561-72.

ELMI, A., WATSON, E., SANDU, P., GUNDOGDU, O., MILLS, D. C., INGLIS, N. F., MANSON, E., IMRIE, L., BAJAJ-ELLIOTT, M., WREN, B. W., SMITH, D. G. & DORRELL, N. 2012. Campylobacter jejuni outer membrane vesicles play an important role in bacterial interactions with human intestinal epithelial cells. *Infect Immun,* 80**,** 4089-98.

ELSINGHORST, E. A., BARON, L. S. & KOPECKO, D. J. 1989. Penetration of human intestinal epithelial cells by Salmonella: molecular cloning and expression of Salmonella typhi invasion determinants in Escherichia coli. *Proc Natl Acad Sci U S A,* 86**,** 5173-7.

ERRAMPALLI, D., LEUNG, K., CASSIDY, M. B., KOSTRZYNSKA, M., BLEARS, M., LEE, H. & TREVORS, J. T. 1999. Applications of the green fluorescent protein as a molecular marker in environmental microorganisms. *J Microbiol Methods,* 35**,** 187-99.

ESSON, D., MATHER, A. E., SCANLAN, E., GUPTA, S., DE VRIES, S. P., BAILEY, D., HARRIS, S. R., MCKINLEY, T. J., MERIC, G., BERRY, S. K., MASTROENI, P., SHEPPARD, S. K., CHRISTIE, G., THOMSON, N. R., PARKHILL, J., MASKELL, D. J.

& GRANT, A. J. 2016. Genomic variations leading to alterations in cell morphology of Campylobacter spp. *Sci Rep,* 6**,** 38303.

EUCKER, T. P. & KONKEL, M. E. 2012. The cooperative action of bacterial fibronectin-binding proteins and secreted proteins promote maximal Campylobacter jejuni invasion of host cells by stimulating membrane ruffling. *Cell Microbiol,* 14**,** 226-38.

EVEREST, P., KETLEY, J., HARDY, S., DOUCE, G., KHAN, S., SHEA, J., HOLDEN, D., MASKELL, D. & DOUGAN, G. 1999. Evaluation of Salmonella typhimurium mutants in a model of experimental gastroenteritis. *Infect Immun,* 67**,** 2815-21.

EVEREST, P. H., GOOSSENS, H., BUTZLER, J. P., LLOYD, D., KNUTTON, S., KETLEY, J. M. & WILLIAMS, P. H. 1992. Differentiated Caco-2 cells as a model for enteric invasion by Campylobacter jejuni and C. coli. *J Med Microbiol,* 37**,** 319-25.

FAUCHERE, J. L., ROSENAU, A., VERON, M., MOYEN, E. N., RICHARD, S. & PFISTER, A. 1986. Association with HeLa cells of Campylobacter jejuni and Campylobacter coli isolated from human feces. *Infect Immun,* 54**,** 283-7.

FERNANDES, A. M., BALASEGARAM, S., WILLIS, C., WIMALARATHNA, H. M., MAIDEN, M. C. & MCCARTHY, N. D. 2015. Partial Failure of Milk Pasteurization as a Risk for the Transmission of Campylobacter From Cattle to Humans. *Clin Infect Dis,* 61**,** 903-9.

FERNANDEZ, H., VERGARA, M. & TAPIA, F. 1985. Dessication resistance in thermotolerant Campylobacter species. *Infection,* 13**,** 197.

FIELD, L. H., HEADLEY, V. L., UNDERWOOD, J. L., PAYNE, S. M. & BERRY, L. J. 1986. The chicken embryo as a model for campylobacter invasion: comparative virulence of human isolates of Campylobacter jejuni and Campylobacter coli. *Infect Immun,* 54**,** 118-25.

FINLAY, B. B. & FALKOW, S. 1988. Comparison of the invasion strategies used by Salmonella cholerae-suis, Shigella flexneri and Yersinia enterocolitica to enter cultured animal cells: endosome acidification is not required for bacterial invasion or intracellular replication. *Biochimie,* 70**,** 1089-99.

FINLAY, B. B. & FALKOW, S. 1990. Salmonella interactions with polarized human intestinal Caco-2 epithelial cells. *J Infect Dis,* 162**,** 1096-106.

FINLAY, B. B., GUMBINER, B. & FALKOW, S. 1988. Penetration of Salmonella through a polarized Madin-Darby canine kidney epithelial cell monolayer. *J Cell Biol,* 107**,** 221-30.

FIOCCA, R., NECCHI, V., SOMMI, P., RICCI, V., TELFORD, J., COVER, T. L. & SOLCIA, E. 1999. Release of Helicobacter pylori vacuolating cytotoxin by both a specific secretion pathway and budding of outer membrane vesicles. Uptake of released toxin and vesicles by gastric epithelium. *J Pathol,* 188**,** 220-6.

FLANAGAN, R. C., NEAL-MCKINNEY, J. M., DHILLON, A. S., MILLER, W. G. & KONKEL, M. E. 2009. Examination of Campylobacter jejuni putative adhesins leads to the identification of a new protein, designated FlpA, required for chicken colonization. *Infect Immun,* 77**,** 2399-407.

FOX, J. G., ROGERS, A. B., WHARY, M. T., GE, Z., TAYLOR, N. S., XU, S., HORWITZ, B. H. & ERDMAN, S. E. 2004. Gastroenteritis in NF-kappaB-deficient mice is produced with wild-type Camplyobacter jejuni but not with C. jejuni lacking cytolethal distending toxin despite persistent colonization with both strains. *Infect Immun,* 72**,** 1116-25.

FRIIS, C., WASSENAAR, T. M., JAVED, M. A., SNIPEN, L., LAGESEN, K., HALLIN, P. F., NEWELL, D. G., TOSZEGHY, M., RIDLEY, A., MANNING, G. & USSERY, D. W.

2010. Genomic characterization of Campylobacter jejuni strain M1. *PLoS One,* 5**,** e12253.
FRIIS, L. M., KEELAN, M. & TAYLOR, D. E. 2009. Campylobacter jejuni drives MyD88-independent interleukin-6 secretion via Toll-like receptor 2. *Infect Immun,* 77**,** 1553-60.
FRIIS, L. M., PIN, C., PEARSON, B. M. & WELLS, J. M. 2005. In vitro cell culture methods for investigating Campylobacter invasion mechanisms. *J Microbiol Methods,* 61**,** 145-60.
FSA 2016. <campylobacter-prog-review-nov2016.pdf>.
GALAN, J. E. 2001. Salmonella interactions with host cells: type III secretion at work. *Annu Rev Cell Dev Biol,* 17**,** 53-86.
GASKIN, D. J., REUTER, M., SHEARER, N., MULHOLLAND, F., PEARSON, B. M. & VAN VLIET, A. H. 2009. Genomics of thermophilic campylobacter species. *Genome Dyn,* 6**,** 91-109.
GATFIELD, J. & PIETERS, J. 2000. Essential role for cholesterol in entry of mycobacteria into macrophages. *Science,* 288**,** 1647-50.
GAYNOR, E. C., CAWTHRAW, S., MANNING, G., MACKICHAN, J. K., FALKOW, S. & NEWELL, D. G. 2004. The genome-sequenced variant of Campylobacter jejuni NCTC 11168 and the original clonal clinical isolate differ markedly in colonization, gene expression, and virulence-associated phenotypes. *J Bacteriol,* 186**,** 503-17.
GERDES, H. H. & KAETHER, C. 1996. Green fluorescent protein: applications in cell biology. *FEBS Lett,* 389**,** 44-7.
GILBREATH, J. J., CODY, W. L., MERRELL, D. S. & HENDRIXSON, D. R. 2011. Change is good: variations in common biological mechanisms in the epsilonproteobacterial genera Campylobacter and Helicobacter. *Microbiol Mol Biol Rev,* 75**,** 84-132.
GODLEWSKA, R., KUCZKOWSKI, M., WYSZYNSKA, A., KLIM, J., DERLATKA, K., WOZNIAK-BIEL, A. & JAGUSZTYN-KRYNICKA, E. K. 2016. Evaluation of a protective effect of in ovo delivered Campylobacter jejuni OMVs. *Appl Microbiol Biotechnol,* 100**,** 8855-64.
GOEBEL, W. & KUHN, M. 2000. Bacterial replication in the host cell cytosol. *Curr Opin Microbiol,* 3**,** 49-53.
GOLZ, G., ROSNER, B., HOFREUTER, D., JOSENHANS, C., KREIENBROCK, L., LOWENSTEIN, A., SCHIELKE, A., STARK, K., SUERBAUM, S., WIELER, L. H. & ALTER, T. 2014. Relevance of Campylobacter to public health--the need for a One Health approach. *Int J Med Microbiol,* 304**,** 817-23.
GORMLEY, F. J., BAILEY, R. A., WATSON, K. A., MCADAM, J., AVENDANO, S., STANLEY, W. A. & KOERHUIS, A. N. 2014. Campylobacter colonization and proliferation in the broiler chicken upon natural field challenge is not affected by the bird growth rate or breed. *Appl Environ Microbiol,* 80**,** 6733-8.
GRANT, C. C., KONKEL, M. E., CIEPLAK, W., JR. & TOMPKINS, L. S. 1993. Role of flagella in adherence, internalization, and translocation of Campylobacter jejuni in nonpolarized and polarized epithelial cell cultures. *Infect Immun,* 61**,** 1764-71.
GRANT, K. A., BELANDIA, I. U., DEKKER, N., RICHARDSON, P. T. & PARK, S. F. 1997. Molecular characterization of pldA, the structural gene for a phospholipase A from Campylobacter coli, and its contribution to cell-associated hemolysis. *Infect Immun,* 65**,** 1172-80.
GRANT, K. A. & PARK, S. F. 1995. Molecular characterization of katA from Campylobacter jejuni and generation of a catalase-deficient mutant of

Campylobacter coli by interspecific allelic exchange. *Microbiology,* 141 (Pt 6)**,** 1369-76.

GREGSON, N. A., REES, J. H. & HUGHES, R. A. 1997. Reactivity of serum IgG anti-GM1 ganglioside antibodies with the lipopolysaccharide fractions of Campylobacter jejuni isolates from patients with Guillain-Barre syndrome (GBS). *J Neuroimmunol,* 73**,** 28-36.

GUERRY, P. 2007. Campylobacter flagella: not just for motility. *Trends Microbiol,* 15**,** 456-61.

GUERRY, P., ALM, R. A., POWER, M. E., LOGAN, S. M. & TRUST, T. J. 1991. Role of two flagellin genes in Campylobacter motility. *J Bacteriol,* 173**,** 4757-64.

GUERRY, P., EWING, C. P., HICKEY, T. E., PRENDERGAST, M. M. & MORAN, A. P. 2000. Sialylation of lipooligosaccharide cores affects immunogenicity and serum resistance of Campylobacter jejuni. *Infect Immun,* 68**,** 6656-62.

GUNDOGDU, O., BENTLEY, S. D., HOLDEN, M. T., PARKHILL, J., DORRELL, N. & WREN, B. W. 2007. Re-annotation and re-analysis of the Campylobacter jejuni NCTC11168 genome sequence. *BMC Genomics,* 8**,** 162.

GUNDOGDU, O., DA SILVA, D. T., MOHAMMAD, B., ELMI, A., MILLS, D. C., WREN, B. W. & DORRELL, N. 2015. The Campylobacter jejuni MarR-like transcriptional regulators RrpA and RrpB both influence bacterial responses to oxidative and aerobic stresses. *Front Microbiol,* 6**,** 724.

GUNDOGDU, O., DA SILVA, D. T., MOHAMMAD, B., ELMI, A., WREN, B. W., VAN VLIET, A. H. & DORRELL, N. 2016. The Campylobacter jejuni Oxidative Stress Regulator RrpB Is Associated with a Genomic Hypervariable Region and Altered Oxidative Stress Resistance. *Front Microbiol,* 7**,** 2117.

GUNDOGDU, O., MILLS, D. C., ELMI, A., MARTIN, M. J., WREN, B. W. & DORRELL, N. 2011. The Campylobacter jejuni transcriptional regulator Cj1556 plays a role in the oxidative and aerobic stress response and is important for bacterial survival in vivo. *J Bacteriol,* 193**,** 4238-49.

HADDOCK, G., MULLIN, M., MACCALLUM, A., SHERRY, A., TETLEY, L., WATSON, E., DAGLEISH, M., SMITH, D. G. & EVEREST, P. 2010. Campylobacter jejuni 81-176 forms distinct microcolonies on in vitro-infected human small intestinal tissue prior to biofilm formation. *Microbiology,* 156**,** 3079-84.

HALL, A. 1990. The cellular functions of small GTP-binding proteins. *Science,* 249**,** 635-40.

HALL, A. 1999. Signal transduction pathways regulated by the Rho family of small GTPases. *Br J Cancer,* 80 Suppl 1**,** 25-7.

HALL, A. & NOBES, C. D. 2000. Rho GTPases: molecular switches that control the organization and dynamics of the actin cytoskeleton. *Philos Trans R Soc Lond B Biol Sci,* 355**,** 965-70.

HAMILTON, J. P., XIE, G., RAUFMAN, J. P., HOGAN, S., GRIFFIN, T. L., PACKARD, C. A., CHATFIELD, D. A., HAGEY, L. R., STEINBACH, J. H. & HOFMANN, A. F. 2007. Human cecal bile acids: concentration and spectrum. *Am J Physiol Gastrointest Liver Physiol,* 293**,** G256-63.

HANEL, I., BORRMANN, E., MULLER, J., MULLER, W., PAULY, B., LIEBLER-TENORIO, E. M. & SCHULZE, F. 2009. Genomic and phenotypic changes of Campylobacter jejuni strains after passage of the chicken gut. *Vet Microbiol,* 136**,** 121-9.

HANNU, T., MATTILA, L., RAUTELIN, H., PELKONEN, P., LAHDENNE, P., SIITONEN, A. & LEIRISALO-REPO, M. 2002. Campylobacter-triggered reactive arthritis: a population-based study. *Rheumatology (Oxford),* 41**,** 312-8.

HARDING, C. R., SCHROEDER, G. N., COLLINS, J. W. & FRANKEL, G. 2013. Use of Galleria mellonella as a model organism to study Legionella pneumophila infection. *J Vis Exp*, e50964.

HARDING, C. R., SCHROEDER, G. N., REYNOLDS, S., KOSTA, A., COLLINS, J. W., MOUSNIER, A. & FRANKEL, G. 2012. Legionella pneumophila pathogenesis in the Galleria mellonella infection model. *Infect Immun,* 80**,** 2780-90.

HARDT, W. D., CHEN, L. M., SCHUEBEL, K. E., BUSTELO, X. R. & GALAN, J. E. 1998. S. typhimurium encodes an activator of Rho GTPases that induces membrane ruffling and nuclear responses in host cells. *Cell,* 93**,** 815-26.

HARVEY, P., BATTLE, T. & LEACH, S. 1999. Different invasion phenotypes of Campylobacter isolates in Caco-2 cell monolayers. *J Med Microbiol,* 48**,** 461-9.

HARVEY, P. & LEACH, S. 1998. Analysis of coccal cell formation by Campylobacter jejuni using continuous culture techniques, and the importance of oxidative stress. *J Appl Microbiol,* 85**,** 398-404.

HAWKINS, P. T., EGUINOA, A., QIU, R. G., STOKOE, D., COOKE, F. T., WALTERS, R., WENNSTROM, S., CLAESSON-WELSH, L., EVANS, T., SYMONS, M. & ET AL. 1995. PDGF stimulates an increase in GTP-Rac via activation of phosphoinositide 3-kinase. *Curr Biol,* 5**,** 393-403.

HEIM, R., PRASHER, D. C. & TSIEN, R. Y. 1994. Wavelength mutations and posttranslational autoxidation of green fluorescent protein. *Proc Natl Acad Sci U S A,* 91**,** 12501-4.

HEITMUELLER, M., BILLION, A., DOBRINDT, U., VILCINSKAS, A. & MUKHERJEE, K. 2017. Epigenetic Mechanisms Regulate Innate Immunity against Uropathogenic and Commensal-Like Escherichia coli in the Surrogate Insect Model Galleria mellonella. *Infect Immun,* 85.

HENDERSON, B., NAIR, S., PALLAS, J. & WILLIAMS, M. A. 2011. Fibronectin: a multidomain host adhesin targeted by bacterial fibronectin-binding proteins. *FEMS Microbiol Rev,* 35**,** 147-200.

HENDRIXSON, D. R. 2006. A phase-variable mechanism controlling the Campylobacter jejuni FlgR response regulator influences commensalism. *Mol Microbiol,* 61**,** 1646-59.

HENDRIXSON, D. R. 2008. Restoration of flagellar biosynthesis by varied mutational events in Campylobacter jejuni. *Mol Microbiol,* 70**,** 519-36.

HESSULF, F., LJUNGBERG, J., JOHANSSON, P. A., LINDGREN, M. & ENGDAHL, J. 2016. Campylobacter jejuni-associated perimyocarditis: two case reports and review of the literature. *BMC Infect Dis,* 16**,** 289.

HICKEY, T. E., MAJAM, G. & GUERRY, P. 2005. Intracellular survival of Campylobacter jejuni in human monocytic cells and induction of apoptotic death by cytholethal distending toxin. *Infect Immun,* 73**,** 5194-7.

HICKEY, T. E., MCVEIGH, A. L., SCOTT, D. A., MICHIELUTTI, R. E., BIXBY, A., CARROLL, S. A., BOURGEOIS, A. L. & GUERRY, P. 2000. Campylobacter jejuni cytolethal distending toxin mediates release of interleukin-8 from intestinal epithelial cells. *Infect Immun,* 68**,** 6535-41.

HIDALGO, I. J., RAUB, T. J. & BORCHARDT, R. T. 1989. Characterization of the human colon carcinoma cell line (Caco-2) as a model system for intestinal epithelial permeability. *Gastroenterology,* 96**,** 736-49.

HIRAYAMA, J., SEKIZUKA, T., TAZUMI, A., TANEIKE, I., MOORE, J. E., MILLAR, B. C. & MATSUDA, M. 2009. Structural analysis of the full-length gene encoding a fibronectin-binding-like protein (CadF) and its adjacent genetic loci within Campylobacter lari. *BMC Microbiol,* 9**,** 192.

HOBBIE, S., CHEN, L. M., DAVIS, R. J. & GALAN, J. E. 1997. Involvement of mitogen-activated protein kinase pathways in the nuclear responses and cytokine production induced by Salmonella typhimurium in cultured intestinal epithelial cells. *J Immunol,* 159**,** 5550-9.
HOFFMAN, P. S. & GOODMAN, T. G. 1982. Respiratory physiology and energy conservation efficiency of Campylobacter jejuni. *J Bacteriol,* 150**,** 319-26.
HOFFMANN, J. A. 1995. Innate immunity of insects. *Curr Opin Immunol,* 7**,** 4-10.
HOFREUTER, D., NOVIK, V. & GALAN, J. E. 2008. Metabolic diversity in Campylobacter jejuni enhances specific tissue colonization. *Cell Host Microbe,* 4**,** 425-33.
HORSTMAN, A. L. & KUEHN, M. J. 2002. Bacterial surface association of heat-labile enterotoxin through lipopolysaccharide after secretion via the general secretory pathway. *J Biol Chem,* 277**,** 32538-45.
HU, L. & HICKEY, T. E. 2005. Campylobacter jejuni induces secretion of proinflammatory chemokines from human intestinal epithelial cells. *Infect Immun,* 73**,** 4437-40.
HU, L. & KOPECKO, D. J. 1999. Campylobacter jejuni 81-176 associates with microtubules and dynein during invasion of human intestinal cells. *Infect Immun,* 67**,** 4171-82.
HU, L., MCDANIEL, J. P. & KOPECKO, D. J. 2006. Signal transduction events involved in human epithelial cell invasion by Campylobacter jejuni 81-176. *Microb Pathog,* 40**,** 91-100.
HU, L., TALL, B. D., CURTIS, S. K. & KOPECKO, D. J. 2008. Enhanced microscopic definition of Campylobacter jejuni 81-176 adherence to, invasion of, translocation across, and exocytosis from polarized human intestinal Caco-2 cells. *Infect Immun,* 76**,** 5294-304.
HUMPHREY, C. D., MONTAG, D. M. & PITTMAN, F. E. 1986. Morphologic observations of experimental Campylobacter jejuni infection in the hamster intestinal tract. *Am J Pathol,* 122**,** 152-9.
HUMPHREY, S., CHALONER, G., KEMMETT, K., DAVIDSON, N., WILLIAMS, N., KIPAR, A., HUMPHREY, T. & WIGLEY, P. 2014. Campylobacter jejuni is not merely a commensal in commercial broiler chickens and affects bird welfare. *MBio,* 5**,** e01364-14.
HURLEY, B. P. & MCCORMICK, B. A. 2003. Translating tissue culture results into animal models: the case of Salmonella typhimurium. *Trends Microbiol,* 11**,** 562-9.
HURLEY, B. P., PIRZAI, W., EATON, A. D., HARPER, M., ROPER, J., ZIMMERMANN, C., LADICS, G. S., LAYTON, R. J. & DELANEY, B. 2016. An experimental platform using human intestinal epithelial cell lines to differentiate between hazardous and non-hazardous proteins. *Food Chem Toxicol,* 92**,** 75-87.
ISLAM, A., RAGHUPATHY, R. & ALBERT, M. J. 2010. Recombinant PorA, the major outer membrane protein of Campylobacter jejuni, provides heterologous protection in an adult mouse intestinal colonization model. *Clin Vaccine Immunol,* 17**,** 1666-71.
JAN, A. T. 2017. Outer Membrane Vesicles (OMVs) of Gram-negative Bacteria: A Perspective Update. *Front Microbiol,* 8**,** 1053.
JANDER, G., RAHME, L. G. & AUSUBEL, F. M. 2000. Positive correlation between virulence of Pseudomonas aeruginosa mutants in mice and insects. *J Bacteriol,* 182**,** 3843-5.
JANG, K. S., SWEREDOSKI, M. J., GRAHAM, R. L., HESS, S. & CLEMONS, W. M., JR. 2014. Comprehensive proteomic profiling of outer membrane vesicles from Campylobacter jejuni. *J Proteomics,* 98**,** 90-8.

JERVIS, A. J., BUTLER, J. A., WREN, B. W. & LINTON, D. 2015. Chromosomal integration vectors allowing flexible expression of foreign genes in Campylobacter jejuni. *BMC Microbiol,* 15**,** 230.

JIN, S., JOE, A., LYNETT, J., HANI, E. K., SHERMAN, P. & CHAN, V. L. 2001. JlpA, a novel surface-exposed lipoprotein specific to Campylobacter jejuni, mediates adherence to host epithelial cells. *Mol Microbiol,* 39**,** 1225-36.

JONES, D. M., SUTCLIFFE, E. M. & CURRY, A. 1991. Recovery of viable but non-culturable Campylobacter jejuni. *J Gen Microbiol,* 137**,** 2477-82.

JONES, M. A., MARSTON, K. L., WOODALL, C. A., MASKELL, D. J., LINTON, D., KARLYSHEV, A. V., DORRELL, N., WREN, B. W. & BARROW, P. A. 2004. Adaptation of Campylobacter jejuni NCTC11168 to high-level colonization of the avian gastrointestinal tract. *Infect Immun,* 72**,** 3769-76.

JOSLIN, S. N. & HENDRIXSON, D. R. 2009. Activation of the Campylobacter jejuni FlgSR two-component system is linked to the flagellar export apparatus. *J Bacteriol,* 191**,** 2656-67.

KADIOGLU, A., SHARPE, J. A., LAZOU, I., SVANBORG, C., OCKLEFORD, C., MITCHELL, T. J. & ANDREW, P. W. 2001. Use of green fluorescent protein in visualisation of pneumococcal invasion of broncho-epithelial cells in vivo. *FEMS Microbiol Lett,* 194**,** 105-10.

KAHANA, J. A., SCHNAPP, B. J. & SILVER, P. A. 1995. Kinetics of spindle pole body separation in budding yeast. *Proc Natl Acad Sci U S A,* 92**,** 9707-11.

KALE, A., PHANSOPA, C., SUWANNACHART, C., CRAVEN, C. J., RAFFERTY, J. B. & KELLY, D. J. 2011. The virulence factor PEB4 (Cj0596) and the periplasmic protein Cj1289 are two structurally related SurA-like chaperones in the human pathogen Campylobacter jejuni. *J Biol Chem,* 286**,** 21254-65.

KALYANARAMAN, B. & ZIELONKA, J. 2017. Green fluorescent proteins induce oxidative stress in cells: A worrisome new wrinkle in the application of the GFP reporter system to biological systems? *Redox Biol,* 12**,** 755-757.

KARLYSHEV, A. V., LINTON, D., GREGSON, N. A. & WREN, B. W. 2002. A novel paralogous gene family involved in phase-variable flagella-mediated motility in Campylobacter jejuni. *Microbiology,* 148**,** 473-80.

KARLYSHEV, A. V. & WREN, B. W. 2005. Development and application of an insertional system for gene delivery and expression in Campylobacter jejuni. *Appl Environ Microbiol,* 71**,** 4004-13.

KAWAI, F., PAEK, S., CHOI, K. J., PROUTY, M., KANIPES, M. I., GUERRY, P. & YEO, H. J. 2012. Crystal structure of JlpA, a surface-exposed lipoprotein adhesin of Campylobacter jejuni. *J Struct Biol,* 177**,** 583-8.

KELLEY, L. A., MEZULIS, S., YATES, C. M., WASS, M. N. & STERNBERG, M. J. 2015. The Phyre2 web portal for protein modeling, prediction and analysis. *Nat Protoc,* 10**,** 845-58.

KELLY, D. J. 2001. The physiology and metabolism of Campylobacter jejuni and Helicobacter pylori. *Symp Ser Soc Appl Microbiol***,** 16S-24S.

KETLEY, J. M. 1997. Pathogenesis of enteric infection by Campylobacter. *Microbiology,* 143 (Pt 1)**,** 5-21.

KIEHLBAUCH, J. A., ALBACH, R. A., BAUM, L. L. & CHANG, K. P. 1985. Phagocytosis of Campylobacter jejuni and its intracellular survival in mononuclear phagocytes. *Infect Immun,* 48**,** 446-51.

KIST, M. 1986. [Who discovered Campylobacter jejuni/coli? A review of hitherto disregarded literature]. *Zentralbl Bakteriol Mikrobiol Hyg A,* 261**,** 177-86.

KLIMENTOVA, J. & STULIK, J. 2015. Methods of isolation and purification of outer membrane vesicles from gram-negative bacteria. *Microbiol Res,* 170C**,** 1-9.

KNODLER, L. A. & STEELE-MORTIMER, O. 2003. Taking possession: biogenesis of the Salmonella-containing vacuole. *Traffic,* 4**,** 587-99.

KOCHAN, T. J., SOMERS, M. J., KAISER, A. M., SHOSHIEV, M. S., HAGAN, A. K., HASTIE, J. L., GIORDANO, N. P., SMITH, A. D., SCHUBERT, A. M., CARLSON, P. E., JR. & HANNA, P. C. 2017. Intestinal calcium and bile salts facilitate germination of Clostridium difficile spores. *PLoS Pathog,* 13**,** e1006443.

KOEPPEN, K., HAMPTON, T. H., JAREK, M., SCHARFE, M., GERBER, S. A., MIELCARZ, D. W., DEMERS, E. G., DOLBEN, E. L., HAMMOND, J. H., HOGAN, D. A. & STANTON, B. A. 2016. A Novel Mechanism of Host-Pathogen Interaction through sRNA in Bacterial Outer Membrane Vesicles. *PLoS Pathog,* 12**,** e1005672.

KOHLER, H., RODRIGUES, S. P. & MCCORMICK, B. A. 2002. Shigella flexneri Interactions with the Basolateral Membrane Domain of Polarized Model Intestinal Epithelium: Role of Lipopolysaccharide in Cell Invasion and in Activation of the Mitogen-Activated Protein Kinase ERK. *Infect Immun,* 70**,** 1150-8.

KOHLER, H., SAKAGUCHI, T., HURLEY, B. P., KASE, B. A., REINECKER, H. C. & MCCORMICK, B. A. 2007. Salmonella enterica serovar Typhimurium regulates intercellular junction proteins and facilitates transepithelial neutrophil and bacterial passage. *Am J Physiol Gastrointest Liver Physiol,* 293**,** G178-87.

KONKEL, M. E., CHRISTENSEN, J. E., KEECH, A. M., MONTEVILLE, M. R., KLENA, J. D. & GARVIS, S. G. 2005. Identification of a fibronectin-binding domain within the Campylobacter jejuni CadF protein. *Mol Microbiol,* 57**,** 1022-35.

KONKEL, M. E. & CIEPLAK, W., JR. 1992. Altered synthetic response of Campylobacter jejuni to cocultivation with human epithelial cells is associated with enhanced internalization. *Infect Immun,* 60**,** 4945-9.

KONKEL, M. E., CORWIN, M. D., JOENS, L. A. & CIEPLAK, W. 1992a. Factors that influence the interaction of Campylobacter jejuni with cultured mammalian cells. *J Med Microbiol,* 37**,** 30-7.

KONKEL, M. E., GARVIS, S. G., TIPTON, S. L., ANDERSON, D. E., JR. & CIEPLAK, W., JR. 1997. Identification and molecular cloning of a gene encoding a fibronectin-binding protein (CadF) from Campylobacter jejuni. *Mol Microbiol,* 24**,** 953-63.

KONKEL, M. E., GRAY, S. A., KIM, B. J., GARVIS, S. G. & YOON, J. 1999a. Identification of the enteropathogens Campylobacter jejuni and Campylobacter coli based on the cadF virulence gene and its product. *J Clin Microbiol,* 37**,** 510-7.

KONKEL, M. E., HAYES, S. F., JOENS, L. A. & CIEPLAK, W., JR. 1992b. Characteristics of the internalization and intracellular survival of Campylobacter jejuni in human epithelial cell cultures. *Microb Pathog,* 13**,** 357-70.

KONKEL, M. E. & JOENS, L. A. 1989. Adhesion to and invasion of HEp-2 cells by Campylobacter spp. *Infect Immun,* 57**,** 2984-90.

KONKEL, M. E., KIM, B. J., RIVERA-AMILL, V. & GARVIS, S. G. 1999b. Bacterial secreted proteins are required for the internaliztion of Campylobacter jejuni into cultured mammalian cells. *Mol Microbiol,* 32**,** 691-701.

KONKEL, M. E., KIM, B. J., RIVERA-AMILL, V. & GARVIS, S. G. 1999c. Identification of proteins required for the internalization of Campylobacter jejuni into cultured mammalian cells. *Adv Exp Med Biol,* 473**,** 215-24.

KONKEL, M. E., KLENA, J. D., RIVERA-AMILL, V., MONTEVILLE, M. R., BISWAS, D., RAPHAEL, B. & MICKELSON, J. 2004. Secretion of virulence proteins from Campylobacter jejuni is dependent on a functional flagellar export apparatus. *J Bacteriol,* 186**,** 3296-303.

KONKEL, M. E., LARSON, C. L. & FLANAGAN, R. C. 2010. Campylobacter jejuni FlpA binds fibronectin and is required for maximal host cell adherence. *J Bacteriol,* 192**,** 68-76.

KONKEL, M. E., MEAD, D. J., HAYES, S. F. & CIEPLAK, W., JR. 1992c. Translocation of Campylobacter jejuni across human polarized epithelial cell monolayer cultures. *J Infect Dis,* 166**,** 308-15.

KONKEL, M. E. & MIXTER, P. F. 2000. Flow cytometric detection of host cell apoptosis induced by bacterial infection. *Methods Cell Sci,* 22**,** 209-15.

KONKEL, M. E., SAMUELSON, D. R., EUCKER, T. P., SHELDEN, E. A. & O'LOUGHLIN, J. L. 2013. Invasion of epithelial cells by Campylobacter jejuni is independent of caveolae. *Cell Commun Signal,* 11**,** 100.

KOPECKO, D. J., HU, L. & ZAAL, K. J. 2001. Campylobacter jejuni--microtubule-dependent invasion. *Trends Microbiol,* 9**,** 389-96.

KORLATH, J. A., OSTERHOLM, M. T., JUDY, L. A., FORFANG, J. C. & ROBINSON, R. A. 1985. A point-source outbreak of campylobacteriosis associated with consumption of raw milk. *J Infect Dis,* 152**,** 592-6.

KRAUSE-GRUSZCZYNSKA, M., BOEHM, M., ROHDE, M., TEGTMEYER, N., TAKAHASHI, S., BUDAY, L., OYARZABAL, O. A. & BACKERT, S. 2011. The signaling pathway of Campylobacter jejuni-induced Cdc42 activation: Role of fibronectin, integrin beta1, tyrosine kinases and guanine exchange factor Vav2. *Cell Commun Signal,* 9**,** 32.

KRAUSE-GRUSZCZYNSKA, M., ROHDE, M., HARTIG, R., GENTH, H., SCHMIDT, G., KEO, T., KONIG, W., MILLER, W. G., KONKEL, M. E. & BACKERT, S. 2007a. Role of the small Rho GTPases Rac1 and Cdc42 in host cell invasion of Campylobacter jejuni. *Cell Microbiol,* 9**,** 2431-44.

KRAUSE-GRUSZCZYNSKA, M., VAN ALPHEN, L. B., OYARZABAL, O. A., ALTER, T., HANEL, I., SCHLIEPHAKE, A., KONIG, W., VAN PUTTEN, J. P., KONKEL, M. E. & BACKERT, S. 2007b. Expression patterns and role of the CadF protein in Campylobacter jejuni and Campylobacter coli. *FEMS Microbiol Lett,* 274**,** 9-16.

KUEHN, M. J. & KESTY, N. C. 2005. Bacterial outer membrane vesicles and the host-pathogen interaction. *Genes Dev,* 19**,** 2645-55.

KULKARNI, H. M. & JAGANNADHAM, M. V. 2014. Biogenesis and multifaceted roles of outer membrane vesicles from Gram-negative bacteria. *Microbiology,* 160**,** 2109-21.

KULP, A. & KUEHN, M. J. 2010. Biological functions and biogenesis of secreted bacterial outer membrane vesicles. *Annu Rev Microbiol,* 64**,** 163-84.

KUROKI, S., SAIDA, T., NUKINA, M., HARUTA, T., YOSHIOKA, M., KOBAYASHI, Y. & NAKANISHI, H. 1993. Campylobacter jejuni strains from patients with Guillain-Barre syndrome belong mostly to Penner serogroup 19 and contain beta-N-acetylglucosamine residues. *Ann Neurol,* 33**,** 243-7.

LAFONT, F. & VAN DER GOOT, F. G. 2005. Bacterial invasion via lipid rafts. *Cell Microbiol,* 7**,** 613-20.

LARA-TEJERO, M. & GALAN, J. E. 2000. A bacterial toxin that controls cell cycle progression as a deoxyribonuclease I-like protein. *Science,* 290**,** 354-7.

LARSON, C. L., SAMUELSON, D. R., EUCKER, T. P., O'LOUGHLIN, J. L. & KONKEL, M. E. 2013. The fibronectin-binding motif within FlpA facilitates Campylobacter jejuni adherence to host cell and activation of host cell signaling. *Emerging Microbes & Infections,* 2**,** e65.

LARSON, C. L., SHAH, D. H., DHILLON, A. S., CALL, D. R., AHN, S., HALDORSON, G. J., DAVITT, C. & KONKEL, M. E. 2008. Campylobacter jejuni invade chicken LMH

cells inefficiently and stimulate differential expression of the chicken CXCLi1 and CXCLi2 cytokines. *Microbiology,* 154**,** 3835-47.

LAUKOETTER, M. G., NAVA, P. & NUSRAT, A. 2008. Role of the intestinal barrier in inflammatory bowel disease. *World J Gastroenterol,* 14**,** 401-7.

LAVINE, M. D. & STRAND, M. R. 2002. Insect hemocytes and their role in immunity. *Insect Biochem Mol Biol,* 32**,** 1295-309.

LAZARO, B., CARCAMO, J., AUDICANA, A., PERALES, I. & FERNANDEZ-ASTORGA, A. 1999. Viability and DNA maintenance in nonculturable spiral Campylobacter jejuni cells after long-term exposure to low temperatures. *Appl Environ Microbiol,* 65**,** 4677-81.

LEE, M. D. & NEWELL, D. G. 2006. Campylobacter in poultry: filling an ecological niche. *Avian Dis,* 50**,** 1-9.

LERTPIRIYAPONG, K., GAMAZON, E. R., FENG, Y., PARK, D. S., PANG, J., BOTKA, G., GRAFFAM, M. E., GE, Z. & FOX, J. G. 2012. Campylobacter jejuni type VI secretion system: roles in adaptation to deoxycholic acid, host cell adherence, invasion, and in vivo colonization. *PLoS One,* 7**,** e42842.

LI, C. Y., XUE, P., TIAN, W. Q., LIU, R. C. & YANG, C. 1996. Experimental Campylobacter jejuni infection in the chicken: an animal model of axonal Guillain-Barre syndrome. *J Neurol Neurosurg Psychiatry,* 61**,** 279-84.

LIM, J. S., CHOY, H. E., PARK, S. C., HAN, J. M., JANG, I. S. & CHO, K. A. 2010. Caveolae-mediated entry of Salmonella typhimurium into senescent nonphagocytotic host cells. *Aging Cell,* 9**,** 243-51.

LINDMARK, B., ROMPIKUNTAL, P. K., VAITKEVICIUS, K., SONG, T., MIZUNOE, Y., UHLIN, B. E., GUERRY, P. & WAI, S. N. 2009. Outer membrane vesicle-mediated release of cytolethal distending toxin (CDT) from Campylobacter jejuni. *BMC Microbiol,* 9**,** 220.

LOUWEN, R., NIEUWENHUIS, E. E., VAN MARREWIJK, L., HORST-KREFT, D., DE RUITER, L., HEIKEMA, A. P., VAN WAMEL, W. J., WAGENAAR, J. A., ENDTZ, H. P., SAMSOM, J., VAN BAARLEN, P., AKHMANOVA, A. & VAN BELKUM, A. 2012. Campylobacter jejuni translocation across intestinal epithelial cells is facilitated by ganglioside-like lipooligosaccharide structures. *Infect Immun,* 80**,** 3307-18.

LOUWEN, R. P., VAN BELKUM, A., WAGENAAR, J. A., DOORDUYN, Y., ACHTERBERG, R. & ENDTZ, H. P. 2006. Lack of association between the presence of the pVir plasmid and bloody diarrhea in Campylobacter jejuni enteritis. *J Clin Microbiol,* 44**,** 1867-8.

LUDIN, B., DOLL, T., MEILI, R., KAECH, S. & MATUS, A. 1996. Application of novel vectors for GFP-tagging of proteins to study microtubule-associated proteins. *Gene,* 173**,** 107-11.

LYNCH, T., LIVINGSTONE, S., BUENAVENTURA, E., LUTTER, E., FEDWICK, J., BURET, A. G., GRAHAM, D. & DEVINNEY, R. 2005. Vibrio parahaemolyticus disruption of epithelial cell tight junctions occurs independently of toxin production. *Infect Immun,* 73**,** 1275-83.

MACCALLUM, A., HADDOCK, G. & EVEREST, P. H. 2005a. Campylobacter jejuni activates mitogen-activated protein kinases in Caco-2 cell monolayers and in vitro infected primary human colonic tissue. *Microbiology,* 151**,** 2765-72.

MACCALLUM, A., HARDY, S. P. & EVEREST, P. H. 2005b. Campylobacter jejuni inhibits the absorptive transport functions of Caco-2 cells and disrupts cellular tight junctions. *Microbiology,* 151**,** 2451-8.

MACCALLUM, A. J., HARRIS, D., HADDOCK, G. & EVEREST, P. H. 2006. Campylobacter jejuni-infected human epithelial cell lines vary in their ability to secrete

interleukin-8 compared to in vitro-infected primary human intestinal tissue. *Microbiology,* 152**,** 3661-5.

MACKAY, D. J., NOBES, C. D. & HALL, A. 1995. The Rho's progress: a potential role during neuritogenesis for the Rho family of GTPases. *Trends Neurosci,* 18**,** 496-501.

MADI, A., SVINAREFF, P., ORANGE, N., FEUILLOLEY, M. G. & CONNIL, N. 2010. Pseudomonas fluorescens alters epithelial permeability and translocates across Caco-2/TC7 intestinal cells. *Gut Pathog,* 2**,** 16.

MAHDAVI, J., PIRINCCIOGLU, N., OLDFIELD, N. J., CARLSOHN, E., STOOF, J., ASLAM, A., SELF, T., CAWTHRAW, S. A., PETROVSKA, L., COLBORNE, N., SIHLBOM, C., BOREN, T., WOOLDRIDGE, K. G. & ALA'ALDEEN, D. A. 2014. A novel O-linked glycan modulates Campylobacter jejuni major outer membrane protein-mediated adhesion to human histo-blood group antigens and chicken colonization. *Open Biol,* 4**,** 130202.

MALIK-KALE, P., PARKER, C. T. & KONKEL, M. E. 2008. Culture of Campylobacter jejuni with sodium deoxycholate induces virulence gene expression. *J Bacteriol,* 190**,** 2286-97.

MAMELLI, L., PAGES, J. M., KONKEL, M. E. & BOLLA, J. M. 2006. Expression and purification of native and truncated forms of CadF, an outer membrane protein of Campylobacter. *Int J Biol Macromol,* 39**,** 135-40.

MANIE, S. N., DE BREYNE, S., VINCENT, S. & GERLIER, D. 2000. Measles virus structural components are enriched into lipid raft microdomains: a potential cellular location for virus assembly. *J Virol,* 74**,** 305-11.

MAYRAND, D. & GRENIER, D. 1989. Biological activities of outer membrane vesicles. *Can J Microbiol,* 35**,** 607-13.

MCBROOM, A. J. & KUEHN, M. J. 2005. Outer Membrane Vesicles. *EcoSal Plus,* 1.

MCBROOM, A. J. & KUEHN, M. J. 2007. Release of outer membrane vesicles by Gram-negative bacteria is a novel envelope stress response. *Mol Microbiol,* 63**,** 545-58.

MEADE, K. G., NARCIANDI, F., CAHALANE, S., REIMAN, C., ALLAN, B. & O'FARRELLY, C. 2009. Comparative in vivo infection models yield insights on early host immune response to Campylobacter in chickens. *Immunogenetics,* 61**,** 101-10.

MEDEMA, G. J., SCHETS, F. M., VAN DE GIESSEN, A. W. & HAVELAAR, A. H. 1992. Lack of colonization of 1 day old chicks by viable, non-culturable Campylobacter jejuni. *J Appl Bacteriol,* 72**,** 512-6.

MELLITS, K. H., MULLEN, J., WAND, M., ARMBRUSTER, G., PATEL, A., CONNERTON, P. L., SKELLY, M. & CONNERTON, I. F. 2002. Activation of the transcription factor NF-kappaB by Campylobacter jejuni. *Microbiology,* 148**,** 2753-63.

MENARD, R., SANSONETTI, P. J. & PARSOT, C. 1993. Nonpolar mutagenesis of the ipa genes defines IpaB, IpaC, and IpaD as effectors of Shigella flexneri entry into epithelial cells. *J Bacteriol,* 175**,** 5899-906.

MERESSE, S., STEELE-MORTIMER, O., FINLAY, B. B. & GORVEL, J. P. 1999. The rab7 GTPase controls the maturation of Salmonella typhimurium-containing vacuoles in HeLa cells. *EMBO J,* 18**,** 4394-403.

MILLER, W. G., BATES, A. H., HORN, S. T., BRANDL, M. T., WACHTEL, M. R. & MANDRELL, R. E. 2000. Detection on surfaces and in Caco-2 cells of Campylobacter jejuni cells transformed with new gfp, yfp, and cfp marker plasmids. *Appl Environ Microbiol,* 66**,** 5426-36.

MILLS, D. C., GUNDOGDU, O., ELMI, A., BAJAJ-ELLIOTT, M., TAYLOR, P. W., WREN, B. W. & DORRELL, N. 2012. Increase in Campylobacter jejuni invasion of

intestinal epithelial cells under low-oxygen coculture conditions that reflect the in vivo environment. *Infect Immun,* 80**,** 1690-8.

MIN, T., VEDADI, M., WATSON, D. C., WASNEY, G. A., MUNGER, C., CYGLER, M., MATTE, A. & YOUNG, N. M. 2009. Specificity of Campylobacter jejuni adhesin PEB3 for phosphates and structural differences among its ligand complexes. *Biochemistry,* 48**,** 3057-67.

MIXTER, P. F., KLENA, J. D., FLOM, G. A., SIEGESMUND, A. M. & KONKEL, M. E. 2003. In vivo tracking of Campylobacter jejuni by using a novel recombinant expressing green fluorescent protein. *Appl Environ Microbiol,* 69**,** 2864-74.

MONTEVILLE, M. R. & KONKEL, M. E. 2002. Fibronectin-Facilitated Invasion of T84 Eukaryotic Cells by Campylobacter jejuni Occurs Preferentially at the Basolateral Cell Surface. *Infection and Immunity,* 70**,** 6665-6671.

MONTEVILLE, M. R., YOON, J. E. & KONKEL, M. E. 2003. Maximal adherence and invasion of INT 407 cells by Campylobacter jejuni requires the CadF outer-membrane protein and microfilament reorganization. *Microbiology,* 149**,** 153-65.

MONTROSE, M. S., SHANE, S. M. & HARRINGTON, K. S. 1985. Role of litter in the transmission of Campylobacter jejuni. *Avian Dis,* 29**,** 392-9.

MOORE, J. E., CORCORAN, D., DOOLEY, J. S., FANNING, S., LUCEY, B., MATSUDA, M., MCDOWELL, D. A., MEGRAUD, F., MILLAR, B. C., O'MAHONY, R., O'RIORDAN, L., O'ROURKE, M., RAO, J. R., ROONEY, P. J., SAILS, A. & WHYTE, P. 2005. Campylobacter. *Vet Res,* 36**,** 351-82.

MOORES, S. L., SABRY, J. H. & SPUDICH, J. A. 1996. Myosin dynamics in live Dictyostelium cells. *Proc Natl Acad Sci U S A,* 93**,** 443-6.

MORAN, A. P. & UPTON, M. E. 1986. A comparative study of the rod and coccoid forms of Campylobacter jejuni ATCC 29428. *J Appl Bacteriol,* 60**,** 103-10.

MOSER, I., SCHROEDER, W. & SALNIKOW, J. 1997. Campylobacter jejuni major outer membrane protein and a 59-kDa protein are involved in binding to fibronectin and INT 407 cell membranes. *FEMS Microbiol Lett,* 157**,** 233-8.

MOUNIER, J., BAHRANI, F. K. & SANSONETTI, P. J. 1997. Secretion of Shigella flexneri Ipa invasins on contact with epithelial cells and subsequent entry of the bacterium into cells are growth stage dependent. *Infect Immun,* 65**,** 774-82.

MUKHERJEE, K., ALTINCICEK, B., HAIN, T., DOMANN, E., VILCINSKAS, A. & CHAKRABORTY, T. 2010. Galleria mellonella as a model system for studying Listeria pathogenesis. *Appl Environ Microbiol,* 76**,** 310-7.

MUND, N. L., MASANTA, W. O., GOLDSCHMIDT, A. M., LUGERT, R., GROSS, U. & ZAUTNER, A. E. 2016. Association of Campylobacter Jejuni ssp. Jejuni Chemotaxis Receptor Genes with Multilocus Sequence Types and Source of Isolation. *Eur J Microbiol Immunol (Bp),* 6**,** 162-177.

MURAOKA, W. T. & ZHANG, Q. 2011. Phenotypic and genotypic evidence for L-fucose utilization by Campylobacter jejuni. *J Bacteriol,* 193**,** 1065-75.

MYERS, J. D. & KELLY, D. J. 2005. A sulphite respiration system in the chemoheterotrophic human pathogen Campylobacter jejuni. *Microbiology,* 151**,** 233-42.

NACHAMKIN, I., ALLOS, B. M. & HO, T. 1998. Campylobacter species and Guillain-Barre syndrome. *Clin Microbiol Rev,* 11**,** 555-67.

NACHAMKIN, I., YANG, X. H. & STERN, N. J. 1993. Role of Campylobacter jejuni flagella as colonization factors for three-day-old chicks: analysis with flagellar mutants. *Appl Environ Microbiol,* 59**,** 1269-73.

NAPPI, A. J. & CHRISTENSEN, B. M. 2005. Melanogenesis and associated cytotoxic reactions: applications to insect innate immunity. *Insect Biochem Mol Biol,* 35**,** 443-59.

NAPPI, A. J. & VASS, E. 2001. Cytotoxic reactions associated with insect immunity. *Adv Exp Med Biol,* 484**,** 329-48.

NATARO, J. P., HICKS, S., PHILLIPS, A. D., VIAL, P. A. & SEARS, C. L. 1996. T84 cells in culture as a model for enteroaggregative Escherichia coli pathogenesis. *Infect Immun,* 64**,** 4761-8.

NAZ, N., MILLS, D. C., WREN, B. W. & DORRELL, N. 2013. Enteric bacterial invasion of intestinal epithelial cells in vitro is dramatically enhanced using a vertical diffusion chamber model. *J Vis Exp***,** e50741.

NEAL-MCKINNEY, J. M. & KONKEL, M. E. 2012. The Campylobacter jejuni CiaC virulence protein is secreted from the flagellum and delivered to the cytosol of host cells. *Front Cell Infect Microbiol,* 2**,** 31.

NEMELKA, K. W., BROWN, A. W., WALLACE, S. M., JONES, E., ASHER, L. V., PATTARINI, D., APPLEBEE, L., GILLILAND, T. C., JR., GUERRY, P. & BAQAR, S. 2009. Immune response to and histopathology of Campylobacter jejuni infection in ferrets (Mustela putorius furo). *Comp Med,* 59**,** 363-71.

NICHOLS, G. L. 2005. Fly transmission of Campylobacter. *Emerg Infect Dis,* 11**,** 361-4.

NOBES, C. D. & HALL, A. 1995a. Rho, rac and cdc42 GTPases: regulators of actin structures, cell adhesion and motility. *Biochem Soc Trans,* 23**,** 456-9.

NOBES, C. D. & HALL, A. 1995b. Rho, rac, and cdc42 GTPases regulate the assembly of multimolecular focal complexes associated with actin stress fibers, lamellipodia, and filopodia. *Cell,* 81**,** 53-62.

NOBES, C. D., HAWKINS, P., STEPHENS, L. & HALL, A. 1995. Activation of the small GTP-binding proteins rho and rac by growth factor receptors. *J Cell Sci,* 108 (Pt 1)**,** 225-33.

NORKIN, L. C. 1999. Simian virus 40 infection via MHC class I molecules and caveolae. *Immunol Rev,* 168**,** 13-22.

NOVIK, V., HOFREUTER, D. & GALAN, J. E. 2009. Characterization of a Campylobacter jejuni VirK protein homolog as a novel virulence determinant. *Infect Immun,* 77**,** 5428-36.

NOVIK, V., HOFREUTER, D. & GALAN, J. E. 2010. Identification of Campylobacter jejuni genes involved in its interaction with epithelial cells. *Infect Immun,* 78**,** 3540-53.

O CROININ, T. & BACKERT, S. 2012. Host epithelial cell invasion by Campylobacter jejuni: trigger or zipper mechanism? *Front Cell Infect Microbiol,* 2**,** 25.

OBAFEMI, M. T. & DOUGLAS, H. 2017. Campylobacter jejuni myocarditis: A journey from the gut to the heart. *SAGE Open Med Case Rep,* 5**,** 2050313X17713148.

OBERMEIER, A., AHMED, S., MANSER, E., YEN, S. C., HALL, C. & LIM, L. 1998. PAK promotes morphological changes by acting upstream of Rac. *EMBO J,* 17**,** 4328-39.

OELSCHLAEGER, T. A., GUERRY, P. & KOPECKO, D. J. 1993. Unusual microtubule-dependent endocytosis mechanisms triggered by Campylobacter jejuni and Citrobacter freundii. *Proc Natl Acad Sci U S A,* 90**,** 6884-8.

OGAWA, M. & SASAKAWA, C. 2006. Intracellular survival of Shigella. *Cell Microbiol,* 8**,** 177-84.

OLLIARO, P. & CASTELLI, F. 1997. Plasmodium falciparum: an electronmicroscopy study of caveolae and trafficking between the parasite and the extracellular medium. *Int J Parasitol,* 27**,** 1007-12.

PANKOV, R. & YAMADA, K. M. 2002. Fibronectin at a glance. *J Cell Sci,* 115**,** 3861-3.

PARKHILL, J., WREN, B. W., MUNGALL, K., KETLEY, J. M., CHURCHER, C., BASHAM, D., CHILLINGWORTH, T., DAVIES, R. M., FELTWELL, T., HOLROYD, S., JAGELS, K., KARLYSHEV, A. V., MOULE, S., PALLEN, M. J., PENN, C. W., QUAIL, M. A., RAJANDREAM, M. A., RUTHERFORD, K. M., VAN VLIET, A. H., WHITEHEAD, S. & BARRELL, B. G. 2000. The genome sequence of the food-borne pathogen Campylobacter jejuni reveals hypervariable sequences. *Nature,* 403**,** 665-8.

PARTON, R. G. & LINDSAY, M. 1999. Exploitation of major histocompatibility complex class I molecules and caveolae by simian virus 40. *Immunol Rev,* 168**,** 23-31.

PATRIARCHI, A., MAUNSELL, B., O'MAHONY, E., FOX, A., FANNING, S., BUCKLEY, J. & BOLTON, D. J. 2009. Prevalence of Campylobacter spp. in a subset of intensive poultry flocks in Ireland. *Lett Appl Microbiol,* 49**,** 305-10.

PATRONE, V., CAMPANA, R., VALLORANI, L., DOMINICI, S., FEDERICI, S., CASADEI, L., GIOACCHINI, A. M., STOCCHI, V. & BAFFONE, W. 2013. CadF expression in Campylobacter jejuni strains incubated under low-temperature water microcosm conditions which induce the viable but non-culturable (VBNC) state. *Antonie Van Leeuwenhoek,* 103**,** 979-88.

PEI, Z. & BLASER, M. J. 1993. PEB1, the major cell-binding factor of Campylobacter jejuni, is a homolog of the binding component in gram-negative nutrient transport systems. *J Biol Chem,* 268**,** 18717-25.

PEI, Z., BURUCOA, C., GRIGNON, B., BAQAR, S., HUANG, X. Z., KOPECKO, D. J., BOURGEOIS, A. L., FAUCHERE, J. L. & BLASER, M. J. 1998. Mutation in the peb1A locus of Campylobacter jejuni reduces interactions with epithelial cells and intestinal colonization of mice. *Infect Immun,* 66**,** 938-43.

PENA, L. A. & FISHBEIN, M. C. 2007. Fatal myocarditis related to Campylobacter jejuni infection: a case report. *Cardiovasc Pathol,* 16**,** 119-21.

PERKINS-JONES, K., HOLMAN, R. L. & FROST, F. 1982. Waterborne transmission of campylobacter. *West J Med,* 137**,** 339.

PESCI, E. C., COTTLE, D. L. & PICKETT, C. L. 1994. Genetic, enzymatic, and pathogenic studies of the iron superoxide dismutase of Campylobacter jejuni. *Infect Immun,* 62**,** 2687-94.

PHE 2016. <Campylobacter_2016_Data.pdf>.

PHILPOTT, D. J., YAMAOKA, S., ISRAEL, A. & SANSONETTI, P. J. 2000. Invasive Shigella flexneri activates NF-kappa B through a lipopolysaccharide-dependent innate intracellular response and leads to IL-8 expression in epithelial cells. *J Immunol,* 165**,** 903-14.

PIGNATA, S., MAGGINI, L., ZARRILLI, R., REA, A. & ACQUAVIVA, A. M. 1994. The enterocyte-like differentiation of the Caco-2 tumor cell line strongly correlates with responsiveness to cAMP and activation of kinase A pathway. *Cell Growth Differ,* 5**,** 967-73.

POGACAR, M. S., KLANCNIK, A., MOZINA, S. S. & CENCIC, A. 2010. Attachment, invasion, and translocation of Campylobacter jejuni in pig small-intestinal epithelial cells. *Foodborne Pathog Dis,* 7**,** 589-95.

POLY, F., EWING, C., GOON, S., HICKEY, T. E., ROCKABRAND, D., MAJAM, G., LEE, L., PHAN, J., SAVARINO, N. J. & GUERRY, P. 2007. Heterogeneity of a Campylobacter jejuni protein that is secreted through the flagellar filament. *Infect Immun,* 75**,** 3859-67.

POLY, F. & GUERRY, P. 2008. Pathogenesis of Campylobacter. *Curr Opin Gastroenterol,* 24**,** 27-31.

POLY, F., THREADGILL, D. & STINTZI, A. 2005. Genomic diversity in Campylobacter jejuni: identification of C. jejuni 81-176-specific genes. *J Clin Microbiol,* 43**,** 2330-8.

PURDY, D. & PARK, S. F. 1994. Cloning, nucleotide sequence and characterization of a gene encoding superoxide dismutase from Campylobacter jejuni and Campylobacter coli. *Microbiology,* 140 (Pt 5)**,** 1203-8.

PUTHENEDAM, M., WILLIAMS, P. H., LAKSHMI, B. S. & BALAKRISHNAN, A. 2007. Modulation of tight junction barrier function by outer membrane proteins of enteropathogenic Escherichia coli: role of F-actin and junctional adhesion molecule-1. *Cell Biol Int,* 31**,** 836-44.

RAMABU, S. S., BOXALL, N. S., MADIE, P. & FENWICK, S. G. 2004. Some potential sources for transmission of Campylobacter jejuni to broiler chickens. *Lett Appl Microbiol,* 39**,** 252-6.

REES, J. H., SOUDAIN, S. E., GREGSON, N. A. & HUGHES, R. A. 1995. Campylobacter jejuni infection and Guillain-Barre syndrome. *N Engl J Med,* 333**,** 1374-9.

RICHARDSON, J. F., FROST, J. A., KRAMER, J. M., THWAITES, R. T., BOLTON, F. J., WAREING, D. R. & GORDON, J. A. 2001. Coinfection with Campylobacter species: an epidemiological problem? *J Appl Microbiol,* 91**,** 206-11.

RICHARDSON, J. S. 1985. Describing patterns of protein tertiary structure. *Methods Enzymol,* 115**,** 341-58.

RIDLEY, A. J. & HALL, A. 1992. Distinct patterns of actin organization regulated by the small GTP-binding proteins Rac and Rho. *Cold Spring Harb Symp Quant Biol,* 57**,** 661-71.

RIDLEY, A. J., PATERSON, H. F., JOHNSTON, C. L., DIEKMANN, D. & HALL, A. 1992. The small GTP-binding protein rac regulates growth factor-induced membrane ruffling. *Cell,* 70**,** 401-10.

RIVERA-AMILL, V., KIM, B. J., SESHU, J. & KONKEL, M. E. 2001. Secretion of the virulence-associated Campylobacter invasion antigens from Campylobacter jejuni requires a stimulatory signal. *J Infect Dis,* 183**,** 1607-16.

RIVERA-AMILL, V. & KONKEL, M. E. 1999. Secretion of Campylobacter jejuni Cia proteins is contact dependent. *Adv Exp Med Biol,* 473**,** 225-9.

ROLHION, N., BARNICH, N., CLARET, L. & DARFEUILLE-MICHAUD, A. 2005. Strong decrease in invasive ability and outer membrane vesicle release in Crohn's disease-associated adherent-invasive Escherichia coli strain LF82 with the yfgL gene deleted. *J Bacteriol,* 187**,** 2286-96.

ROLLINS, D. M. & COLWELL, R. R. 1986. Viable but nonculturable stage of Campylobacter jejuni and its role in survival in the natural aquatic environment. *Appl Environ Microbiol,* 52**,** 531-8.

ROPPER, A. H. 1992. The Guillain-Barre syndrome. *N Engl J Med,* 326**,** 1130-6.

ROPPER, A. H. & ADELMAN, L. 1992. Early Guillain-Barre syndrome without inflammation. *Arch Neurol,* 49**,** 979-81.

ROTHBERG, K. G., HEUSER, J. E., DONZELL, W. C., YING, Y. S., GLENNEY, J. R. & ANDERSON, R. G. 1992. Caveolin, a protein component of caveolae membrane coats. *Cell,* 68**,** 673-82.

ROYDEN, A., WEDLEY, A., MERGA, J. Y., RUSHTON, S., HALD, B., HUMPHREY, T. & WILLIAMS, N. J. 2016. A role for flies (Diptera) in the transmission of Campylobacter to broilers? *Epidemiol Infect,* 144**,** 3326-3334.

RUBINCHIK, S., SEDDON, A. M. & KARLYSHEV, A. V. 2014. A negative effect of Campylobacter capsule on bacterial interaction with an analogue of a host cell receptor. *BMC Microbiol,* 14**,** 141.

RUSSELL, R. G. & BLAKE, D. C., JR. 1994. Cell association and invasion of Caco-2 cells by Campylobacter jejuni. *Infect Immun,* 62**,** 3773-9.

RUSSELL, R. G., BLASER, M. J., SARMIENTO, J. I. & FOX, J. 1989. Experimental Campylobacter jejuni infection in Macaca nemestrina. *Infect Immun,* 57**,** 1438-44.

RUSSELL, R. G., O'DONNOGHUE, M., BLAKE, D. C., JR., ZULTY, J. & DETOLLA, L. J. 1993. Early colonic damage and invasion of Campylobacter jejuni in experimentally challenged infant Macaca mulatta. *J Infect Dis,* 168**,** 210-5.

SAMUEL, M. C., VUGIA, D. J., SHALLOW, S., MARCUS, R., SEGLER, S., MCGIVERN, T., KASSENBORG, H., REILLY, K., KENNEDY, M., ANGULO, F., TAUXE, R. V. & EMERGING INFECTIONS PROGRAM FOODNET WORKING, G. 2004. Epidemiology of sporadic Campylobacter infection in the United States and declining trend in incidence, FoodNet 1996-1999. *Clin Infect Dis,* 38 Suppl 3**,** S165-74.

SAMUELSON, D. R., EUCKER, T. P., BELL, J. A., DYBAS, L., MANSFIELD, L. S. & KONKEL, M. E. 2013. The Campylobacter jejuni CiaD effector protein activates MAP kinase signaling pathways and is required for the development of disease. *Cell Commun Signal,* 11**,** 79.

SANGER, J. M., CHANG, R., ASHTON, F., KAPER, J. B. & SANGER, J. W. 1996. Novel form of actin-based motility transports bacteria on the surfaces of infected cells. *Cell Motil Cytoskeleton,* 34**,** 279-87.

SANSONETTI, P. J. 2001. Rupture, invasion and inflammatory destruction of the intestinal barrier by Shigella, making sense of prokaryote-eukaryote cross-talks. *FEMS Microbiol Rev,* 25**,** 3-14.

SATO, T. & CLEVERS, H. 2013. Growing self-organizing mini-guts from a single intestinal stem cell: mechanism and applications. *Science,* 340**,** 1190-4.

SCANLAN, E., ARDILL, L., WHELAN, M. V., SHORTT, C., NALLY, J. E., BOURKE, B. & T, O. C. 2017. Relaxation of DNA supercoiling leads to increased invasion of epithelial cells and protein secretion by Campylobacter jejuni. *Mol Microbiol,* 104**,** 92-104.

SCHEIFFELE, P., RIETVELD, A., WILK, T. & SIMONS, K. 1999. Influenza viruses select ordered lipid domains during budding from the plasma membrane. *J Biol Chem,* 274**,** 2038-44.

SCHNEIDER, A., RUNZI, M., PEITGEN, K., VON BIRGELEN, C. & GERKEN, G. 2000. Campylobacter jejuni-induced severe colitis--a rare cause of toxic megacolon. *Z Gastroenterol,* 38**,** 307-9.

SCHRODER, W. & MOSER, I. 1997. Primary structure analysis and adhesion studies on the major outer membrane protein of Campylobacter jejuni. *FEMS Microbiol Lett,* 150**,** 141-7.

SCHUBERT, K., OLDE DAMINK, S. W. M., VON BERGEN, M. & SCHAAP, F. G. 2017. Interactions between bile salts, gut microbiota, and hepatic innate immunity. *Immunol Rev,* 279**,** 23-35.

SCOTT, N. E., MARZOOK, N. B., DEUTSCHER, A., FALCONER, L., CROSSETT, B., DJORDJEVIC, S. P. & CORDWELL, S. J. 2010. Mass spectrometric characterization of the Campylobacter jejuni adherence factor CadF reveals post-translational processing that removes immunogenicity while retaining fibronectin binding. *Proteomics,* 10**,** 277-88.

SENIOR, N. J., BAGNALL, M. C., CHAMPION, O. L., REYNOLDS, S. E., LA RAGIONE, R. M., WOODWARD, M. J., SALGUERO, F. J. & TITBALL, R. W. 2011. Galleria mellonella as an infection model for Campylobacter jejuni virulence. *J Med Microbiol,* 60**,** 661-9.

SHANE, S. M., MONTROSE, M. S. & HARRINGTON, K. S. 1985. Transmission of Campylobacter jejuni by the housefly (Musca domestica). *Avian Dis,* 29**,** 384-91.

SHANKER, S., LEE, A. & SORRELL, T. C. 1986. Campylobacter jejuni in broilers: the role of vertical transmission. *J Hyg (Lond),* 96**,** 153-9.

SHANKER, S., LEE, A. & SORRELL, T. C. 1990. Horizontal transmission of Campylobacter jejuni amongst broiler chicks: experimental studies. *Epidemiol Infect,* 104**,** 101-10.

SHIN, J. S., GAO, Z. & ABRAHAM, S. N. 2000. Involvement of cellular caveolae in bacterial entry into mast cells. *Science,* 289**,** 785-8.

SHORTT, C., SCANLAN, E., HILLIARD, A., COTRONEO, C. E., BOURKE, B. & T, O. C. 2016. DNA Supercoiling Regulates the Motility of Campylobacter jejuni and Is Altered by Growth in the Presence of Chicken Mucus. *MBio,* 7.

SIMONS, K. & TOOMRE, D. 2000. Lipid rafts and signal transduction. *Nat Rev Mol Cell Biol,* 1**,** 31-9.

SINGAMSETTY, V. K., WANG, Y., SHIMADA, H. & PRASADARAO, N. V. 2008. Outer membrane protein A expression in Enterobacter sakazakii is required to induce microtubule condensation in human brain microvascular endothelial cells for invasion. *Microb Pathog,* 45**,** 181-91.

SNELLING, W. J., MATSUDA, M., MOORE, J. E. & DOOLEY, J. S. 2005. Campylobacter jejuni. *Lett Appl Microbiol,* 41**,** 297-302.

SONG, Y. C., JIN, S., LOUIE, H., NG, D., LAU, R., ZHANG, Y., WEERASEKERA, R., AL RASHID, S., WARD, L. A., DER, S. D. & CHAN, V. L. 2004. FlaC, a protein of Campylobacter jejuni TGH9011 (ATCC43431) secreted through the flagellar apparatus, binds epithelial cells and influences cell invasion. *Mol Microbiol,* 53**,** 541-53.

SPILLER, R. C. 2007. Role of infection in irritable bowel syndrome. *J Gastroenterol,* 42 Suppl 17**,** 41-7.

ST CHARLES, J. L., BELL, J. A., GADSDEN, B. J., MALIK, A., COOKE, H., VAN DE GRIFT, L. K., KIM, H. Y., SMITH, E. J. & MANSFIELD, L. S. 2017. Guillain Barre Syndrome is induced in Non-Obese Diabetic (NOD) mice following Campylobacter jejuni infection and is exacerbated by antibiotics. *J Autoimmun,* 77**,** 11-38.

STAHL, M., RIES, J., VERMEULEN, J., YANG, H., SHAM, H. P., CROWLEY, S. M., BADAYEVA, Y., TURVEY, S. E., GAYNOR, E. C., LI, X. & VALLANCE, B. A. 2014. A novel mouse model of Campylobacter jejuni gastroenteritis reveals key pro-inflammatory and tissue protective roles for Toll-like receptor signaling during infection. *PLoS Pathog,* 10**,** e1004264.

STEELE-MORTIMER, O. 2008. The Salmonella-containing vacuole: moving with the times. *Curr Opin Microbiol,* 11**,** 38-45.

STEELE-MORTIMER, O., BRUMELL, J. H., KNODLER, L. A., MERESSE, S., LOPEZ, A. & FINLAY, B. B. 2002. The invasion-associated type III secretion system of Salmonella enterica serovar Typhimurium is necessary for intracellular proliferation and vacuole biogenesis in epithelial cells. *Cell Microbiol,* 4**,** 43-54.

STEELE-MORTIMER, O., ST-LOUIS, M., OLIVIER, M. & FINLAY, B. B. 2000. Vacuole acidification is not required for survival of Salmonella enterica serovar typhimurium within cultured macrophages and epithelial cells. *Infect Immun,* 68**,** 5401-4.

SULAEMAN, S., HERNOULD, M., SCHAUMANN, A., COQUET, L., BOLLA, J. M., DE, E. & TRESSE, O. 2012. Enhanced adhesion of Campylobacter jejuni to abiotic

surfaces is mediated by membrane proteins in oxygen-enriched conditions. *PLoS One,* 7**,** e46402.
TAKEUCHI, A. 1967. Electron microscope studies of experimental Salmonella infection. I. Penetration into the intestinal epithelium by Salmonella typhimurium. *Am J Pathol,* 50**,** 109-36.
TAREEN, A. M., DASTI, J. I., ZAUTNER, A. E., GROSS, U. & LUGERT, R. 2011. Sulphite : cytochrome c oxidoreductase deficiency in Campylobacter jejuni reduces motility, host cell adherence and invasion. *Microbiology,* 157**,** 1776-85.
TAUXE, R. V. & BLAKE, P. A. 1992. Epidemic cholera in Latin America. *JAMA,* 267**,** 1388-90.
THOMPSON, J. D., HIGGINS, D. G. & GIBSON, T. J. 1994. CLUSTAL W: improving the sensitivity of progressive multiple sequence alignment through sequence weighting, position-specific gap penalties and weight matrix choice. *Nucleic Acids Res,* 22**,** 4673-80.
TOMBOLINI, R., VAN DER GAAG, D. J., GERHARDSON, B. & JANSSON, J. K. 1999. Colonization pattern of the biocontrol strain Pseudomonas chlororaphis MA 342 on barley seeds visualized by using green fluorescent protein. *Appl Environ Microbiol,* 65**,** 3674-80.
TRAN VAN NHIEU, G., CARON, E., HALL, A. & SANSONETTI, P. J. 1999. IpaC induces actin polymerization and filopodia formation during Shigella entry into epithelial cells. *EMBO J,* 18**,** 3249-62.
TRIEU-CUOT, P., KLIER, A. & COURVALIN, P. 1985. DNA sequences specifying the transcription of the streptococcal kanamycin resistance gene in Escherichia coli and Bacillus subtilis. *Mol Gen Genet,* 198**,** 348-52.
TURNER, K. L., CAHILL, B. K., DILELLO, S. K., GUTEL, D., BRUNSON, D. N., ALBERTI, S. & ELLIS, T. N. 2015. Porin Loss Impacts the Host Inflammatory Response to Outer Membrane Vesicles of Klebsiella pneumoniae. *Antimicrob Agents Chemother,* 60**,** 1360-9.
UNAL, C. M., SCHAAR, V. & RIESBECK, K. 2011. Bacterial outer membrane vesicles in disease and preventive medicine. *Semin Immunopathol,* 33**,** 395-408.
URDANETA, V. & CASADESUS, J. 2017. Interactions between Bacteria and Bile Salts in the Gastrointestinal and Hepatobiliary Tracts. *Front Med (Lausanne),* 4**,** 163.
VALDIVIA, R. H., HROMOCKYJ, A. E., MONACK, D., RAMAKRISHNAN, L. & FALKOW, S. 1996. Applications for green fluorescent protein (GFP) in the study of host-pathogen interactions. *Gene,* 173**,** 47-52.
VAN ALPHEN, L. B., BLEUMINK-PLUYM, N. M., ROCHAT, K. D., VAN BALKOM, B. W., WOSTEN, M. M. & VAN PUTTEN, J. P. 2008. Active migration into the subcellular space precedes Campylobacter jejuni invasion of epithelial cells. *Cell Microbiol,* 10**,** 53-66.
VAN PUTTEN, J. P., DUENSING, T. D. & COLE, R. L. 1998. Entry of OpaA+ gonococci into HEp-2 cells requires concerted action of glycosaminoglycans, fibronectin and integrin receptors. *Mol Microbiol,* 29**,** 369-79.
VAN RHIJN, I., VAN DEN BERG, L. H., ANG, C. W., ADMIRAAL, J. & LOGTENBERG, T. 2003. Expansion of human gammadelta T cells after in vitro stimulation with Campylobacter jejuni. *Int Immunol,* 15**,** 373-82.
VAN SPREEUWEL, J. P., DUURSMA, G. C., MEIJER, C. J., BAX, R., ROSEKRANS, P. C. & LINDEMAN, J. 1985. Campylobacter colitis: histological immunohistochemical and ultrastructural findings. *Gut,* 26**,** 945-51.
VAN TRIEST, M., DE ROOIJ, J. & BOS, J. L. 2001. Measurement of GTP-bound Ras-like GTPases by activation-specific probes. *Methods Enzymol,* 333**,** 343-8.

VANAJA, S. K., RUSSO, A. J., BEHL, B., BANERJEE, I., YANKOVA, M., DESHMUKH, S. D. & RATHINAM, V. A. K. 2016. Bacterial Outer Membrane Vesicles Mediate Cytosolic Localization of LPS and Caspase-11 Activation. *Cell,* 165**,** 1106-1119.
VOGEL, H., ALTINCICEK, B., GLOCKNER, G. & VILCINSKAS, A. 2011. A comprehensive transcriptome and immune-gene repertoire of the lepidopteran model host Galleria mellonella. *BMC Genomics,* 12**,** 308.
WALKER, R. I., SCHMAUDER-CHOCK, E. A., PARKER, J. L. & BURR, D. 1988. Selective association and transport of Campylobacter jejuni through M cells of rabbit Peyer's patches. *Can J Microbiol,* 34**,** 1142-7.
WASSENAAR, T. M. & BLASER, M. J. 1999. Pathophysiology of Campylobacter jejuni infections of humans. *Microbes Infect,* 1**,** 1023-33.
WASSENAAR, T. M., BLEUMINK-PLUYM, N. M. & VAN DER ZEIJST, B. A. 1991. Inactivation of Campylobacter jejuni flagellin genes by homologous recombination demonstrates that flaA but not flaB is required for invasion. *EMBO J,* 10**,** 2055-61.
WASSENAAR, T. M., FRY, B. N., LASTOVICA, A. J., WAGENAAR, J. A., COLOE, P. J. & DUIM, B. 2000. Genetic characterization of Campylobacter jejuni O:41 isolates in relation with Guillain-Barre syndrome. *J Clin Microbiol,* 38**,** 874-6.
WASSENAAR, T. M., GEILHAUSEN, B. & NEWELL, D. G. 1998. Evidence of genomic instability in Campylobacter jejuni isolated from poultry. *Appl Environ Microbiol,* 64**,** 1816-21.
WASSENAAR, T. M., VAN DER ZEIJST, B. A., AYLING, R. & NEWELL, D. G. 1993. Colonization of chicks by motility mutants of Campylobacter jejuni demonstrates the importance of flagellin A expression. *J Gen Microbiol,* 139 Pt 6**,** 1171-5.
WATSON, E., SHERRY, A., INGLIS, N. F., LAINSON, A., JYOTHI, D., YAGA, R., MANSON, E., IMRIE, L., EVEREST, P. & SMITH, D. G. 2014. Proteomic and genomic analysis reveals novel Campylobacter jejuni outer membrane proteins and potential heterogeneity. *EuPA Open Proteom,* 4**,** 184-194.
WATSON, R. O. & GALAN, J. E. 2005. Signal transduction in Campylobacter jejuni-induced cytokine production. *Cell Microbiol,* 7**,** 655-65.
WATSON, R. O. & GALAN, J. E. 2008. Campylobacter jejuni survives within epithelial cells by avoiding delivery to lysosomes. *PLoS Pathog,* 4**,** e14.
WATSON, R. O., NOVIK, V., HOFREUTER, D., LARA-TEJERO, M. & GALAN, J. E. 2007. A MyD88-deficient mouse model reveals a role for Nramp1 in Campylobacter jejuni infection. *Infect Immun,* 75**,** 1994-2003.
WEI, H., ZHANG, Y., FAN, Z. Z., GE, H. Y., ARENDT-NIELSEN, L., JIANG, H., YAO, W. & YUE, S. W. 2013. Effects of colchicine-induced microtubule depolymerization on TRPV4 in rats with chronic compression of the dorsal root ganglion. *Neurosci Lett,* 534**,** 344-50.
WESSLER, S. & BACKERT, S. 2008. Molecular mechanisms of epithelial-barrier disruption by Helicobacter pylori. *Trends Microbiol,* 16**,** 397-405.
WESTLING, K. & EVENGARD, B. 2001. Myocarditis associated with Campylobacter infection. *Scand J Infect Dis,* 33**,** 877-8.
WILLISON, H. J. & O'HANLON, G. M. 1999. The immunopathogenesis of Miller Fisher syndrome. *J Neuroimmunol,* 100**,** 3-12.
WINE, E., CHAN, V. L. & SHERMAN, P. M. 2008. Campylobacter jejuni mediated disruption of polarized epithelial monolayers is cell-type specific, time dependent, and correlates with bacterial invasion. *Pediatr Res,* 64**,** 599-604.
WOOLDRIDGE, K. G., WILLIAMS, P. H. & KETLEY, J. M. 1996. Host signal transduction and endocytosis of Campylobacter jejuni. *Microb Pathog,* 21**,** 299-305.

WOSTEN, M. M., WAGENAAR, J. A. & VAN PUTTEN, J. P. 2004. The FlgS/FlgR two-component signal transduction system regulates the fla regulon in Campylobacter jejuni. *J Biol Chem,* 279**,** 16214-22.

YANAGAWA, Y., TAKAHASHI, M. & ITOH, T. 1994. [The role of flagella of Campylobacter jejuni in colonization in the intestinal tract in mice and the cultured-cell infectivity]. *Nihon Saikingaku Zasshi,* 49**,** 395-403.

YANG, F., MOSS, L. G. & PHILLIPS, G. N., JR. 1996. The molecular structure of green fluorescent protein. *Nat Biotechnol,* 14**,** 1246-51.

YAO, R., BURR, D. H., DOIG, P., TRUST, T. J., NIU, H. & GUERRY, P. 1994. Isolation of motile and non-motile insertional mutants of Campylobacter jejuni: the role of motility in adherence and invasion of eukaryotic cells. *Mol Microbiol,* 14**,** 883-93.

YAO, R., BURR, D. H. & GUERRY, P. 1997. CheY-mediated modulation of Campylobacter jejuni virulence. *Mol Microbiol,* 23**,** 1021-31.

YAP, A. S., MULLIN, J. M. & STEVENSON, B. R. 1998. Molecular analyses of tight junction physiology: insights and paradoxes. *J Membr Biol,* 163**,** 159-67.

YONEZAWA, H., OSAKI, T., KURATA, S., FUKUDA, M., KAWAKAMI, H., OCHIAI, K., HANAWA, T. & KAMIYA, S. 2009. Outer membrane vesicles of Helicobacter pylori TK1402 are involved in biofilm formation. *BMC Microbiol,* 9**,** 197.

YOUNG, K. T., DAVIS, L. M. & DIRITA, V. J. 2007. Campylobacter jejuni: molecular biology and pathogenesis. *Nat Rev Microbiol,* 5**,** 665-79.

YUKI, N. 1997. Molecular mimicry between gangliosides and lipopolysaccharides of Campylobacter jejuni isolated from patients with Guillain-Barre syndrome and Miller Fisher syndrome. *J Infect Dis,* 176 Suppl 2**,** S150-3.

YUKI, N., SUSUKI, K., KOGA, M., NISHIMOTO, Y., ODAKA, M., HIRATA, K., TAGUCHI, K., MIYATAKE, T., FURUKAWA, K., KOBATA, T. & YAMADA, M. 2004. Carbohydrate mimicry between human ganglioside GM1 and Campylobacter jejuni lipooligosaccharide causes Guillain-Barre syndrome. *Proc Natl Acad Sci U S A,* 101**,** 11404-9.

YUKI, N., TAKAHASHI, M., TAGAWA, Y., KASHIWASE, K., TADOKORO, K. & SAITO, K. 1997. Association of Campylobacter jejuni serotype with antiganglioside antibody in Guillain-Barre syndrome and Fisher's syndrome. *Ann Neurol,* 42**,** 28-33.

ZAUTNER, A. E., HERRMANN, S., CORSO, J., TAREEN, A. M., ALTER, T. & GROSS, U. 2011. Epidemiological association of different Campylobacter jejuni groups with metabolism-associated genetic markers. *Appl Environ Microbiol,* 77**,** 2359-65.

ZAUTNER, A. E., OHK, C., TAREEN, A. M., LUGERT, R. & GROSS, U. 2012. Epidemiological association of Campylobacter jejuni groups with pathogenicity-associated genetic markers. *BMC Microbiol,* 12**,** 171.

ZILBAUER, M., DORRELL, N., BOUGHAN, P. K., HARRIS, A., WREN, B. W., KLEIN, N. J. & BAJAJ-ELLIOTT, M. 2005. Intestinal innate immunity to Campylobacter jejuni results in induction of bactericidal human beta-defensins 2 and 3. *Infect Immun,* 73**,** 7281-9.

ZILBAUER, M., DORRELL, N., WREN, B. W. & BAJAJ-ELLIOTT, M. 2008. Campylobacter jejuni-mediated disease pathogenesis: an update. *Trans R Soc Trop Med Hyg,* 102**,** 123-9.

ZIPRIN, R. L., YOUNG, C. R., BYRD, J. A., STANKER, L. H., HUME, M. E., GRAY, S. A., KIM, B. J. & KONKEL, M. E. 2001. Role of Campylobacter jejuni potential virulence genes in cecal colonization. *Avian Dis,* 45**,** 549-57.

ZIPRIN, R. L., YOUNG, C. R., STANKER, L. H., HUME, M. E. & KONKEL, M. E. 1999. The absence of cecal colonization of chicks by a mutant of Campylobacter jejuni not expressing bacterial fibronectin-binding protein. *Avian Dis,* 43**,** 586-9.

Appendix 1

ClustalW output for NCTC11168 CadF and FlpA alignment

```
########################################
# Program: water
# Rundate: Thu 27 Apr 2017 11:34:18
# Commandline: water
#    -auto
#    -stdout
#    -asequence emboss_water-I20170427-113417-0026-88836252-
oy.asequence
#    -bsequence emboss_water-I20170427-113417-0026-88836252-
oy.bsequence
#    -datafile EBLOSUM62
#    -gapopen 10.0
#    -gapextend 0.5
#    -aformat3 pair
#    -sprotein1
#    -sprotein2
# Align_format: pair
# Report_file: stdout
########################################

#=======================================
#
# Aligned_sequences: 2
# 1: CadFNTCC11168(Cj1478c)
# 2: FlpANCTC11168(Cj1279c)
# Matrix: EBLOSUM62
# Gap_penalty: 10.0
# Extend_penalty: 0.5
#
# Length: 283
# Identity:      55/283 (19.4%)
# Similarity:    91/283 (32.2%)
# Gaps:         101/283 (35.7%)
# Score: 52.0
#
#
#=======================================

CadFNTCC11168     16 GADNNVK--
FEITPTLNYNYFEGNLDMDNRYAPGIRLGYHFDDFWLDQLE     63
                     |.|...|  .|:...||..|.:.:|..:...:..| :...|:
FlpANCTC11168    174 GDDKEFKKIAEVKNRLNAEYIDSDLKPNENSSYRI-
IAVSFN--------    214

CadFNTCC11168     64
FGLEHYSDVKYTNTNKTTDITRTYLSAIKGIDVGEKFYFYGLAGGGYEDF
113
                     |::..|....::|:|.......:|||  ..|...|......| ..||||
```

```
FlpANCTC11168    215 -GIKSGSSQVVSSTSKALPPQVEHLSA--
STDGSSKIILTWDA-PTYEDF    260

CadFNTCC11168    114
SNAAYDNKSGGFGHYGAGVKFRLSDSLALRLETRDQINFNHANHNWVSTL
163
                 |.....:.|..|
FlpANCTC11168    261 SYYKVYSTSSSF-----------------------------------    272

CadFNTCC11168    164 GISFGFGGKKEK-
AVEEVADTRATPQAKCPVEPREGA---------LLDE    203
                  :.|....|.:| :.|::.             |||         ::|:
FlpANCTC11168    273 -LPFSVLAKTDKNSYEDIV----------
EGAGKSKYYKVTMVDK    306

CadFNTCC11168    204
NGCEKTISLEGHFGFDKTTINPTFQEKIKEIAKVLDENERYDTILEGHTD    253
                 :|.|..:..:|..|  ||..||        :|..:        ||...|
FlpANCTC11168    307 DGLESPMPKDGVEG--KTLGNP--------LAPSI--------
ILAQST-    337

CadFNTCC11168    254 NIGSRAYNQKLSERRAKSVANELEKYGVEKSRI
286
                   |...|.:.|:...::|..|:.:||.|::.:
FlpANCTC11168    338 ---SEGINLEWSDNDTRAVEYEVRRYGGEQNAV
367


#---------------------------------------
#---------------------------------------
```

Appendix 2

ClustalW output for NCTC11168 and 81-176 FlpA alignment

```
########################################
# Program: water
# Rundate: Thu 27 Apr 2017 11:27:44
# Commandline: water
#    -auto
#    -stdout
#    -asequence emboss_water-I20170427-112743-0196-93760291-
oy.asequence
#    -bsequence emboss_water-I20170427-112743-0196-93760291-
oy.bsequence
#    -datafile EBLOSUM62
#    -gapopen 10.0
#    -gapextend 0.5
#    -aformat3 pair
#    -sprotein1
#    -sprotein2
# Align_format: pair
# Report_file: stdout
########################################

#=======================================
#
# Aligned_sequences: 2
# 1: FlpANCTC11168
# 2: FlpA81-176
# Matrix: EBLOSUM62
# Gap_penalty: 10.0
# Extend_penalty: 0.5
#
# Length: 410
# Identity:     403/410 (98.3%)
# Similarity:   405/410 (98.8%)
# Gaps:           0/410 ( 0.0%)
# Score: 2057.0
#
#
#=======================================

FlpANCTC11168      2
MKRFRLSFYLSFLTLLLSACSVSQMNSLASSKEPAVNESLPKVESLKSLS
51
                   ||||||.||||||||||||||||||||||||||||||||||||||||||
FlpA81-176         1
MKRFRLGFYLSFLTLLLSACSVSQMNSLASSKEPAVNESLPKVESLKSLS
50
```

FlpANCTC11168 52
DMSNIAFEWEPLYNENIKGFYLYRSSDENPDFKLVGTIKDKFQTHYVDTK
101

FlpA81-176 51
DMSNIAFEWESLYNENIKGFYLYRSSDENPDFKLVGTIKDKFQTHYVDTK
100

FlpANCTC11168 102
LEPGTKYRYMMKSFNEQGQISEDGKVIEVSTAPRLEAVPFVQAVTNLPNR
151

FlpA81-176 101
LEPGTKYRYMMKSFNEQGQISEDGKVIEVSTAPRLEAVPFVQAVTNLPNR
150

FlpANCTC11168 152
IKLIWRPHPDFRVDSYIIERTKGDDKEFKKIAEVKNRLNAEYIDSDLKPN 201

FlpA81-176 151
IKLIWRPHPDFRVDSYIIERTKGDDKEFKKIAEVKNRLNAEYIDSDLKPN 200

FlpANCTC11168 202
ENSSYRIIAVSFNGIKSGSSQVVSSTSKALPPQVEHLSASTDGSSKIILT 251

FlpA81-176 201
ENSSYRIIAVSFNGIKSEPSQVVSSTSKALPPQVEHLSASTDGSNKIMLT
250

FlpANCTC11168 252
WDAPTYEDFSYYKVYSTSSSFLPFSVLAKTDKNSYEDIVEGAGKSKYYKV
301

FlpA81-176 251
WDAPTYEDFSYYKVYSTSSSFLPFSVLAKTDKNSYEDIVEGVGKSKYYKV
300

FlpANCTC11168 302
TMVDKDGLESPMPKDGVEGKTLGNPLAPSIILAQSTSEGINLEWSDNDTR
351

FlpA81-176 301
TMVDKDGLESPMPKDGVEGKTLGNPLAPSIILAQSTSEGINLEWSDNDTR
350

FlpANCTC11168 352
AVEYEVRRYGGEQNAVFKGIKEKRLKDVKALPGVEYSYEVIAIDSAGLRS
401

FlpA81-176 351
AVEYEVRRYGGEQNAVFKGIKEKRLKDVKALPGVEYSYEVIAIDSAGLRS
400

FlpANCTC11168 402 EPSSKVKAAQ 411

FlpA81-176 401 EPSSKVKAAQ 410

#---------------------------------------
#---------------------------------------

Appendix 3

ClustalW output for NCTC11168 and 81-176 CadF alignment

```
########################################
# Program: water
# Rundate: Thu 27 Apr 2017 11:23:41
# Commandline: water
#    -auto
#    -stdout
#    -asequence emboss_water-I20170427-112335-0274-85685520-
oy.asequence
#    -bsequence emboss_water-I20170427-112335-0274-85685520-
oy.bsequence
#    -datafile EBLOSUM62
#    -gapopen 10.0
#    -gapextend 0.5
#    -aformat3 pair
#    -sprotein1
#    -sprotein2
# Align_format: pair
# Report_file: stdout
########################################

#=======================================
#
# Aligned_sequences: 2
# 1: CadFNTCC11168
# 2: CadF81-176
# Matrix: EBLOSUM62
# Gap_penalty: 10.0
# Extend_penalty: 0.5
#
# Length: 319
# Identity:     315/319 (98.7%)
# Similarity:   315/319 (98.7%)
# Gaps:           0/319 ( 0.0%)
# Score: 1668.0
#
#
#=======================================

CadFNTCC11168      1
MKKIFLCLGLASVLFGADNNVKFEITPTLNYNYFEGNLDMDNRYAPGIRL
50
                   |||||.||||||||||.||||||||||||||||||||||||||||||||||
CadF81-176         1
MKKILLCLGLASVLFSADNNVKFEITPTLNYNYFEGNLDMDNRYAPGIRL
50
```

```
CadFNTCC11168     51
GYHFDDFWLDQLEFGLEHYSDVKYTNTNKTTDITRTYLSAIKGIDVGEKF
100
                  ||||||||||||||||||||||||||||||||||||||||||||||||||
CadF81-176        51
GYHFDDFWLDQLEFGLEHYSDVKYTNTNKTTDITRTYLSAIKGIDVGEKF
100

CadFNTCC11168     101
YFYGLAGGGYEDFSNAAYDNKSGGFGHYGAGVKFRLSDSLALRLETRDQI
150
                  ||||||||||||||||||||||||||||||||||||||||||||||||||
CadF81-176        101
YFYGLAGGGYEDFSNAAYDNKSGGFGHYGAGVKFRLSDSLALRLETRDQI
150

CadFNTCC11168     151
NFNHANHNWVSTLGISFGFGGKKEKAVEEVADTRATPQAKCPVEPREGAL
200
                  ||||||||||||||||||||||||||||||||||..|||||||||||||||
CadF81-176        151
NFNHANHNWVSTLGISFGFGGKKEKAVEEVADTRPAPQAKCPVEPREGAL
200

CadFNTCC11168     201
LDENGCEKTISLEGHFGFDKTTINPTFQEKIKEIAKVLDENERYDTILEG     250
                  ||||||||||||||||||||||||||||||||||||||||||||||||||
CadF81-176        201
LDENGCEKTISLEGHFGFDKTTINPTFQEKIKEIAKVLDENERYDTILEG     250

CadFNTCC11168     251
HTDNIGSRAYNQKLSERRAKSVANELEKYGVEKSRIKTVGYGQDNPRSSN
300
                  ||||||||||||||||||||||||||||||||||||||||||||||||||
CadF81-176        251
HTDNIGSRAYNQKLSERRAKSVANELEKYGVEKSRIKTVGYGQDNPRSSN
300

CadFNTCC11168     301 DTKEGRADNRRVDAKFILR     319
                  |||||||||||||||||||
CadF81-176        301 DTKEGRADNRRVDAKFILR     319


#---------------------------------------
#---------------------------------------
```